Investigating the Immune System in Parkinson's Disease

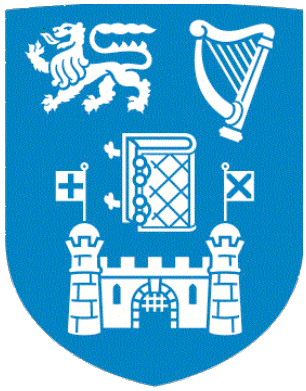

Thesis submitted for the degree of

Doctor of Philosophy, Physiology

2024

Adina MacMahon Copas

Supervised by
Prof. Maeve Caldwell and Assoc. Prof. Jean Fletcher

Department of Physiology, School of Medicine

and

Trinity College Institute of Neuroscience, Llyod Institute
Trinity College Dublin, Ireland

Declaration and statement of plagiarism

I declare that this thesis has not been submitted as an exercise for a degree at this or any other university and it is entirely my own work. The unpublished and/or published work of others, has been duly acknowledged in the text wherever included.

Prof. Maeve Caldwell and Prof. Jean Fletcher were involved in study design, analysis and interpretation of data. Dr Sarah McComish, carried out the dose-responses for TNFα, IL-17A and $CD4^+$ conditioned media. Dr. Andreea Petrasca, generated the $CD4^+$ conditioned media (Chapter 3), designed the flow cytometry panel and aided in initial acquisition and analysis (Chapter 6). The Neurology clinic at the Mater hospital, in particular, Professor Tim Lynch, Dr. Connor Fearon, Dr. Dimitra Chaity and John Innocentes are to thank for the patient samples used throughout this PhD. Students Anna Stricker, Rachel McCormack, Daniel Ivers, Harriet O'Leary, Katarzyna Plesniar, Amy Doyle and Patricia Sim aided in various experiments during their respective projects.

I agree to deposit this thesis in the University's open access institutional repository or allow the Library to do so on my behalf, subject to Irish Copyright Legislation and Trinity College Library conditions of use and acknowledgement.

I consent to the examiner retaining a copy of the thesis beyond the examining period, should they so wish (EU GDPR May 2018).

Signed:

Date: 31.03.2024

Summary

Parkinson's disease (PD) is a chronic neurodegenerative disease in which loss of the dopaminergic neurons of the substantia nigra *pars compacta* and alpha synuclein accumulation are considered hallmarks. However, the involvement of neuroinflammation and indeed astrocyte reactivity in disease pathogenesis is becoming more widely recognised. In recent years the infiltration of peripheral immune cells into the brain and their contribution to the pathogenesis of PD has been demonstrated. While the study of peripheral immune cell populations in PD continues to yield varying results, the contribution of these cells to neuronal damage is apparent. In particular, T lymphocytes have been implicated in causing the damage observed in these studies. However, the effects these two cell populations on one another has yet to be fully elucidated. Therefore this thesis aimed to investigate the role of inflammation in contributing to PD, with particular focus on T lymphocytes and astrocyte reactivity.

In order to do this induced pluripotent stem cells (iPSC) were utilised to generate the cell type of interest, the astrocyte of the midbrain. This study found that $CD4^+$ T cell associated cytokines, induced a chronic pro-inflammatory phenotype in midbrain astrocytes. This inflammatory phenotype consisted of increased gene expression, protein secretion and morphological changes consistent with reactive astrocytes. Furthermore, these astrocytes demonstrated signs of damage, with increased DNA damage marker, yH2AX and an increase in the release of lactate dehydrogenase, an indicator of cell membrane damage.

To increase the translatability of this research, we aimed to generate iPSC from individuals with PD. Human dermal fibroblasts from PD patients were reprogrammed back to a pluripotent state, successfully producing multiple new PD iPSC lines.

Furthermore, midbrain astrocytes were then differentiated from one of those PD iPSC lines and a healthy control iPSC line. Once stimulated a difference in reactivity profile was observed between the PD and healthy control astrocytes, with the PD astrocytes illustrating a more prominent pro-inflammatory phenotype.

Finally, blood samples were collected from PD individuals and healthy age-matched controls in order to assess the peripheral immune cell landscape in PD. Analysis of peripheral immune cells and their cytokines resulted in a number of differences being observed between PD patient and age-matched healthy control cohorts.

Overall, the data generated in this thesis adds to current literature suggesting a prominent role for peripheral and central immune cell activation in contributing to PD pathogenesis. Future work to expand on the data presented here could aid in identification of immune-based targets for the treatment of PD.

Acknowledgments

Firstly, I want to whole-heartedly extend my gratitude and thanks to my primary supervisor Prof. Maeve Caldwell. I can genuinely say that I would not have made it through this PhD if it weren't for you. Your support, guidance, understanding and resourcefulness have been invaluable to the completion of this thesis. You have helped me gain confidence in myself and because of this I have achieved so many things I wouldn't have thought I could. You have been an amazing mentor throughout these past few years and hopefully for many more to come.

To my secondary supervisor, Assoc. Prof. Jean Fletcher, thank you from the bottom of my heart for your continued support throughout this PhD. Thank you for all of your immunology expertise, for answering my endless questions and for always being willing to help, I am so thankful to you!

The Caldwell lab, Sarah, Maddie, Julia, Jessica and Lei. How do I even begin thanking you all for everything that you have done. Sarah, thank you for taking me under your wing and teaching everything you know from summer student to PhD candidate, I can't thank you enough. Maddie, thank you for your continued support, for picking me up when I'm down, and for reminding me to eat! I never expected to find such an amazing friend during this PhD and I am so thankful for you! Julia, thank god you joined our lab! Honestly, you have been such a constant support through me finishing up this PhD, thank you for proof reading and answering my endless questions! Jessica, thank you for the Lucozade sport, for hiding me in your office while I cried and for solidarity in overthinking and anxiety! Lei, thank you for your help with processing the last of the blood samples! You are some of the most inspiring, strong and intelligent women I have had the pleasure of knowing. Thank you so much for all of your support, I'm here to return the favour whenever you need!

To my 'work colleagues', i.e. the Harkin lab *et al*. You have seen me through all the emotional states of doing a PhD, thank you for making it so much fun, thank you for all the chocolate, laughs, drinks and karaoke. I feel very lucky to work with such an amazing group of people and I am going to miss seeing you all every day, evening, weekend and holiday, cheers to having a work-life balance!

To the members of the Fletcher lab, Andreea and Conor, thank you for welcoming me so openly into your lab! I cannot thank you enough for making the process of trying to learn flow cytometry so seamless!

Thank you to my masters, undergraduate and summer students over the years who have helped with much of the data in this thesis; Katarzyna, Amy, Daniel, Anna, Harriet, Rachel, Patricia, and Patricia.

Thank you to our collaborators in Tim Lynch's group and the Neurology Clinic in the Mater Hospital. To John and Dimitra, thank you for all of your help in obtaining and coordinating collection of all the patient samples used in this thesis!

To my friends who have had to listen to me for the last three and a half years talking about science and complaining about cells not growing. Thank you for listening, for the care-packages, for the words of encouragement, for booking spontaneous holidays, thank you for being the best friends I could ask for!

Last but certainly not least, thank you to my family. To my mam, Sinead and dad, Aidan. There are no words to thank you for all that you do to support me. Thank you for the tea and biscuits, for the coffee every morning on the way to the train, for collecting me when I was in the lab late at night and too tired to drive, for making sure I remembered to eat while writing this thesis! Thank you to my sister Thea for the treats and support! Thank you to my sister Ayaisha who always tells me I'm great! Thank you, thank you, thank you!

Ps. Thank you to my laptop for holding it together while I wrote this thesis, and finally " I want to thank me for believing in me, I want to thank me for doing all this hard work." ~Snoop dog

Table of contents

DECLARATION AND STATEMENT OF PLAGIARISM 2

SUMMARY 3

ACKNOWLEDGMENTS 5

TABLE OF CONTENTS 7

LIST OF FIGURES 14

LIST OF TABLES 18

ABBREVIATIONS 19

CHAPTER 1 : INTRODUCTION 23

1.1. PARKINSON'S DISEASE A HISTORY; FROM SHAKING PALSY TO DOPAMINERGIC DEGENERATION 24

1.2. DISEASE STAGING 25

1.3. PARKINSON'S DISEASE, A GLOBAL ISSUE 26

1.4. PARKINSON'S ASSOCIATED GENETICS 28

1.5. ALPHA SYNUCLEIN; A MISFOLDED MENACE 32

1.6. DEGENERATION OF THE MIDBRAIN 34

1.7. DOPAMINE AND ITS ACTIONS 36

1.8. NEUROINFLAMMATION IN PARKINSON'S DISEASE 37

1.8.1. ASTROCYTES; THE HOMEOSTATIC REGULATORS OF THE CNS 37

1.8.2. Astrogliosis; harmful or helpful 40
1.8.3. The peripheral immune system; a novel contender? 43
1.9. Modelling PD with induced pluripotent stem cells 46
1.9.1. Evolution of the Yamanaka protocol 47
1.9.1.1. Genetic material 47
1.9.1.2. Methods of delivery 48
1.10. What existed before this? 50
1.10.1. Post-mortem brain tissue 52
1.10.2. Animal models 52
1.10.3. Direct reprogramming 55
1.11. Advantages and disadvantages of iPSC 56
1.12. Overarching aims and hypotheses 58

CHAPTER 2 : MATERIALS AND METHODS 60

2.1. Cryopreservation and thawing of cells 61
2.2. Counting cells 61
2.3. Enzyme-linked immunosorbent assay 62
2.4. Quantitative real time polymerase chain reaction (qRT-PCR) 62
2.4.1. Sample preparation 62
2.4.2. RNA isolation 63
2.4.3. Complementary DNA manufacture 63
2.4.4. qRT-PCR 64
2.5. Immunocytochemistry 66
2.6. Statistical methods 67

CHAPTER 3: CD4+ T CELL-ASSOCIATED CYTOKINES INDUCE A CHRONIC PRO-INFLAMMATORY PHENOTYPE IN INDUCED PLURIPOTENT STEM CELL-DERIVED MIDBRAIN ASTROCYTES 68

ABSTRACT 70

3.1. INTRODUCTION....71

3.2. METHODS....73

3.2.1. CULTURE OF IPSC-DERIVED ASTROCYTES 73

3.2.3. IMMUNOCYTOCHEMISTRY/IMMUNOFLUORESCENCE AND IMAGING....74

3.2.4. RT-QPCR 75

3.2.5. ELISA 76

3.2.6. LACTATE DEHYDROGENASE ASSAY....76

3.2.7. QUANTIFICATION AND STATISTICAL ANALYSIS 77

3.3. RESULTS 78

3.3.1. $CD4^+$ T CELL CONDITIONED MEDIA INDUCES NFKB TRANSLOCATION IN VMASTROS. 78

3.3.2. $CD4^+$ T CELL CONDITIONED MEDIA INDUCES ACUTE AND CHRONIC ALTERATIONS IN VMASTROS REACTIVITY PROFILE. 80

3.3.3. NFKB TRANSLOCATION INDUCED BY TNFA AND IL-17A 82

3.3.4. VMASTROS RESPOND ROBUSTLY, AND CHRONICALLY TO THE SYNERGISTIC ACTION OF TNFA AND IL-17A 85

3.3.5. MORPHOLOGICAL ALTERATIONS INDICATIVE OF REACTIVE ASTROCYTE PHENOTYPE INDUCED BY CHRONIC CYTOKINE EXPOSURE....87

3.3.6. CHRONIC CYTOKINE EXPOSURE RESULTS IN INCREASED DNA DAMAGE AND LDH RELEASE FROM VMASTROS....89

3.4. DISCUSSION 91

3.5. SUPPLEMENTAL....96

CHAPTER 4 : GENERATING PARKINSON'S DISEASE PATIENT DERIVED IPSC...103

4.1. INTRODUCTION 104

4.1.1. CHARACTERISATION OF INDUCED PLURIPOTENT STEM CELLS 104

4.1.2. AIMS 106

4.2. MATERIALS AND METHODS 108

4.2.1. DERMAL PUNCH BIOPSY 108

4.2.1.1. Preparation of dermal punch biopsy 108

4.2.1.2. Culture and expansion of human dermal fibroblasts 109

4.2.1.3. Mouse embryonic fibroblasts as a feeder layer for iPSC 109

4.2.2. REPROGRAMMING OF HUMAN FIBROBLASTS TO IPSC 110

4.2.2.1. Nucleofection of human fibroblasts 110

4.2.2.2. Culture of reprogramming cells 111

4.2.2.3. Transition of cells from MEF feeder layer to a feeder free system 112

4.2.2.4. Removal of spontaneous differentiation 112

4.2.3. TRILINEAGE DIFFERENTIATION 113

4.3. RESULTS 114

4.3.1. THE SUCCESSFUL REPROGRAMMING OF HUMAN DERMAL FIBROBLASTS INTO PLURIPOTENT STEM CELLS 114

4.3.2. CONFIRMATION OF THE SUCCESSFUL REPROGRAMMING OF HUMAN DERMAL FIBROBLASTS TO PLURIPOTENT STEM CELLS. 118

4.3.3. GENERATED IPSC DEMONSTRATE THE ABILITY TO DIFFERENTIATE INTO CELLS OF THE THREE GERM LAYERS. 123

4.4. DISCUSSION 126

CHAPTER 5 : UTILISING IPSC TO DIFFERENTIATE CELLS OF THE VENTRAL MIDBRAIN 131

5.1. INTRODUCTION 132

5.1.1. WHAT NEURONS ARE OF INTEREST IN PD? 132

5.1.2. THE GLIOGENIC SWITCH 135

5.2. AIMS 136

5.3. MATERIALS AND METHODS 137

5.3.2. INDUCE PLURIPOTENT STEM CELL LINES 137

5.3.3. VMNPC DIFFERENTIATION 137

5.3.4. VMASTROS DIFFERENTIATION 137

5.3.5. STIMULATING ASTROCYTES WITH MICROGLIAL-SECRETED CYTOKINES 138

5.3. RESULTS 140

5.3.1. DIFFERENTIATION OF VMNPC FROM IPSC. 140

5.3.2. CONFIRMATION OF THE SUCCESSFUL DIFFERENTIATION OF VMNPC. 141

5.3.3. DIFFERENTIATION OF VMASTROS FROM VMNPC. 143

5.3.4. DIFFERENTIATED VMASTROS EXPRESS MARKERS ASSOCIATED WITH MATURE ASTROCYTES. 145

5.3.5. VMASTROS RESPOND TO PRO-INFLAMMATORY CYTOKINES TO PRODUCE A REACTIVE ASTROCYTE PHENOTYPE 147

5.3.6. PD05 VMASTROS DEMONSTRATE DIFFERING PROTEIN AND GENE EXPRESSION COMPARED TO NAS2 VMASTROS. 151

5.4. DISCUSSION 153

5.4.1. GENERATION OF IPSC-DERIVED VENTRAL MIDBRAIN NEURAL PROGENITOR CELLS 153

5.4.2. DIFFERENTIATION OF VMASTROS 156

5.4.3. ASTROCYTES DEMONSTRATE DIFFERENCES IN THEIR REACTIVE PHENOTYPE 157

CHAPTER 6 : INVESTIGATING THE PERIPHERAL IMMUNE SYSTEM IN PARKINSON'S DISEASE....161

6.1. INTRODUCTION....162

6.1.1. THE PERIPHERAL IMMUNE SYSTEM IN PARKINSON'S DISEASE....162

6.2. AIMS....171

6.2. MATERIALS AND METHODS....173

6.2.1. PROCESSING OF BLOOD SAMPLES....173

6.2.1.1. Isolation of plasma....173

6.2.1.2. Isolation of peripheral blood mononuclear cells....173

6.2.2. GENERATION OF CONDITIONED MEDIA....174

6.2.3. FLOW CYTOMETRY....174

6.3. RESULTS....176

6.3.1. ANALYSIS OF PLASMA FROM INDIVIDUALS WITH PARKINSON'S AND AGE-MATCHED CONTROLS.....176

6.3.2. INVESTIGATING DIFFERENCES IN STIMULATED PBMCS PROTEIN RELEASE. 177

6.3.3. INVESTIGATION OF T CELL POPULATIONS USING FLOW CYTOMETRY.....181

6.4. DISCUSSION....187

CHAPTER 7 : FINAL DISCUSSION....194

7.1. SUMMARY....195

7.2. PERIPHERAL IMMUNE CELLS CONTRIBUTE TO CHRONIC ASTROGLIOSIS 197

7.4. CELL REPLACEMENT THERAPY....200

7.3. REACTIVE PHENOTYPE DIFFERENCES IN PD VMASTROS....200

7.4. ALTERATIONS IN PERIPHERAL IMMUNE CELL POPULATIONS 201

7.5. TARGETING THE IMMUNE SYSTEM THERAPEUTICALLY 204

7.6. CONCLUSIONS 206

APPENDIX 1 207

APPENDIX 2 212

BIBLIOGRAPHY 214

List of figures

FIGURE 1.1.1. TIMELINE FOR KEY EARLY DISCOVERIES IN PARKINSON'S DISEASE 26

FIGURE 1.1.2. ASTROCYTES ARE KEY HOMEOSTATIC REGULATORS OF THE CNS. 39

FIGURE 1.1.3. POTENTIAL INTERACTIONS BETWEEN ASTROCYTES, MICROGLIA AND T LYMPHOCYTES IN PARKINSON'S DISEASE. 42

FIGURE 1.1.4. MHC CLASS PRESENTATION TO $CD8^+$ AND $CD4^+$ T CELLS. 44

FIGURE 1.1.5. DIFFERENTIATION OF $CD4^+$ T CELL SUBTYPES. 45

FIGURE 3.3.1. ACTIVATION OF NFKB PATHWAY SIGNALLING IN VMASTROS FOLLOWING EXPOSURE TO $CD4^+$ T CELL CONDITIONED MEDIA (CD4CM). 79

FIGURE 3.3.2. CD4CM INDUCED REACTIVE GENE EXPRESSION AND PROTEIN SECTION FROM VMASTROS. 81

FIGURE 3.3.3. VMASTROS RESPOND TO TNFA AND IL-17A BY INDUCING NFKB TRANSLOCATION TO THE NUCLEUS. 84

FIGURE 3.3.4. TNFA AND IL-17A INDUCED VARIABLE ALTERATIONS IN VMASTROS REACTIVITY ASSOCIATED GENE EXPRESSION AND PROTEIN SECRETION. 86

FIGURE 3.3.5. CYTOKINE STIMULATION RESULTS IN SIGNIFICANT MORPHOLOGICAL CHANGES IN VMASTROS. 88

90

FIGURE 3.3.6. CHRONIC STIMULATION WITH TNFA+IL-17A INDUCED DISTRESS IN VMASTROS. 90

98

SUPPLEMENTAL FIGURE 1. 98

SUPPLEMENTARY FIGURE 2. GENE AND PROTEIN ANALYSIS OF VMASTROS FOLLOWING STIMULATION WITH CD4CM. 99

Supplementary Figure 3. Gene expression and protein secretion from vmAstros following stimulation with TNFa, IL-17A or TNFa+IL-17A. 100
Supplementary Figure 4. Immunocytochemical analysis of S100b intensity changes in vmAstros following stimulation. 101
Supplementary Figure 5. Morphological analysis of vmAstros following 24 h stimulation with cytokines TNFa, and IL-17A. 101
Supplementary Figure 6. Immunocytochemical analysis of gH2AX expression in vmAstros following stimulation. 101
Figure 4.1.1. Major changes to the protocol for deriving induce pluripotent stem cells since its initial discovery. 104
Figure 4.2.1. Timeline highlighting the key points of iPSC generation from HDF. . 113
Figure 4.3.1. Generation iPSC from HDF. 116
Figure 4.3.2. Troubleshooting the protocol for generation of iPSC. 116
117
Figure 4.3.3. Morphological changes and GFP expression indicate successful reprogramming. 117
Figure 4.3.4. Transition of iPSC colonies from MEF feeder system to a feeder-free, xeno-free culture system. 117
Figure 4.3.5. PD05 iPSC expresses intra and extracellular markers of pluripotency. 119
Figure 4.3.6. PD03 iPSC expresses intra and extracellular markers of pluripotency. 120
Figure 4.3.7. PD06 iPSC expresses intra and extracellular markers of pluripotency. 121

FIGURE 4.3.8. PD04 IPSC EXPRESS INTRA AND EXTRACELLULAR MARKERS OF PLURIPOTENCY. 122
FIGURE 4.3.9. GENERATED IPSC LINES PD05, PD03 AND PD06 EXPRESS PLURIPOTENCY GENES. 123
FIGURE 4.3.10. TIMELINE FOR TRILINEAGE DIFFERENTIATION FROM IPSC 124
FIGURE 4.3.11. ASSESSING GENE EXPRESSION OF PLURIPOTENCY AND TRILINEAGE ASSOCIATED GENES FOLLOWING TRILINEAGE DIFFERENTIATION. 125
FIGURE 5.3.1. DIFFERENTIATION OF VMNPC CELLS FROM IPSC. 141
FIGURE 5.3.2. CONFIRMATION OF VMNPC DIFFERENTIATION FROM NAS2 IPSC. 142
FIGURE 5.3.3. CONFIRMATION OF VMNPC DIFFERENTIATION FROM PD05 IPSC. 143
FIGURE 5.3.4. PROTOCOL FOR THE DIFFERENTIATION OF VMAPC FROM VMNPC. 144
FIGURE 5.3.5. NAS2 VMASTROS EXPRESSION KEY ASTROCYTE PROTEINS. 146
FIGURE 5.3.6. PD05 VMASTROS EXPRESSION KEY ASTROCYTE MARKERS. 147
FIGURE 5.3.7. NAS2 VMASTROS RESPOND TO INFLAMMATORY CYTOKINES BY INCREASING SECRETION AND GENE EXPRESSION OF PRO-INFLAMMATORY ASSOCIATED FACTORS. 149
FIGURE 5.3.8. PD05 VMASTROS RESPOND TO INFLAMMATORY BY INCREASING SECRETION AND GENE EXPRESSION OF PRO-INFLAMMATORY MARKERS. 150
FIGURE 5.3.9. PD05 VMASTROS DEMONSTRATE AN ALTERED PROTEIN AND GENE EXPRESSION PHENOTYPE COMPARED WITH CONTROL NAS2 VMASTROS. 152
FIGURE 6.3.1. ANALYSIS OF PLASMA FROM INDIVIDUALS WITH PD AND AGED-MATCHED HC. 179
FIGURE 6.3.2. ANALYSIS OF THE CYTOKINES RELEASED BY STIMULATED PBMC. 180
FIGURE 6.3.3. OUTLINE OF THE FLOW CYTOMETRY GATING STRATEGY. 183
FIGURE 6.3.4. ANALYSIS OF T CELL POPULATIONS 184
FIGURE 6.3.5. ANALYSIS OF CD4 T CELL CYTOKINES. 185

FIGURE 6.3.6. ANALYSIS OF CD8 T CELL CYTOKINES. 186

List of tables

TABLE 1.1.1. PROPOSED PARKINSON'S ASSOCIATED GENETIC MUTATIONS 29

TABLE 2.1. QRT-PCR PRIMERS.....65

TABLE 2.2. IMMUNOCYTOCHEMISTRY ANTIBODIES.....67

SUPPLEMENTAL TABLE 1. IMMUNOCYTOCHEMISTRY ANTIBODIES 96

SUPPLEMENTAL TABLE 2. RT-QPCR PRIMERS 97

TABLE 4.2.1. PATIENT CELL LINE INFORMATION. 109

TABLE 4.2.2. REPROGRAMMING PLASMIDS 111

TABLE 5.1.1. SUMMARY OF KEY MIDBRAIN NEURON DIFFERENTIATION PROTOCOLS 134

TABLE 5.2.1. TREATMENT PLAN FOR VMASTROS 138

TABLE 6.1.1. EVIDENCE FOR T CELL INVOLVEMENT IN PARKINSON'S DISEASE 164

TABLE 6.2.1. FLOW CYTOMETRY ANTIBODY PANEL. 175

TABLE 6.3.1. OVERVIEW OF PARTICIPANTS INVOLVED IN THIS STUDY. 177

TABLE 1. HUMAN FIBROBLAST MEDIUM.....207

TABLE 2. MOUSE EMBRYONIC FIBROBLAST MEDIUM 207

TABLE 3. HUMAN EMBRYONIC STEM CELL MEDIUM 207

TABLE 4. REPROGRAMMING MEDIUM.....208

TABLE 5. EMBRYOID BODY MEDIUM 208

TABLE 6. COMPLETED RPMI 209

TABLE 7. NEURAL DIFFERENTIATION MEDIUM 209

TABLE 8. NEURAL MAINTENANCE MEDIUM.....210

TABLE 9. ASTROCYTE MEDIUM 210

TABLE 10. ASTROCYTE MATURATION MEDIUM 211

Abbreviations

α-syn	Alpha Synuclein
6-OHDA	6 hydroxydopamine
A	
AA	Arachidonic Acid
AD	Alzheimer's disease
ALDH1A1	Aldehyde dehydrogenase 1 A 1
AM	Astrocyte medium
AMM	Astrocyte maturation medium
ANOVA	Analysis of variance
APC	Astrocyte progenitor cell
ATP	Adenosine triphosphate
B	
BARHL1	BarH like homeobox 1
BBB	Blood brain barrier
BDNF	Brain derived neurotrophic factor
BMP4	Bone morphogenetic protein 4
C	
c-Myc	Cellular Myc
C1q	Complement component 1 q
C3	Complement component 3
CCL5	Chemokine ligand 5
CD4CM	$CD4^+$ T cell conditioned media
cDNA	Complementary deoxyribonucleic acid
CNPY1	Canopy FGF signalling regulator 1
CNS	Central nervous system
CNTF	Ciliary neurotrophic factor
CTLA-4	Cytotoxic T lymphocyte associated protein 4
CX43	Connexin 43
CXCL10	C-X-C motif chemokine ligand 10
D	
DMSO	Dimethyl sulfoxide
DNA	Deoxyribonucleic acid
E	
EAAT1	Excitatory amino acid transporter 1
EB	Embryoid body
EDTA	Ethylenediaminetetraacetic acid
EET	epoxyeicosatrienoic acids
EGF	Epidermal growth factor
EN1	Engrailed 1
EOPD	Early onset Parkinson's disease
ESC	Embryonic stem cell

F

FBS	Foetal bovine serum
FGF2	Fibroblast growth factor 2
FOXP3	Forkhead box P3

G

GATA3	GATA-binding protein 3
GBA	Glucocerebrosidase
GDNF	Glial cell line derived neurotrophic factor
GFAP	Glial fibrillary acidic protein
GFP	Green fluorescent protein
GLP-1	Glucagon-like peptide 1
GM-CSF	Granulocyte macrophage colony stimulating factor
GWAS	Genome-wide association studies

H

HC	Healthy control
HDF	Human dermal fibroblasts
hES	Human embryonic stem cell medium
HLA	Human leukocyte antigen
hLIF	Human leukaemia inhibitory factor
HRP	Horseradish peroxidase

I

ICAM-1	Intracellular adhesion molecule 1
IFN-γ	Interferon gamma
IL-1α	Interleukin 1 alpha
IL-17A	Interleukin 17 A
IL-1β	Interleukin 1 beta
iPSC	Induced pluripotent stem cells
ITGA6	Integrin subunit alpha 6

J

JAK	Janus kinase
JNK	c-Jun N-terminal kinase

K

Klf4	Krüppel-like factor 4

L

LCN2	Lipocalin 2
LFA-1	Lymphocyte function associated antigen 1
LMX1A	LIM homeobox transcription factor 1 alpha
LOPD	Late onset Parkinson's disease
LPS	Lipopolysaccharide
LRRK2	Leucine-rich repeat kinase 2

M

MAPK	Mitogen activated protein kinase

MDS-UPDRS	Movement disorder society unified PD rating scale
MEF	Mouse embryonic fibroblasts
MHC	Major histocompatibility complex
MPP+	1-methyl-4-phenylpyridinium
MPTP	1-methyl-4-phenyl-1,2,3,6-tetrahydropyridine
MRC1	Mitochondrial respiration complex 1

N

NAC	Non amyloid beta component
NAS2	Non-affected sibling 2
NDM	Neural differentiation medium
NFκB	Nuclear factor kappa B
NGS	Normal goat serum
NMM	Neural maintenance medium
NPC	Neural progenitor cell

O

Oct3/4	Octamer-binding transcription factor 3 or 4
OTX2	Orthodenticle homeobox 2

P

PBMC	Peripheral blood mononuclear cells
PBS-T	Phosphate buffered saline Triton X
PD	Parkinson's disease
PGE	Prostaglandin
PINK1	PTEN-induced kinase 1
PITX2	Paired-like homeodomain transcription factor 2
PMA	Para methoxyamphetamine
PTX3	Pentraxin 3

Q

qRT-PCR	Quantitative real time polymerase chain reaction

R

ROCK	Rho kinase
RT	Room temperature

S

S100β	S100 calcium binding protein beta
SEM	Standard error of the mean
SERPINA3	Serpin peptidase inhibitor clade A member 3
SHH	Sonic hedgehog
shRNA	Short hairpin ribonucleic acid
SNARE	Soluble N-ethylmaleimide sensitive factor activating protein receptor
SNCA	Synuclein alpha
SNpc	Substantia nigra pars compacta
SOC	Alpha synuclein origin and connectome model
Sox2	SRY-box 2
STAT3	Signal transducer and activator of transcription 3

T

T regs	T regulatory cell
TGFβ	Transforming growth factor beta
TH	Tyrosine hydroxylase
Th	T helper cell
TMB	3,3',5,5' Tetramethylbenzidine
TNFα	Tumour necrosis factor alpha

V

VEGF	Vascular endothelial growth factor
vmAstros	Ventral midbrain astrocytes
vmNPC	Ventral midbrain neural progenitor cells
VPS35	Vacuolar protein sorting 35
VTA	Ventral tegmental area

Chapter 1 : Introduction

1.1. Parkinson's disease a history; from shaking palsy to dopaminergic degeneration

Parkinson's disease (PD) was first described by James Parkinson in 1817 (Parkinson, 2002). Parkinson described a 'shaking palsy', wherein individuals develop a minor tremor usually in one hand or arm, eventually progressing to affect most of the body and impeding everyday tasks (Parkinson, 2002). He does note for a time individuals find a brief respite in walking, however eventually this too becomes impossible. The disease brings with it alterations in gait, first noticed as a loss of upright posture. Which eventually develops into a forward leaning gait, with individuals walking on the balls of their feet and toes. Parkinson further describes the non-motor symptoms such as sleep disturbances, with individuals being awoken by the shaking of their limbs, as well as the symptoms of constipation, and speech impediment. He continues on, outlining the presence of these symptoms in multiple case studies (Parkinson, 2002). While Parkinson's essay was released in 1817 it was not until 1872 that it was named PD after his descriptions and identification of the symptoms for what they were (Charcot, 1892). It was Charcot in 1872 who first uses Parkinson's name to describe the disease, he also associates the symptom of bradykinesia with PD, describing individuals as having a slowness to their movements (Charcot, 1892).

As we now know, degeneration of dopaminergic neurons in the substantia nigra *pars compacta* (SNpc) of the midbrain accompanied by alpha synuclein (α-syn) accumulation are characteristic of PD (Poewe et al., 2017). While it is easy to look back and pinpoint these moments of first discovery, it was not until 1892 that Blocq and Marinesco established that the SN may be linked to PD due to a patient presenting with Parkinson's symptoms later having been found at autopsy to have a tumour that destroyed their SN (Blocq & Marinescu, 1892). In 1899 Brissaud and colleagues linked the motor symptoms of PD to damage of the SN of the

midbrain (Brissaud, 1899). Following after this, Fredrick Lewy, described aggregated inclusions in 1912, which were observed in the SN and named Lewy bodies by Tretiakoff in 1919 (Lewy, 1912; Trétiakoff, 1919). Despite these discoveries confirming the involvement of this region in the brain with the presenting symptoms of PD, the molecular basis connecting the two was still to be established. Carlsson described dopamine as a neurotransmitter in the brain involved in motor function in 1959 (Carlsson, 1959), while its role in PD was solidified by Hornykiewicz in 1960 who observed that dopamine was in fact reduced in the striatum of people with PD (Ehringer & Hornykiewicz, 1960). This led to the implementation of L-dopa, the dopamine precursor, as a therapeutic for PD. While the pathophysiology of this disease was still being unravelled, it was in 1973 that decreased striatal dopamine was correlated with loss of neurons in the SN by Bernheimer and colleagues (Bernheimer et al., 1973). This was followed by a key discovery in 1997 by Spillantini and colleagues demonstrating that α-syn proteins were present in those intracellular inclusions previously described by Fredrick Lewy (Spillantini et al., 1997).

1.2. Disease staging

These discoveries, which are summarised in Fig. 1.1.1. below, paved the way for methods of disease staging. In 1967, Hoehn and Yahr proposed the first staging system for PD (Hoehn & Yahr, 1967). This scale uses functional disability as a method of staging, beginning with stage 1, representing symptoms unilaterally and ending with stage 5, describing the patient as wheelchair bound or bedridden (Hoehn & Yahr, 1967). In 2003, Braak, described a subsequent staging method for PD which takes into account pathology spread within the brain (Braak, Del Tredici, et al., 2003). This scale consists of 6 stages, denoting lesion spread throughout the brain as disease progresses. At stage 3 lesions within the SNpc are observed (Braak, Del Tredici, et al., 2003). However, there are obvious limitations to the use of this scale clinically,

and indeed for research purposes. The movement disorder society-unified PD rating scale (MDS-UPDRS) is a modified version of the original 1987 UPDRS, the MDS-UPDRS was created in 2007 and is still the gold-standard for staging PD (Goetz et al., 2007). The MDS-UPDRS takes into account all aspects of disease, both motor and non-motor and incorporates the Hoehn and Yahr staging system (Goetz et al., 2007; Skorvanek et al., 2017).

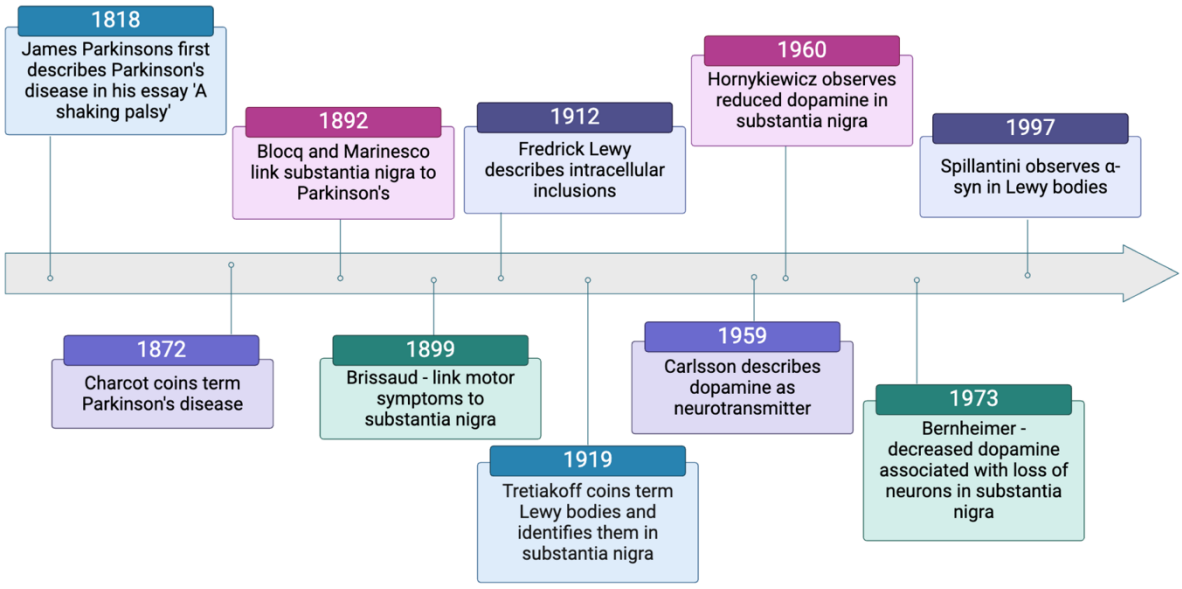

Figure 1.1.1. Timeline for key early discoveries in Parkinson's disease

Generated with biorender.

1.3. Parkinson's disease, a global issue

PD is the second most common neurodegenerative disease globally, coming second only to Alzheimer's disease (AD; Mishra et al., 2018). The number of cases of PD globally is increasing rapidly year-on-year, with cases having increased to 6.2. million between 1990 and 2015, representing an 118% increase (Dorsey et al., 2018). Cases are expected to continue rising exponentially, so that it is estimated by 2040 there will be over 12 million cases of PD worldwide (Dorsey et al., 2018) and it is currently estimated that 1-2% of people over 60 have

PD (Mishra et al., 2018). There is a bias towards males for risk of developing PD, with approximately 1.5 times more males having the disease compare to females (Wooten et al., 2004). It is thought that dopaminergic neurons in females are less vulnerable due to differential expression of key genes such as D1 and D2 receptors, while males have increased expression of genes associated with pathological mechanisms in PD such as α-syn (Cerri et al., 2019). Furthermore, the natural hormonal differences between males and females is thought to contribute to reduced incidence in females due to the anti-inflammatory effects of oestrogen. Furthermore, it is also thought that females have better energy capacities within their neurons compared to males, contributing to higher functional capacity and reduced oxidative stress (Cerri et al., 2019). However, interestingly, an increased prevalence of leucine-rich repeat kinase 2 (LRRK2)-associated PD has been demonstrated in females, in particular, the G2019S mutation (W. Chen et al., 2020). While the increase in PD cases worldwide is commonly attributed to the increasing survival into old age, there are of course a number of other factors involved, including, sex, socioeconomic status, race, ethnicity, geographical location and numerous others (for review see; Ben-Shlomo et al., 2024). Countries with high socio-demographic index continue to have high rates of PD, however those countries with a mid-level socio-demographic index demonstrating increasing rates of prevalence (Collaborators, 2018). While it is not fully known, there are a number of potential contributing factors to the increased rates of PD in certain geographical locations. It is thought that increased environmental exposure to compounds such as pesticides in countries which are developing rapidly may contribute to increased PD. Interestingly, reduced smoking in a country, is associated with increased incidence of PD. Other factors such as increased access to health care and thus living longer into old-age may also be contributing to the increased PD cases in certain countries (Collaborators, 2018).

1.4. Parkinson's associated genetics

While the majority of PD cases are sporadic in origin, there remains a large number of genes that infer increased risk (Table 1.1.1.; Bandres-Ciga et al., 2020; Blauwendraat et al., 2020; Dulski et al., 2022; Klein & Westenberger, 2012; Yang et al., 2019). Those genetic mutations that are autosomal dominant in nature include the α-syn (SNCA) mutation, as well as the LRRK2 and vacuolar protein sorting 35 (VPS35) mutations. In 1997, the SNCA mutation was first discovered and associated with PD (Polymeropoulos et al., 1997). SNCA encodes for α-syn, which is important in soluble N-ethylmaleimide-sensitive fusion protein attachment protein receptors (SNARE) complex formation and vesicle trafficking (Emamzadeh, 2016). Another major PD-associated genetic mutation is that of LRRK2, which encodes the LRRK2 protein. Involvement of LRRK2 was first discovered in 2004, this protein is involved in autophagy, vesicular transport and the cytoskeleton, it is known to have important kinase and GTPase functions also (Paisan-Ruiz et al., 2004; Zimprich et al., 2004). LRRK2 was demonstrated to be the most common PD associated genetic mutation in the Japanese population, while interestingly it is rare in the Irish population (Funayama et al., 2023; Olszewska et al., 2020). More recently, in 2011, the VPS35 gene mutation was discovered thanks to exome sequencing. VPS35 affects intracellular processes of trafficking between the endosome and Golgi apparatus, it also impedes the recycling of proteins from the cell membrane (Vilarino-Guell et al., 2011). Autosomal recessive genetic mutations include PTEN-induced putative kinase 1 (PINK1), which is associated with mitochondrial function and is closely linked to Parkin, another genetic mutation associated with PD. PINK1 and Parkin work together to get rid of damaged or dysfunctional mitochondria (Ge et al., 2020). DJ-1 mutations are another autosomal recessive mutation, the protein of which is important in sensing oxidative stress and aiding in proper protein folding (Bonifati et al., 2003; Dolgacheva et al., 2019). The glucocerebrosidase (GBA) mutation is a sometimes forgotten about mutation due

to being missed initially in genome-wide association studies (GWAS) studies and its lack of complete penetrance (Huh et al., 2023). GBA mutations affect the glycolipid metabolism enzyme, β-glucocerebrosidase (Huh et al., 2023). The Irish population were demonstrated to have a relatively high proportion of GBA mutation associated PD cases comparatively to the rest of Europe (Olszewska et al., 2020). New genetic mutations associated with increased risk of PD are continuously being discovered, in large part thanks to the increasing GWAS being undertaken, however, many of these genes still remain to be validated (Table 1.1.1.; Bandres-Ciga et al., 2020; Blauwendraat et al., 2020; Dulski et al., 2022; Klein & Westenberger, 2012; Yang et al., 2019).

Table 1.1.1. **Proposed** ***Parkinson's associated genetic mutations***

Gene	***Protein***	***Function***	***Inheritance***
SNCA	α-syn	Vesicle Trafficking, SNARE formation	Autosomal dominant
PRKN	Parkin	Removal of dysfunctional mitochondria (works with PINK1)	Autosomal recessive
UCHL1	UCHL1	Ubiquitination	Autosomal dominant
PINK1	PINK1	Removal of dysfunctional mitochondria (works with Parkin)	Autosomal recessive
DJ-1	DJ-1	Senses oxidative stress, aids in protein folding	Autosomal recessive
LRRK2	LRRK2	Autophagy, cytoskeleton, vesicular transport, GTPase and kinase functions	Autosomal dominant
VPS35	VPS35	Membrane protein recycling and intracellular trafficking	Autosomal dominant
GBA	Glucocerebrosidase	Glycolipid metabolism	Autosomal dominant/

			Incomplete penetrance
HTRA2	HTRA2	Pro-apoptotic serine protease	Autosomal dominant
ATP13A2	ATP13A2	Lysosomal K^+/H^+ ATPase	Autosomal recessive
FBXO7	FBXO7	E3 ligase, proteosome, mitochondrial clearance, cell cycle regulation	Autosomal recessive
GIGYF2	GIGYF2	Vesicle transport, IGF-1 signalling	Autosomal dominant
PLA2G6	iPLA2β/PLA2G6	Trafficking between Golgi and ER, phospholipid metabolism	Autosomal recessive
EIF4G1	EIF4G1	EIF4F complex, protein synthesis	Autosomal dominant
DNAJC6	Auxilin	Clathrin-mediated endocytosis	Autosomal recessive
DNAJC13	DNAJC13	Endosomal trafficking, interacts with HSPA8	Autosomal dominant
CHCHD2	CHCHD2	Oxidative phosphorylation, inhibition of apoptosis	Autosomal dominant
VPS13C	VPS13C	Interacts with PINK1/Parkin to maintain mitochondrial homeostasis	Autosomal recessive
PSAP	Prosaposin	Intracellular lysosomal functions, secreted neurotrophic effects	Autosomal dominant
LRP10	LRP10	Endosomal protein involved in trans-Golgi trafficking	Autosomal dominant
TREM230	TREM230	Retromer trafficking, secretory autophagy, Golgi vesicle secretion	Autosomal dominant
SYNJ1	Synaptojanin 1	Synaptic and endosomal trafficking, autophagy	Autosomal recessive
POLG	DNA polymerase gamma	Maintaining mitochondrial DNA	Autosomal dominant

SMPD1	Acid sphingomyelinase	Sphingolipid metabolism	Autosomal recessive
NUS1	Nogo-B receptor	Cholesterol trafficking, protein glycosylation	Autosomal dominant
ARSA	Arylsulfatase A	Lysosomal enzyme, hydrolyses sulfatides	Autosomal recessive
BST1	CD157	Calcium homeostasis, innate immune functions	Autosomal dominant
SLC44A1	Choline transporter-like 1	Choline/H^+ antiporter	Autosomal recessive
ADRA2A	Adrenoreceptor α2A	Inhibition of cAMP, regulates norepinephrine release	Autosomal recessive
GCH1	GTP cyclohydrolase 1	Production of BH4 which helps produce dopamine	Autosomal dominant
MAPT	Tau	Stabilises microtubules	Autosomal dominant
TH	Tyrosine hydroxylase	Production of dopamine	Autosomal recessive
L2HGDH	L-2-hydroxyglutarate dehydrogenase	Production of α-ketoglutarate	Autosomal recessive
SLC30A10	SLC30A10	Manganese efflux transporter	Autosomal recessive
ATP10B	ATP10B	Endo-lysosomal lipid flippase	Autosomal recessive
DCTN1	DCTN1	Largest subunit of dynactin complex, important for dynein, which are cytoskeletal motor protein	Autosomal dominant
CSMD1	CSMD1	Inhibits complement cascade, immune suppressive	Autosomal recessive
WASL	Neural Wiskott-Aldrich syndrome protein	Regulates polymerisation of actin filaments	Autosomal recessive

1.5. Alpha synuclein; a misfolded menace

α-syn is crucial to the pathogenesis of PD. As mentioned above, mutations in α-syn were the first attributed risk to developing PD. Furthermore, α-syn was demonstrated to be present in identified pathological hallmarks, now coined as Lewy bodies. α-syn is a small 14kDa protein, of 140 amino acids, composed of an N-terminal, a non-amyloid β central region (NAC) and an acidic C-terminal (Emamzadeh, 2016). The N-terminal tends towards an α-helix formation and is important in helping the protein interact with lipids and membranes. The NAC region is hydrophobic and tends to aggregate. The C-terminal tail region is needed for the role α-syn plays as a chaperone protein and in calcium binding (Calabresi et al., 2023). α-syn exists endogenously as monomers and tetramers, usually dependant on location and function (Calabresi et al., 2023).

While the extent of all the roles α-syn plays remains to be fully elucidated, it is a key protein for the homeostatic maintenance of the brain. α-syn is important in regulating many processes that if dysregulated contribute to PD. It is important at regulating dopamine production in neurons, it down-regulates tyrosine hydroxylase (TH) production, thus preventing dopamine overproduction, which reduces harmful oxidative stress (Emamzadeh, 2016). However, complete removal of α-syn is demonstrated to reduce striatal dopamine (Abeliovich et al., 2000). Another way α-syn reduces oxidative stress is through its insertion in lipid membranes. Monomeric forms of α-syn have been demonstrated to aid in prevention of lipid oxidation using this method (Emamzadeh, 2016). α-syn also works to suppress apoptosis, through inhibition of the c-Jun N-terminal kinase (JNK) pathway, caspase activation and reduction of protein kinase C (Emamzadeh, 2016). This protein also plays an important role in the formation of the SNARE complex in the pre-synaptic neuronal terminal and is key to neurotransmitter vesicle trafficking (Calabresi et al., 2023).

Considering its many important functions it is not hard to believe that a mutation of this protein is associated with such a debilitating disease. In PD α-syn is observed to accumulate in cells and indeed α-syn overexpression is utilised as a model to study this disease (Emamzadeh, 2016). In PD α-syn tends towards a β-sheet conformation which attracts monomers, eventually forming oligomers and finally fibrils (Calabresi et al., 2023). It is these aggregates of α-syn that are deposited intracellularly and commonly known as Lewy bodies and neurites (Calabresi et al., 2023). α-syn phosphorylation plays a large role in its aggregation, in particular phosphorylation at the serine 129 residue (Parra-Rivas et al., 2023). Neurons have even been demonstrated to transfer their α-syn to astrocytes in an attempt to clear the protein, while aggregation of α-syn has also been demonstrated to induce microgliosis, contributing to an inflammatory environment in PD (Long et al., 2022; Loria et al., 2017). Interestingly, recent studies have demonstrated α-syn specific T cells in the periphery of PD patients, as well as α-syn being suggested as a potential trigger for immune infiltration from the periphery. A recent study has provided further information to back up this theory. McFleder and colleagues demonstrated using an A53T mouse model of PD that CD11c+, microglial-like cells traffic α-syn to the ileum (McFleder et al., 2023).

Furthermore, there are numerous hypotheses attempting to describe the origin and spread of PD that are linked to α-syn. As mentioned previously, Braak and colleagues proposed a staging system that takes into account pathological spread of α-syn throughout the brain. Braak and colleagues proposed that PD originated from an unknown pathogen entering the body through the gut and travelling to the brain via the vagus nerve (Braak, Rub, et al., 2003). This hypothesis stimulated much discussion and subsequent research, after which a dual-hit hypothesis was proposed (Hawkes et al., 2007). This hypothesis described a disease causing pathogen entering

the brain via the nasal cavity and simultaneously, the vagus nerve via the gut. However, a recent study examining post-mortem PD cases has added evidence suggesting that this is not the case (Borghammer et al., 2022). Another hypothesis for α-syn pathogenesis in PD is the brain-first, body-first approach. This theory implies that α-syn accumulation begins in either the olfactory bulb, brain-first, or the enteric nervous system, body-first. The α-syn is then proposed to spread through the vagus nerve intro the central nervous system (CNS) for body-first pathology. Recently a new model, the α-syn origin site and connectome (SOC) model, was proposed which builds upon this brain-first/body-first hypothesis. This model acknowledges other contributing factors to disease pathogenesis such as inflammation, genetics, mitochondrial dysfunction among others, while also providing mechanisms to explain variation in presentation of disease and pathology spread (Borghammer, 2021). While, these hypothesis provide interesting points for consideration, it is difficult to know which is most accurate until we have a better understanding of the disease as a whole.

1.6. Degeneration of the midbrain

Accompanying the accumulation of α-syn, is the degeneration of dopaminergic neurons in the midbrain. The loss of these cells and their secretion of dopamine is the basis for the symptoms of PD, with motor symptoms becoming apparent after loss of up to 80% of these neurons (Masato et al., 2019). Dopaminergic neurons are distributed throughout the brain, however, it is the A9 dopaminergic neurons of the SNpc that are selectively vulnerable in PD (Kamath et al., 2022). Catecholamine producing neurons within the brain have been divided into subclasses of nuclei referred to as A1-17 and C1-3. This system divides catecholamine producing neurons based on anatomical location, and the neurotransmitter produced, this system allows for comparison across species (Bjorklund & Dunnett, 2007). The subclasses of relevance to us are the three nuclei responsible for making up the midbrain. These include the

A8, retrorubal, the A9, SN, and the A10 ventral tegmental area (VTA) (Damier et al., 1999). Preceding these nuclei are the A1-A7 noradrenergic nuclei of the brainstem (Gok-Yurtseven et al., 2019), and directly after are the A11 dopamine producing nuclei, which project downwards through the spinal cord and are thought to be important for migraine pathogenesis (C. Li et al., 2023). The A8-A10 dopaminergic neurons from the midbrain project towards the striatum, limbic region and cortex forming the mesostriatal, mesolimbic and mesocortical pathways respectively (German & Manaye, 1993). The A10 dopaminergic neurons from the VTA project towards the ventral striatum, mainly the nucleus accumbens, an important component of the limbic system (Luo & Huang, 2016; Ziolkowska, 2021). Thus these neurons form part of the mesolimbic pathway and are important in reward behaviour and response to aversive stimuli (Ziolkowska, 2021). The A9 SN dopaminergic neurons project towards the dorsal striatum, forming the well-known nigrostriatal pathway. These neurons are important in regulating voluntary movement, thus it is no surprise that their degeneration produces the motor symptoms associated with PD (Luo & Huang, 2016).

The SN itself has been further subdivided into the *pars compacta*, *pars reticulata* and the lesser discussed region of the *pars lateralis* (Bentivoglio & Morelli, 2005; Fuxe et al., 2006). The SN was first discovered in 1786 by Félix Vicq d'Azyr, despite for many years it being named Sommering's spot due to his description of the structure a number of years later (Bentivoglio & Morelli, 2005). Vicq d-Azyr described the neuromelanin-pigmented area as '*locus niger crurum cerebri'* meaning dark region of cerebral peduncles (d'Azyr, 1786). It is the loss of this neuromelanin-pigmented area that makes degeneration of the SNpc so apparent. Neuromelanin has been suggested as a potential contributing factor to the selective vulnerability of these midbrain dopaminergic neurons. Neuromelanin is demonstrated to contribute to the toxic effects of MPP+, as it binds to the toxin, helping it remain within the neurons while it exerts its toxic effects (D'Amato et al., 1987). Furthermore, a recent study utilised adenoviral

overexpression of human tyrosine to induce neuromelanin accumulation, similar to that observed with aging. This resulted in Lewy body pathology, inflammatory activation and loss of dopaminergic neurons, resulting in depigmentation of the SNpc (Chocarro et al., 2023). These data further contributes to a link between neuromelanin and selective vulnerability in PD. While it is widely accepted that it is dopaminergic neurons of the SNpc that are selectively vulnerable in PD, a recent study uncovered that within this population there are different levels of vulnerability (Kamath et al., 2022). Kamath and colleagues aimed to investigate why certain dopamine neurons are lost in early disease, while others remain present late into pathogenesis. Using post-mortem brain tissue and RNA-sequencing, this study identified a SOX6_AGTR1 subpopulation that was located ventrally within the SNpc and was selectively vulnerable in PD (Kamath et al., 2022). This study provides novel insights into the selective vulnerability of these neurons in PD and the potential for identifying new therapeutic targets.

1.7. Dopamine and its actions

The above mentioned A9 dopaminergic neurons of course produce and release dopamine, the main neurotransmitter associated with PD. Dopamine is produced by tyrosine, which is converted to L-dopa the dopamine precursor and is the current gold standard therapeutic for PD. TH is the enzyme responsible for this conversion and is the rate limiting step in the production of dopamine. L-dopa is then finally converted to dopamine with the help of an aromatic amino acid decarboxylase (Elsworth & Roth, 1997; Juarez Olguin et al., 2016). Dopamine also acts as a precursor compound to the production of other catecholaminergic neurotransmitters, noradrenaline and adrenaline (Juarez Olguin et al., 2016), highlighting the importance of this compound across the brain and how it's loss can have wide-reaching implications. Dopamine exerts its effects through a number of dopamine receptors. These

receptors are divided into D1-like, D1 and D5 receptors and D2-like receptors, D2, D3 and D4 receptors (Mishra et al., 2018). D1-like receptors increase adenylate cyclase activity, whereas D2-like receptors inhibit this activity. Dopamine receptor agonists are currently used as a therapeutic for PD, with a bias for activation of the D2-like receptor family, which has been demonstrated to delay the use of L-Dopa (Isaacson et al., 2023; Mishra et al., 2018).

1.8. Neuroinflammation in Parkinson's disease

While α-syn accumulation and degeneration of dopaminergic neurons have long since been established as pathological hallmarks of PD, in recent years mounting evidence demonstrates the contribution of the immune system to PD pathogenesis (MacMahon Copas et al., 2021). Glial cells, which are present at a 1:1 ratio with neurons in the brain, are crucial to the CNS immune response (Azevedo et al., 2009). Within the CNS, microglia, are the resident immune cell. Their primary functions revolve around the surveillance of the environment for pathogens and the subsequent removal of said pathogens, should they arise (Qin et al., 2023). Microglia have been demonstrated to induce a reactive astrocyte phenotype through the release of pro-inflammatory cytokines (Liddelow & Barres, 2017). While the immune-related process of microglial activation, microgliosis, has been long established in PD (McGeer et al., 1988), astrocyte reactivity, also known as astrogliosis, is a newer phenomenon (Mohamed et al., 2022).

1.8.1. Astrocytes; the homeostatic regulators of the CNS

It was Michael von Lenhossek in the 1890's who first coined the term Astrocyte, naming the cells after its star-lie shape (Mv, 1895). Astrocytes are widely established as the major homeostatic regulators of the CNS. These cells have a plethora of functions including,

maintenance of the blood brain barrier (BBB), regulation of blood-flow, as well as buffering the extracellular environment (Fig. 1.1.2.). The BBB consists of endothelial cells, pericytes and astrocytic end feet which form the barrier checkpoint for materials entering and leaving the CNS. It is thought that astrocytes contribute to BBB control through release of trophic factors such as vascular endothelial growth factor (VEGF), brain-derived neurotrophic factor (BDNF) and fibroblast growth factor 2 (FGF2) (Cabezas et al., 2014). Their homeostatic regulation of potassium and water balance at the BBB is also achieved through their aquaporin 4 channel and inward-rectifying potassium 4.1 channels (Alvarez et al., 2013). Astrocytes have also been found to play an important role in regulating cerebral blood flow through their secretion of prostaglandins (PGE), epoxyeicosatrienoic acids (EET), arachidonic acids (AA) and potassium (MacVicar & Newman, 2015). These cells also form part of the tripartite synapse, alongside pre- and post-synaptic neuron terminals, aiding in regulation of neurotransmission. Astrocytes have important roles in the uptake of neurotransmitters from the extracellular space. Glutamate is a major excitatory neurotransmitter and poor clearance of glutamate from the synapse can lead to overstimulation of neurons and eventual excitotoxicity (Gwag et al., 1995). Astrocyte to astrocyte communication and transport networks are key to them carrying out their functions. The astrocyte specific connexin, connexin 43 (CX43), helps form gap junctions between astrocytes, through which they can communicate and transport molecules (Dong et al., 2022). Astrocytes use this networking system to activate neighbouring astrocytes via calcium signalling, helping to maintain homeostasis (De Bock et al., 2014). Another way that astrocytes aid in neuronal function and survival is through the astrocyte-neuron lactate shuttle (Bhatti & Frostig, 2023). It is demonstrated that while neurons utilise glucose, at times of high energy requirement or lack of glucose, neurons switch their metabolism to utilise lactate (Bhatti & Frostig, 2023). Astrocytes are known for their preference of glycolysis rather than oxidative phosphorylation, and have been demonstrated to uptake glucose from the blood more readily

than neurons (Barros & Weber, 2018; Bhatti & Frostig, 2023). Astrocytes produce lactate from glucose and can store and provide this to neurons in times of high demand or stress (Barros & Weber, 2018; Bhatti & Frostig, 2023). Fig. 1.1.2. below summaries some of the main homeostatic functions of the astrocytes within the CNS.

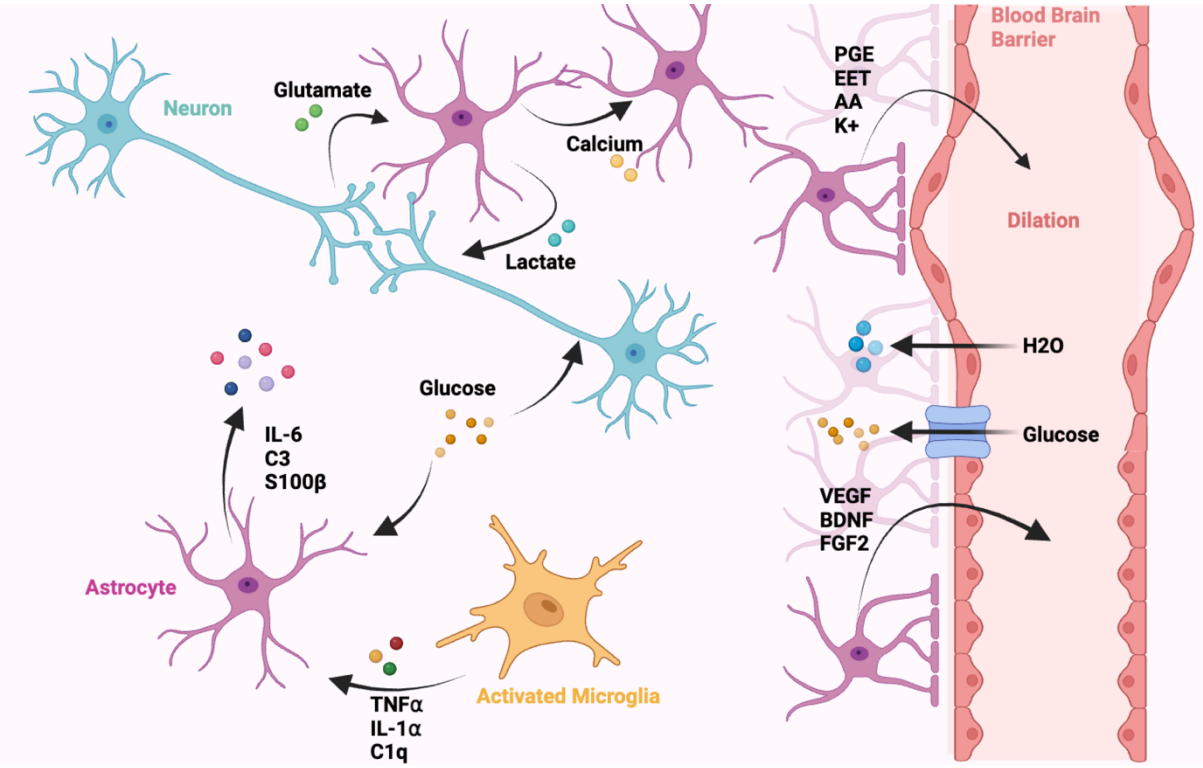

Figure 1.1.2. Astrocytes are key homeostatic regulators of the CNS.

Astrocytes have numerous functions within the CNS. Astrocytes form part of the tripartite synapse with pre- and post-synaptic neurons. They uptake neurotransmitters such as glutamate from the extracellular space, preventing excitotoxicity. Astrocytes signal to one another via calcium transport between cells. In times of increased energy demand astrocytes provide lactate as an energy source to neurons. Astrocytes play important parts in generating and

maintaining the BBB, as well as blood flow. In times of infection, astrocytes can become reactive producing inflammatory cytokines in response to microglial stimulation. Figure generated with biorender.

1.8.2. Astrogliosis; harmful or helpful

Astrogliosis, is the process by which astrocytes take on a reactive phenotype consistent with release of inflammatory cytokines and chemokines (Liddelow & Barres, 2017; Mohamed et al., 2022). While astrogliosis is considered more of an immune related process, fighting pathogens is crucial to restoring brain homeostasis therefore it is not unsurprising that astrocytes are keen to get involved (Fig. 1.1.2.). These reactive astrocytes can be both pro- and anti-inflammatory in nature and contribute to the immune response within the CNS (Liddelow & Barres, 2017). Originally, reactive astrocytes were split into A1 and A2 subcategories, delineating a pro- and anti-inflammatory phenotype respectively (Escartin et al., 2021). However, recently the field has moved away from this constricting nomenclature due to the heterogeneity of astrocytic responses to stimuli (Escartin et al., 2021). Reactive astrocytes can be induced by microglia through their secretion of inflammatory cytokines such as tumour necrosis factor alpha (TNFα), interleukin-1 alpha (IL-1α) and complement component 1q (C1q) demonstrated by Liddelow and colleagues in 2017 (Liddelow et al., 2017). Liddelow and colleagues also demonstrated the presence of pro-inflammatory reactive astrocytes in the post-mortem brain tissue of PD patients, identified by the marker, complement component 3 (C3). C3 is a component of the complement cascade and it's expression in astrocytes, is associated with a pro-inflammatory phenotype (Liddelow et al., 2017). While pro-inflammatory astrocytes have been linked to neurodegenerative disease, anti-inflammatory astrocytes have also been associated with neurological cases, such as ischaemia (Liddelow et al., 2017). The process of mounting an immune response to damage or disease, is of course

normal and necessary, however in the case of PD, this immune response may become aberrant (Wang et al., 2021). Reactive astrocytes, have been observed to fail in carrying out their necessary homeostatic roles (Wang et al., 2021). PD derived iPSC-astrocytes from individuals with the LRRK2 mutation demonstrated a failed ability to form a functional BBB in a 3-D BBB-on-a-chip model (de Rus Jacquet et al., 2023). This group established that it is likely to be due to the activation of MEK1/2 signalling, as its inhibition attenuated the effects observed (de Rus Jacquet et al., 2023). For instance, reactive astrocytes fail to monitor the BBB correctly, contributing to a leaky barrier which allows infiltration of unwanted substances from the periphery. Similarly, reactive astrocytes demonstrate poor regulation of glutamate homeostasis among other things, which contributes to dysfunction of cellular processes (Yang et al., 2024).

Astrocytes have recently been described as potential antigen presenting cells, expressing the co-stimulatory molecules required for activation of $CD4^+$ T cells, CD80, CD86 and CD40 (Rostami et al., 2020). They have also recently been illustrated to have immune memory (Fig. 1.1.3.; Lee et al., 2024). Lee and colleagues exposed astrocytes to an initial pro-inflammatory stimulus of TNFα and interleukin 1 beta (IL-1β). A reactive phenotype was triggered, after which astrocytes returned to baseline. When presented with a second bout of the same stimulus, a more robust inflammatory response was observed. Indicating that the astrocytes maintained memory of the initial stimulus, and were 'primed' for the second insult (Lee et al., 2024). The group linked this memory induced response to epigenetic changes within the astrocytes following the initial stimulus. This follows the known memory route the peripheral immune system implements. This has interesting connotations for neurological disease, if the cells remember stimuli, it provides evidence to back up theories in which it is thought that early life infection may increase risk of developing neurological disease later in life (Lee et al., 2024). Astrocytes expressing adhesion molecule intracellular adhesion molecule 1 (ICAM-1) have

been co-localised to lymphocyte function antigen 1 (LFA-1) expressing macrophages and microglia in post-mortem brain tissue of PD patients (Brochard et al., 2009). Together these data indicates a role for astrocytes in co-ordination and propagation of immune cell responses, both peripheral and central (Fig. 1.1.3).

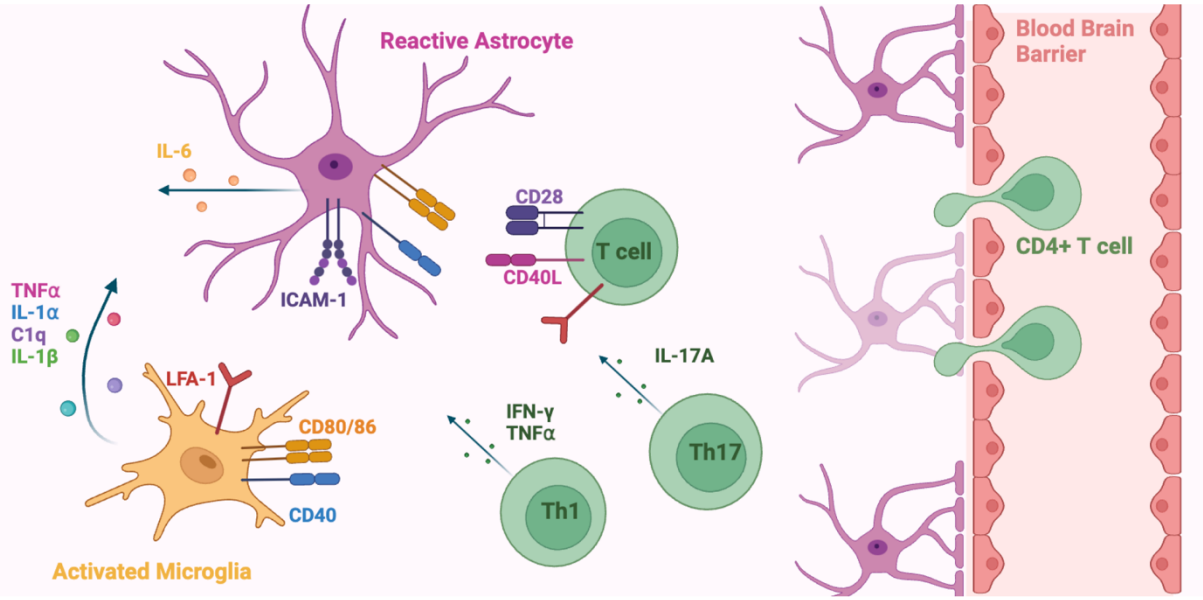

Figure 1.1.3. Potential interactions between astrocytes, microglia and T lymphocytes in Parkinson's disease.

It had been demonstrated that peripheral CD4$^+$ T cells enter the brain, aided by the leaky BBB present in PD. Once present these T cells secrete pro-inflammatory cytokines such as TNFα, interferon gamma (IFN-γ) and interleukin 17 A (IL-17A). Astrocytes have recently been demonstrated to express T cell co-stimulatory molecules CD80/86 and CD40 in response to α-syn. LFA-1 expressing microglia and leukocytes have been observed co-localised to ICAM-1 expressing astrocytes. Activated microglia release pro-inflammatory cytokines which are capable of inducing a robust pro-inflammatory astrocyte. Figure generated with biorender.

1.8.3. The peripheral immune system; a novel contender?

The peripheral immune system can be split into two arms; the innate and the adaptive. The innate immune system is the body's first line of defence, it consists of various cellular and humoral responses. The innate immune system also acts as first responders eliminating pathogens and sending out a call for help to other immune cells which have more specialised skill sets, i.e. the adaptive immune system (Marshall et al., 2018). The adaptive immune system takes a bit longer to boot into action but it is the more specified response and consists of B and T lymphocytes which can use the memory of pathogen to mount a targeted response (Marshall et al., 2018). Naïve T cells differentiate into either $CD4^+$ or $CD8^+$ T cells based on the recognition of their antigen presented to them via major histocompatibility complex (MHC) molecules on the surface of antigen presenting cells (Pennock et al., 2013). MHC1 will bind $CD8^+$ T cells, while MHCII will bind $CD4^+$ T cells (Fig. 1.1.4.). Differentiated effector T cells have specialised functions that are tailored to the specific infection taking place. $CD4^+$ T cells differentiate into multiple subsets, the main ones being; T helper (Th) 1, Th2 and Th17 cells (Fig. 1.1.5.; Pennock et al., 2013). IFNγ and IL-12 activate the T-bet transcription factor, which is what induces differentiation of $CD4^+$ T cells into a Th1 cells. These Th1 cells secrete IFNγ and TNFα mainly, and are critical in the phagocytosis of pathogens and activation of B cells (Pennock et al., 2013). Th2 cells are generated from the activation of the GATA-binding protein 3 (GATA3) transcription factors by IL-4. Th2 cells secrete IL-4, IL-5 and IL-13 mainly. Th2 cells are largely considered to have more anti-inflammatory tendencies. Transforming growth factor beta (TGFβ), IL-6, IL-1 and IL-23 can stimulate differentiation of Th17 cells through activation of the Th17 cell transcription factor, RAR-related orphan receptor gamma (RORγt; Pennock et al., 2013). Th17 cells are largely associated with their secretion of the IL-17 cytokine. Stimulation of transcription factors forkhead box P3 (FOXP3) by TGFβ induces differentiation of T regulatory cells (T regs). T regs secrete IL-10 and TGFβ, which are known

for their anti-inflammatory actions (Fig.1.1.5.). $CD8^+$ T cells produced cytotoxic T lymphocytes which are crucial mediator of apoptosis in targeted cells, without disturbing the nearby healthy tissues (Pennock et al., 2013). Naïve B cells are stimulated to differentiate into plasma cells once they have bound to their antigen and in response to T cell cytokines. These plasma cells produce and secrete antibodies which are antigen specific and aid in phagocytosis of pathogens (Pennock et al., 2013).

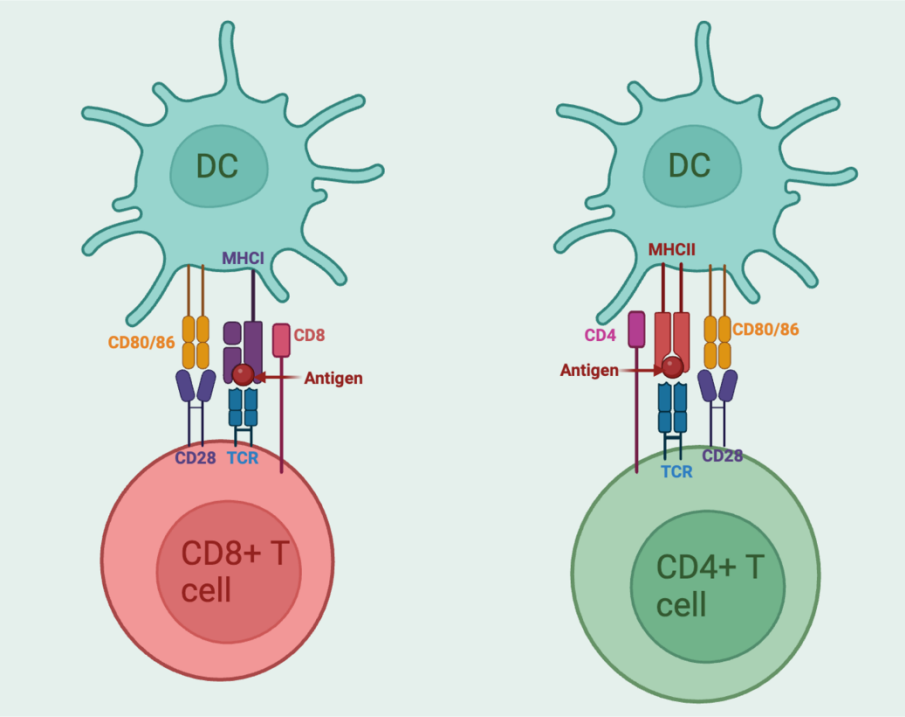

Figure 1.1.4. MHC class presentation to $CD8^+$ and $CD4^+$ T cells.

Antigen presenting cells, such as dendritic cells (DC), process antigens and present them on their surface via MHC complexes. MHC1 is recognised by $CD8^+$ T cells and MHCII by $CD4^+$ T cells via their T cell receptor (TCR). Co-stimulatory molecules CD80/86 on the DC are also required to bind their counterpart CD28 on the T cell. Figure generated with Biorender

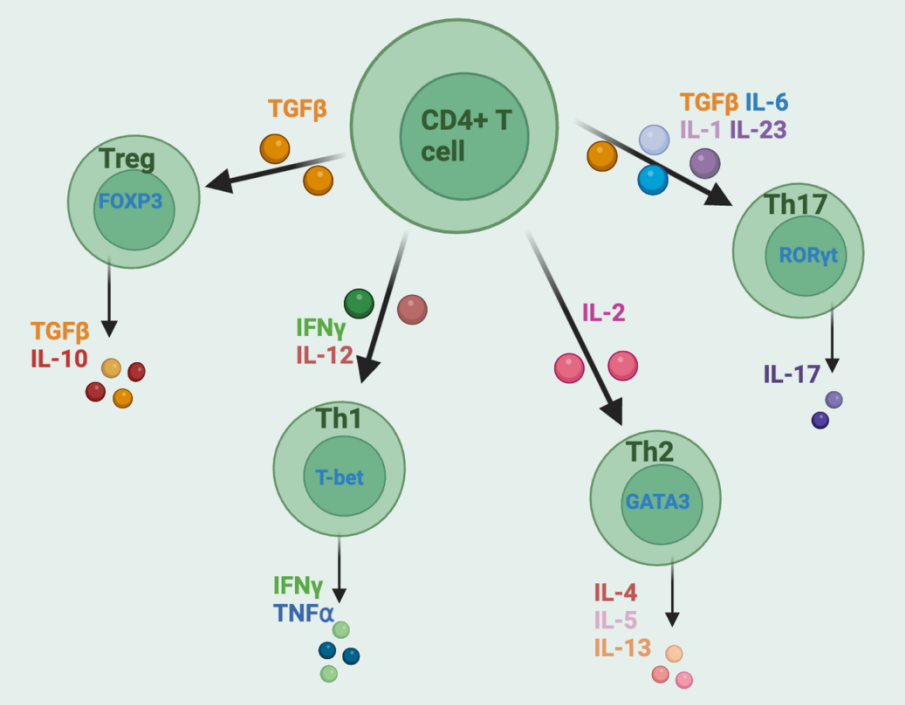

Figure 1.1.5. Differentiation of CD4⁺ T cell subtypes.

CD4⁺ T cells will differentiate into different subtypes dependent on the cytokine they are exposed to and the transcription factor activated, e.g. TGFβ and FOXP3 activation produces Tregs which produce TGFβ and IL-10. Figure generated with biorender.

Whilst the immune system is an extremely complex and effective system at dealing with the broad range of pathogens we are exposed to daily, it has also been known to contribute to disease when it produces an uninhibited chronic inflammatory response, or indeed response to self-antigens producing autoimmune disease. The brain has previously been considered an immune privileged organ, whilst in the last number of years, there has been increasing evidence to support the presence of peripheral immune cells in the brain in PD (Gray & Woulfe, 2015; Liu et al., 2019). Brochard and colleagues identified $CD4^+$ and $CD8^+$ T cells in the post-mortem brain tissues of PD patients (Brochard et al., 2009). This has also been corroborated in animal models of the disease (Brochard et al., 2009; Liu et al., 2017). BBB disruption has been observed in multiple studies of PD and is thought to contribute to the infiltration of these cells

into the brain (Gray & Woulfe, 2015; Liu et al., 2017; Liu et al., 2019). Peripheral immune cells have been observed localised to the SN itself, which is the key area of pathology in PD (Liu et al., 2017; Liu et al., 2019). The presence of these cells has been demonstrated to induce degeneration of neurons, and increased cytokine production. Brochard and colleagues also demonstrated that it appeared to be $CD4^+$ T cells specifically that are contributing to these pathological symptoms (Brochard et al., 2009). Whilst Sommer and colleagues demonstrated that the $CD4^+$ Th17 cells induced dopaminergic neuron degeneration (Sommer et al., 2018). Taken together these data highlights a potential role for peripheral immune cells in PD pathogenesis (Fig. 1.1.3.).

1.9. Modelling PD with induced pluripotent stem cells

Induced pluripotent stem cells (iPSC) are generated from somatic cells which have been reprogrammed back to a pluripotent state (Hochedlinger & Jaenisch, 2015). Pluripotency is a desirable feature as it means the cells have the capability of differentiating into, in theory, any cell type of the human body (Hochedlinger & Jaenisch, 2015). The generation of iPSC was first described by Yamanaka and colleagues in 2006, when they managed to induce pluripotency in mouse embryonic fibroblasts (MEFs; Takahashi & Yamanaka, 2006). Following extensive analysis of 24 different genes that might infer pluripotency, the group was able to narrow the list down to 4 necessary factors. These four factors; Octamer binding transcription factor (Oct3/4), SRY-box 2 (Sox2), cellular Myc (c-Myc) and Krüppel-like factor 4 (Klf4), have since been coined the 'Yamanaka factors' (Karami et al., 2022; Liu et al., 2020). The group established that using retroviral infection, the forced expression of these four genes was sufficient to induce the cells back to a pluripotent state (Takahashi & Yamanaka, 2006). The cells generated exhibited similar morphology to embryonic stem cells (ESC), in that they demonstrated a scant cytoplasm, large nucleoli and were round in shape with defined borders,

expressed a similar gene profile and demonstrated the ability to form teratomas consisting of cells of all three germ layers (Takahashi & Yamanaka, 2006). Concluding that these cells were truly pluripotent and behaved similarly to ESC, they proceeded to attempt the same reprogramming using human dermal fibroblasts (HDF) which, similarly, successfully reprogrammed into iPSC using this technique (Yamanaka, 2007). This novel approach to generating stem cells was so ground-breaking that Yamanaka was jointly awarded the Nobel Prize in Physiology or Medicine in 2012, a mere number of years after the discovery.

1.9.1. Evolution of the Yamanaka protocol

The protocol for generation of iPSC described by Yamanaka and colleagues was the first of its kind, however, naturally it had some aspects that could be improved upon (Takahashi et al., 2007; Takahashi & Yamanaka, 2006; Yamanaka, 2007). Two main aspects of the protocol have been targeted for updating; (i) the genetic material being delivered, and (ii) how it is delivered.

1.9.1.1. Genetic material

Numerous studies have since investigated the Yamanaka factors; Oct3/4, Sox2, Klf-4 and c-Myc. Yamanaka and colleagues have outlined that Oct3/4 and Sox2 are core pluripotency associated genes and are necessary for the generation of iPSC (Takahashi et al., 2007; Takahashi & Yamanaka, 2006). However, in their initial studies they were unable to produce ESC-like iPSC without the addition of Klf-4 and c-Myc (Takahashi & Yamanaka, 2006). It is believed that the addition of these two genes allows for the modification of chromatin structure to allow the 'core' pluripotency genes to bind to their target sites (Takahashi & Yamanaka, 2006). Klf-4 also acts as a suppressor of p53. p53 is demonstrated to inhibit Nanog, which is an established pluripotency-related factor, therefore Klf-4 may act to promote Nanog signalling through p53 suppression (Takahashi et al., 2007; Takahashi & Yamanaka, 2006). However, in

addition to the fact c-Myc is an oncogene, the discovery that c-Myc lead to differentiation and cell death in ESC prompted the iPSC community to quickly investigate alternative pluripotency gene combinations to facilitate the removal of this factor (Yu et al., 2007). Enter, Yu and colleagues, who were able to demonstrate that the combination of core pluripotency genes, Oct3/4 and Sox2 with Nanog and Lin28 replacing c-Myc and Klf-4 being sufficient to generate pluripotent cells (Yu et al., 2007). Lin28 represents a novel factor that was not in the original Yamanaka panel of 24 genes (Takahashi & Yamanaka, 2006). Nanog is a well-established factor in the maintenance of pluripotency so it's involvement here is no surprise (Yamanaka, 2007). Some alterations to this combination were made again when trying to move away from retroviral transfection of cells. The re-addition of Klf-4 and c-Myc was used to improve efficiency of reprogramming (Yu et al., 2009). In 2011, Okita and colleagues described an episomal plasmid vector-based reprogramming of HDF toward iPSC using the combination of Oct3/4, Sox2, Klf-4, Lin28, L-Myc and a p53 short hairpin ribonucleic acid (shRNA) (Okita et al., 2011). This protocol does not require the use of oncogenic c-Myc, and the episomal plasmid vectors are non-viral and non-integrating, providing an optimal protocol for generating clinically useable iPSC (Okita et al., 2011).

1.9.1.2. Methods of delivery

The second largest change to the original Yamanaka protocol has been the method of inserting the pluripotent gene cocktail into the cells. In the original study, retroviral transfection was used (Takahashi & Yamanaka, 2006). While this was highly effective at the time, it was always understood to be a roadblock when it came to the potential use of these cells therapeutically (Takahashi et al., 2007; Yamanaka, 2007). Since then, naturally, a variety of different methods have been assessed (Karami et al., 2022; Omole & Fakoya, 2018), both integrating and non-integrating. The main issue with retroviral transfection, is that it involves integration into the

host cells genome, and while the retroviral genes are usually silenced, there is a high probability of their reactivation, which presents issues if your goal is to transplant these cells into humans (Karami et al., 2022; Omole & Fakoya, 2018). The use of lentivirus transfection improved the reprogramming process compared to other retroviral vectors; however, it still carries with it the same set of issues as the above, including the inability to maintain pluripotency in the absence of external factors and insertional mutagenesis (Karami et al., 2022; Omole & Fakoya, 2018). While non-integrative viral approaches also exist such as the use of adenovirus or sendai virus, these processes have a very low reprogramming efficiency and involve a lot of work in the production of the viruses and the cleaning of the cells post-transfection (Karami et al., 2022; Omole & Fakoya, 2018). In terms of non-integrative, non-viral reprogramming methods, there are episomal plasmid vectors and delivery of messenger RNA (Karami et al., 2022; Omole & Fakoya, 2018). While the use of RNA gene delivery, provides a non-integrative approach, it does require frequent re-transfection and has been demonstrated to potentially trigger immune responses (Karami et al., 2022; Omole & Fakoya, 2018). The use of episomal plasmid vectors, currently present the best option for reprogramming the cells to be used in any clinical setting. Episomal plasmids allow the insertion of pluripotency genes into the target cell, where the episome can act independently from integrating into the host genome to produce expression of genes of interest (Karami et al., 2022; Omole & Fakoya, 2018; Van Craenenbroeck et al., 2000). In addition, the plasmid deoxyribonucleic acid (DNA) will eventually leave the cell, with cell proliferation, meaning that there is no fear of the process being reactivated in future, as is the case with viral transfections (Karami et al., 2022; Omole & Fakoya, 2018). Okita and colleagues in 2011 demonstrated the ability to produce iPSC using these episomal plasmid vectors with the pluripotency cocktail of Oct3/4, Sox2, Klf-4, Lin28 and p53 shRNA (Okita et al., 2011). Actual methods of inserting these episomal plasmid vectors differ also, there are both physical and chemical delivery methods (Okita et al., 2007; Okita et al., 2011). Physical

methods such as electroporation provide access to the cell for the plasmids by disrupting the membrane of the target cell through electrical impulses (Mulia et al., 2021). The chemical methods, taking Lipofectamine, for example, enables the formation of liposomes containing the genetic material, which can then enter the cell via endocytosis (Mulia et al., 2021). Physical methods are highly effective, however, produce greater amounts of cell death. While chemical methods are straightforward as can be added directly to media but are not as effective (Mulia et al., 2021).

1.10. What existed before this?

Prior to the discovery of iPSC, there were still a number of options for pluripotent stem cell generation. Initial studies to demonstrate reprogramming of terminally differentiated cells to a pluripotent state used nuclear transfer of genetic material into oocytes (Gurdon et al., 1971). This technology is what would enable the cloning of a whole sheep, widely known as Dolly the sheep (Wilmut et al., 1997). Between the initial success of this process and the production of Dolly the sheep, the first generation of ESC from mice occurred, these cells were demonstrated to be pluripotent and maintained their pluripotency long-term in culture *ex vivo* (Evans & Kaufman, 1981). Human ESC have also since been generated and are still widely used in research due to the well-characterised nature of the cells and their ability to be directed towards any cell type of interest (Thomson et al., 1998). While ESC are a highly reliable cell type for research, they do not come without drawbacks, the three largest concerns around the use of these cells is of course, that obtaining the cells, which are derived from the inner cell mass of the blastocyst stage embryo, results in destruction of the embryo (Okita et al., 2007; Omole & Fakoya, 2018). The second concern surrounding ESC is that they bring with them the risk of teratoma formation, which poses a great risk for their use as transplantation therapies. Studies have demonstrated the spontaneous formation of teratomas following

transplantation of ESC-derivatives into animal models (Cao et al., 2006; Chaudhry et al., 2009). In addition, if used for cell transplantation therapies, they bring with them the risk of immune complications due to not being derived from the same host (Okita et al., 2007; Omole & Fakoya, 2018). Unless derived from the specific patient, this same issue can apply to iPSC, however, certain groups have found ways to overcome these issues as best as is possible, such as human leukocyte antigen (HLA)-matching, and they have been brought forward for clinical trial, it is not ideal however, as immunosuppressants were still required (Yamanaka, 2020). The use of iPSC allows generation of cells which are person-specific and would hopefully negate this immune-rejection risk (Schweitzer et al., 2020). Confirming this point, Schweitzer and colleagues demonstrated in a single case-study, that the autologous transplant of iPSC-derived dopaminergic neural progenitor cells did not require immunosuppressants (Schweitzer et al., 2020). Other methods to generate pluripotent cells include the fusion of cells with ESC (Cowan et al., 2005; Miller & Ruddle, 1976; Tada et al., 2001; Yu et al., 2006) as well as spontaneous reprogramming with prolonged culture of cells (Jiang et al., 2002). Although these present similar disadvantages and iPSC remain the cell type of choice due to their ability to provide patient-specific therapeutic approaches. However, it is important to note that the cost of producing iPSC reduces the accessibility of these cell as therapeutics. The generation of a single iPSC line from tissue to cell line has been estimated to cost anywhere between 10,000-20,000 dollars (Bravery, 2015). This is also an extensively time-consuming process, taking upwards of 6 months to achieve, which simply adds to the cost generated. However, to then generate cGMP grade iPSC lines required for therapeutic intervention, the cost extends to approximately 800,000 dollars per line to account for the extensive testing (Bravery, 2015). However, continuing research in this area aims to improve efficiency and reduce the cost associated with the production of these cell lines so that they may be a more feasible therapeutic avenue in the future (Lin et al., 2019).

1.10.1. Post-mortem brain tissue

Post-mortem brain tissue was first used to study PD in the late 1950s (Carlsson, 1959; Ehringer & Hornykiewicz, 1960). Post-mortem tissue studies have aided in the identification of most PD associated hallmarks, including accumulations of α-syn aggregates as well as the degeneration of dopamine neurons, visualised as the classic loss of pigmentation in the SN (Farrer et al., 2004; Singleton et al., 2003; Spillantini et al., 1997). Post-mortem tissue has also aided in the confirmation of findings in animal and cellular models of PD (Liddelow et al., 2017; Sommer et al., 2018). It still remains an invaluable tool in the study of this disease, however, it does of course have its limitations. Post-mortem tissue is only a representation of end-stage disease, not enabling us to follow the progression and identify potential mechanisms at play.

1.10.2. Animal models

Animal models provide an invaluable, whole-system model to study disease. Without such models many scientific discoveries would not come about, and it is doubtful many drugs would have made it to clinical trials. There are a wide range of different animal models used to study PD each offering different pathological features associated with the disease. Advantages and disadvantages to each model exist, and some examples of these models are discussed below (for review see; Dovonou et al., 2023). An example of the α-syn based models is the very commonly used A53T mouse model. This model consists of mice which overexpress the A53T mutation to the human α-syn gene (Giasson et al., 2002). The resulting mice overexpress phosphorylated and aggregated α-syn, demonstrate signs of inflammation, and dysfunctional mitochondria (Dovonou et al., 2023; Martin et al., 2006; Sorrentino et al., 2018). Despite this, the model does not recapitulate neuronal loss or the accompanying drop in dopamine levels. Due to the importance of α-syn in PD, there are understandably numerous models targeting

this aspect of the disease, including a pre-formed fibril model, wild-type human α-syn models, as well as a model utilising the viral overexpression of α-syn (Dovonou et al., 2023). Other examples of genetic models of PD include those focusing of the PRKN/PINK1, LRRK2, GBA and DJ-1 mutations (Dovonou et al., 2023). Apart from genetic causes of PD, a number of toxins have been associated with development of this disease. Rotenone is a pesticide that has been linked to development of PD, and thus it is no surprise that it should form the basis for an animal model of this disease (Tanner et al., 2011). Rotenone was first described as a model of PD in 2000 by Betarbet and colleagues, which recapitulated many of the hallmarks of PD including, α-syn accumulation, oxidative stress, and loss of dopaminergic neurons in the SNpc (Betarbet et al., 2000). This model can be used to recapitulate PD in rodents, *C. elegans* and *Drosophila*. Whilst the major drawback for this model is the variability in the response produced (Dovonou et al., 2023). Another toxin-based model for the study of PD is that of Paraquat. Paraquat, is thought to be converted to PQ+ which can be up-taken through dopamine acid transporters into dopamine neurons (Rappold et al., 2011). This model produces mild dopaminergic degeneration, α-syn accumulation and microglial, and astrocyte activation (Dovonou et al., 2023). However, to produce a more robust model it is often combined with maneb (Thiruchelvam et al., 2000). Another such neurotoxin, 1-methyl-4-phenyl-1,2,3,6-tetrahydropyridine (MPTP) crosses the BBB and is metabolized by astrocytes releasing the active form 1-methyl-4-phenylpyridinium (MPP+) (Ransom et al., 1987). MPP+ is then up taken by dopaminergic neurons and inhibits the mitochondrial respiration complex 1 (MRC1), increases adenosine triphosphate (ATP), reactive oxygen species and induces neuronal cell death (Du et al., 2001; Nicklas et al., 1987). This model produces motor symptoms of PD, loss of dopaminergic neurons and depletion of dopamine, as well as α-syn accumulation making it a robust model for studying PD (Betarbet et al., 2000; Dovonou et al., 2023; Sherer et al., 2003). 6-Hydroxidopamine (6-OHDA) is a widely used toxin induced PD model. Due to its

inability to cross the BBB, 6-OHDA is injected into the desired brain region, most commonly the medial forebrain, but also the SNpc and striatum (Simola et al., 2007). 6-OHDA is a catecholamine analogue and thus targets all catecholaminergic neurons. In order to increase specificity of the model and prevent targeting of the noradrenergic system, it is usually administered alongside Desipramine, a noradrenergic reuptake inhibitor (Murillo et al., 2020). This model produces inhibition of the MRC1, dopaminergic degeneration, oxidative stress, inflammation (Dovonou et al., 2023) and presentation of PD-like motor symptoms. Although, α-syn accumulation is not a feature of this model (Simola et al., 2007). A neuroinflammation based model of PD is induced using lipopolysaccharide (LPS). LPS can be administered both systemically and locally. This model produces motor deficits, microglial and astrocyte activation, degeneration of dopaminergic neurons and α-syn accumulation (Dovonou et al., 2023). However, it should be noted that this model is also used to recapitulate AD in which amyloid-β, and Tau accumulation is observed (Wang et al., 2018).

Based on the information discussed above it is important to consider what makes an animal model an appropriate system to study a human disease. The concepts of face, construct and predictive validity must be considered. Face validity refers to the ability of the model to replicate the disease at a face level, in the case of PD, does it replicate any of the outwardly facing symptoms of the disease? Taking into account the models I've mentioned above, the 6-OHDA model for example is capable of replicating the motor symptoms of PD as well as non-motor symptoms of cognitive impairment and GI dysfunction. Similarly, the MPTP model also replicates motor symptoms including bradykinesia, rigidity and tremor (Dovonou et al., 2023). The second aspect to consider is do they replicate the underlying pathology of the disease, i.e. construct validity. As I have mentioned above, while each of the models do not replicate all the pathological hallmarks of PD, they do represent many aspects of the disease including,

degeneration of dopaminergic neurons, accumulation of α-syn and even mitochondrial dysfunction. Finally, we need to consider predictive validity, i.e. does the model respond as expected to therapeutic intervention for the disease in question. The 6-OHDA model is known for inducing contralateral rotation indicative of restoration of function on the lesioned side following administration of the therapeutic of interst. Similarly, addition of PD therapeutics to the MPTP model results in attenuation of motor symptoms associated with this model (Lane & Dunnett, 2008). Considering these set criteria, the current animal models of PD, while not perfect, do validly represent the disease.

While animal models clearly provide excellent systems for studying PD, they do have their disadvantages. Mainly, the lack of ability to study mechanisms at a cellular level, including studying disease at the single cell level. However, there are other techniques available which make this possible.

1.10.3. Direct reprogramming

Induced cells, or direct reprogramming of somatic cells to the cell type of interest is a relatively novel method of generating a new cell from a previously defined cell. Somatic cells can be directly reprogrammed to say a midbrain dopaminergic neuron, to enable the study of PD (Caiazzo et al., 2015; Pfisterer et al., 2011; Vierbuchen et al., 2010). These cells skip the pluripotent stem cell stage and forgo the extensive pre-differentiation process required with these cells (Stoker et al., 2018; Vierbuchen et al., 2010). Thus, making them an ideal option for many researchers, although the poor reprogramming efficiency yields low levels of cells making it difficult to maintain sufficient numbers for research (Ng et al., 2021).

1.11. Advantages and disadvantages of iPSC

iPSC of course, present the phenomenal ability to generate patient and disease-specific cell lines (Kouroupi et al., 2020; Park et al., 2008; Schweitzer et al., 2020; Shuvalova et al., 2020; Soldner et al., 2009). Patient-specific cells represent opportunities to directly replace disease cells with the patient's own healthy counterparts, the therapeutic potential is exciting and there are numerous clinical trials targeting this approach (Schweitzer et al., 2020; Yamanaka, 2020). Disease-specific cells, allow us to investigate disease associated cellular phenotypes at the level of a single cell. Furthermore, the iPSC can also be derived from people with disease-associated genetic mutations (Grigor'eva et al., 2023; Kawatani et al., 2021; Schmid et al., 2021; Schondorf et al., 2014; Shuvalova et al., 2020), this allows the study of how specific genetic mutations can alter the function and responses of cells. In addition to this, iPSC allow the generation of isogenic cell lines, providing the truly remarkable ability to study cells with a genetic mutation and compare it directly to a cell line that remains genetically identical, apart from that one genetic mutation which has been corrected (Kawatani et al., 2021; Schmid et al., 2021). An excellent example of how these points have come together to provide insight into disease pathogenesis, is in terms of AD, and the apolipoprotein gene mutation (Schmid et al., 2021). However, iPSC generated from people with a disease of idiopathic origin, as in PD, allow us the ability to have a near endless supply of cells to study *in vitro*. They also allow us to gain an unprecedented understanding of how cell types, especially those of the brain which are otherwise nearly impossible to obtain, function in isolation in response to outside stimulus or therapeutics. Comparisons and differences in how genetic and idiopathic disease presents at a cellular level can also be investigated in this manner.

In addition to the ability to truly study cellular mechanisms at a single-cell level, iPSC are also commonly used to study cells in co-culture, tri-culture and multi-cellular systems (McComish

et al., 2022). The ability to build the culture system that best aids in investigating your research question, is a large part of the appeal of iPSC. A great example is how iPSC have been used to generate brain spheroids/organoids with neural precursors differentiating into neurons and astrocytes, and the insertion of mesenchymal-originating microglia-like cells (Eichmuller & Knoblich, 2022; McComish et al., 2022). This gives an almost mini brain like structure in which you can study disease at a multi-cellular level.

These cells also provide an excellent model to test potential therapeutics in an *in vitro*, disease-relevant system (Cappella et al., 2021; Chehelgerdi et al., 2023; Ko & Gelb, 2014). The ability to assess drug responses on idiopathic and genetic cases of disease, and on single or multi-cellular systems, opens the door for identification of certain subsets of individuals who may respond better to certain therapeutics, allowing for precision-based, patient-specific medicine.

Despite the endless benefits to iPSC use, there are of course pitfalls to this technology. The main issue with iPSC, is that they are not a fully formed mammalian system, in this sense, animal models are still the gold-standard in enabling us to understand how potential therapeutics work in a fully functioning system. Furthermore, there are still roadblocks to the use of iPSC, mainly because of their novelty and the lack of a complete understanding of how they function. The issue of the reprogramming process reverting the cells back to age zero and therefore losing all the epigenetic changes that contribute so often to disease phenotypes manifesting is a concern (Horvath, 2013; Kerepesi et al., 2021; Maherali et al., 2007; Mertens et al., 2015). While many studies have investigated this and have found methods to overcome this, it has not fully been rectified yet (Kerepesi et al., 2021). Interestingly, one such method that aims to bypass this, is the direct reprogramming of somatic cells to cell type of interesting, skipping over the pluripotent stem cell step and therefore preventing the cells being stripped of

their epigenetic identities (Ladewig et al., 2012; Liu et al., 2013). This is a rapidly growing area and while it is going to aid in overcoming some of the downsides to iPSC research, it is of course also, in its novelty and comes with its own limitations.

1.12. Overarching aims and hypotheses

PD is a chronic, neurodegenerative disease, affecting millions of people worldwide. Currently there are no disease modifying therapeutics available for this disease, and the current symptomatic treatments have a time-limit. The introduction of iPSC technology brings with it the exciting potential for patient specific therapeutics, be it implantation of patient cells or drugs targeting individual PD cases. The recent identification of inflammation as a key contributor to the disease, brings with the potential of novel therapeutic targets. However, in order to be in a position to fully utilise these factors, we need to fully understand them. Therefore, this study aims to take what is known and to delve deeper into the role of the peripheral and central immune system in terms of PD pathogenesis. Furthermore, this study aims to utilise iPSC based technology to study these mechanisms at a cellular levels, and translate these findings to the human disease by using patient derived iPSC and peripheral immune cells.

A summary of the aims of this project are;

1. Investigate the interaction between peripheral immune cell secreted cytokines and midbrain astrocytes
2. Generate patient specific iPSC in order to study PD
3. Differentiate midbrain astrocytes in order to investigate disease specific mechanisms
4. Analyse peripheral immune cell populations in PD patients

The hypothesis of this study is that peripheral immune cell populations are altered in PD. These peripheral immune cells may be contributing to an increase in reactive astrocytes in the midbrain in PD. This increase in a pro-inflammatory environment may have negative effects on all structures within the brain and therefore be contributing to disease pathogenesis.

Chapter 2 : Materials and methods

2.1. Cryopreservation and thawing of cells

Cells were dissociated from the plate using the appropriate enzymatic disassociation agent and then centrifuged for 3 min, 178 x g, room temperature (RT). The cells were resuspended in CryoStor cryopreservation medium (Sigma Aldrich) and added to cryovials, freezing at a rate of 1°C per min using a MrFrosty at -80°C, then transferred to liquid nitrogen for long term storage. To thaw cells, the cryovials were placed into a water bath at 37°C, until only a small chunk of ice remained. Cells were diluted 1:10 in appropriate medium to dilute the dimethyl sulfoxide (DMSO) and then centrifuged for 3 min, RT, at 178 x g. The cell pellet was then resuspended in the appropriate cell medium adding a rho-kinase (ROCK) inhibitor, Y-27632 [10 μM; BioTechne] to aid cell survival, added to the pre-coated vessel and incubated at 37°C, 5% CO_2.

2.2. Counting cells

Disassociated cells were centrifuged then resuspended in a known volume of corresponding media. The cells were diluted 1:5 in media, then 1:1 in Trypan Blue. This cell/trypan blue suspension was loaded onto a haemocytometer, where 4 squares are counted and averaged. Trypan Blue labels dead cells, thus the number of cells trypan negative cells was divided by 4 to find the average per square and then multiplied by the dilution factor, in this case 10, and subsequently multiplied by 10^4 to determine the number of cells in the original 1 ml cell suspension. This number was then used to determine the volume of cells required to achieve the density desired.

2.3. Enzyme-linked immunosorbent assay

ELISAs was performed following manufacturers guidelines (R&D Systems, USA; Biolegend, USA). The plate was coated with capture antibody and sealed to incubate overnight. The capture antibody was removed and the plate washed three times with 0.05% PBS-tween (PBS-T). 1% bovine serum albumin (reagent diluent) was used to block for 1 h at room temperature (RT). Reagent diluent was removed and the plate washed three times with 0.05% PBS-T. Standards were prepared according to the manufacturers specifications and added to the plate. Following this samples were added, and the plate was left to incubate for 2 h at RT on a shaker. The Samples and standards were removed and plate was washed three times with 0.05% PBS-T. Detection antibody was added and incubated for 2 h at RT, following removal of the detection antibody the plate was washed three times with 0.05% PBS-T. Streptavidin-horse radish peroxidase (HRP) was added and left to incubated at RT for 30 minutes, Subsequently the plate was washed three times with 0.05% PBS-T. The tetramethylbenzidine (TMB) substrate solution was added and incubated at RT in the dark for 5-30 m. H2SO4 stop solution was added once reaction was complete. The plate was then resealed and read using a plate reader (Synergy HT, BioTek Instruments, USA) at 450 nm, subtracting the 540/570 nm wavelength to correct for optical imperfections within the plate.

2.4. Quantitative real time polymerase chain reaction (qRT-PCR)

2.4.1. Sample preparation

Sample preparation was carried out as per the NucleoSpin RNA isolation kit (Macherey Nagel Bioanalysis, Fisher Scientific Ltd). Lysis buffer was prepared by diluting β-mercaptoethanol in RA1 lysis buffer (1:100). Lysis buffer was applied to the cells and cells were scraped from

the wells. Cell lysates were collected into RNAse-free eppendorfs and stored at -80°C until use.

2.4.2. RNA isolation

RNA isolations were carried out following manufacturers protocol (NucleoSpin RNA isolation kit; Macherey Nagel Bioanalysis, Fisher Scientific Ltd). Samples were pipetted to redistribute lysate following freeze-thaw. The lysate was added to a violet ring filter and centrifuged at 11,000 x g for 1 min to clear the lysate. The violet filter was discarded and samples were diluted 1:1 with 70% ethanol. Samples were pipetted a homogenous solution was achieved, this adjusts RNA binding conditions. The ethanol-lysate mix was then added to the blue ring filter and centrifuged at 11,000 x g for 30 s, this allows RNA to bind to the filter. Membrane desalting buffer is then added to the blue ring filter to remove excess salt the membrane and centrifuged at 11,000 x g for 1 min. rDNase reaction mix was added to the blue ring filter and incubated for 15 min at RT. This step acts to digest DNA. RAW2 was added to inactivate this reaction and centrifuged at 11,000 x g for 30 s. RA3 buffer was added to wash the filter and centrifuged for 30 s at 11,000 x g. The flow-through was discarded and a further wash with RA3 buffer was performed, centrifuging for 2 min at 11,000 x g. The blue ring filter is then finally placed into an RNAse-free Eppendorf and RNAse-free water is added. The filter is centrifuged at 11,000 x g for 1 min to elute the RNA. RNA was then stored at -80°C until use.

2.4.3. Complementary DNA manufacture

Prior to complementary DNA (cDNA) manufacture, the isolated RNA concentration was measured using a nanodrop (Nanodrop 2000 spectrophotometer, ThermoFisher Scientific). RNA concentrations were equalised to the lowest concentration using RNAse-free water.

Equalised RNA can also be stored at -80°C. cDNA was manufactured using the high-capacity cDNA reverse transcription kit following the manufacturers protocol (Applied Biosystems, ThermoFisher Scientific). The reverse transcription master mix was prepared, then diluted 1:1 with equalised RNA. Samples were centrifuged at 1,200 x g for 1 min. The samples are added to the thermocycler (PTC-200 Peltier Thermal Cycler, MJ Research) for the following protocol; 25°C 10 min, 37°C 120 min, 85°C 5 min, 4°C ∞. Once cDNA has been manufactured, samples were stored at -20°C.

2.4.4. qRT-PCR

PCR master mix was prepared by combining Taqman master mix, with an endogenous control primer (1:12; see Table 2.1.) and the target primer (1:12; see Table 2.1.). cDNA was diluted 1:4 with RNAse-free water before use. Diluted cDNA and PCR master mix were added to a MicroAmp® Fast Optical 96-Well Reaction Plate. Once loaded, the plate was sealed and centrifuged at 1,200 x g for 1 min. Samples were then run in the StepOne Real-Time PCR System (Applied Biosystems; ThermoFisher Scientific) for the following program; Holding stage 1: 50°C, 2 min, Holding stage 2: 95°C, 20 s, cycling stage 1: 95°C, 1 s, cycling stage 2: 60°C, 20 s. Results were analysed using the Design and Analysis software (version 2.7.0; Applied Biosystems, ThermoFisher Scientific) using the comparative CT method.

Table 2.1. qRT-PCR primers

Primers	***Gene Name***	***Company***	***Assay Number***
GAPDH	Endogenous control primer; Glyceraldehyde-3-Phosphate Dehydrogenase	ThermoFisher Scientific	Hs02786624_g1
IL-17RA	Interleukin 17 receptor A	ThermoFisher Scientific	Hs01056316_m1
IL-6	Interleukin 6	ThermoFisher Scientific	Hs00174131_m1
PTX3	Pentraxin-related protein	ThermoFisher Scientific	Hs00173615_m1
C3	Complement component 3	ThermoFisher Scientific	Hs00163811_m1
GFAP	Glial fibrillary acidic protein	ThermoFisher Scientific	Hs00909233_m1
ICAM1	Intracellular adhesion molecule 1	ThermoFisher Scientific	Hs00164932_m1
ITGA6	Integrin subunit alpha 6	ThermoFisher Scientific	Hs01041011_m1
SERPINA3	Serpin family A member 3	ThermoFisher Scientific	Hs00153674_m1
TIMP1	TIMP metallopeptidase 1	ThermoFisher Scientific	Hs01092512_g1
IL-1β	Interleukin 1 β	ThermoFisher Scientific	Hs01555410_m1
CXCL10	C-X-C motif chemokine ligand 10	ThermoFisher Scientific	Hs00171042_m1
LCN2	Lipocalin 2	ThermoFisher Scientific	Hs01008571_m1
VIM	Vimentin	ThermoFisher Scientific	Hs00958111_m1
POU5F1	Oct3/4	ThermoFisher Scientific	Hs04260367_gH
NANOG	Nanog	ThermoFisher Scientific	Hs02387400_g1
SOX1	Sry-box transcription factor 1	ThermoFisher Scientific	Hs01057642_s1

ALB	Albumin	ThermoFisher Scientific	Hs00609411_m1
HAND1	Heart and neural crest derivatives expressed 1	ThermoFisher Scientific	Hs02330376_s1

2.5. Immunocytochemistry

Cells were fixed using 4% paraformaldehyde solution, 15 min at RT. Coverslips can then be stored at 4°C until use. Coverslips were washed three times with 0.02% Triton-X in PBS before being incubated in blocking buffer (10% normal goat serum (NGS), 0.3% Triton-X in PBS), 2 h, RT. Primary antibody was diluted (Table 2.2.) in buffer containing 2% NGS, 0.06% Triton-X in PBS and incubated overnight at 4°C. Coverslips were washed three times in 0.02% Triton-X in PBS before secondary antibody (Table 2.2.) was incubated for 2 h, RT, in the dark. The secondary antibody was washed from the cells with 0.02% Triton-X in PBS three times. Hoechst was diluted 1:1000 in PBS and added to the cells for 30 min, RT, in the dark. Following this coverslips were washed with PBS and mounted on slides in ProLong™ (ThermoFisher Scientific) antifade mounting medium and left to dry overnight at RT protected from light. Mounted coverslips were stored at 4°C until imaging took place using a fluorescent microscope (Carl Zeiss Axio Imager Z1 microscope). Cells were analysed using CellProfiler software.

Table 2.2. Immunocytochemistry antibodies

Manufacturer	*Target*	*Antibody*	*Dilution*
Sigma-Aldrich	S100β	S2532	1 in 1000
Sigma-Aldrich	GFAP	AB5541	1 in 1000
Cell Signalling	NFκB	8242	1 in 500
Cell Signalling	gH2AX	9718	1 in 1000
Bio-Techne	EAAT1	NBPI-20135	1 in 1000
Sigma	αConnexin-43	C6219	1 in 1000
Bioss	IL-17RA	BS-2606R	1 in 100
Merk	LMX1A	AB10533	1 in 1000
ThermoFisher Scientific	Donkey anti-mouse	Alexa Fluor 488, A21202	1 in 500
ThermoFisher Scientific	Goat anti-rabbit	Alexa Fluor 555, A21428	1 in 500
abcam	Goat anti-chicken	Alexa Fluor 488, ab150169	1 in 500

2.6. Statistical methods

Statistical analysis was carried out using Microsoft Excel and GraphPad prism software version 9. A two-tailed unpaired t-test was used when comparing two groups. A one-way analysis of variance (ANOVA) was used for data with one independent variable and three or more groups. A two-way ANOVA was used for data with two independent variables. A three-way ANOVA for when data had three independent variables. Tukey's post-hoc was used when significance was observed in the ANOVA. For iPSC and iPSC-derived cellular experiments, N, refers to experimental replicates. For each experiment between 2 and 3 technical replicates were performed. For human peripheral blood mononuclear cells (PBMC) and plasma experiments N, denotes biological replicates. Data was expressed as mean ± standard error of the mean (SEM), except where mean ± standard deviation is specified and statistical significance was set at $p<0.05$.

Chapter 3: $CD4^+$ T cell-associated cytokines induce a chronic pro-inflammatory phenotype in induced pluripotent stem cell-derived midbrain astrocytes

---

3. $CD4^+$ T cell-associated cytokines induce a chronic pro-inflammatory phenotype in induced pluripotent stem cell-derived midbrain astrocytes

Authors list

Adina N. MacMahon Copas[1,2], Sarah F. McComish[1,2], Andreea Petrasca[3], Rachel McCormack[1,2], Daniel Ivers[1,2], Anna Stricker[1,2], Jean M. Fletcher[3,4], Maeve A. Caldwell[1,2,*]

1. Discipline of Physiology, School of Medicine, Trinity Biomedical Sciences Institute, Trinity College Dublin, Dublin, Ireland.
2. Trinity College Institute for Neuroscience, Trinity College, Dublin, Ireland.
3. School of Biochemistry and Immunology, Trinity Biomedical Sciences Institute, Trinity College Dublin, Dublin, Ireland.
4. School of Medicine, Trinity Biomedical Sciences Institute, Trinity College Dublin, Dublin, Ireland.

*Corresponding author: Maeve Caldwell maeve.caldwell@tcd.ie

Author contributions

ANM, JMF and MAC designed and coordinated the study and interpreted data. ANM performed experiments, data analysis, interpretation and produced the figures. SFM, AP, RMcM, DI and AS performed experiments and data analysis. ANM and MAC wrote the manuscript. All authors approved the final manuscript.

Abstract

Astrocytes are mediators of homeostasis but contribute to neuroinflammation in Parkinson's disease (PD). Mounting evidence suggests involvement of peripheral immune cells in PD pathogenesis. Therefore, this study aimed to determine the potential role of peripheral immune secreted cytokines in modulating midbrain astrocyte reactivity.

Human iPSC-derived midbrain astrocytes, were exposed to $CD4^+$ T cell conditioned media (CD4CM) for 24 h, 72 h and 7 d to assess chronic exposure. Additionally, astrocytes were exposed to the Th17 cell cytokine, IL-17A, alone and in combination with TNFα to assess potential synergistic effects of both cytokines.

CD4CM induced acute and chronic alterations in midbrain astrocytes. Increased NFκB translocation to the nucleus, increased expression of the proinflammatory genes, *IL-1β, CXCL10* at 24 h, *C3, LCN2, IL-6* at 24 and 48 h, as well as an increase in their release of proinflammatory cytokines IL-6 and CXCL10 at both of these time points was observed. A synergistic response to the combination of IL-17A and TNFα on increasing inflammatory gene expression and cytokine release occurred. IL-17A and TNFα increased intensity of S100β at 24 h, decreased nuclear area and increased circularity of astrocytes at 72 h. A synergistic effect on gH2AX intensity at 72 h and an increase in LDH release at 7 d was observed.

Our results demonstrate that IL-17A and TNFα act synergistically, enhancing midbrain astrocyte reactivity to a similar degree as CD4CM. This highlights the importance of the peripheral immune secreted cytokines in increasing the reactivity status of midbrain astrocytes, implicating their role in PD.

3.1. Introduction

The involvement of immune-related responses such as astrogliosis and microgliosis have been well-established in the pathogenesis of Parkinson's disease (PD) (Kam et al., 2020). It is only in recent years that the involvement of peripheral immune cells in neurodegenerative diseases, such as PD has been evaluated (for review see MacMahon Copas et al., 2021; Sommer et al., 2018). While the presence of T cells in the brain of PD patients has been demonstrated using post-mortem tissue, little is known about their role in disease pathogenesis (Brochard et al., 2009; Sommer et al., 2018). While a consensus remains to be drawn from analysis of peripheral immune cell populations in PD patients, *in vivo* models have demonstrated that manipulating these cells can exacerbate or attenuate disease (Brochard et al., 2009; Sommer et al., 2016). Brochard *et al.,* demonstrated that $CD4^{-/-}$ mice resulted in attenuation of MPTP-induced neurodegeneration, furthermore, Sommer *et al.,* observed a reduction in α-synuclein aggregation in human wild-type α-syn overexpressing, $Rag2^{-/-}$ mice (Brochard et al., 2009; Sommer et al., 2016). These findings have been further validated by *in vitro* studies demonstrating that, in rodent and human cells, peripheral immune cells and their associated cytokines can be detrimental to cells of the CNS (Liu et al., 2019; Sommer et al., 2018).

Recent evidence specifically highlighted $CD4^{+}$ T cells as a potential source of these harmful factors (Brochard et al., 2009; Liu et al., 2019; Sommer et al., 2018). In particular, Th17 cells have emerged as key targets, since inhibition of these cells or their cytokines was demonstrated to attenuate pathological outcomes in numerous studies (Brochard et al., 2009; Liu et al., 2019; Sommer et al., 2018). Interestingly, IL-17A, the signature cytokine of Th17 cells, is known to synergise with other cytokines such as TNFα or IL-1β, producing robust responses from many cell types (Beringer et al., 2018; Chiricozzi et al., 2011; Claire et al., 2013; Elain et al., 2014; Noack et al., 2019; Zrioual et al., 2008). Due to the wide range of cytokines known to be present

in PD disease pathogenesis, the infiltration of IL-17 secreting cells into the brain is likely to have a marked effect on inflammation. However, the implications of this has yet to be investigated in the context of PD. In particular, little is known about the effect of IL-17 on astrocytes, the major homeostatic regulators of the CNS. Therefore, this study aims to investigate the effect of peripheral immune cell secreted cytokines on the reactivity of iPSC-derived midbrain astrocytes (vmAstros).

3.2. Methods

3.2.1. Culture of iPSC-derived astrocytes

The human iPSC line, NAS2 used in this study was kindly provided by Professor Tilo Kunath, University of Edinburgh and from them vmAstros were differentiated as previously described by Crompton *et al.,* 2021 (2021) (supplemental Fig 1 A). Briefly, midbrain neural progenitors were directed towards an astrocytic fate using astrocyte media (Advanced Dulbecco's Modified Eagle Medium, 1% NEAA, 1% GlutaMAX, 1% Penicillin/Streptomycin, 1% N2, 0.1% B27) supplemented with epidermal growth factor (EGF, 20 ng/ml; Sigma Aldrich) and human leukaemia inhibitory factor (hLIF, 20 ng/ml; PeproTech). Astrocytes were continually passaged when confluent until they reached d80. From d80 onwards, astrocyte progenitor cells can be matured for experimentation. Astrocytes were detached using Accutase™ (Stem Cell Technologies), 3 min, RT. Before being counted and seeded at set density; $3x10^5$ cells per coverslip for immunocytochemistry, $5x10^5$ cells per well for ELISA, or $15x10^5$ cells per well for qPCR. Astrocyte progenitor cells were then matured for 7 d using astrocyte media containing bone morphogenetic protein 4 (BMP4, 20 ng/ml, Bio-Techne) and hLIF (20 ng/ml; PeproTech). Once matured, astrocytes were exposed to either $CD4^+$ conditioned media, TNFα (Cell Signalling Technology) or IL-17A (PeproTech) diluted to relevant concentration in astrocyte media.

3.2.2. T cell conditioned media

Conditioned media was prepared as per Petrasca *et al.,* (2020). Briefly, PBMC were isolated from whole blood. $CD4^+$ T cells were isolated by magnetic-activated cell sorting as per manufacturer's instructions (MACS; Miltenyi Biotec). Once isolated the $CD4^+$ T cells were stimulated with anti-CD3 (BD Biosciences) and anti-CD28 (eBioscience) in cRPMI and

incubated (5 d, 37°C. 5% CO2). The conditioned media was then collected and stored at -20°C until use.

3.2.3. Immunocytochemistry/Immunofluorescence and Imaging

Astrocytes were fixed using 4% paraformaldehyde. Coverslips were washed 3 times with 0.02% Triton-X in PBS and incubated in blocking buffer (10% normal goat serum (NGS), 0.3% Triton-X in PBS) for 2 h, RT. Primary antibody was diluted (supplemental Table 1) in buffer containing 2% NGS, 0.06% Triton-X in PBS and incubated overnight at 4°C. Coverslips were washed 3 times in 0.02% Triton-X in PB before secondary antibody (supplemental Table 1) was added for 2 h, RT, dark. Hoechst was added to the cells for 30 min, RT, dark following washing coverslips 3 times in 0.02% Triton-X in PBS. Following this coverslips were washed with PBS and mounted on slides in ProLong™ (ThermoFisher Scientific) antifade mounting medium and left to dry overnight. Mounted coverslips were stored at 4°C until imaging took place using a fluorescent microscope (Carl Zeiss Axio Imager Z1 microscope). 15-20 fields were taken per coverslip, one coverslip was imaged per N, for an N=3. Cells were analysed using CellProfiler software for γH2AX, S100β and morphological analysis. 100 cells per N were analysed, meaning a total of 300 cells were analysed per treatment group. CellProfiler first identified the nucleus of the cell based on Hoechst staining and cells were identified from there. Integrated intensity was used for S100β and γH2AX intensity values, integrated intensity within CellProfiler is the additive intensity of the pixel intensity within the cell. Form factor equates to circularity, CellProfiler attempt to calculate how close to 1 the cell is using the formula, of 4xpi(area/perimeter^2). The closer to 1 the cell is the more circular. The perimeter, which indicates the total length around the outer perimeters of the cells and nuclear area, which measures the total area taken up by the identified nucleus were identified also. Cells were analysed using ImageJ for NFκB analysis. 100 cells per N were analysed, meaning a total of

300 cells were analysed per treatment group. NFκB translocation was assessed by counting NFκB positive nuclei and expressing as percentage of total Hoechst positive nuclei per 100 cells i.e. per N.

3.2.4. RT-qPCR

Following manufacturers protocol cells were lysed using a lysis buffer of β-mercaptoethanol and RA1 lysis buffer. The NucleoSpin^{TM} RNA isolation kit (Macherey Nagel Bioanalysis, Fisher Scientific Ltd) was used to isolate the RNA. Isolated RNA was stored at -80°C until use. RNA was equalized with RNase-free H_20 to 40 ng/µl before cDNA was manufactured. Equalized RNA was stored at - 80°C. The RNA was reverse transcribed to give cDNA using a high-capacity cDNA kit and following manufacturers protocol (Applied Biosciences). Reverse transcription master mix was first prepared using multiscribe reverse transcriptase (2X, Biosciences), reverse transcriptase buffer (10X), dNTPs (25X, Biosciences), nuclease-free H_2O and random primers (10X). The RNA:cDNA master mix was added to a Thermocycler (PTC-200 Peltier Thermal Cycler, MJ Research) and left to incubate for the following program; 25°C 10 min, 37°C 120 min, 85°C 5 min, 4°C ∞ and then stored at -20°C. PCR master mix was prepared by combining TaqMan^{TM} master mix (Applied Biosciences), endogenous control primer (GAPDH) and the appropriate target primer (supplemental Table 2; TaqMan^{TM}, ThermoFisher Scientific). Plate was then run in the StepOne^{TM} Real-Time PCR System (Applied Biosystems, ThermoFisher Scientific) for the following settings for 40 cycles; Holding stage 1: 50°C, 2 min, Holding stage 2: 95°C, 20 s, cycling stage 1: 95°C, 1 s, cycling stage 2: 60°C, 20 s. Data was analysed using Microsoft Excel, where replicates were averaged to give a single value for each N, which could then be inserted into GraphPad Prism software for final analysis. An N=3, with 2 experimental replicates per N were analysed for all treatment groups and timepoints.

3.2.5. ELISA

Cell culture media was collected and stored at -20°C before being analysed by ELISA. ELISA was performed following manufacturers guidelines (R&D Systems). Plate was coated with capture antibody overnight at RT. Following 3 washes with 0.05% PBS-Tween20 (Buffer) wells were incubated in 1% BSA for 1 h at RT. Plate was washed with buffer and samples and standards loaded prior to incubation on a shaker for 2 h at RT. Detection antibody was added and incubated for 2 h at RT following washing off the samples and standards. Plate was washed with buffer prior to incubation in Streptavidin-HRP at RT for 30 min. The plate was washed with buffer before tetramethylbenzidine (TMB) substrate solution was added for 10-30 min at RT in the dark. H_2SO_4 stop solution was added to stop the reaction once standards were developed. The plate was read using a plate reader (Synergy HT, BioTek Instruments, USA) at 450 nm, subtracting the 540 nm wavelength to correct for optical imperfections within the plate. GraphPad prism was used to generate the standard curve and determine protein concentrations within the samples. Data was then analysed using Microsoft Excel. At least two experimental replicates were analysed per N, which were averaged to give a single value per N. An N=3 was analysed per treatment group and timepoint. GraphPad Prism was used for final statistical analysis and graph generation.

3.2.6. Lactate dehydrogenase assay

The lactate dehydrogenase assay was carried to assess LDH levels in cell culture supernatants (CyQuant™ LDH Cytotoxicity Assay Kit; Invitrogen). Positive control was prepared by diluting LDH positive control in 1% BSA in PBS. Culture media supernatant samples and positive control were loaded onto the plate. The reaction mix was then added and plate incubated at RT in the dark for 30 min. Stop solution was then added before reading plate at 490 nm and 680 nm (Synergy HT, BioTek Instruments, USA). 680 nm was subtracted from

490 nm to determine LDH activity. Data was analysed using Microsoft Excel. Two experimental replicates were analysed per N, which were averaged to give a single value per N. An N=3 was analysed per treatment group and timepoint. Data was expressed as percentage control at 24 h post-stimulation. GraphPad Prism was used for final statistical analysis and graph generation.

3.2.7. Quantification and Statistical Analysis

Statistical analysis was carried out using Microsoft Excel and GraphPad Prism Software version 9. One, two or three-way ANOVA with Tukey's post-hoc were used dependent on whether there were one, two or three variables present respectively. Data was expressed as mean ± standard error of the mean (SEM) and statistical significance was set at $p<0.05$.

3.3. Results

3.3.1. $CD4^+$ T cell conditioned media induces NFκB translocation in vmAstros.

In order to investigate the effects of peripheral immune cells on astrocytes in the context of PD we utilized vmAstros, described by Crompton *et al.* (2021) (supplemental Fig 1. A). These vmAstros expressed S100 calcium binding protein (S100β), excitatory amino acid transporter 1 (EAAT1) and CX43 confirming their astrocytic phenotype. In addition, they expressed LIM homeobox 1 alpha (LMX1A) indicative of their midbrain identity (Fig. 3.3.1. A). These vmAstros then underwent exposure to conditioned media from CD28/CD3 stimulated $CD4^+$ T cells (CD4CM; Petrasca et al., 2020), at a concentration of 5 and 10%. These concentrations were chosen following determination of their ability to induce secretion of the pro-inflammatory cytokine IL-6. Results showed that 10% CD4CM resulted in a significantly greater secretion of IL-6 than 5% following 24 h exposure (supplemental Fig. 1. B). The study included 4 timepoints to assess different aspects of astrocyte reactivity following stimulation (Fig. 3.3.1. B). As a key pathway involved in astrogliosis, NFκB translocation was assessed following 1 h stimulation with the CD4CM (Fig. 3.3.1. C and D). Analysis demonstrated a significant increase in NFκB translocation to the nucleus of the vmAstros following stimulation with both 5 and 10% concentrations of the CD4CM with 10% having the strongest effect (Fig. 3.3.1. C and D). In summary these results show that vmAstros increase NFκB translocation to the nucleus following CD4CM treatment.

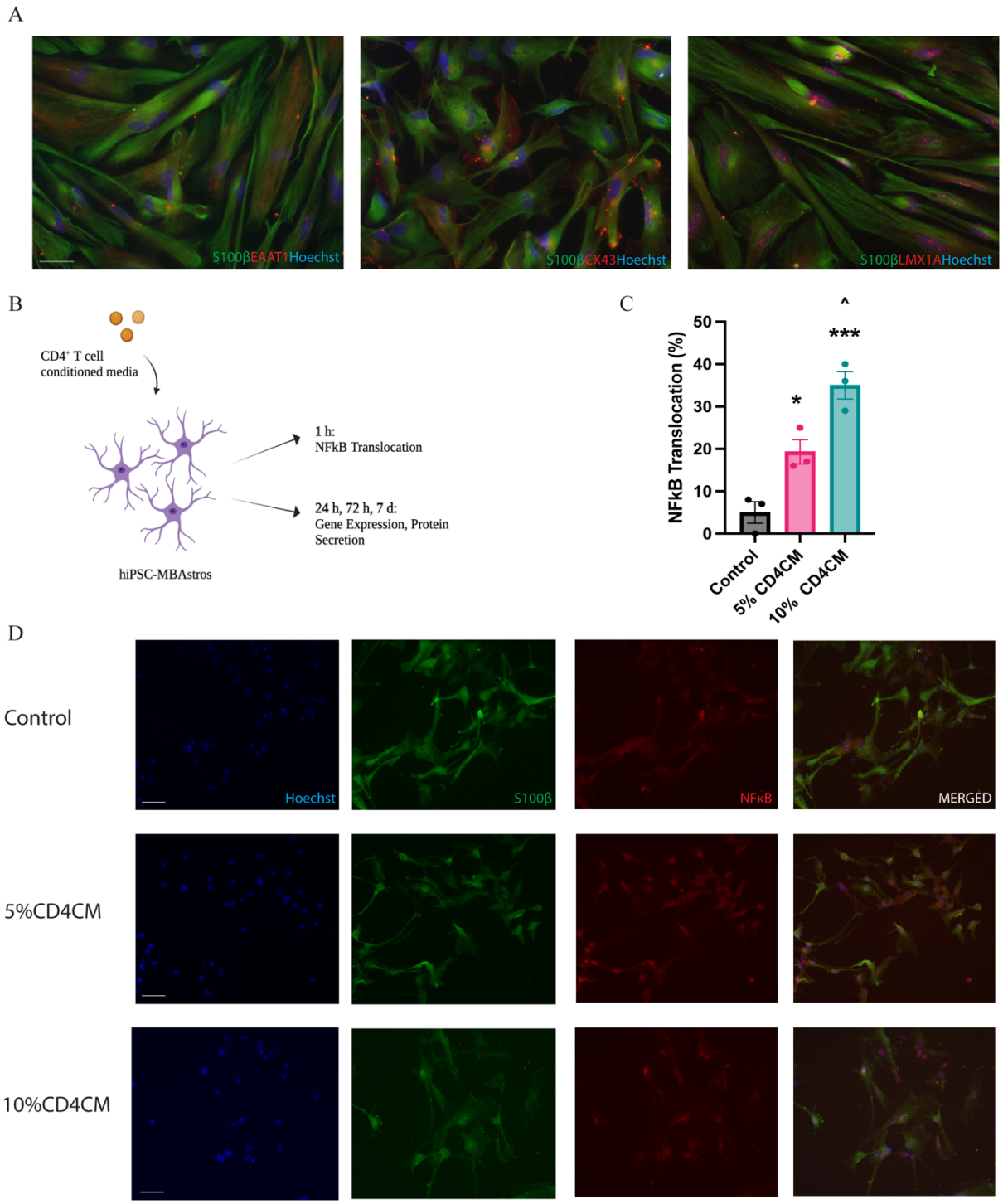

Figure 3.3.1. Activation of NFκB pathway signalling in vmAstros following exposure to CD4⁺ T cell conditioned media (CD4CM).

(A) Immunostaining for expression of astrocyte markers; S100β, EAAT1, CX43 and midbrain marker; LMX1A. (B) Schematic representation of experimental design. (C) NFκB

translocation to the nucleus represented as % positive nuclear expression of NFκB. (D) Representative immunofluorescence of NFκB translocation. Data expressed as ± SEM (N=3). *p<0.05, ***p<0.001 vs control. ^p<0.05 vs 5% CD4CM. One-way ANOVA with Tukey's post hoc. Scale bars, 50 μm.

3.3.2. $CD4^+$ T cell conditioned media induces acute and chronic alterations in vmAstros reactivity profile.

Following evidence of NFκB translocation to the nucleus in response to CD4CM, we next investigated whether this produced alterations in the expression of reactivity associated genes. In order to mimic the chronic nature of PD, astrocytes were exposed to CD4CM for 24 h, 72 h and 7 d and gene expression analysed using RT-qPCR.

The expression of inflammation associated markers *C3, LCN2 and PTX3* were significantly upregulated by the CD4CM for up to 72 h post-stimulation (Fig. 3.3.2. A-C). Interestingly expression of the proinflammatory cytokines *IL-6* (Fig. 3.3.2. D) and *IL-1β* (Fig. 3.3.2. E) were significantly upregulated acutely, following 24 h stimulation, and this upregulation resolved by 72 h post-stimulation. Furthermore, expression of the chemokine *CXCL10*, involved in migration and extravasation of immune cells to sites of inflammation, was significantly upregulated by CD4CM stimulation (Fig. 3.3.2. F). Other reactive astrocyte related genes such as *SERPINA3, ICAM1, GFAP, TIMP1* and *VIM* remained unchanged (supplemental Fig. 2 A-E). Expression of the recently described reactivity-independent astrocyte marker of *ITGA6* remained unaltered following stimulation, providing further confirmation of its use a reliable astrocytic marker (supplemental Fig. 2F; Barbar *et al.,* 2020).

In order to assess protein secretion by the astrocytes following stimulation, secretion of pro-inflammatory IL-6 and IL-1β, as well as anti-inflammatory IL-10 and the chemokines CXCL10 and CCL5 were assessed over the same time course. While levels of IL-10 and IL-1β remained unaltered (supplemental Fig. 2 G and H), levels of IL-6 were significantly upregulated across all three timepoints (Fig. 3.3.2. G), demonstrating a chronic exposure of the astrocytes to pro-inflammatory cytokines, such as IL-6. Interestingly secretion of the chemokine CXCL10 was significantly increased at 24 h post-stimulation (Fig. 3.3.2. H), whilst CCL5 levels remained unchanged (Fig. 3.3.2. I). These results demonstrate that CD4CM induces upregulated expression and secretion of pro-inflammatory associated markers in vmAstros, while typical anti-inflammatory signals remain unchanged.

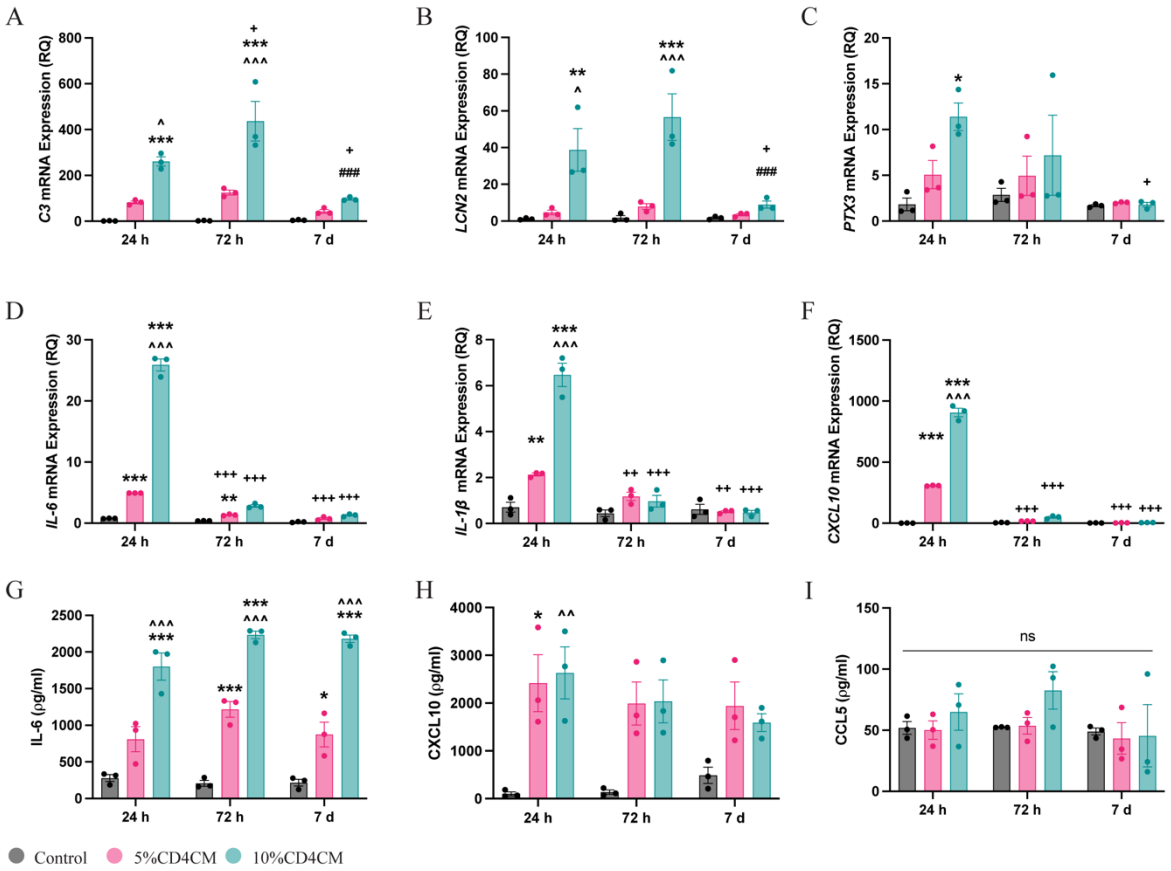

Figure 3.3.2. CD4CM induced reactive gene expression and protein section from vmAstros.

Following stimulation with CD4CM for 24 h, 72 h and 7 d, vmAstros were taken for RT-qPCR and ELISA analysis of reactivity associated cytokines and chemokines. (A) *C3*, (B) *LCN2*, (C) *PTX3*, (D) *IL-6*, (E) *IL-1β*, (F) *CXCL10* gene expression levels and (G) IL-6, (H) CXCL10 and (I) CCL5 protein secretion levels. Data expressed as ± SEM (N=3). *p<0.05, **p<0.01, ***p<0.001 vs control. ^p<0.05, ^^p<0.01, ^^^p<0.001 vs 5% CD4CM. $^{+}$p<0.05, $^{++}$p<0.01, $^{+++}$p<0.001 vs 24 h. $^{\#\#\#}$p<0.001 vs 72 h. Two-way ANOVA with Tukey's post hoc.

3.3.3. NFκB translocation induced by TNFα and IL-17A

Due to the emerging link between Th17 cells and PD pathogenesis, we aimed to establish how much of the response to CD4CM could be due to IL-17A, the signature cytokine of Th17 cells. Also, due to its well-established synergistic capabilities, we investigated its interaction with another cytokine implicated in PD, TNFα (Beringer et al., 2018; Chiricozzi et al., 2011; Claire et al., 2013; Elain et al., 2014; Noack et al., 2019; Zrioual et al., 2008). TNFα, a commonly secreted reactive microglial cytokine, known to induce astrocyte reactivity, and also present in CD4CM, was chosen to investigate this synergistic relationship.

Initially, *IL-17RA* expression by the vmAstros was confirmed using immunocytochemistry and gene expression (Fig. 3.3.3. A and B). Human dermal fibroblasts were used as a positive control, and iPSC as a negative control for gene expression (Fig. 3.3.3. B). Following this a dose-response was carried out, utilizing IL-6 secretion as the readout, to ensure the lowest possible concentration of both TNFα (0.3 ng/ml) and IL-17A (10 ng/ml) were selected to focus on any relationship between the two cytokines (supplemental Fig. 1 C and D).

Following stimulation with TNFα and/or IL-17A for 1 h, translocation of NFκB to the nucleus was assessed (Fig. 3.3.3. D and E). Stimulation with TNFα, as well as TNFα and IL-17A combined significantly increased NFκB translocation to the nucleus of the cells, compared to

control (Fig. 3.3.3. D and E). Although a slight increase can be observed between the TNFα alone group and the combined TNFα and IL-17A group this did not reach significance. Similarly, while IL-17A alone did not significantly stimulate NFκB translocation a trend towards increase can be observed (Fig. 3.3.3. D and E).

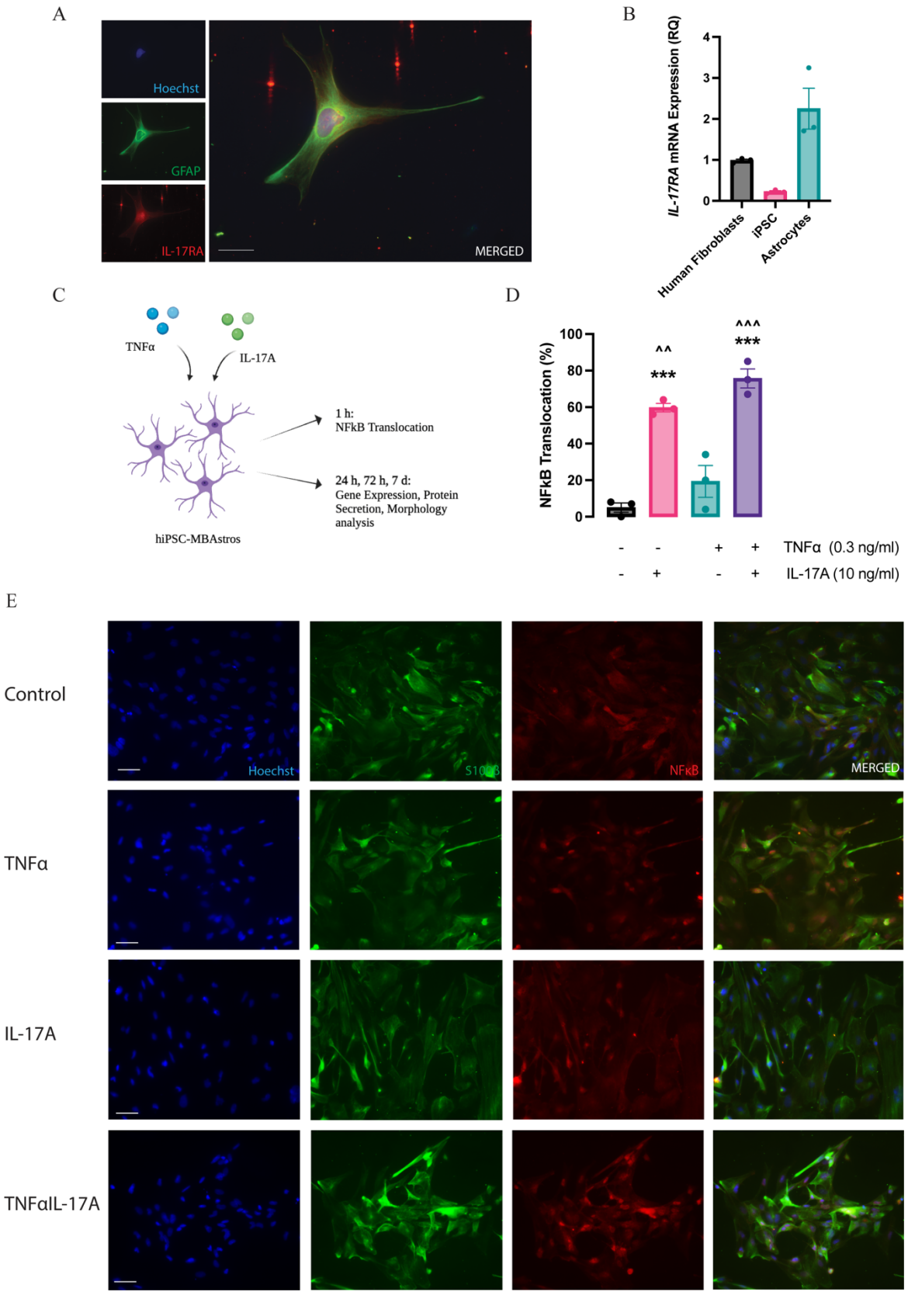

Figure 3.3.3. vmAstros respond to TNFα and IL-17A by inducing NFκB translocation to the nucleus.

*Confirmation of vmAstros expression of IL-17RA via (A) immunocytochemistry and (B) RT-qPCR. (C) Schematic representation experimental design. (D) Quantification of NFκB nuclear translocation following exposure to TNFα, IL-17A or TNFα+IL-17A. (E) Representative images of NFκB translocation in vmAstros. Data expressed as ± SEM (N=3). ***p<0.001 vs control. ^^p<0.01, ^^^p<0.001 vs TNFα. One-way or two-way ANOVA with Tukey's post hoc. Scale bars, 50 µm.*

3.3.4. vmAstros respond robustly, and chronically to the synergistic action of TNFα and IL-17A

Next, we aimed to establish the reactivity profile of the vmAstros following stimulation with TNFα and/or IL-17A, in comparison to that achieved by CD4CM. Similar to the response induced by the CD4CM, TNFα+IL-17A combined induced significant increases in gene expression of *C3* and *LCN2*. However, interestingly the response induced by the combined cytokines was synergistic when compared with the response from either alone (Fig. 3.3.4. A and B). Both *C3* and *LCN2* maintained this significantly increased expression level at 72 h post-stimulation, and while *LCN2* expression decreased over time, for *C3* it remained significantly upregulated compared with control at 7 d post-stimulation (Fig. 3.3.4. A and B).

However, unlike CD4CM, *PTX3* mRNA expression levels remained unaltered by TNFα and IL-17A treatment (Fig. 3.3.4. C). As with CD4CM, acute and synergistic increases in *IL-6* and *IL-1β* expression were observed with TNFα+IL-17A stimulation (Fig. 3.3.4. D and E). Interestingly, while *CXCL10* was significantly upregulated, as was seen with CD4CM stimulation, it was largely due to exposure of the cells to TNFα, rather than to IL-17A or the combination of the two (Fig. 3.3.4. F).

Similar to the above, we aimed to further assess the astrocyte reactivity profile by looking at secretion levels of IL-6, IL-1β, IL-10, CXCL10 and CCL5. While IL-10 and IL-1β remained unaltered (supplemental Fig. 3), as was observed with the CD4CM treatment, IL-6 secretion was significantly and synergistically increased by TNFα and IL-17A combined treatment (Fig. 3.3.4. G). Despite decreasing slightly by 7 d, this increased secretion remained significant compared to control at 7 d (Fig. 3.3.4. G). Interestingly, secretion of the chemokines, CCL5 and CXCL10 was significantly increased, however as with mRNA, this effect was mainly due to the TNFα stimulation alone (Fig. 3.3.4. H). In summary, TNFα and IL-17A can induce synergistic upregulation of pro-inflammatory associated markers in vmAstros.

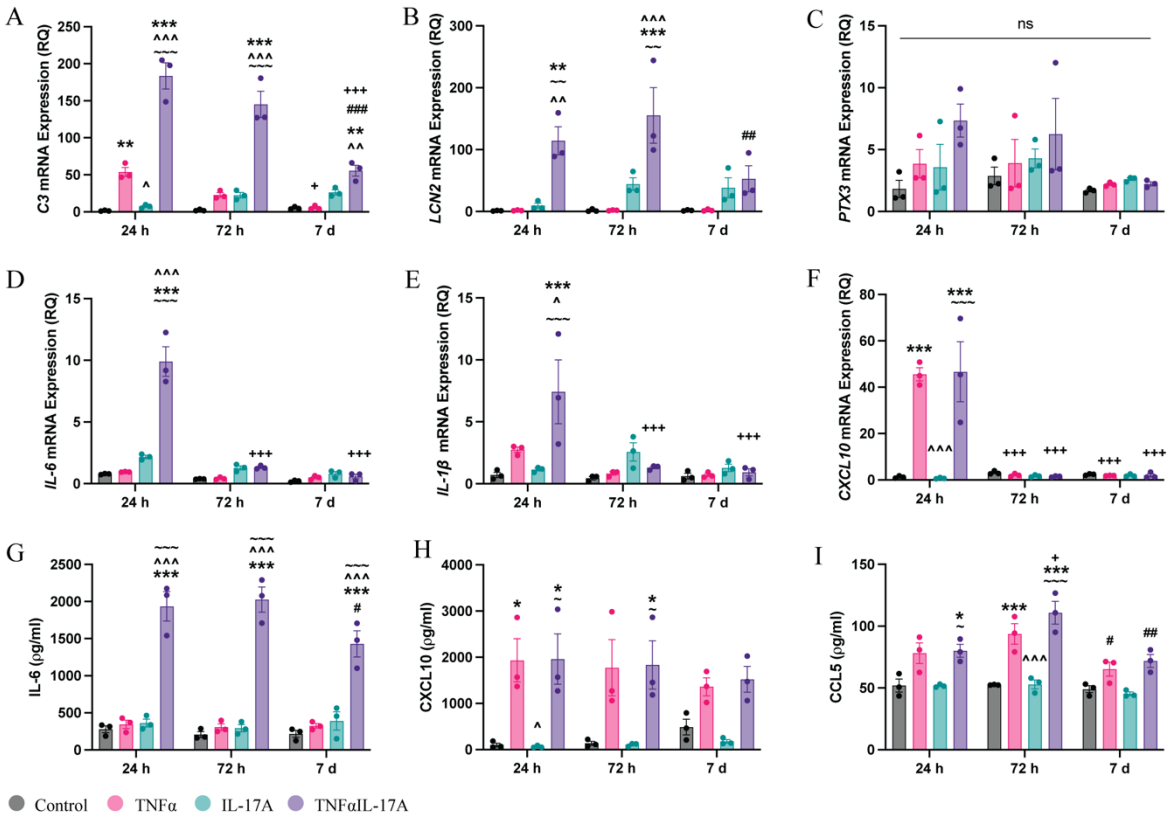

Figure 3.3.4. TNFα and IL-17A induced variable alterations in vmAstros reactivity associated gene expression and protein secretion.

*mRNA expression levels of (A) C3, (B) LCN2, (C) PTX3, (D) IL-6, (E) IL-1β, and (F) CXCL10. Secretion levels of (G) IL-6, (H) CXCL10 and (I) CCL5. Data expressed as ± SEM (N=3). *p<0.05, **p<0.01, ***p<0.001 vs control. ^p<0.05, ^^p<0.01, ^^^p<0.001 vs TNFα. ~p<0.05, ~~p<0.01, ~~~p<0.001 vs IL-17A. $^{+}$p<0.05, $^{+++}$p<0.001 vs 24 h. $^{\#}$p<0.05, $^{\#\#}$p<0.01, $^{\#\#\#}$p<0.001 vs 72 h. Three-way ANOVA with Tukey's post hoc.*

3.3.5. Morphological alterations indicative of reactive astrocyte phenotype induced by chronic cytokine exposure

Astrocytes have been observed to undergo morphological changes in response to induction of reactivity (Hyvarinen et al., 2019; Trindade et al., 2020). In order to assess whether these vmAstros exhibited morphological changes associated with their reactive phenotype, the astrocytes were stained with an antibody specific for S100β, and morphology was assessed. Significant increase in the expression of S100β at 24 h post-stimulation with TNFα and/or IL-17A was observed in all treatment groups (Fig 3.3.5. A-C). However, this upregulation was resolved by 72 h and 7 d post-stimulation (supplementary Fig. 4). Furthermore, no significant alteration in morphology was observed 24 h post-stimulation (supplemental Fig. 5). However, a significant reduction in nuclear area was observed for the TNFα+IL-17A group at 72 h, while this resolved by 7 d (Fig. 3.3.5. D and E). vmAstros demonstrated significantly increased circularity in both TNFα and combined TNFα+IL-17A groups at 72 h and 7 d post-stimulation (Fig. 3.3.5. E and F). Perimeter was decreased at 72 h, and 7 d however this only reached significance in the TNFα group (Fig. 3.3.5. D and E). In summary, TNFα and IL-17A exposure results in morphological changes in vmAstros associated with an inflammatory phenotype.

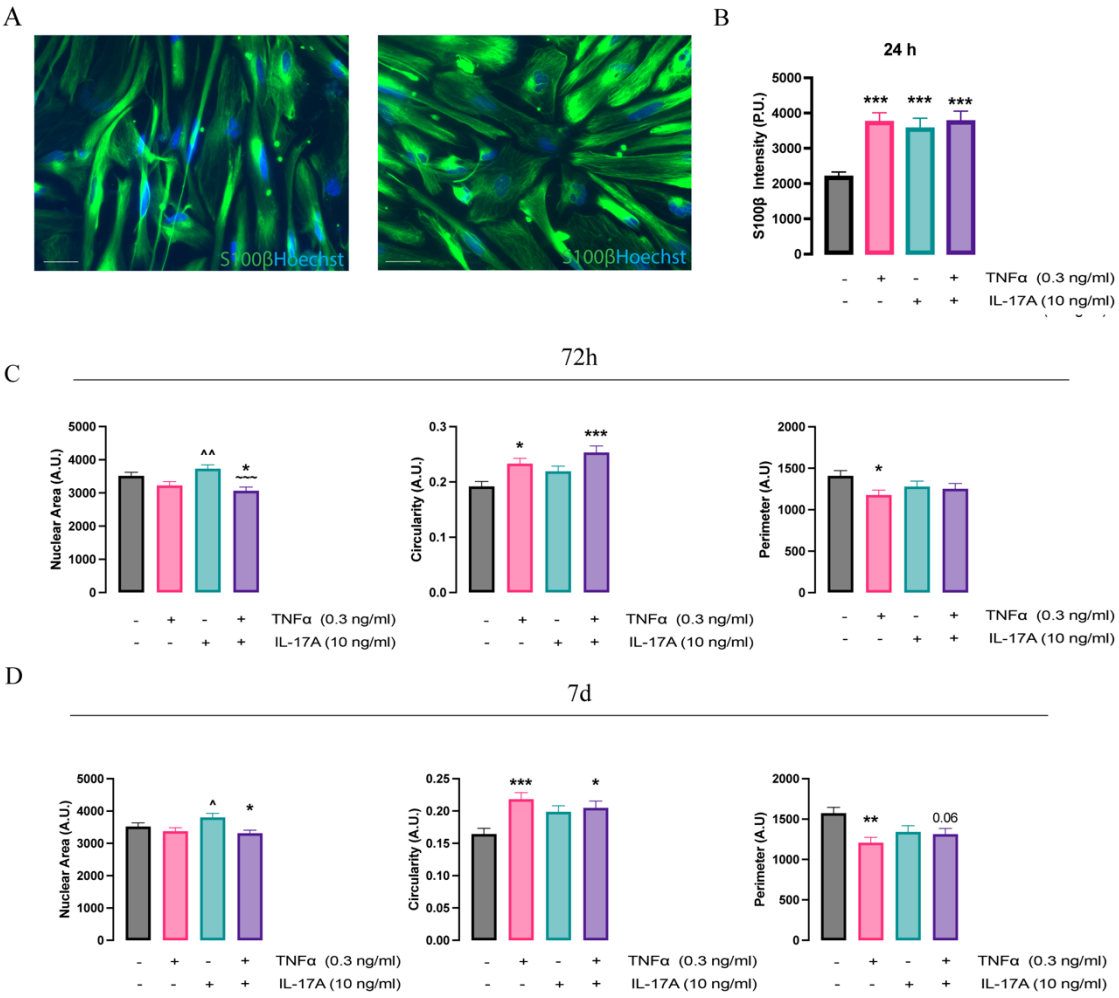

Figure 3.3.5. Cytokine stimulation results in significant morphological changes in vmAstros. *Representative images of S100β intensity changes following 24 h stimulation; (A) Control, (B) TNFα+IL-17A. C) graphical representation of S100β intensity analysis 24 h post-stimulation. Morphological analysis of nuclear area, perimeter, and circularity in vmAstros following (D) 72 h and (E) 7 d stimulation. Data expressed as ± SEM (N=3, where 100 cells were analysed per N). *p<0.05, **p<0.01, ***p<0.001 vs control. ^p<0.05, ^^p<0.01 vs TNFα. ~~~p<0.001 vs IL-17A. One-way ANOVA with Tukey's post hoc. Scale bars, 50 µm.*

3.3.6. Chronic cytokine exposure results in increased DNA damage and LDH release from vmAstros

In order to elucidate potential implications of long-term reactivity induced by TNFα and/or IL-17A on the astrocytes themselves we investigated indicators of cellular distress. Significant increase in the expression of γH2AX, indicative of double-stranded DNA breaks, was observed in the combined TNFα+IL-17A treatment group at 72 h post-stimulation (Fig. 3.3.6. A-C) while no change between groups was observed at the other timepoints (supplementary Fig. 6). Additionally, the vmAstros demonstrated increased secretion of LDH at 7 d post-stimulation, in the combined TNFα+IL-17A group compared with the control at 7 d as well as in comparison to the same treatment group at earlier timepoints, indicative of cell membrane disruption (Fig. 3.3.6. D). Indicating that chronic exposure to the cytokines, TNFα+IL-17A results in signs of cellular distress.

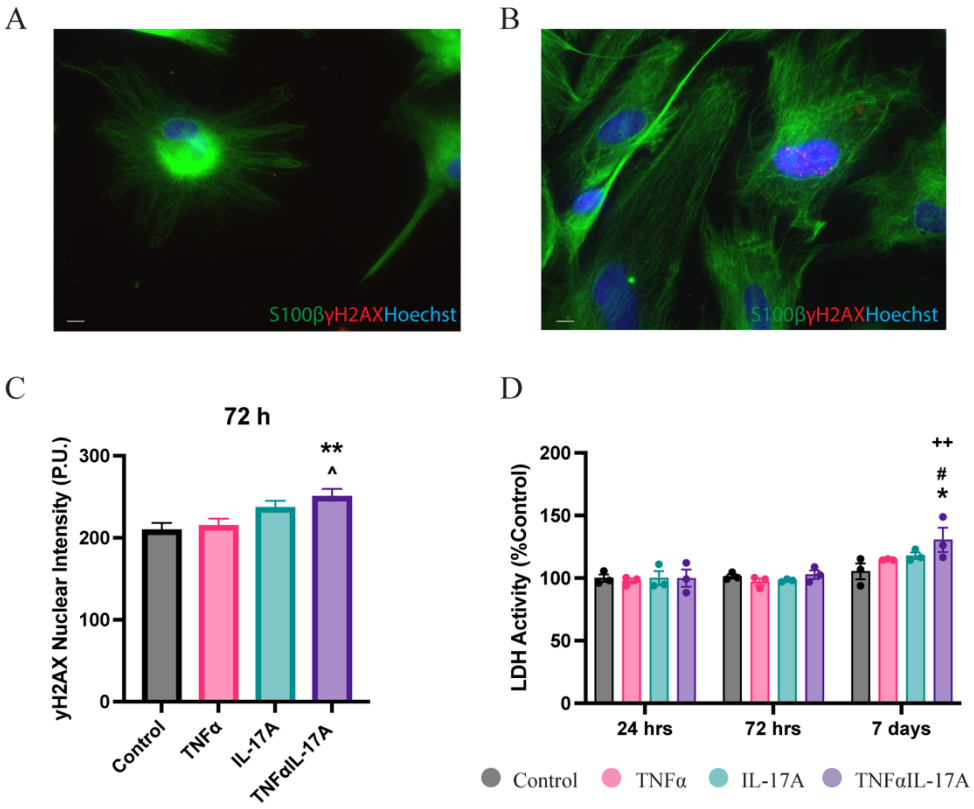

Figure 3.3.6. Chronic stimulation with TNFα+IL-17A induced distress in vmAstros.

*Representative images of γH2AX expression in (A) Control and (B) TNFα+IL-17A, 72 h post-stimulation. C) Analysis of nuclear intensity of γH2AX in vmAstros 72 h post-stimulation. D) Lactate dehydrogenase activity (LDH) represented as percentage of control following 24 h, 72 h and 7 d stimulation with either TNFα, IL-17A or TNFα+IL-17A. Data expressed as ± SEM (N=3, where 100 cells were analysed per N for γH2AX). *p<0.05, **p<0.01 vs control. ^p<0.05 vs TNFα. $^{++}$p<0.01 vs 24 h. $^{\#}$p<0.05 vs 72 h. One-way or two-way ANOVA with Tukey's post hoc. Scale bars, 10 µm.*

3.4. Discussion

The contribution of the immune system to the pathogenesis of Parkinson's disease is increasingly being recognised (for review see MacMahon Copas et al., 2021). However, despite evidence supporting infiltration of T cells into the brain and their subsequent negative effects on neurons as they have been repeatedly implicated in the pathogenesis of PD (Sommer et al., 2018), there is a paucity of information on their effects on glial cells such as astrocytes.

Therefore, the first aim of this study was to establish if and how vmAstros respond to $CD4^+$ T cells, as they have been repeatedly implicated in the pathogenesis of PD (Brochard et al., 2009; Sommer et al., 2018). This was achieved by exposing these cells to conditioned media from $CD4^+$ T cells, and their responsiveness to short- and long-term exposure was characterised. vmAstros responded by establishing a robust pro-inflammatory reactive astrocyte phenotype, including activation of the NFκB pathway at the one hour time point, synonymous with astrocyte reactivity (Lian et al., 2015; Liddelow & Barres, 2017). This is also in agreement with the timeframe of its nuclear translocation previously reported for human iPSC derived astrocytes in response to TNFα (Trindade et al., 2020). In addition, there was subsequent upregulation of key pro-inflammatory associated astrocyte genes (Liddelow et al., 2017), at 24 h including *IL-6, IL-1β, CXCL10* with the protein expression of CXCL10 persisting for 24 h and that of IL-6 persisting up to the 7 d timepoint. Such a persistent increase in IL-6 has previously been reported following treatment with IL-1β and TNFα (Hyvarinen et al., 2019) demonstrating that astrocytes have the ability to respond to a variety of cytokines including those known to be secreted by activated microglia (Liddelow et al., 2017).

While the $CD4^+$ T cell family includes various subsets, Th17 cells have gained the most interest in PD research of late, following studies demonstrating their involvement in inducing

degeneration of neurons (Sommer et al., 2018). In light of this, investigating whether Th17 cells and their signature cytokine, IL-17A, may be at the source of this pro-inflammatory response was the logical next step. Indeed, we show that our human vmAstros express the IL-17A receptor and respond robustly to IL-17A when administered in combination with TNFα. Interestingly, some studies have investigated the effect of IL-17A (Kostic et al., 2017; Yan et al., 2012; You et al., 2017), and TNFα separately on astrocytes (Hyvarinen et al., 2019; Trindade et al., 2020; Zhou et al., 2019), few have investigated the effect of IL-17A and TNFα in combination on human astrocytes. We observed a clear and robust synergistic relationship between TNFα and IL-17A on astrocyte pro-inflammatory gene expression and protein secretion, following a similar pattern to that seen with 10% CD4CM. Despite the lack of studies investigating this synergism on astrocytes differentiated from human iPSCs, the synergistic relationship between TNFα and IL-17A is well established in other cell types, mainly peripheral cells such as synoviocytes and fibroblasts (Beringer et al., 2018; Claire Q.F. Wang, 2013,; Noack et al., 2019; Zrioual et al., 2008). We demonstrated significant upregulation of pro-inflammatory factors such as IL-6 and *LCN2* which has been observed by others (Claire Q.F. Wang, 2013,; Zrioual et al., 2008). Interestingly, this synergistic relationship did not extend to the chemokines assessed; CCL5 and CXCL10 were increased by TNFα stimulation alone and this did not increase further when added with IL-17A. Other studies have observed a decrease in CCL5 following exposure to TNFα and IL-17A in combination, highlighting the differential mechanisms triggered in different cell types (Claire Q.F. Wang, 2013,; Zrioual et al., 2008). The variable of time is also a potential factor in differing responses observed across studies. Here we observed no significant change in CXCL10 at 24 h when both cytokines were administered together, which has been observed by others in a human fetal astrocyte cell line (Elain et al., 2014). However, Elain *et al.,* also noted an increase in CXCL10 prior to 24 h, suggesting the importance of assessing cellular changes across a broader range of time points.

Interestingly, in agreement with results for IL-6 obtained when CD4CM was added to astrocytes, there is a robust synergistic and persistent increase, following addition of TNFα and IL-17A in combination, in the levels of IL-6 over the 7 d examined. Indeed, it was recently reported that astrocytes generated from persons with Parkinson's have a higher baseline level of IL-6 than controls, which in turn was found to induce toxicity in dopamine neurons. Furthermore, these authors demonstrate that when the IL-6 receptor is blocked dopamine neuronal death is prevented (Pons-Espinal et al., 2024), highlighting the potential of IL-6 as a therapeutic target.

As expected the astrocytes express S100β, *GFAP* and *VIM*. Interestingly we did see an increase in the intensity of S100β protein following 24 h treatment with IL-17A, TNFα and both in combination, but the same was not seen for *GFAP* or *VIM* expression. While S100β is a crucial astrocytic protein, involved in a multitude of processes including, calcium homeostasis, cell proliferation, and cytoskeletal reorganisation, it has yet to be fully understood in the context of neurodegenerative disease (Donato et al., 2009). However, the upregulation and release of S100β from astrocytes has been observed in multiple neurological disorders (Langeh & Singh, 2021) and some studies, such as Clementi *et al.,* (2023) have reported an association between S100β upregulation following exposure to amyloid beta and increased cytotoxicity in astrocytes. It has previously been reported that GFAP is not always expressed by astrocytes in human brain tissue (Kettenmann et al., 2011), which could explain why we do not see a change in its expression in response to cytokine exposure in this human based model. Furthermore, in this study, we observed morphological changes at the longer term exposures, so following 72 h and 7 d. Such exposure time resulted in reduced nuclear area, and perimeter from 72 h onwards and increased circularity at 7 d post-stimulation, which has been indicative of a reactive astrocyte phenotype in other studies (Hyvarinen et al., 2019; Trindade et al., 2020).

Interestingly, our study demonstrated an increase in LDH and γH2AX following chronic cytokine exposure, indicative of cellular distress and potential cytotoxicity. DNA damage is associated with increased inflammation and studies have demonstrated that DNA damage can result in increased NFκB induced inflammation (Hinz et al., 2010; Kang et al., 2015). These results highlight a vicious cycle of inflammation, with infiltrating immune cells triggering a chronic reactive phenotype in astrocytes, increasing DNA damage, and potentially resulting in further inflammation. Additionally, LDH release is associated with primary and secondary necrosis (Chan et al., 2013), therefore the increased release of LDH from our astrocytes indicates some sense of distress and damage to the astrocytes occurring between 72 h and 7 d. LDH release is associated with primary and secondary necrosis (Chan et al., 2013). It is probable that mechanisms such as the increased DNA damage, and others are overwhelming the astrocyte. Again, due to the novelty of this area of peripheral immune cell interaction with glia in the context of PD, comparative literature is lacking, however, in agreement with this study Hyvarinen *et al.,* observed an increase in cytotoxicity and reduced viability following chronic stimulation with TNFα and IL1β for 7 d (Hyvarinen et al., 2019).

In summary, this study was able to elucidate the inflammatory response of vmAstros to peripheral immune secreted cytokines, including the combined synergistic effects of IL-17A with TNFα over a chronic period. Importantly, the data alluded to a potential cytotoxic effect of this chronic cytokine exposure on astrocytes. While these initial results have interesting connotations for astrocyte viability with the chronic inflammation present in PD, there is still a wide scope for further investigations uncovering mechanisms underlying this response and how this impacts astrocytes and their surrounding environment. Crucially, a better understanding of how inflammation is mediated in PD may help identify novel therapeutic

targets. Currently, there are a number of drugs which target immune responses in inflammatory diseases such as IL-17 pathway inhibitors which could potentially be repurposed for PD.

3.5. Supplemental

Supplemental Table 1. Immunocytochemistry Antibodies

Manufacturer	*Target*	*Antibody*	*Dilution*
Sigma-Aldrich	S100β	S2532	1 in 1000
Sigma-Aldrich	GFAP	AB5541	1 in 1000
Cell Signalling	NFκB	8242	1 in 500
Cell Signalling	γH2AX	9718	1 in 1000
Bio-Techne	EAAT1	NBPI-20135	1 in 1000
Sigma	αConnexin-43	C6219	1 in 1000
Bioss	IL-17RA	BS-2606R	1 in 100
Merk	LMX1A	AB10533	1 in 1000
ThermoFisher Scientific	Donkey anti-mouse	Alexa Fluor 488, A21202	1 in 500
ThermoFisher Scientific	Goat anti-rabbit	Alexa Fluor 555, A21428	1 in 500
abcam	Goat anti-chicken	Alexa Fluor 488, ab150169	1 in 500

Supplemental Table 2. RT-qPCR Primers

Primers	***Gene Name***	***Company***	***Assay Number***
GAPDH	Endogenous control primer; Glyceraldehyde-3-Phosphate Dehydrogenase	ThermoFisher Scientific	Hs02786624_g1
IL-17RA	Interleukin 17 receptor A	ThermoFisher Scientific	Hs01056316_m1
IL-6	Interleukin 6	ThermoFisher Scientific	Hs00174131_m1
PTX3	Pentraxin-related protein	ThermoFisher Scientific	Hs00173615_m1
C3	Complement component 3	ThermoFisher Scientific	Hs00163811_m1
GFAP	Glial fibrillary acidic protein	ThermoFisher Scientific	Hs00909233_m1
ICAM1	Intracellular adhesion molecule 1	ThermoFisher Scientific	Hs00164932_m1
ITGA6	Integrin subunit alpha 6	ThermoFisher Scientific	Hs01041011_m1
SERPINA3	Serpin family A member 3	ThermoFisher Scientific	Hs00153674_m1
TIMP1	TIMP metallopeptidase 1	ThermoFisher Scientific	Hs01092512_g1
IL-1β	Interleukin 1 β	ThermoFisher Scientific	Hs01555410_m1
CXCL10	C-X-C motif chemokine ligand 10	ThermoFisher Scientific	Hs00171042_m1
LCN2	Lipocalin 2	ThermoFisher Scientific	Hs01008571_m1
VIM	Vimentin	ThermoFisher Scientific	Hs00958111_m1

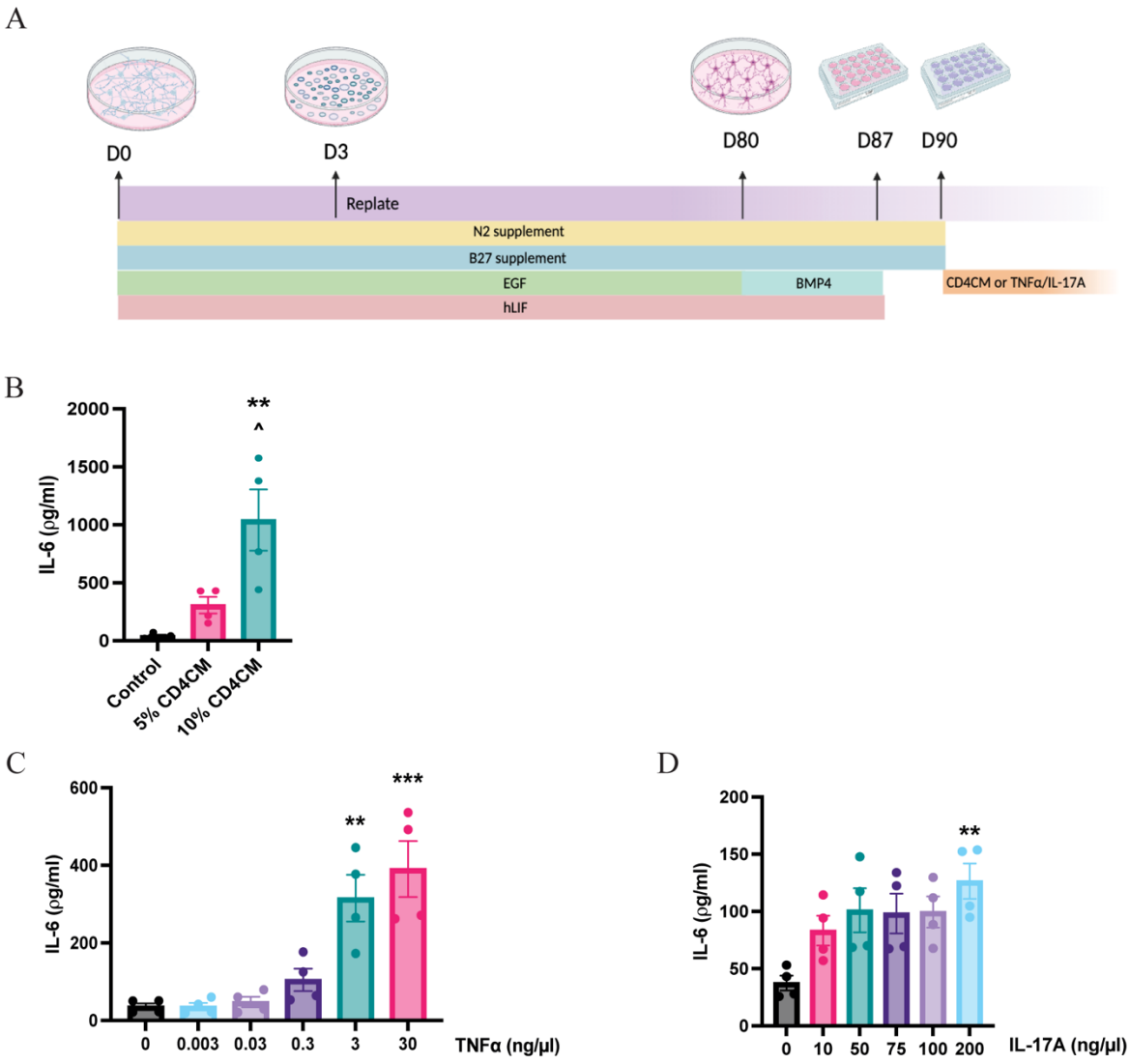

Supplemental Figure 1.

*Astrocyte culture and treatment timeline, as per Crompton et al. (2021) (A) Dose-response for (B) CD4⁺ T cell conditioned media (CD4CM), (C) TNFα, and (D) IL-17A. Data expressed as ± SEM (N=4). **p<0.01, ***p<0.001 vs control. ^p<0.05 vs 5% CD4CM. One-way ANOVA with Tukey's post-hoc.*

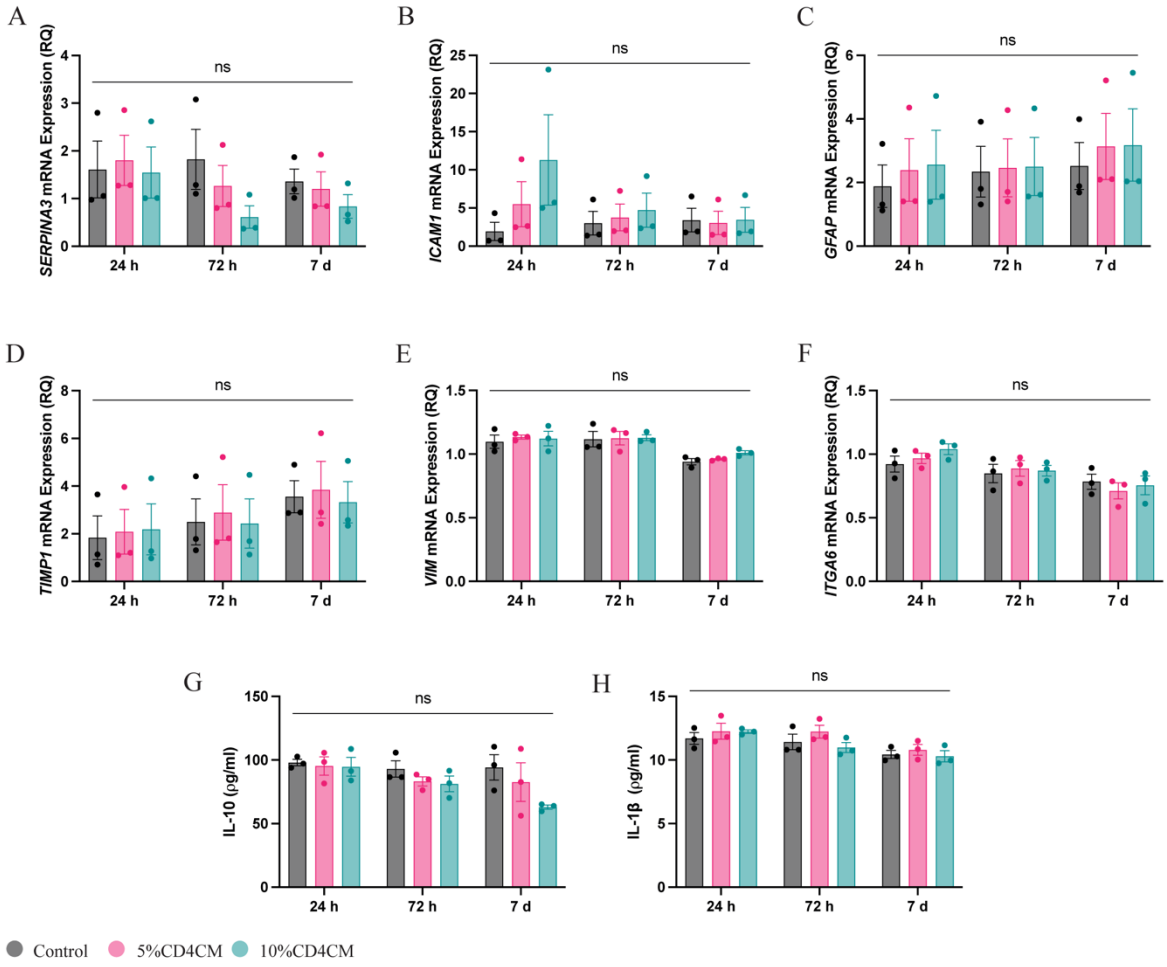

Supplementary Figure 2. Gene and protein analysis of vmAstros following stimulation with CD4CM.

mRNA expression levels of (A) SERPINA3, (B) ICAM1, (C) GFAP, (D) TIMP1, (E) VIM, (F) ITGA6. Protein secretion levels of IL-10 (G) and IL-1β (H). Data expressed as ± SEM (N=3). Two-way ANOVA.

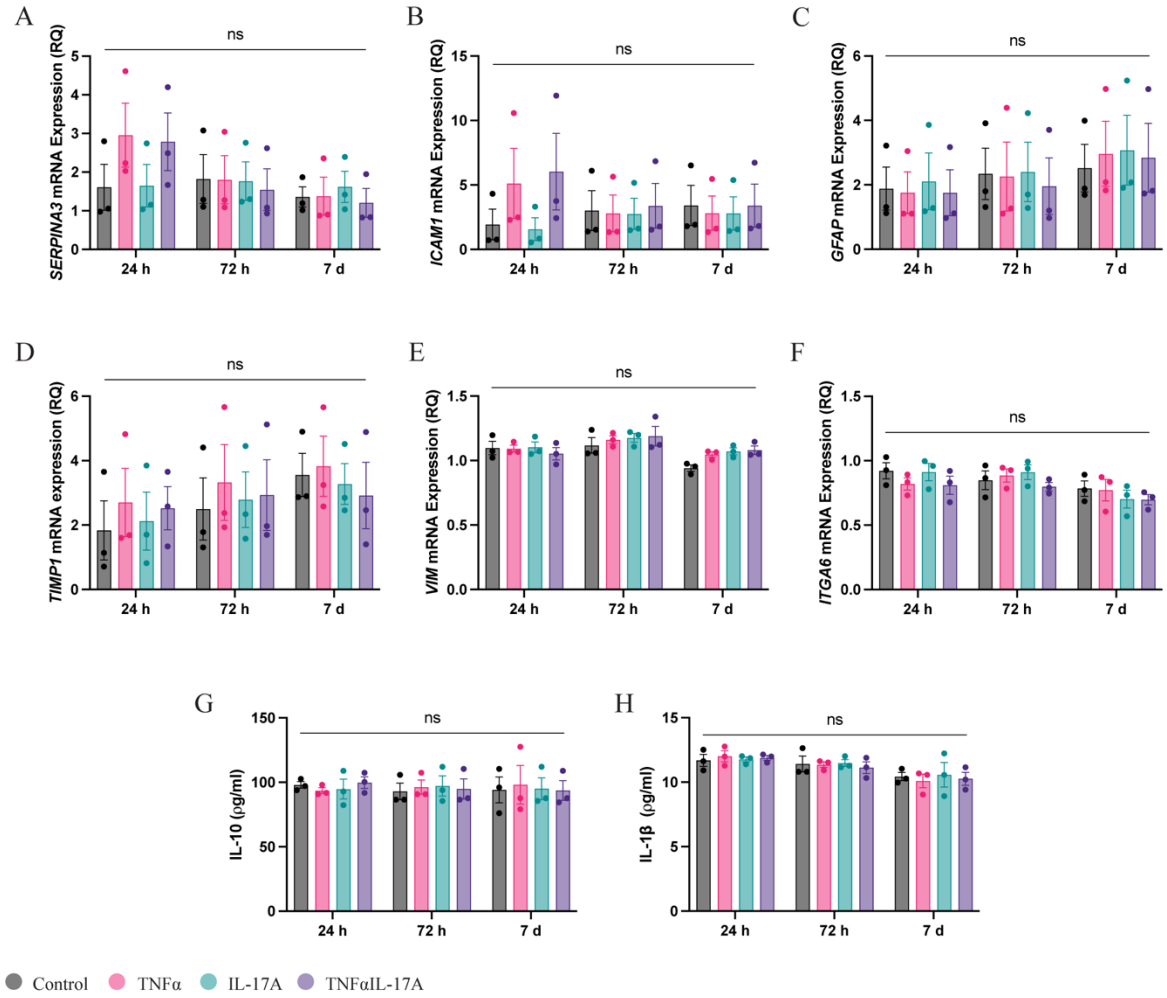

Supplementary Figure 3. Gene expression and protein secretion from vmAstros following stimulation with TNFα, IL-17A or TNFα+IL-17A.

mRNA expression levels of (A) SERPINA3, (B) ICAM1, (C) GFAP, (D) TIMP1, (E) VIM, (F) ITGA6 and protein secretion levels of (G) IL-10, and (H) IL-1β. Data expressed as ± SEM (N=3). Three-way ANOVA.

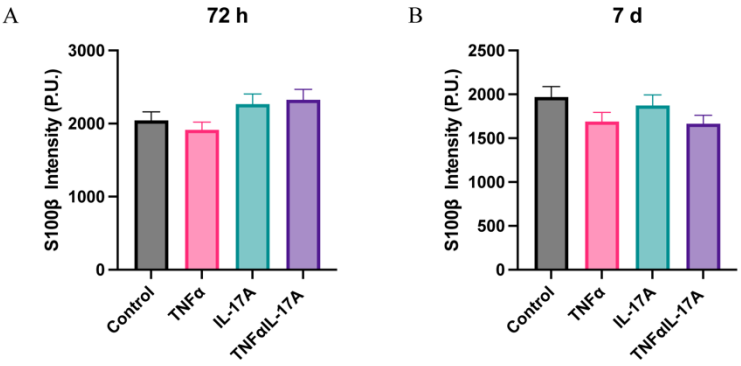

Supplementary Figure 4. **Immunocytochemical analysis of S100β intensity changes in vmAstros following stimulation.**

72 h (A) and 7 d (B). Data expressed as ± SEM (N=3, where 100 cells were analysed per N). One-way ANOVA.

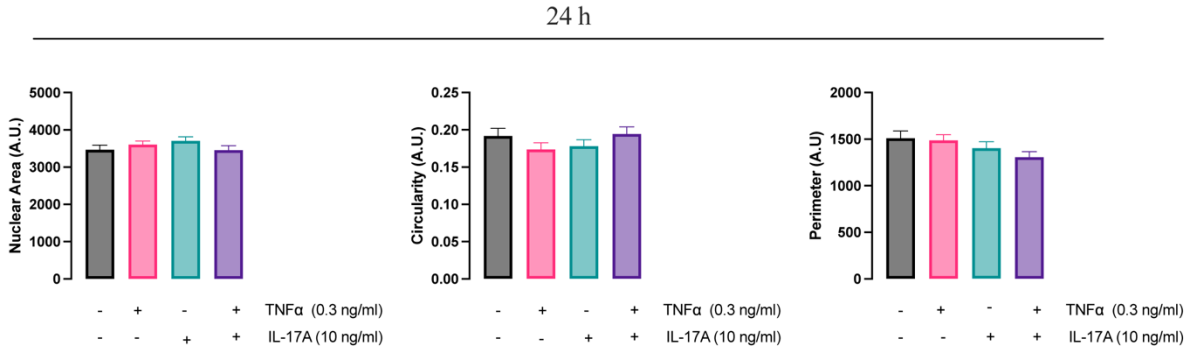

Supplementary Figure 5. Morphological analysis of vmAstros following 24 h stimulation with cytokines TNFα, and IL-17A.

Data expressed as ± SEM (N=3, where 100 cells were analysed per N). One-way ANOVA.

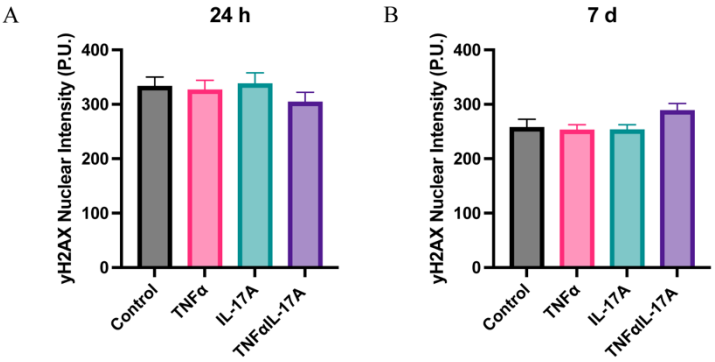

Supplementary Figure 6. Immunocytochemical analysis of γH2AX expression in vmAstros following stimulation.

24 h (A) and 7 d (B). Data expressed as ± SEM (N=3, where 100 cells were analysed per N). One-way ANOVA.

Chapter 4 : Generating Parkinson's disease patient-derived iPSC

4.1. Introduction

Described in detail in Chapter 1, iPSC are pluripotent cells generated from somatic cells, which are capable of differentiating into any cell type of the three germ layers: endoderm, mesoderm and ectoderm. Many alterations have been made to the original protocol outlined by Yamanaka and colleagues in 2006 which are summarised below in Fig. 4.1.1. The protocol we followed in this study is that of Okita and colleagues from 2011, in which they utilise non-integrating episomal plasmid vectors containing the genetic material for OCT3/4, SOX2, KLF-4, L-Myc, Lin 28 and a p53 shRNA (Okita et al., 2011).

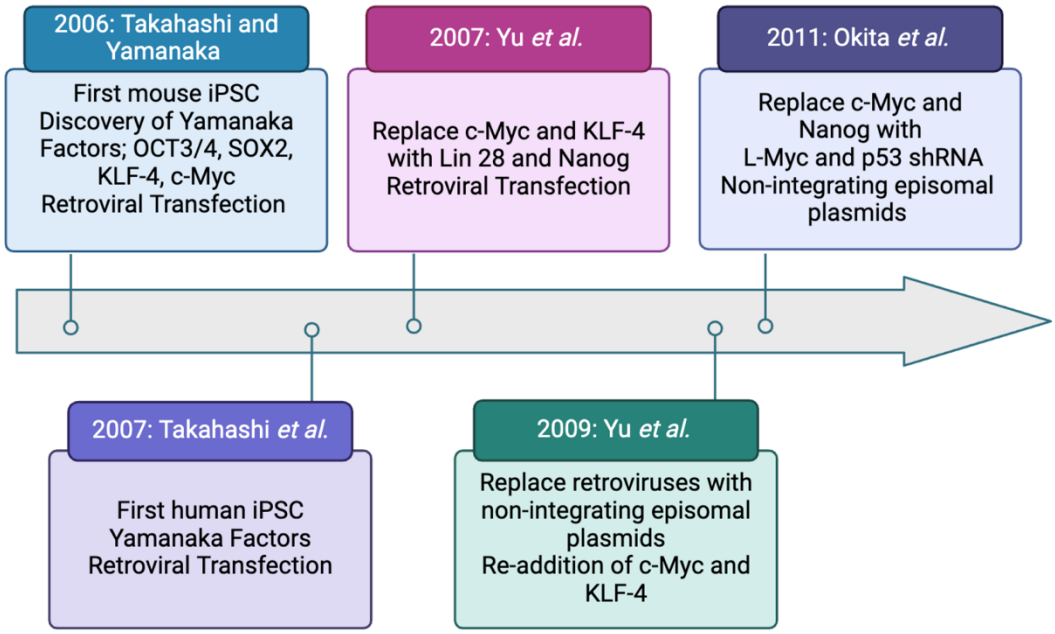

Figure 4.1.1. Major changes to the protocol for deriving induce pluripotent stem cells since its initial discovery.

4.1.1. Characterisation of induced pluripotent stem cells

In order to ensure that the newly reprogrammed cells are in fact pluripotent, there are numerous methods to characterise these cells (Castro-Vinuelas et al., 2020; Okita et al., 2011; Takahashi

et al., 2007; Takahashi & Yamanaka, 2006; Vlahos et al., 2019; Yu et al., 2009). The main determinants of a successful reprogramming are the visible morphological changes consistent with pluripotent stem cells, the expression of pluripotency associated factors and the ability to generate cells of the three germ layers (Okita et al., 2011; Takahashi et al., 2007; Takahashi & Yamanaka, 2006; Yu et al., 2009).

The first indication of a successful reprogramming process is the cells appearing visibly as you would expect ESC and iPSC to appear. The morphological characteristics of stem cells are; scant cytoplasm, large nuclei, round colonies with defined borders (Okita et al., 2011; Takahashi et al., 2007; Takahashi & Yamanaka, 2006; Yu et al., 2009). Following this, iPSC are usually taken for confirmation of the expression of pluripotency markers, both gene and protein expression are usually confirmed (Castro-Vinuelas et al., 2020; Okita et al., 2007; Okita et al., 2011; Takahashi et al., 2007; Vlahos et al., 2019; Yu et al., 2009; Yu et al., 2007). Commonly observed markers are Oct3/4, Sox2, Nanog, Tra-1-60, Tra-1-81, among numerous others. Furthermore, the assessment of the ability of the iPSC to differentiate into cells of the three germ layers; the endoderm, mesoderm and ectoderm can be assessed in different ways; however, all yield the same conclusions (Castro-Vinuelas et al., 2020; Okita et al., 2007; Okita et al., 2011; Takahashi et al., 2007; Vlahos et al., 2019; Yu et al., 2009; Yu et al., 2007). iPSC can either be allowed to form embryoid bodies *in vitro* and left to spontaneously differentiate, which should yield cells from all germ layers, otherwise the cells can be injected *in vivo* and should form teratomas (Castro-Vinuelas et al., 2020; Okita et al., 2007; Okita et al., 2011; Takahashi et al., 2007; Vlahos et al., 2019; Yu et al., 2009; Yu et al., 2007). The cells are then assessed for expression of markers of the three germ layers again either using immunocytochemistry to assess protein expression or PCR to assess gene expression (Castro-Vinuelas et al., 2020; Okita et al., 2007; Okita et al., 2011; Takahashi et al., 2007; Vlahos et

al., 2019; Yu et al., 2009; Yu et al., 2007). In addition to this, alkaline phosphatase activity can be assessed on live cells to determine expression of this common pluripotency associated protein, that is downregulated upon differentiation of cells towards their terminal lineage (Takahashi et al., 2007; Takahashi & Yamanaka, 2006). Furthermore, due to potential genetic issues with the reprogramming of cells, it is common to karyotype the iPSC generated to determine that they possess a normal karyotypic phenotype (Castro-Vinuelas et al., 2020; Okita et al., 2007; Okita et al., 2011; Takahashi et al., 2007; Vlahos et al., 2019; Yu et al., 2009; Yu et al., 2007). This is particularly important to assess before taking the cells into the clinic.

4.1.2. Aims

Patient-derived iPSC provide endless possibilities for the understanding and therapeutic targeting of disease associated mechanisms. Therefore, the aims of this project are as follows.

1. To reprogramme HDF back to a pluripotent state
2. To confirm pluripotency through the expression of pluripotency genes and proteins
3. Provide evidence of the ability of the generated iPSC to from cells of the three germ layers

The hypothesis here is that with electroporation assisted transfer of episomal plasmid vectors containing the pluripotency-associated genes of *OCT3/4, Sox2, KLF-4, Lin28, L-Myc* and shp53, as well as GFP for visualisation of transfection success, into somatic HDF, these cells will reprogramme into a pluripotent state, as described by Okita and colleagues (Okita et al., 2011). This pluripotent state will be confirmed by expression of markers of pluripotency such as TRA-1-60, TRA-1-81, Nanog, Sox2 and OCT3/4. The reprogrammed cells should also be found to behave as ESC-like, iPSC, as previously described, and demonstrate their ability to differentiate into the trilineages, the endoderm, mesoderm and ectoderm (Okita et al., 2011).

This will be apparent through a down-regulation of pluripotency genes, such as *OCT3/4*, and an upregulation of genes representative of the three germ layers, such as *OTX2* (ectoderm), *ALB* (endoderm) and *HAND1* (mesoderm).

4.2. Materials and methods

4.2.1. Dermal punch biopsy

4.2.1.1. Preparation of dermal punch biopsy

Human dermal punch biopsies were collected with consent from 6 PD patients (Table 4.2.1). Biopsies were collected from the upper back/arm of patients by a dermatologist from the Mater Hospital, in collaboration with Professor Tim Lynch's group at the Neurology Clinic, Mater Hospital. The biopsy is minimally invasive, using a 3 mm punch biopsy to acquire the sample. Samples are stored on ice in human dermal fibroblast medium (HDF medium; Appendix 1 Table 1) until processed. Biopsies were cut into 4 equal pieces on a sterile petri dish using a scalpel blade. Each of the 4 pieces were placed into their own well of a 24-well plate coated with a 1X Geltrex solution (Life Tech, ThermoFisher Scientific). Care was taken to ensure the dermis is facing down onto the Geltrex solution. HDF medium was then added slowly to submerge the biopsy, while leaving the tip of the biopsy exposed. The plate was then added to an incubator at 37°C, 5% CO_2. The biopsies were fed every 3 to 4 d removing half of the spent medium and replacing with fresh HDF medium. After approximately 1 week, fibroblasts outgrowth from the biopsy is visible and at this point the well can be flooded with medium, covering the biopsy entirely.

Table 4.2.1. Patient cell line information.

Y = Yes, N= No.

Biopsy Number	***Cell Line Code***	***HDF***	***iPSC***
1	PD01	Y	N
2	PD02	Y	N
3	PD03	Y	Y
4	PD04	Y	Y
5	PD05	Y	Y
6	PD06	Y	Y

4.2.1.2. Culture and expansion of human dermal fibroblasts

Once the fibroblast outgrowth from the biopsy had reached 100% confluency the cells were split. Spent media was removed from the well and discarded. The biopsy containing well was gently washed with PBS and TrypLE^{TM} Express Enzyme (ThermoFisher Scientific) detachment solution was added for 5 min at 37°C. The cells were then collected using HDF medium and the biopsy discarded appropriately. Cells were centrifuged at 178 x g for 3 min at RT. The cells were resuspended in HDF medium and added to a 12 well plate. Fibroblasts were cryopreserved from passage 3 (P3) onwards.

4.2.1.3. Mouse embryonic fibroblasts as a feeder layer for iPSC

Mouse embryonic fibroblasts (MEF) were cultured on 0.1% Gelatin coated plates (30 min, RT; EmbryoMax) in MEF medium (Appendix 1 Table 2). Trypsin EDTA (ThermoFisher Scientific) was used to detach cells for 3 min at 37°C. Between P3 to P5, MEFs can be inactivated using mitomycin C to arrest cell proliferation, allowing them to become a feeder

layer. Spent medium is replaced with 1X mitomycin C solution and incubated for 2 h at 37°C, 5% CO_2. Cells were washed twice with PBS and fresh MEF media added. Inactivated MEFs were then seeded on 0.1% Gelatin coated plates at a density of $6x10^4/cm^2$. Medium was changed to human embryonic stem cell medium (hES; Appendix 1 Table 3) medium 2 h before seeding iPSC.

4.2.2. Reprogramming of human fibroblasts to iPSC

4.2.2.1. Nucleofection of human fibroblasts

HDF which had been expanded to P5 were taken for reprogramming once at 70-90% confluency. Reprogramming was carried out using the HDF nucleofector kit (Lonza). TrypLE™ Express was used to dissociate cells for 3 min at 37°C. Cells were collected in HDF media and centrifuged for 3 min at 178 x g at RT. Cells were counted and $80x10^5$ cells were taken to reprogramme. Cells were centrifuged at 178 x g for 3 min to form a pellet which was then resuspended in transfection buffer (Lonza). Plasmids were added at 1 μg/100 μl (Table 4.2.2.). This solution was then added to the transfection cuvette, ensuring bubbles did not form. The cuvette was added to the nucleofector 2b machine (Lonza) and the U-023 program was run on the sample. Cells were immediately resuspended in HDF medium, which had been added to the MEF feeder layer at least 2 h prior to nucleofection. Avoiding the layer of dead cells, cells were removed from the cuvette and transferred dropwise into the plate containing the MEF feeder layer. Cells were evenly distributed across the well and incubated at 37°C, 5% CO_2.

Table 4.2.2. Reprogramming plasmids

Plasmid name	***Genes***	***Manufacturer***	***Code***
pCE-hSK	SOX2 and KLF4	Addgene	41814
pCE-hUL	human L-MYC and LIN28	Addgene	41855
pCXCLE-hOCT3/4-shp53-F	Human OCT3/4 and shRNA against p53	Addgene	27077
pCE-GFP	Green fluorescent protein (GFP)	addgene	41858

4.2.2.2. Culture of reprogramming cells

D2 post-nucleofection, the media was changed from HDF medium to reprogramming medium (RM; Appendix 1 Table 4). From D1–D16 post-nucleofection green fluorescent protein (GFP) expression was monitored to indicate successful insertion of plasmids. Colonies began to appear from D14 onwards. Between D18 and D20 reduction of inhibitors: PD0325901, CHIR99021, Sodium Butyrate and A-83-01 occurred gradually. Fibroblast growth factor 2 (FGF2) was then reduced by 10-20 ng/ml every 2 d until concentration reached 0 ng/ml, except on passaging days. Early colonies of cells were passaged using mechanical picking. At least 1 h prior to passaging, Y27632 (10 μM) was added to the well and to the prepared plate containing fresh MEF feeder cells. Colonies with typical iPSC morphology of dense tightly packed colonies of cells with scant cytoplasm and defined borders were picked from the well. They were cut out of the MEF feeder layer and transferred in RM to a sterile petri dish. The colonies were dissociated using sterile needles to expose cells at the centre of the colony. The dissociated colony was then transferred into a fresh well of MEF feeder cells in RM. Each individual colony picked from the original well of reprogramming cells is a separate clone of that cell line. Once multiple colonies with consistent morphology appeared in the same well, cells were dissociated using a chemical dissociation agent, ethylenediaminetetraacetic acid

(EDTA; ThermoFisher Scientific) for 3 min at RT, in combination with mechanical passaging. Stocks of reprogrammed cells were cryopreserved from P5 onwards (Fig. 4.2.1.).

4.2.2.3. Transition of cells from MEF feeder layer to a feeder free system

Cells were passaged from the MEF feeder layer directly onto vitronectin (ThermoFisher Scientific) coated plates. Cells were fed with MEF-conditioned hES medium, which was gradually reduced as the cells adjusted, to 100% E8 Flex medium (Fig. 4.2.1.; BioSciences ltd).

4.2.2.4. Removal of spontaneous differentiation

Spontaneous differentiation can commonly occur both with the reduction in FGF2 and transition from feeder to feeder free. Spontaneously differentiating cells can take over iPSC cultures so it is important to monitor cultures for patches of differentiation and remove the differentiating cells as they appear. To attempt to reduce the level of differentiation from contaminating the culture, colonies free of differentiation were marked on the bottom of the well prior to splitting the cells. Then a P200 pipette was used to dislodge those cells to be split, leaving any differentiation to be discarded.

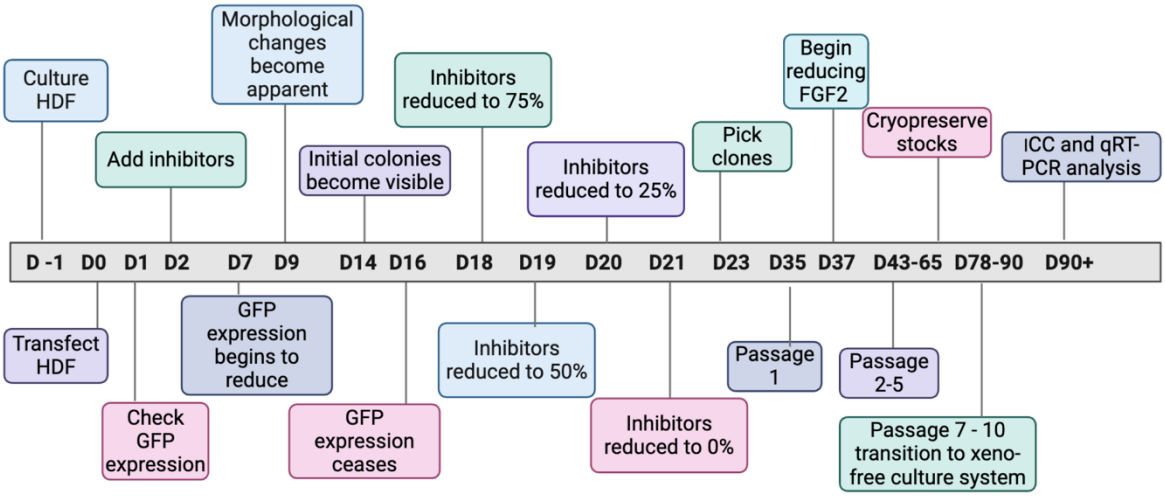

Figure 4.2.1. Timeline highlighting the key points of iPSC generation from HDF.

4.2.3. Trilineage differentiation

In order to assess the ability of the iPSC to differentiate into cells of the three germ layers they were forced to form embryoid bodies which were then allowed to differentiate spontaneously. To generate embryoid bodies, iPSC were detached using EDTA for 3 min at RT. Cells were added to ultra-low adherence plates (Greiner Bio-One International GmbH) to cause the iPSC to form embryoid bodies. After 6 d embryoid bodies were seeded on 0.1% Gelatin coated plates and allowed to differentiate unchecked for 14 d in embryoid body medium (EB; Appendix 1 Table 5). Following this the cells were lysed for RT-qPCR. An N=3 with 2 experimental replicates was analysed. The 1st replicate of the 1st N of iPSC was set to 1 for the gene POU5F1, while 1st replicate of the 1st N of the embryoid body samples was set to 1 for the genes *ALB, HAND1 and OTX2.* The replicates were averaged in Microsoft Excel to give a single value per N before final statistical analysis was carried out in GraphPad Prism using an unpaired T-test.

4.3. Results

4.3.1. The successful reprogramming of HDF into iPSC.

In order to investigate the cellular mechanisms at play in PD pathogenesis, we first needed to develop an appropriate cellular model of disease. Dermal punch biopsies were obtained from six people with sporadic PD (Fig. 4.3.1.). These biopsies could then be cultured in the lab to obtained dermal fibroblasts (Fig. 4.3.1.). To initiate reprogramming the fibroblasts were nucleofected with a cocktail of plasmids containing pluripotency-associated genes (Fig. 4.3.1.;Okita et al., 2011). To aid in determining the success of the nucleofection, the cocktail also contained a plasmid for GFP (Fig. 4.3.1.). The GFP fluoresces up until D7 post-nucleofection and continues to decline thereafter until D16 post-transfection at which point the genetic influence of the nucleofection has ceased in the cell (Fig. 4.3.1.).

Unfortunately, the generation of iPSC is not a straightforward process, and required some optimization. The initial reprogramming attempts failed due to attempting to place the nucleofected fibroblasts directly into a feeder free iPSC culture system. This resulted in a large amount of cell death and subsequent unsuccessful reprogramming (Fig. 4.3.2. A and B). As can be seen in Fig. 4.3.2. A and B below, there are very few cells, and those cells that do not appear to be fibroblast-like are exhibiting signs of spontaneous differentiation and do not display morphological characteristics of pluripotent stem cells (Fig. 4.3.2. B). Furthermore, the GFP expression in these reprogramming attempts was extremely low (Fig. 4.3.2. A), with approximately 1 cell in every field expressing GFP. Fig. 4.3.2. B demonstrates the unusual cell morphology experienced following transfection into a feeder free system (Fig. 4.3.2. B). Fig. 4.3.2 C below demonstrates poor reprogramming of HDF towards iPSC. The ‘fuzzy’ borders of the colonies depicted in Fig. 3.2. C are typical of cells which have not completely reprogrammed and thus do not display the characteristic iPSC defined borders. Fig. 4.3.2. D

also depicts another issue with iPSC culture and generation, through the process of initial colony formation and the transition of iPSC from the feeder system to feeder free, spontaneous differentiation can occur quite readily (Fig. 4.3.2. D). If not properly identified and removed, this spontaneous differentiation can quickly grow out of hand and take over an entire culture, rendering the cells no longer pluripotent.

However, upon transitioning to using a feeder layer of MEFs, the nucleofected cells exhibited much better survival rates (Fig. 4.3.3. A). The early morphological changes observed with reprogramming towards a pluripotent state can be seen in Fig. 4.3.3. A. The areas where morphological changes were evident, correlated to areas of high GFP expression which can be observed in Fig. 4.3.3. B.

Despite, the issues with iPSC generation, eventually successful reprogramming occurred and cells which demonstrated typical iPSC characteristics, such as formation of colonies of dense and tightly packed cells with a high nucleus to cytoplasm ratio and well-defined borders were observed (Fig. 4.3.4. A). These initial colonies were manually picked and expanded in culture to continue to reprogramming process until well-established iPSC colonies were achieved (Fig. 4.2.1). Past passage 5 the cells could be cryopreserved. Unfortunately, to achieve a xeno-free culture system, the generated iPSC needed to be transitioned off the MEF feeder layer. This involves the transition of the colonies of iPSC to a xeno-free extracellular matrix coating and the gradual titration of serum containing media to a completely xeno-free medium. Fig. 4 below depicts the iPSC colonies in the MEF feeder layer system (Fig. 4.3.4. A) and in the feeder-free, xeno-free culture system (Fig. 4.3.4. B). In total, six out of six biopsies were successfully cultured, four out of six were successfully reprogrammed to iPSC, and three out of six were taken forward for full characterization due to time constraints (Table 4.2.1.).

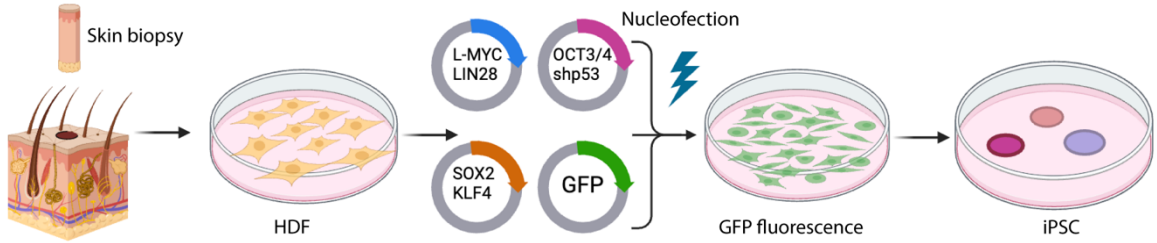

Figure 4.3.1. Generation iPSC from HDF.

Skin biopsy is obtained using a minute 3 mm dermal punch. Biposies are then cultured to give HDF which are subcultured to generate stocks. Episomal plasmids containing pluripotency genes are nucleofected into HDF. Cells reprogramme in culture. Generated with biorender.

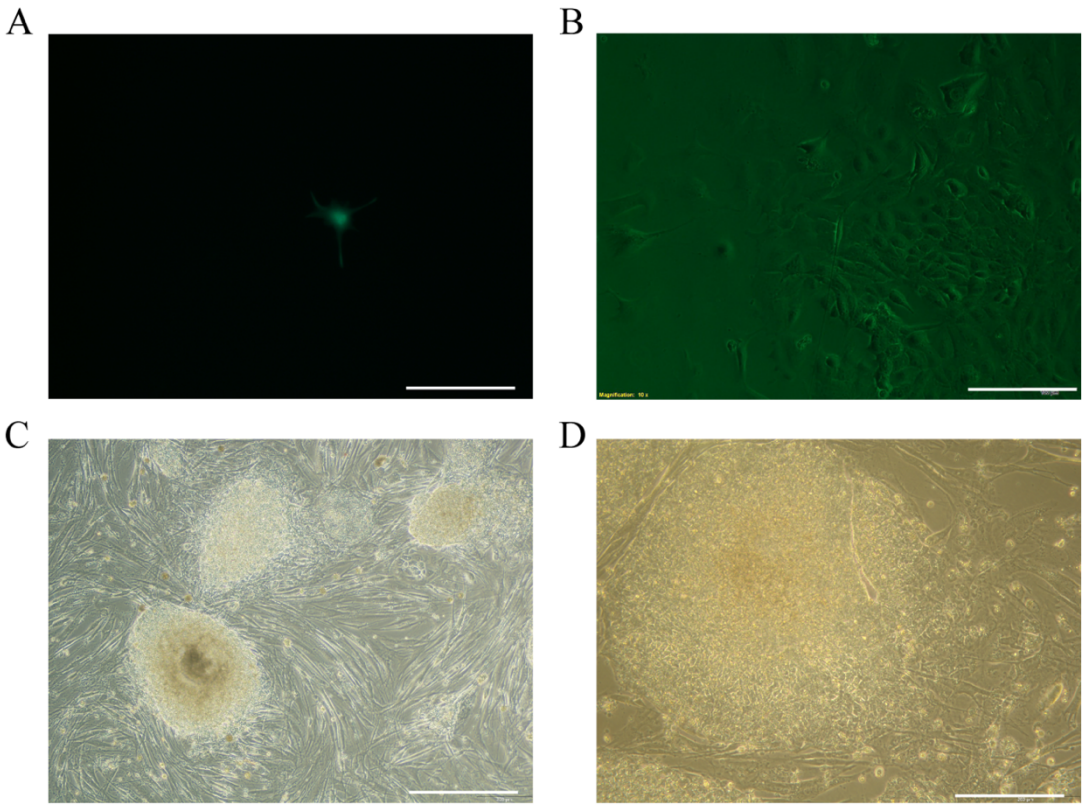

Figure 4.3.2. Troubleshooting the protocol for generation of iPSC.

Poor GFP expression post-nucleofection is linked to improper differentiation of cells to iPSC (A and B). Brightfield image demonstrates incomplete reprogramming of HDF to iPSC (C).

Brightfield image displays spontaneous differentiation of iPSC colonies, a common issue in iPSC culture (D). Scale bar, 200 µm.

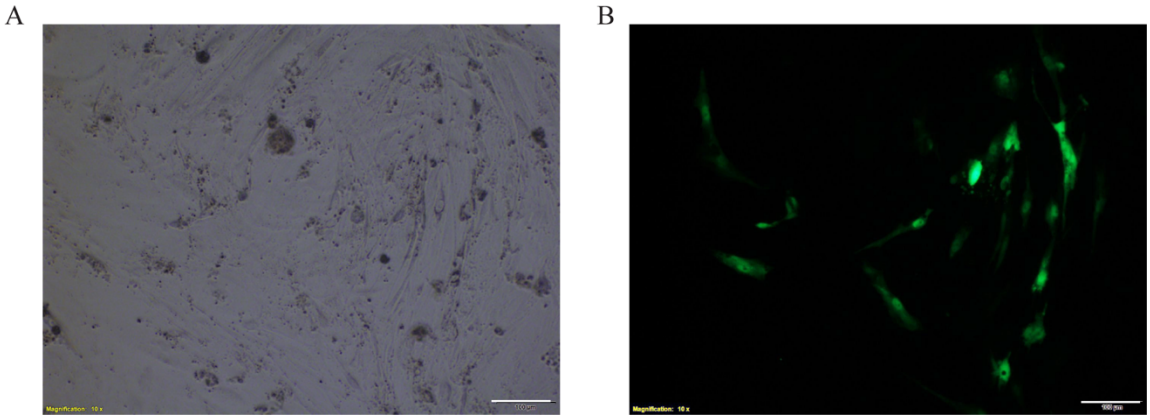

Figure 4.3.3. Morphological changes and GFP expression indicate successful reprogramming.

Corresponding Brightfield image (A) and GFP image (B) demonstrates early morphological changes associated reprogramming from HDF to iPSC. Scale bar, 100 µm.

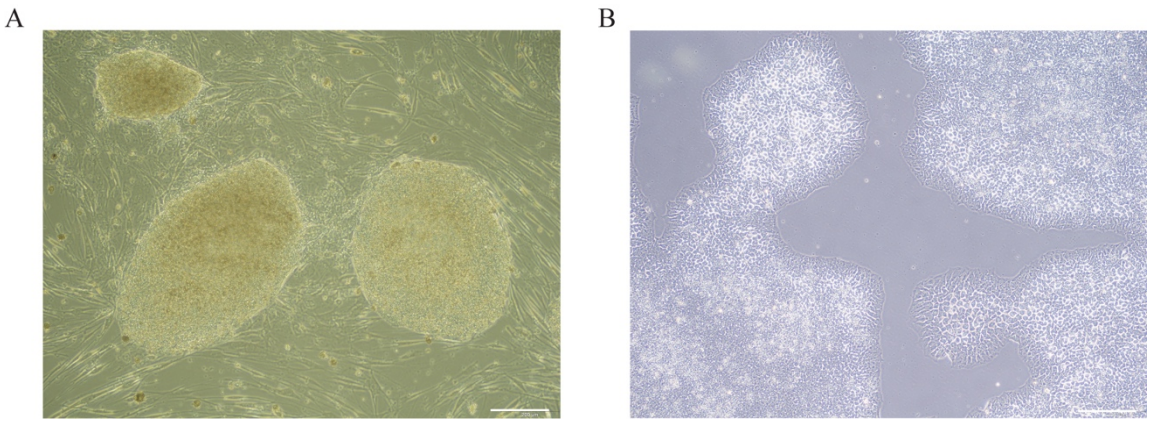

Figure 4.3.4. Transition of iPSC colonies from MEF feeder system to a feeder-free, xeno-free culture system.

A) Brightfield image demonstrating iPSC colonies on top of a bed of MEF feeder cells. B) Brightfield image illustrating iPSC colonies in a feeder-free system. Scale bar, 200 µm.

4.3.2. Confirmation of the successful reprogramming of HDF to iPSC.

In order to confirm that these cells have in fact been successfully reprogrammed from HDF and are truly pluripotent in nature. The first step in this process was to confirm that they express markers that are synonymous with pluripotent stem cells. We used immunocytochemistry to confirm the expression of intra and extracellular proteins found in all pluripotent stem cells. Intracellular markers of SOX2, NANOG, and OCT3/4 were expressed by all four iPSC lines generated (Fig. 4.3.5-8) as well as the extracellular markers of TRA-1-60 or TRA-1-81 (Fig. 4.3.5-8).

To further confirm their pluripotent state, we followed up assessment of protein expression with confirmation of gene expression of pluripotency genes (Fig. 4.3.9). The iPSC lines generated were assessed for their expression of pluripotency genes *POU5F1* and *NANOG* (Fig. 4.3.9 A and B). The well-characterised NAS2 iPSC line is used as a positive control and HDF are used as a negative control as they will not express the markers of pluripotency *POU5F1* and *NANOG* (Fig. 4.3.9).

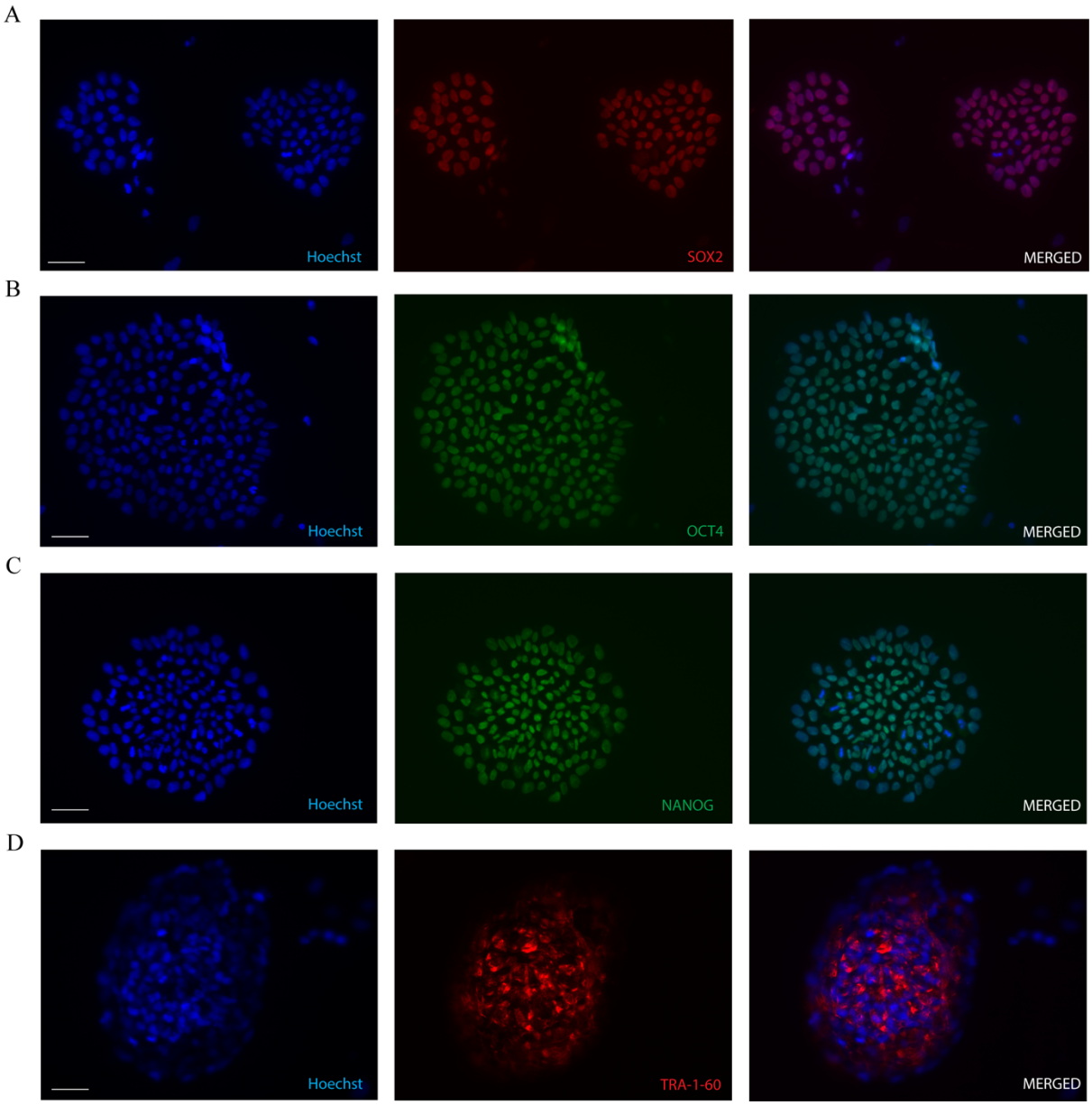

Figure 4.3.5. PD05 iPSC expresses intra and extracellular markers of pluripotency.

Immunocytochemistry staining demonstrates positive expression of intracellular markers of pluripotency; SOX2 (A), OCT4 (B), NANOG (C) and extracellular marker of pluripotency, TRA-1-60 (D). Scale bar, 50 µm.

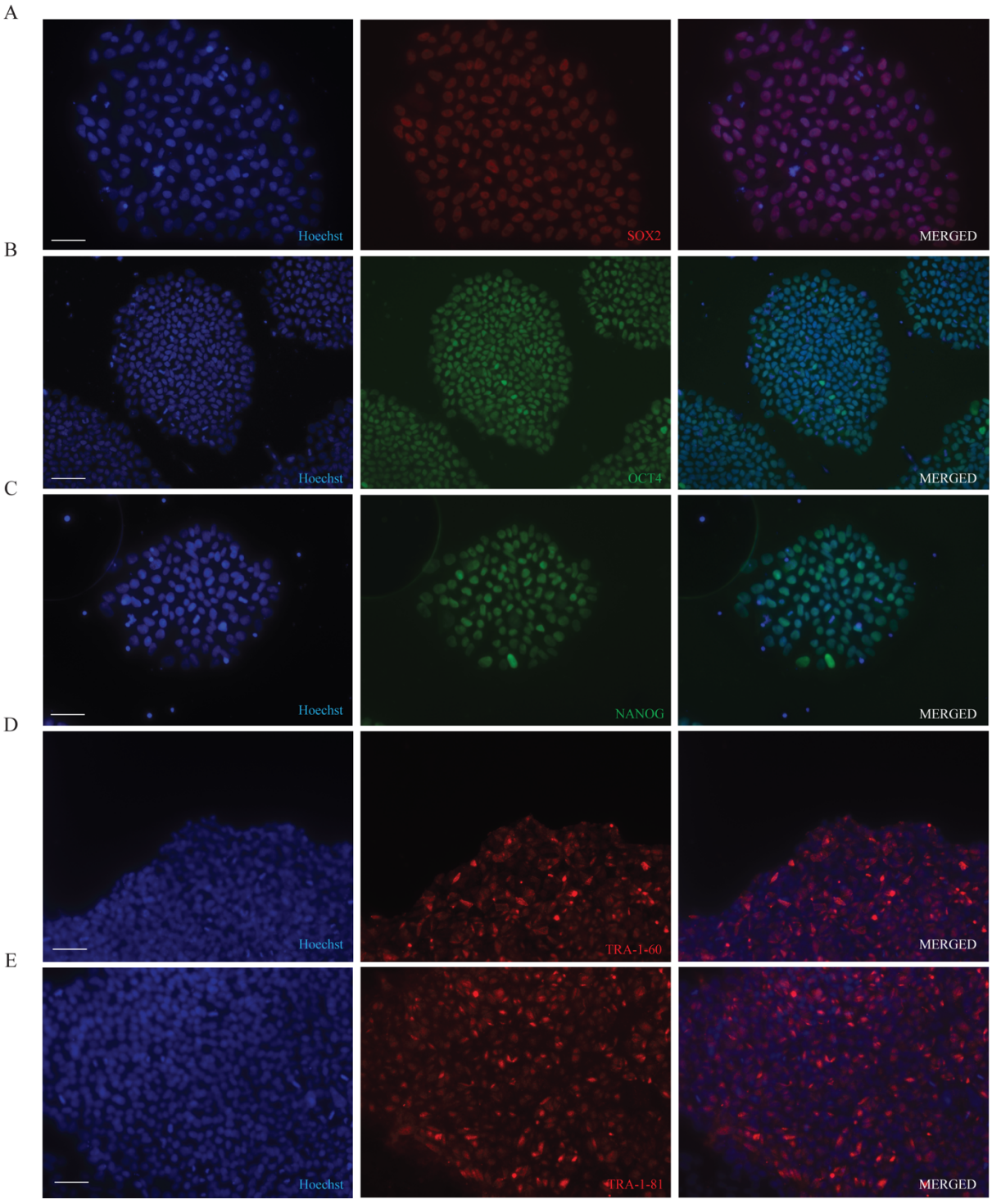

Figure 4.3.6. PD03 iPSC expresses intra and extracellular markers of pluripotency.

Immunocytochemistry staining demonstrates positive expression of intracellular markers of pluripotency; SOX2 (A), OCT4 (B), NANOG (C) and extracellular markers of pluripotency, TRA-1-60 (D) and TRA-1-81 (E). Scale bar, 50 µm.

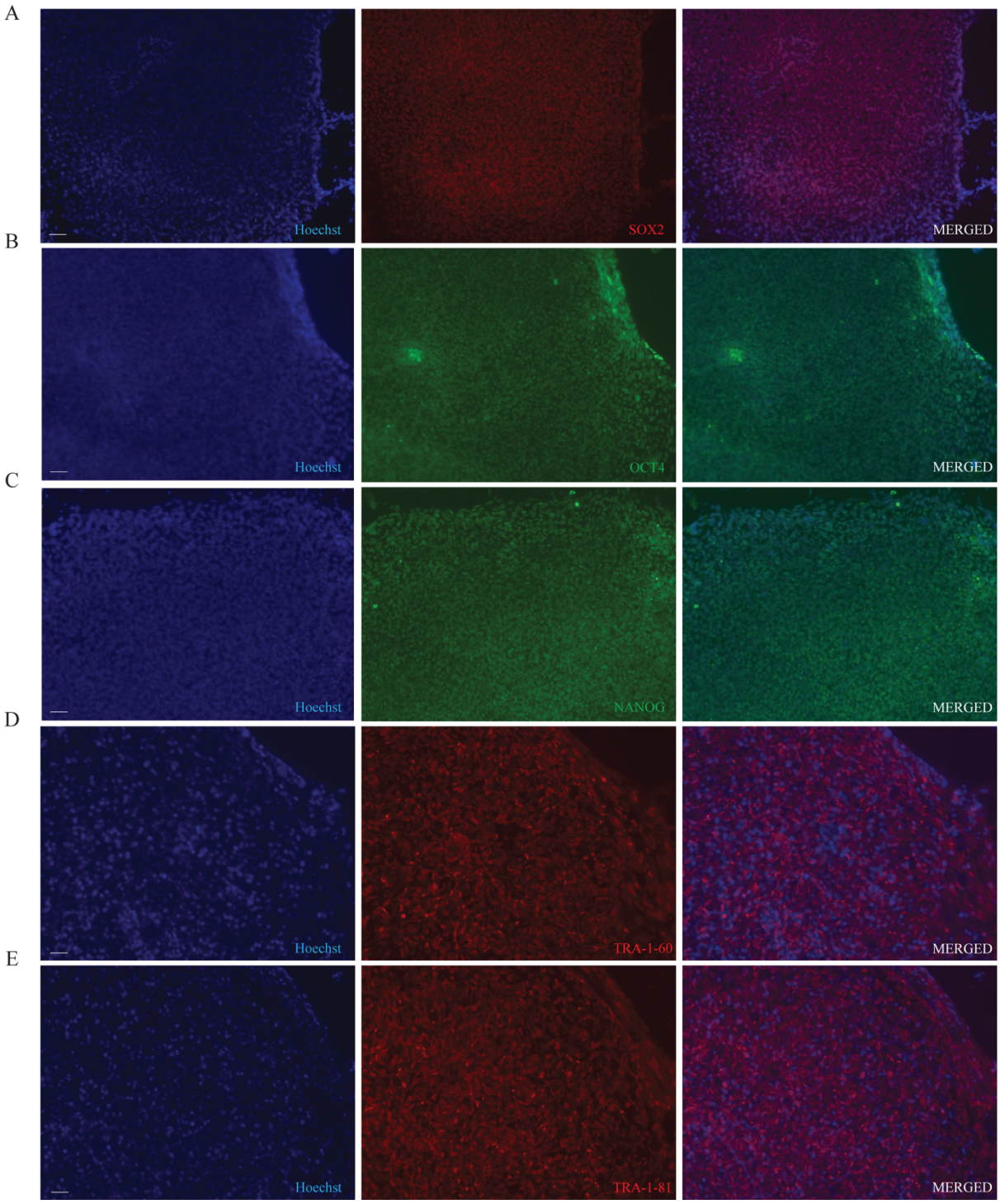

Figure 4.3.7. PD06 iPSC expresses intra and extracellular markers of pluripotency.

Immunocytochemistry staining demonstrates positive expression of intracellular markers of pluripotency; SOX2 (A), OCT4 (B), NANOG (C) and extracellular markers of pluripotency, TRA-1-60 (D) and TRA-1-81 (E). Scale bar, 50 µm.

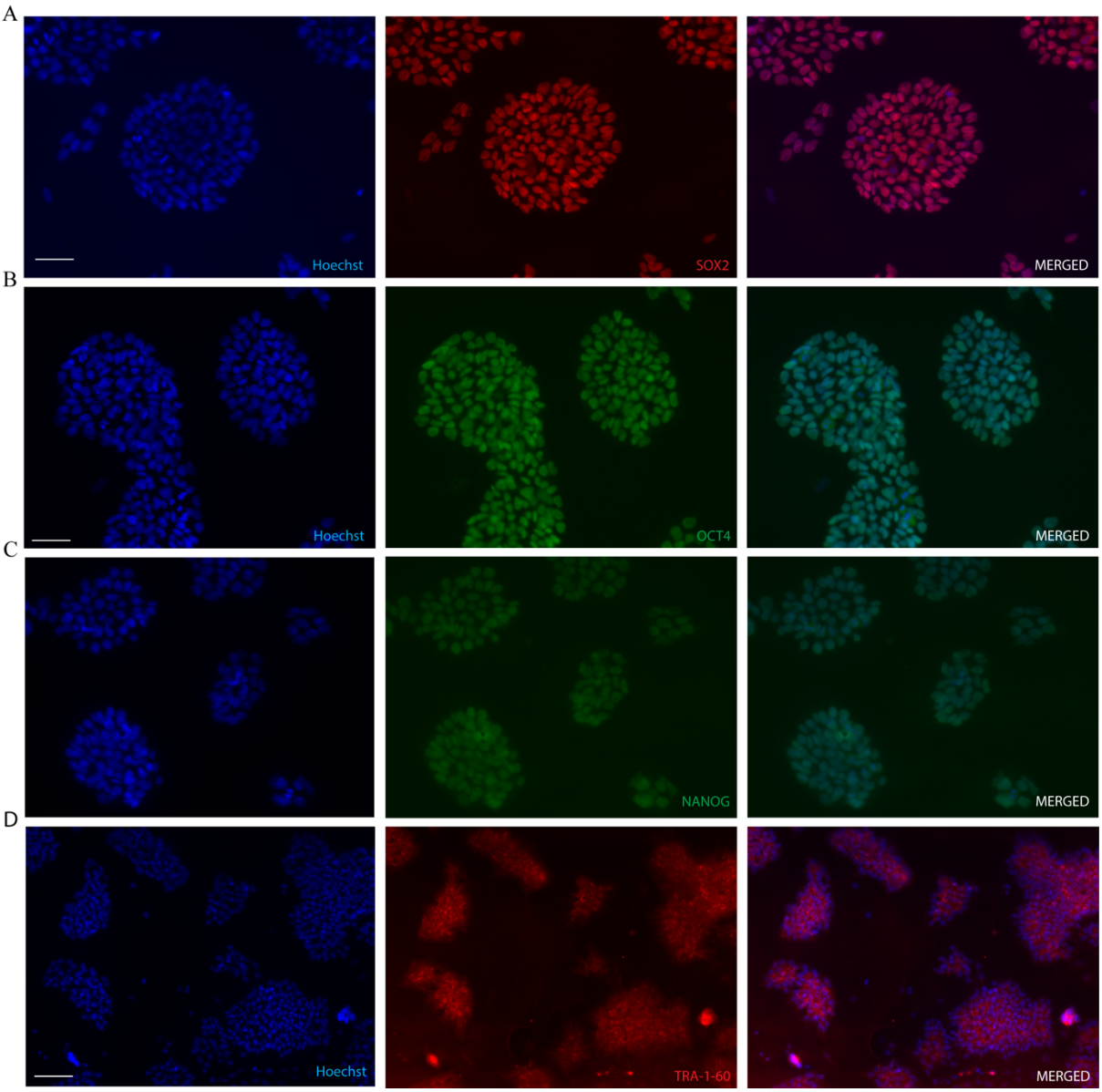

Figure 4.3.8. PD04 iPSC express intra and extracellular markers of pluripotency.

Immunocytochemistry staining demonstrates positive expression of intracellular markers of pluripotency; SOX2 (A), OCT4 (B), NANOG (C) and extracellular marker of pluripotency, TRA-1-60 (D). Scale bar, 50 µm.

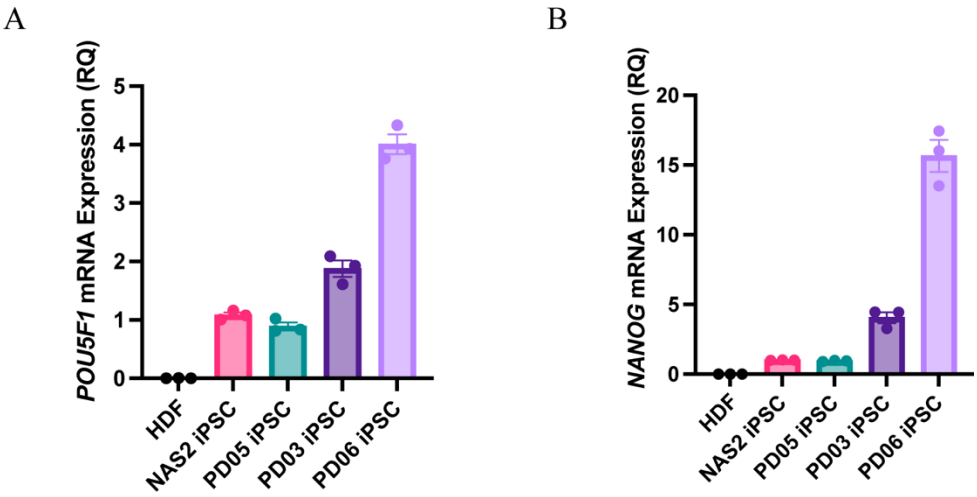

Figure 4.3.9. Generated iPSC lines PD05, PD03 and PD06 express pluripotency genes. *mRNA expression levels of POU5F1 (A) and NANOG (B). NAS2 iPSC act as a positive control, while HDF act as a negative control. Data expressed as ± SEM (N=3).*

4.3.3. Generated iPSC demonstrate the ability to differentiate into cells of the three germ layers.

A further method of confirming that iPSC are in fact pluripotent is assessing their ability to differentiate into the cell types of the three germ layers of the embryo: the endoderm, mesoderm and ectoderm. In order to assess this, the iPSC were cultured in suspension to allow them to aggregate into embryoid bodies (Fig. 4.3.10. A). Following this the EB's are adhered to a culture vessel and allowed to differentiate uninfluenced for two weeks (Fig. 4.3.10. B). Following this the cells should have differentiated into cells of the three germ layers (Fig. 4.3.10. C). To assess the production of cells of the three germs layers, we used qRT-PCR to assess the expression levels of sample genes from each of the three germ layers. Initially, we confirmed that the iPSC down-regulate their expression of the pluripotent marker POU5F1 (Fig. 4.3.11. A). Following this, we assesed *SOX1* (Fig. 4.3.11. B) for the ectoderm, *ALB* for

endoderm (Fig. 4.3.11. C), and finally *HAND1* for mesoderm (Fig. 4.3.11. D). These genes are not expressed in the corresponding iPSC (Fig. 4.3.11. B-D).

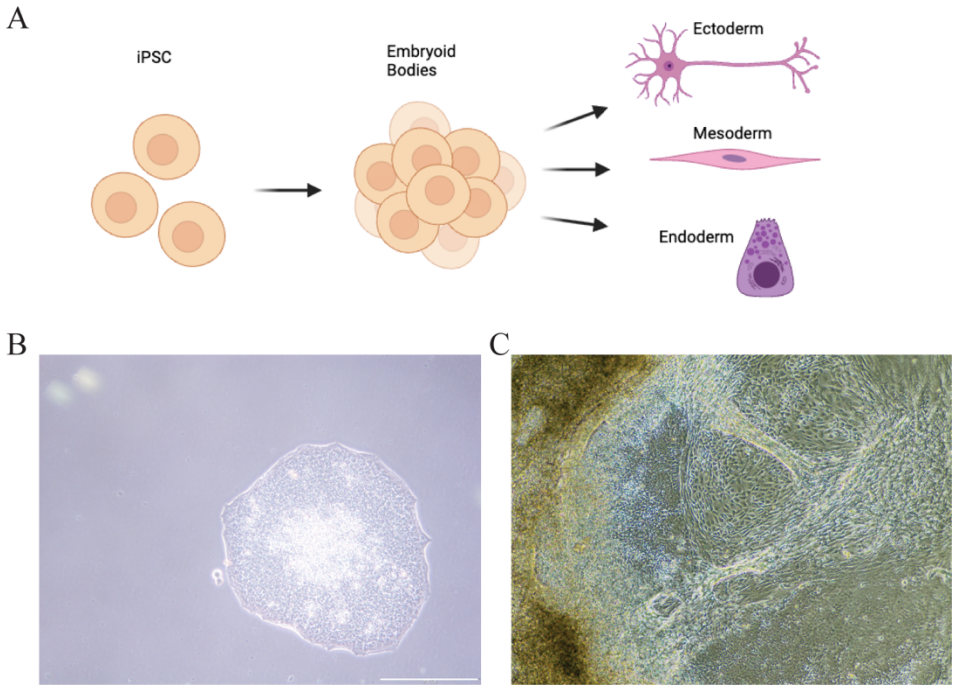

Figure 4.3.10. Timeline for trilineage differentiation from iPSC.

A) Graphical depiction of trilineage differentiation protocol from iPSC. Brightfield images demonstrating the cells prior to differentiation (B) and following differentiation of trilineage cells (C). Scale bar, 200 µm.

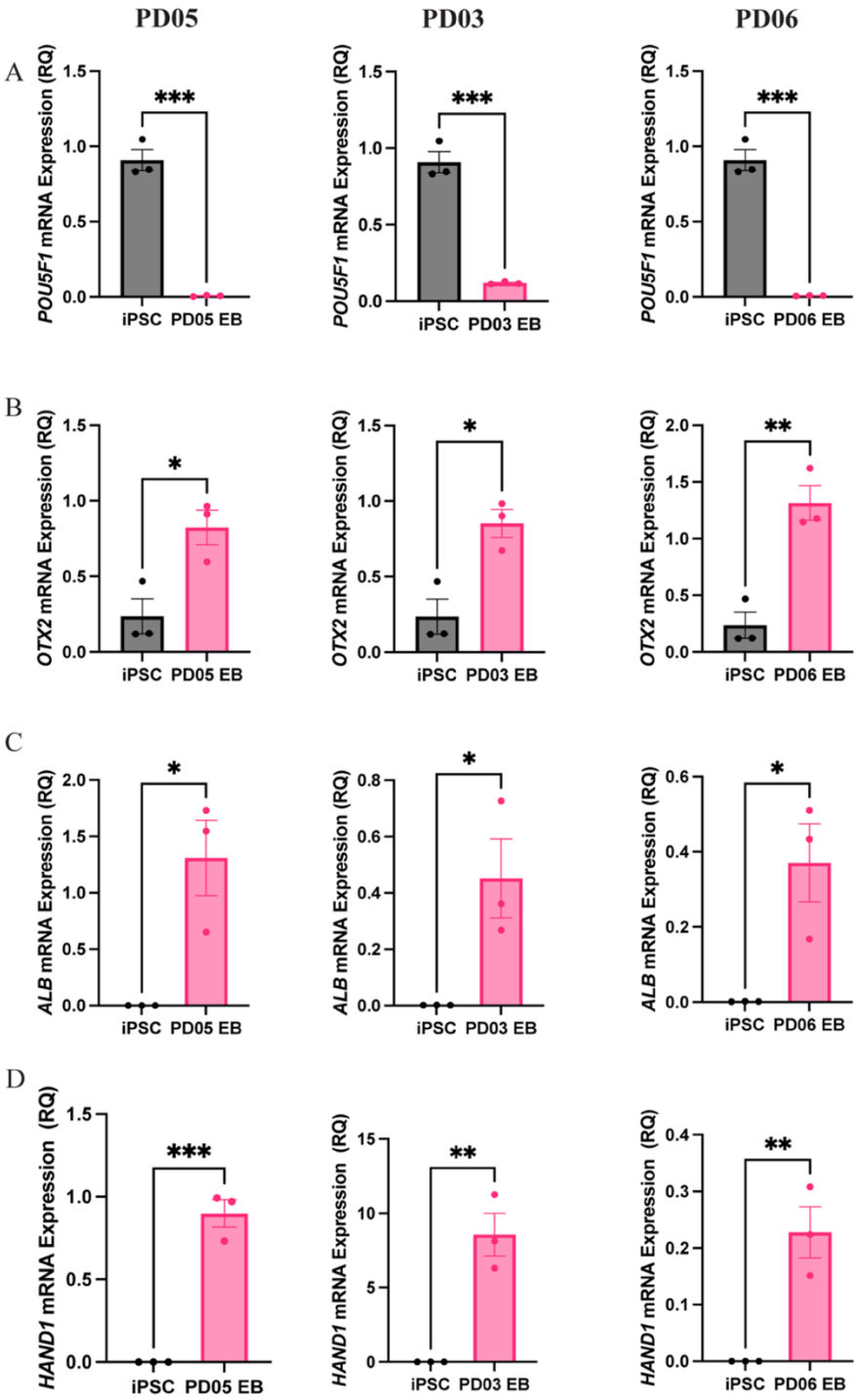

Figure 4.3.11. Assessing gene expression of pluripotency and trilineage associated genes following trilineage differentiation.

*mRNA expression levels of POU5F1 (A), OTX2 (B), ALB (C), and HAND1 (D) in the iPSC and differentiated cells from PD05, PD03 and PD06. iPSC successfully differentiated cells of all three germ layers. Data expressed as ± SEM (N=3). *p<0.05, **p<0.01, ***p<0.001. Unpaired T-test.*

4.4. Discussion

As has been described previously in this thesis, the importance of iPSC as a model system for studying disease is particularly applicable to PD. PD is a chronic neurodegenerative disease and as such presents a multitude of problems when it comes its study. Issues that arise, include, not being able to access cells of the diseased tissue easily. Post-mortem brain tissue provides the option to study patient tissue however it has its limitations. This tissue represents the disease at a single timepoint and while it is important, it makes it difficult for us to assess the mechanisms that have led to this point in pathology. There is also the issue of multiple cell types being present in tissue samples and this makes it difficult to identify which cells are contributing to pathology. iPSC allow us the ability to differentiate cells of interest when studying PD, including neurons and astrocytes of the midbrain. Somatic cells can be gathered from participants, usually either blood cells obtained through a simple blood draw, or dermal fibroblasts obtained through a minute skin punch biopsy. In this study we aimed to generate iPSC from dermal fibroblasts obtained from people with sporadic PD. We follow the protocol described by Okita and colleagues in 2011, which used nucleofection to insert non-integrating episomal plasmid vectors into dermal fibroblasts in order to force them to reprogram into a pluripotent stem cell state (Okita et al., 2011).

A number of protocols have proposed the use of various small molecules to improve the reprogramming efficiency in integration and feeder free systems. In this study we implemented the use of some of these small molecules to aid in the reprogramming process. We utilised the combined action of an inhibitor cocktail containing PD0325901, A-83-01, CHIR99021, and sodium butyrate. PD0325901, A-83-01, CHIR99021, have been demonstrated previously to improve reprogramming, through their inhibition of MEK, TGF-β and glycogen synthase kinase 3 (GSK-3) pathways respectively (Li et al., 2016; Yu et al., 2011). Sodium butyrate is

a histone deacetylase inhibitor that has been demonstrated to improve reprogramming through increasing the activity of OCT3/4 (Zhang et al., 2014). Alongside this we also utilised FGF2 which has been demonstrated to improve reprogramming efficiency, and also can be utilised to maintain pluripotency in cultures long-term (Jiao et al., 2013). However, FGF2 is a very unstable compound and thus means cultures must be fed daily (Lotz et al., 2013). This is in part the benefit of transitioning the cultures to a feeder free system, such as the E8 system used here, while also producing a defined and xeno-free culture system (Wang et al., 2013).

After much troubleshooting, we were able to obtain iPSC-like cells from the HDF. The iPSC-like cells displayed typical iPSC morphology of colonies of tightly packed cells with well-defined borders (Okita et al., 2011; Takahashi et al., 2007; Takahashi & Yamanaka, 2006). In order to confirm that the cells were fully reprogrammed to a pluripotent state, we implemented many of the well-established techniques outlined previously. Cells were taken initially to assess the expression of pluripotency associated markers, both intracellular and extracellular. The intracellular markers of OCT3/4, SOX2 and NANOG were assessed, and all four iPSC lines were observed to express these markers. OCT3/4 is an octamer-binding transcription factor originally identified in the 1990's. While the expression of this transcription factor was identified specifically in undifferentiated embryonic stem cells, it had yet to be confirmed. It was Nichols and colleagues in 1998 who determined that OCT3/4 was essential for maintenance of pluripotency. This group determined that knockout of this transcription factor resulted in loss of pluripotency in the cells of the inner cell mass of the embryo (Nichols et al., 1998). OCT3/4 maintains pluripotency by suppressing genes such as FOXA1 and 2, and tau interferon gamma which aim to drive differentiation of these cells. OCT3/4 and SOX2 have also been demonstrated to work together in order to increase expression of FGF4, and important stem cell growth factor (Pan et al., 2002). SOX2, is another transcription factor

determined to be expressed within the inner cell mass of the developing embryo and downregulated upon terminal differentiation. Lack of SOX2 leads to improper differentiation of cells towards the trophoblast lineage rather than producing the epiblast (Avilion et al., 2003). While important for pluripotency, it is thought that the main role of SOX2 is in enhancing effects of OCT3/4 (Masui et al., 2007). Nanog, was named after Tír na nÓg, the land of the ever young, due to its pluripotent abilities. The first description of Nanog in 2003 was shared by two groups, Chambers *et al*, and Mitsui *et al*. Mitsui and colleagues demonstrated that Nanog deletion resulted in loss of pluripotency, while Chambers and colleagues described the ability of Nanog to maintain pluripotency *in vitro* (Chambers et al., 2003; Mitsui et al., 2003). The extracellular markers of TRA-1-60 or TRA-1-81 were also assessed, and again, all iPSC lines expressed these extracellular markers of pluripotency. TRA-1-60 and TRA-1-81 were originally identified in embryonic carcinoma cell research (Andrews et al., 1984). While the exact surface protein they target is still being debated, the presence of these markers in pluripotent cells and not in their differentiated counterparts is widely accepted (Natunen et al., 2011). The gene expression levels of pluripotency associated genes *POU5F1* which encodes for OCT3/4 and *NANOG* which encodes for NANOG were also assessed. The iPSC lines demonstrated expression levels comparable to a well-characterised iPSC line, NAS2. As the genes for NANOG, TRA-1-60 and TRA-1-81 were not in the plasmids inserted, their expression confirms that the cells have fully reprogrammed and that they are not simply expressing those factors that were inserted. The pluripotency related markers assessed here are commonly used throughout iPSC generation literature and produce similar results to those observed in this thesis (Castro-Vinuelas et al., 2020; Okita et al., 2007; Okita et al., 2011; Takahashi et al., 2007; Vlahos et al., 2019; Yu et al., 2009; Yu et al., 2007). Together these data gives the primary identification that these cells are in fact pluripotent.

Following this initial assessment of pluripotency, we next confirmed their ability to carry out the major function of pluripotent cells, which is to generate the cells of the three germ layers: the endoderm, the mesoderm and the ectoderm. In order to do this the cells were allowed to aggregate together to form embryoid bodies mimicking development. These embryoid bodies were then seeded and allow to differentiate uninhibited for 2 weeks, at which point cells from the three germ layers should be present (Bhargava et al., 2019; Kumar et al., 2018). We assessed that the differentiating iPSC lost their expression of pluripotency associated genes and gained the expression of genes representative of the three germ layers. Three of the four iPSC lines were taken forward for this characterisation step: PD05, PD03 and PD06. All three iPSC lines lost their expression of the pluripotency gene *POU5F1*, which is follows what is observed in development (Kuang et al., 2019; Pan et al., 2002). Similarly, as would be expected of iPSC, all three lines gained the expression of genes associated with the endoderm (*ALB*) and mesoderm (*HAND1*) and ectoderm (*OTX2*) (Garcia et al., 2024; Kamishibahara et al., 2023; Stanberry et al., 2023). While the trilineage differentiation method used here is quite widely utilised, there are also various other methods for the differentiation of iPSC, including assessing their ability to form teratomas upon injection into animals, or utilising differentiation medium kits from scientific companies which include factors to direct the differentiation (Ross et al., 2017; Takahashi et al., 2007). Together these data provides evidence that these human dermal fibroblasts have been successfully differentiated into iPSC. These cells express markers of pluripotency and are capable of generating cells of the three germ layers.

Furthermore, karyotyping of iPSC should be carried out on all newly generated iPSC lines in order to ensure that there are no genetic abnormalities. Karyotype analysis enables the identification of numerical and structural chromosomal alterations in the iPSC (Vaz et al., 2021). The presence of these abnormalities can alter the responses of these cells in culture,

increased proliferation rate and tumorgenicity are examples of such aberrant responses (Vaz et al., 2021). This obviously has negative connotations for the potential implantation of these cells as therapeutics, but also for any research studying cellular mechanisms themselves.

Overall, this chapter outlines the successful generation of iPSC lines from patient dermal fibroblasts following established protocols. These cells represent the potential for generation of disease associated cell types in order for us to investigate pathological mechanisms at play in PD.

Chapter 5 : Utilising iPSC to differentiate cells of the ventral midbrain

5.1. Introduction

5.1.1. What neurons are of interest in PD?

In PD, it is the A9 dopaminergic neurons of the SNpc of the ventral midbrain that degenerate (German et al., 1989). The issue with generating these cells is the very minute area which they occupy, comparatively to other areas of the brain, such as the cortex (Hirsch, 1994). There have been countless protocols generated over the years and these are still evolving, which aim to produce the most precise differentiation conditions to achieve these cells (Schwarz et al., 2006). The major concerns are neurons directly in the surrounding areas of the brain which are incredibly close in developmental origin (Perrier et al., 2004). The main areas of issue when developing A9 neurons, are of course the A8, retrorubral neurons, A10, VTA and the neurons of the subthalamic nucleus due to their proximity in developmental pathways (Perrier et al., 2004).

While ensuring we are generating neurons of the minute target area of the SNpc is crucial, we must first try to generate neural cells. While, of course, over the years there have been many methods generated to do this, the protocol most used presently, is that outlined by Chambers and colleagues in 2009. This protocol outlines a method of utilising dual SMAD inhibition to force the iPSC towards a neuroectodermal lineage as opposed to mesoderm or endoderm (Chambers et al., 2009). The combined action of Noggin and SB431542 act to synergistically downregulate pluripotency associated proteins such as Nanog, while inhibiting mesoderm/endoderm differentiation, and promoting neuroectoderm differentiation (Chambers et al., 2009). Noggin acts to inhibit BMP signalling, whilst SB431542 inhibits lefty/activin/TGFβ pathways (Chambers et al., 2009). Homologs of noggin, such as LDN or dorsomorphin are also now commonly used (Alekseenko et al., 2022; Crompton et al., 2021; Devine et al., 2011). Now that we've established how to direct the cells towards a neuronal

lineage, the specification of the ventral midbrain region can be addressed. Unfortunately, this is less straightforward. Differentiation protocols follow developmental cues, and like developmental biology would suggest, this is a very precise and sensitive process. The key protocols that have been outlined for the generation of midbrain neurons are summarised below (Table 5.1.1.). The main components of these protocols, after you take into account the dual SMAD inhibition (Chambers et al., 2009), are those that stimulate the sonic hedgehog (SHH) pathway, and inhibitors of GSK3. GSK3 inhibition functions to activate WNT signalling, which is important for midbrain regionality, it acts in concert with FGF8 to delineate the midbrain/hindbrain boundary (Arenas et al., 2015). SHH signalling is important in production of the ventral floor plate of the midbrain (Ribes et al., 2010). SHH and WNT signalling act to balance ventro-dorsal and rostro-caudal patterning of the midbrain, respectively (Joksimovic et al., 2009). Some protocols also implement the use of FGF8 which of course is crucial in midbrain development, secreted by the isthmus organiser along the midbrain/hindbrain boundary (Arenas et al., 2015). It is thought that FGF8 is important in fine-tuning the caudalisation of the neurons (Nolbrant et al., 2017). Retinoic acid has also been introduced as it is demonstrated to be important in caudalisation and has been demonstrated to generate midbrain neurons (Alekseenko et al., 2022).

Table 5.1.1. Summary of key midbrain neuron differentiation protocols

Patterning Factors	***Neurotrophic/ Maturation***	***Starting population***	***Duration***	***Markers***	***Reference***
SB431542, Noggin, SHH, Purmorphine, Chir, FGF8	BDNF GDNF Ascorbic acid TGFβ3 DAPT dbcAMP	hESC	D11+ NPC D50 neurons	Nestin/TUJ1 FOXA2/LMX 1a TH/Nurr1	Kriks 2011
SB431542, Noggin, Dorsomorphin, SHH, WNT1, Dkk1 inhibitor	BDNF Ascorbic acid FGF8 GDNF TGFβ3 dbcAMP	iPSC	D23-31	TUJ1 TH/LMX1B/Nurr1/LMX1A DAT	Devine 2011
SB431542, Noggin, SHH, CT99021(Chir)	BDNf GDNF Ascorbic acid dbcAMP DAPT	hESC	>30 d	FOXA2/LMX 1A EN1 MAP2 TH/Corin/Nurr 1	Kirkeby 2012
SB431542, Noggin, SHH, Chir, FGF8	BDNF GDNF Ascorbic acid dcCAmp DAPT	hiPSC	D16+ NPC D42+ neurons	LMX1A/FOXA2/OTX2 Corin/EN1 TH/GIRK2/MAP2	Nolbrant 2017
SB431542, DMH1, SAG1.3, Chir, RA	BDNF GDNF Ascorbic acid		>24 d	LMX1A/LMX 1B OTX2/Nurr1 TUJ1/MAP2 EN1/DAT/TH Girk2/Sox6	Alekseenko 2022

5.1.2. The gliogenic switch

There remain very few protocols for the differentiation of astrocytes from iPSC, let alone, region specific astrocytes. The protocol followed in this study closely resembles that of Crompton and colleagues from 2021, which describes the generation of midbrain astrocytes from iPSC (Crompton et al., 2021). To begin, neural progenitor cells are first generated from iPSC, which has been described in detail above. Following development, to generate astrocytes, we need to induce a gliogenic switch. Factors which have been demonstrated to induce such as switch include, BMPs, EGF, ciliary neurotrophic factor (CNTF) and LIF (Markey et al., 2023). It has been observed that EGF is important in stimulating upregulation of EGF receptors which increase astrocyte responsiveness to factors such as LIF and induces signal transducer and activator of transcription 3 (STAT3) phosphorylation. However, factors such as BMP and CNTF have been demonstrated to act independently of this pathway (Viti et al., 2003). Studies have demonstrated that BMP signalling, in particular that of BMP2 and BMP4 induces astrocytic maturation through the phosphorylation of the SMAD1/5/8 pathway (Scholze et al., 2014). CNTF, is known to induce differentiation of astrocytes and exerts its affects through Janus tyrosine kinase (JAK)/STAT signalling and phosphorylation of STAT3 (Hughes et al., 1988; Shaltouki et al., 2013). Krencik and colleagues' paper from 2011 is one of the first protocols which outlined astrocyte differentiation from hESC. They cultured PSC as neurospheres exposed to EGF and FGF2, to generate functional astrocytes, CNTF was added to cultures (Krencik & Zhang, 2011). Following this, Roybon and colleagues utilised FGF2 and EGF to force neurospheres towards an astrocytic lineage, they supplemented media with foetal bovine serum (FBS) once cells were a monoculture to aid in their survival (Roybon et al., 2013). Serio and colleagues in 2013, first outlined a protocol for the generation of iPSC-derived astrocytes without the need for serum, using EGF and LIF for initial gliogenic induction and final maturation with CNTF (Serio et al., 2013). Crompton and colleagues then

built upon this to generate midbrain astrocytes. The protocol describes differentiation of midbrain neural progenitor cells (NPC), a gliogenic switch is then triggered using EGF and hLIF (Crompton et al., 2021). After culturing the cells for 50+ d, they are finally matured using BMP4. Generated midbrain astrocytes were demonstrated to expression typical astrocyte markers, as well as those of the midbrain (Crompton et al., 2021).

5.2. Aims

Understanding the cellular mechanisms underlying PD allows for the identification of novel therapeutic targets, therefore, the aims of this study are as follows.

1. To generate ventral midbrain neural progenitor cells (vmNPC)
2. To differentiate vmAstros
3. To induce a reactive astrocyte phenotype in vmAstros

The hypothesis for this study is that by applying factors associated with development of ventral midbrain neurons, SB431542, LDN, SHH, Chir and FGF8b and astrocytes, EGF, hLIF and BMP4, that iPSC can directed towards these terminal cell fates. Furthermore, these differentiated cells will express markers such as TUJI, LMX1A, FOXA2, and SOX6 in relation to the midbrain neurons and GFAP, S100β, CX43, EAAT1 and LMX1A in relation to midbrain astrocytes. Furthermore, the iPSC-derived midbrain astrocytes should respond to the inflammatory stimuli of TNFα, IL-1α and C1q by upregulating pro-inflammatory genes, such as *C3, LCN2* and *IL-6*, and proteins such as IL-6.

5.3. Materials and methods

5.3.2. Induce pluripotent stem cell lines

The non-affected sibling 2 (NAS2) iPSC line was used as a control line for this study. The NAS2 line was generated by the Kunath Lab (Devine et al 2011; https://ebisc.org/EDi002-A/). The PD05 sporadic PD cell line generated in this study was chosen to be taken forward for the following experiments (see Chapter 4 for more detail).

5.3.3. vmNPC differentiation

vmNPC were differentiated largely following the Nolbrant, 2017 protocol (Fig. 5.3.1; Nolbrant et al., 2017). First iPSC were detached from culture plates using EDTA (3 min, RT). Cells were counted and seeded onto vitronectin coated plates at a density of $1x10^5$ cells per cm^2. Cells were seeded straight into neural differentiation medium (NDM; Appendix 1 Table 7) containing Y-27632 (10 μM) to aid cell survival. A complete media change to remove the Y-27632 was carried out on D2. By D7 cells were approximately 90% confluent. Media was changed from NDM on D9 to N2B27 medium containing FGF8b (100 ng/ml). On D11, the cells are passaged onto Poly-Ornithine (20 min, RT) and Laminin (2 h, 37°C) coated plates, using Accutase™ (10 min, 37°C) to detach cells. From this point cells were treated as neural progenitor cells. Media was changed to neural maintenance medium (NMM; Appendix 1 Table 8) with added FGF8b (100 ng/ml). FGF8b was removed from the media at D16. From D16 to D25 vmNPC were taken for characterisation. Stocks of confirmed vmNPC were cryopreserved.

5.3.4. vmAstros differentiation

vmAstros were differentiated following Crompton and colleagues, 2021 (Fig. 5.3.4.; Crompton et al., 2021). vmNPC that have reached approximately 100% confluency had their media

changed to astrocyte medium (AM; Appendix 1 Table 9). On D3 on astrocyte differentiation cells were passaged using Accutase™ (10 min, 37°C) onto Geltrex coated plates at a ratio of 1:7.5. The cells were continuously cultured in AM at high split ratios for approximately 50 d until they had reached D80 post-neuralisation. From D80 onwards, cells were taken for characterisation to confirm a successful differentiation to astrocyte progenitor cell (APC). From D80 AM was changed to astrocyte maturation medium (AMM; Appendix 1 Table 10) to generate mature astrocytes which were used in experiments. AMM was added for 7 d after which media was replaced with AM minus EGF and hLIF for 3 d. This was to remove any inflammatory phenotype potentially triggered by hLIF before experiments. Astrocytes were seeded at densities of 4-5x10^5 cell per coverslip for ICC, 20x10^5 cell per 24-well for RT-qPCR and 5x10^5 for ELISA. Stocks of APC and vmAstros were cryopreserved.

5.3.5. Stimulating astrocytes with microglial-secreted cytokines

vmAstros were stimulated with the Liddelow Factors to confirm their maturation and ability to respond to inflammatory stimulus (Liddelow et al., 2017). All media was removed from the cells and replaced with corresponding treatments outlined below (Table 5.2.1). Cells were incubated for 24 h at 37°C, 5% CO_2. Cell conditioned media was collected for ELISA, and cells were lysed for PCR. For ELISA, and PCR an N=3 with 2 experimental replicates was analysed. For PCR analysis, where CT remained undetermined, the RQ was calculated using the delta-delta CT method from the control N which had a CT value within the cycle limits.

Table 5.2.1. Treatment plan for vmAstros

Code	*Treatment*	*Concentration*
Control	AM -EGF -hLIF	N/A

Factors	TNFα	30 ng/ml
	IL-1α	3 ng/ml
	C1q	400 ng/ml

5.3. Results

5.3.1. Differentiation of vmNPC from iPSC.

In order to utilize the generated iPSC as a cellular model of PD, we aimed to guide their differentiation into the cell type mainly impacted in PD. These cells are the A9, dopamine neurons, of the SNpc of the midbrain (German et al., 1989). In neurodevelopmental terms, these cells are derived from the ventral midbrain (Hegarty et al., 2013). In order to achieve this, we followed a protocol that combined the precise addition of factors to direct the iPSC towards a vmNPC fate (Fig. 5.3.1. A). These factors originated from studies of embryonic development and closely follow these processes (Hegarty et al., 2013). Initially the cells were exposed to SB431542 and LDN193189 which forces the iPSC towards a neuroectoderm lineage, utilising dual SMAD inhibition (Chambers et al., 2009). For differentiation of cells of the ventral midbrain specifically, the factors, SHH and CHIR are crucial. These factors aim to caudalise and ventralise the cells respectively (Kirkeby et al., 2012; Kriks et al., 2011; Nolbrant et al., 2017). Recent literature has demonstrated that further caudalisation with FGF8b from D9-11 can improve the yield of vmNPC. However, the timing of this addition is also crucial (Nolbrant et al., 2017). Factors such as BDNF, glial cell-line derived neurotrophic factor (GDNF) and ascorbic acid were added to aid in the expansion of cells in culture. NPC can be clearly distinguished from their iPSC origins due to their vastly differing and distinct morphology (Fig. 5.3.1. B and C). The entire protocol take approximately 16-25 d before cells are ready to be characterized as vmNPC, from here, the cells can be further matured, cryopreserved, or taken for subsequent differentiation of vmAstros (see section 5.3.3. below).

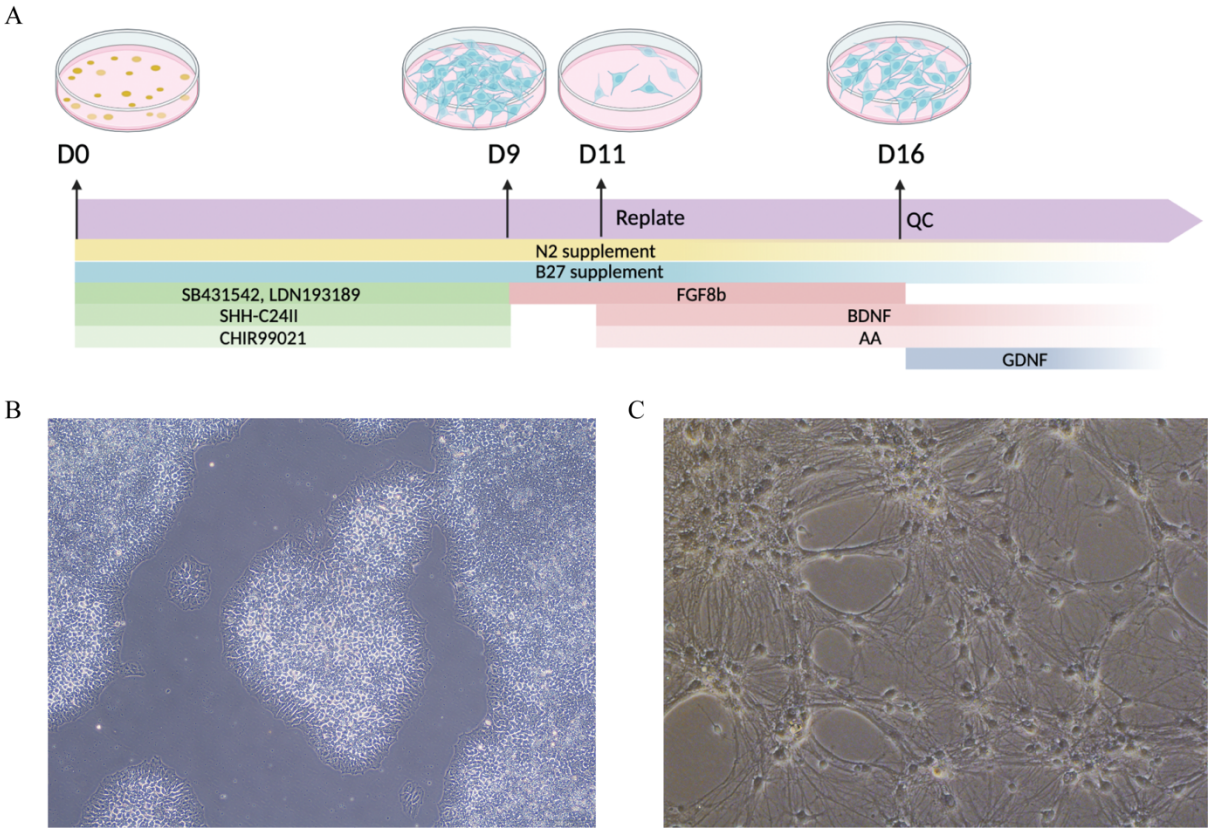

Figure 5.3.1. Differentiation of vmNPC cells from iPSC.

Timeline depicting the differentiation protocol for achieving vmNPC (A). Brightfield images demonstrate morpholgoical changes between the iPSC and the newly differentiated NPC (B). Figure generated with Biorender.

5.3.2. Confirmation of the successful differentiation of vmNPC.

The above protocol was utilised to differentiate vmNPC from one of the generated PD iPSC lines, PD05 and the control iPSC line, NAS2. A single PD line was chosen in the interest of time, while NAS2 vmNPC were required to act as a comparative cell line throughout subsequent expreiments. In order to confirm that the protcol is successful and that these morphological changes do in fact indicate neural progenitor cell identity, we assessed the expression of a variety of proteins in the cells via immunocytochemistry. The initial step is to assess the cells expression of the neural marker, TUJI (Fig. 5.3.2. A-B, Fig. 5.3.3. A) indiciating

that the cells have been successfully pushed towards a neural terminal fate. Following this, we assess whether we had successfully achieved cells of the ventral midbrain. To achieve this we assessed the expression of midbrain markers such as: LIM homeobox transcription factor 1 alpha (LMX1A) (Fig. 5.3.2. A and C and Fig. 5.3.3. A), FOXA2 (Fig. 5.3.2. C and Fig. 5.3.3. B) and SOX6 (Fig. 5.3.2. B). The NAS2 iPSC line and PD05 iPSC line both demonstrated typical NPC morphology and expressed these key neural and midbrain markers, indicating the successful differentiation of the cell type of interest, the vmNPC.

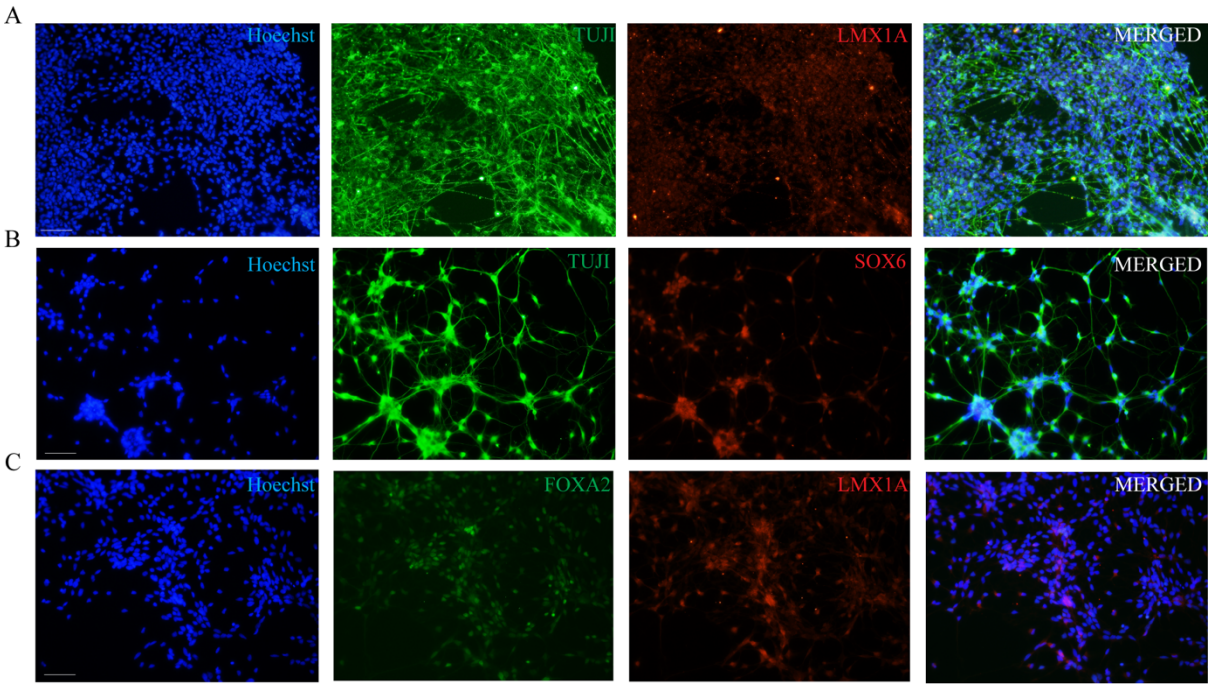

Figure 5.3.2. Confirmation of vmNPC differentiation from NAS2 iPSC.

Immunocytochemistry analysis demonstrates differentiated vmNPC express markers TUJ1 (A and B), LMX1A (A and C), SOX6 (B) and FOXA2 (C). Scale bar, 50 µm.

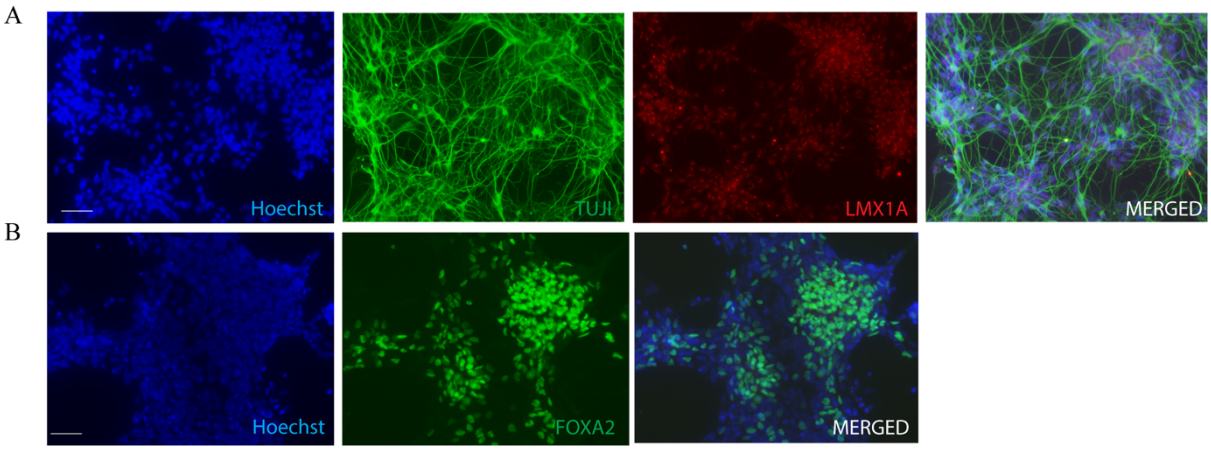

Figure 5.3.3. Confirmation of vmNPC differentiation from PD05 iPSC.

Immunocytochemistry analysis demonstrates differentiated vmNPC express markers TUJ1 (A), LMX1A (A) and FOXA2 (B). Scale bar, 50 µm.

5.3.3. Differentiation of vmAstros from vmNPC.

Once successful differentiation of vmNPC had been achieved and confirmed, these NPC could be taken to further differentiate into vmAstros. In order to do this the NPC were expanded for 50 d from D30 post-neuralisation to D80 post-neuralisation (Fig. 5.3.4. A). These cells were expanded with a high split ratio and in medium containing the factors, EGF and hLIF in order to stimulate differentiation towards an astrocytic fate (Fig. 5.3.4. A). From D80 the astrocyte progenitor cells could be fully matured by replacing EGF with BMP4 (Fig. 5.3.4. A). After 7 d exposed to BMP4 and hLIF, the astrocytes were considered to be mature. To confirm the success of this differentiation and the functionality of the mature astrocytes, the cells must undergo a variety of characterisation steps, discussed below (see section 5.3.4. and 5.3.5.). As with the iPSC generation and subsequent NPC differentiation, morphology plays a large role in indicating a successful differentiation of astrocytes also. Astrocytes are typically larger and have a bigger nucleus than NPC. They are also known for their ‘star’ shape morphology from which they derive their name (Baldwin et al., 2023). Fig. 5.3.4. below depicts morphological

changes that can be observed during the differentiation process that would indicate successful differentiation (Fig. 5.3.4. B-D). The first image demonstrates a typical neuronal morphology (Fig. 5.3.4. B) and is the cell type we begin the neuralisation with, the second image depicts an intermediate stage of the protocol where we have astrocyte progenitor cells (APC; Fig. 5.3.4. C), the cells are beginning to display more of an astrocytic morphology and have transitioned away from a neuronal morphology, whilst the last image demonstrates the fully matured final morphology of the astrocyte, characteristic morphology is evident (Fig. 5.3.4. D).

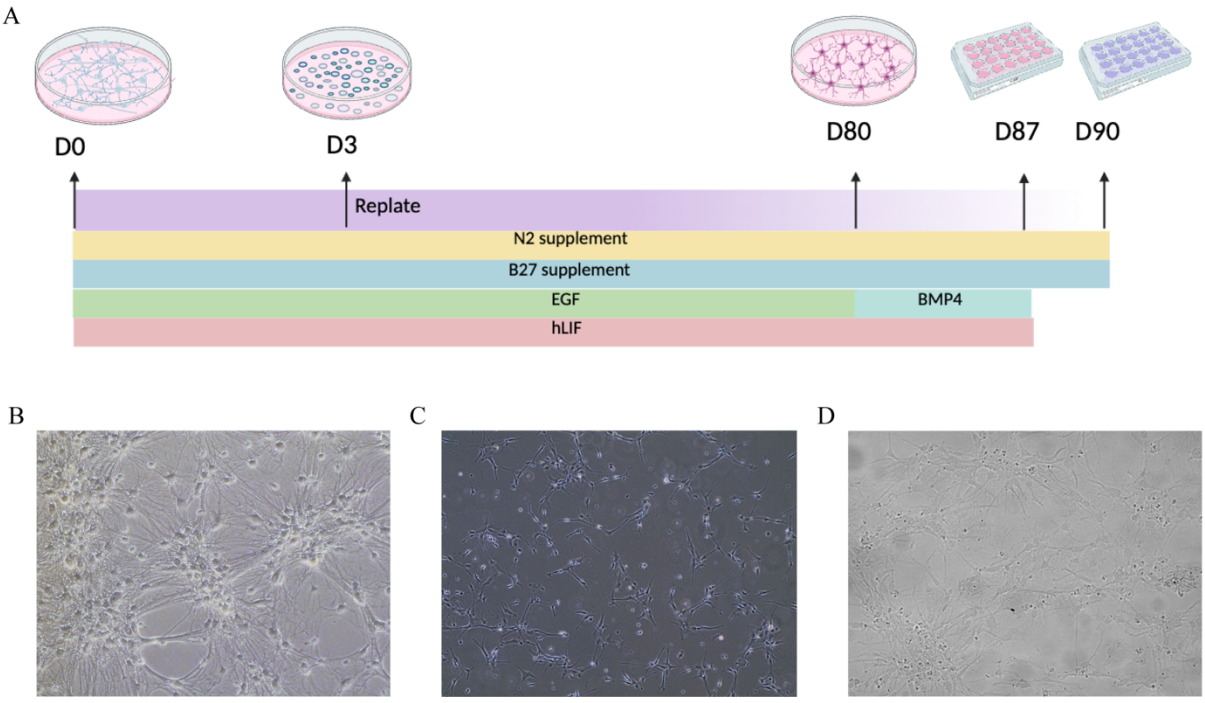

Figure 5.3.4. Protocol for the differentiation of vmAPC from vmNPC.

A) Visual timeline depicting key steps in the differentiation protocol. Brightfield images demonstrating morphological differences in the cells at different stages of the protocol, B) NPC, C) APC, D) Astrocytes.

5.3.4. Differentiated vmAstros express markers associated with mature astrocytes.

Despite the differentiated cells behaving as astrocytes and appearing morphologically similar, their identity must be confirmed by assessing observed characteristics of iPSC-derived astrocytes. Initially, we confirmed their expression of astrocytic proteins via immunocytochemistry. The expression of S100β, and GFAP tell us the cells are of the astrocyte lineage (Fig. 5.3.5. A and Fig. 5.3.6. A). While expression of CX43 (Fig. 5.3.5. B and Fig. 5.3.6. B), and EAAT1 (Fig. 5.3.5. C and Fig. 5.3.6. C) help us to confirm the maturity of the astrocytes, as they should indicate their ability to carry out typical astrocyte functions. Finally, as we are interested in assessing midbrain astrocytes specifically, we confirmed their expression of midbrain marker, LMX1A (Fig. 5.3.5. D and Fig. 5.3.6. D; Crompton et al., 2021). The NAS2 and PD05 differentiated astrocytes expressed all mentioned astrocytic markers, confirming their successful differentiation (Fig. 5.3.5. and 5.3.6.).

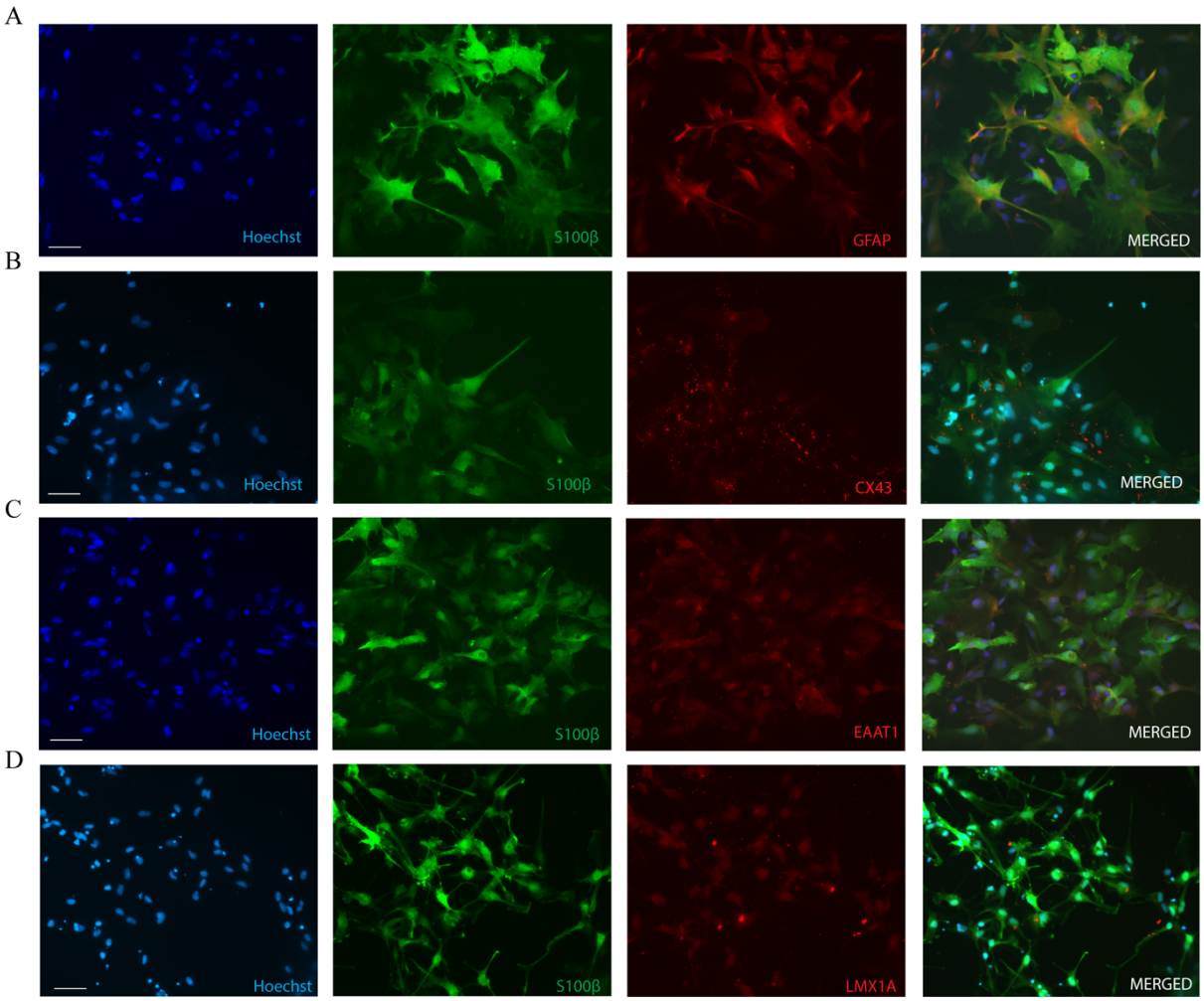

Figure 5.3.5. NAS2 vmAstros expression key astrocyte proteins.

Immunocytochemistry confirms astrocytic expression of A) S100β and GFAP, B) S100β and CX43, C) S100β and EAAT1, D) S100β and LMX1A. Scale bar, 50 µm.

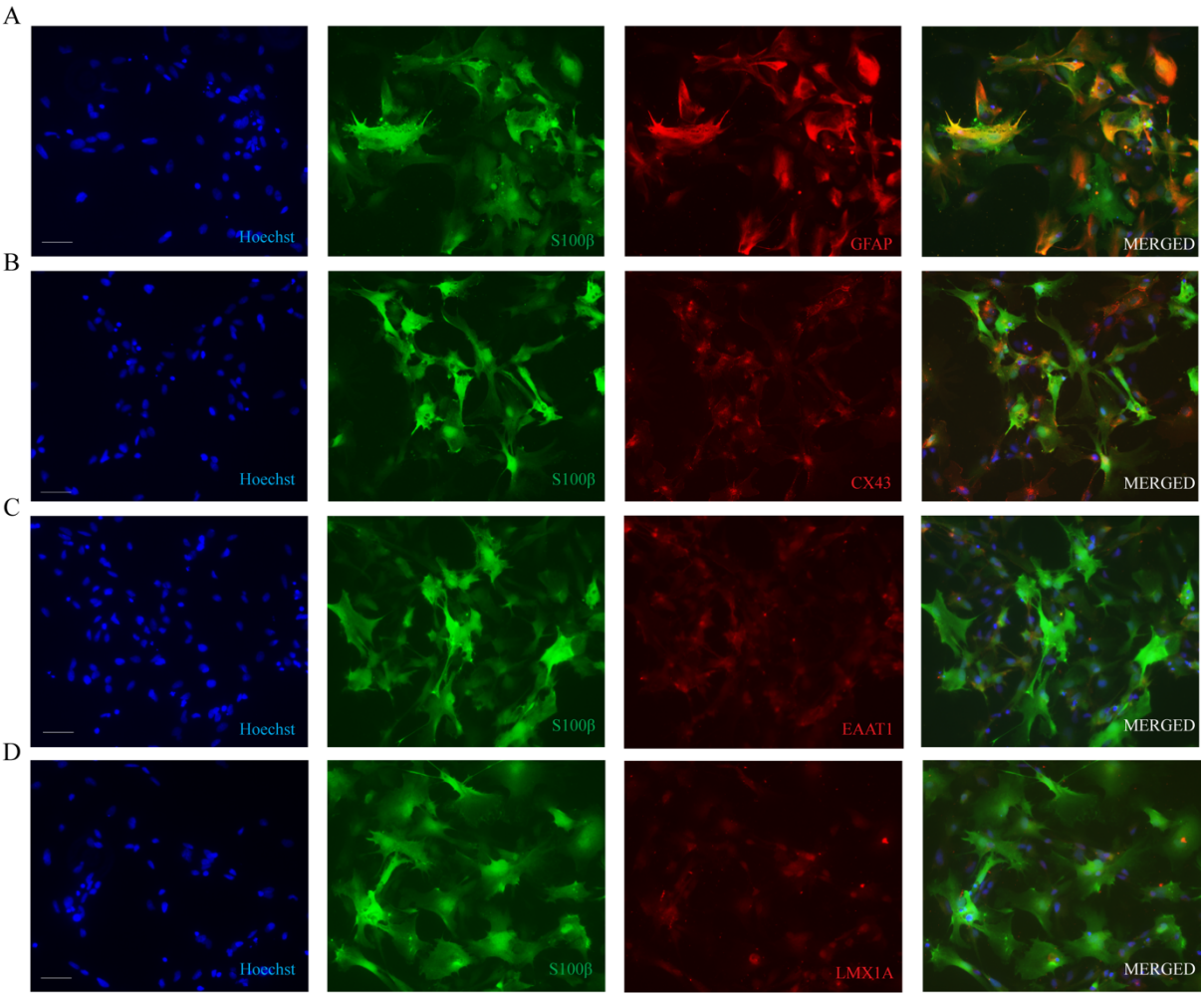

Figure 5.3.6. PD05 vmAstros expression key astrocyte markers.

Immunocytochemistry confirms astrocytic expression of A) S100β and GFAP, B) S100β and CX43, C) S100β and EAAT1, D) S100β and LMX1A. Scale bar, 50 µm.

5.3.5. vmAstros respond to pro-inflammatory cytokines to produce a reactive astrocyte phenotype.

Next, in order to assess the functionality of the astrocytes and due to our interest in reactive astrocytes, we assessed their ability to respond as expected to the Liddelow factors, demonstrated to produce a robust reactive astrocyte phenotype (Liddelow et al., 2017). The combined action of microglial secreted cytokines, TNFα, IL-1α and C1q was determined by

Liddelow and colleagues to produce the most robust reactive astrocyte phenotype (Liddelow et al., 2017). In order to assess their ability to become reactive, we exposed the astrocytes to the combination of these factors for a typical period of 24 h. Protein secretion and gene expression of markers associated with reactive astrocytes were assessed. Following exposure to the pro-inflammatory cytokines, both the NAS2 and PD05 vmAstros demonstrated a significant secretion of IL-6 indicating their switch to a reactive state (Fig. 5.3.7. A and Fig. 5.3.8. A). Following on from this, gene expression analysis demonstrated the increased expression of pro-inflammatory genes; *C3* ($p<0.001$; Fig. 5.3.7. B, p0.006; Fig. 5.3.8. B), *LCN2 (*Fig. 5.3.7. and 5.3.8. C), *CXCL10* ($p<0.001$; Fig. 5.3.7. D, $p<0.001$; Fig. 5.3.8. D), *IL-6* ($p<0.001$; Fig. 5.3.7. E, Fig. 5.3.8. E), and *PTX3* ($p<0.001$; Fig. 5.3.7. F, $p<0.001$; Fig. 5.3.8. F). The expression of *GFAP* was observed to decrease significantly following stimulation ($p<0.001$; Fig. 5.3.7. G, $p<0.001$; Fig. 5.3.8. G). *ITGA6* expression significantly decreased with reactivity in the astrocytes (p0.005; Fig 5.3.7. H, p0.02; Fig. 5.3.8. H), following a similar response as *GFAP*. Some differences in responses were observed between the NAS2 and PD05 lines, mainly NAS2 vmAstros demonstrated a significant decrease in *SERPINA3* (p0.010; Fig. 5.3.7. I) following exposure to the Liddelow factors, whilst PD05 vmAstros produced a significant increase in *SERPINA3* ($p<0.001$; Fig. 5.3.8. I). Furthermore, the PD05 astrocytes appear to be expressing greater levels of *CXCL10* mRNA (Fig. 5.3.8. D) than their NAS2 counterparts (Fig. 5.3.7. D). Altogether these data confirms the success of the vmAstros differentiation of NAS2 and PD05, demonstrating their expression of astrocyte markers and their ability to function as astrocytes and become reactive upon stimulation.

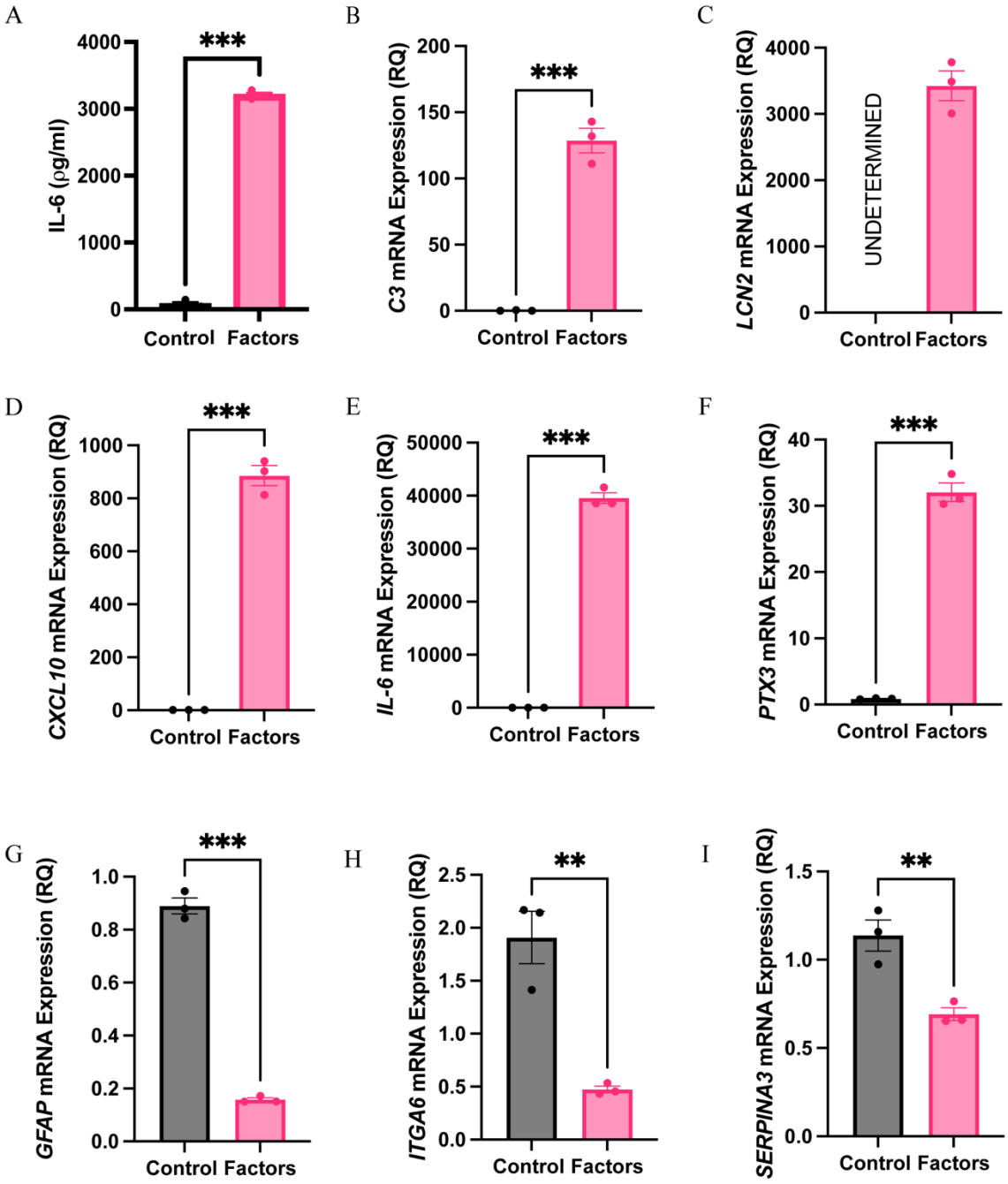

Figure 5.3.7. NAS2 vmAstros respond to inflammatory cytokines by increasing secretion and gene expression of pro-inflammatory associated factors.

*A) IL-6 protein secretion. Gene expression levels of C3 (B), LCN2 (C), CXCL10 (D), IL-6 (E), PTX3 (F), GFAP (G), ITGA6 (H), SERPINA3 (I). Data expressed as ± SEM (N=3). **p<0.01, ***p<0.001. Unpaired T-test.*

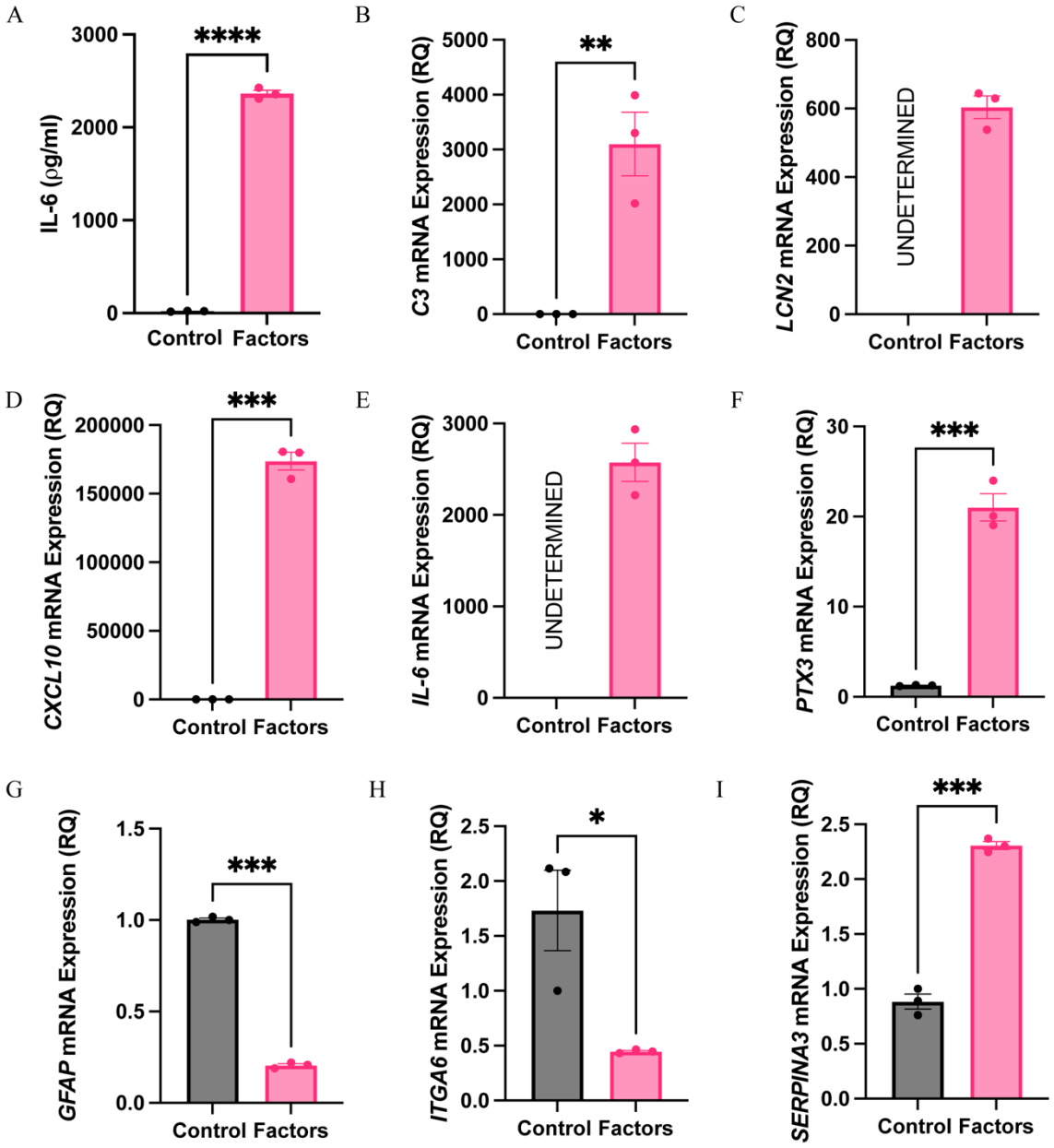

Figure 5.3.8. PD05 vmAstros respond to inflammatory by increasing secretion and gene expression of pro-inflammatory markers.

*A) IL-6 protein secretion. Gene expression levels of C3 (B), LCN2 (C), CXCL10 (D), IL-6 (E), PTX3 (F), GFAP (G), ITGA6 (H), SERPINA3 (I). Data expressed as ± SEM (N=3). *p<0.05, **p<0.01, ***p<0.001. Unpaired T-test.*

5.3.6. PD05 vmAstros demonstrate differing protein and gene expression compared to NAS2 vmAstros.

In order to investigate the potential differences between the PD05 and NAS2 cell lines we directly compared their protein secretion and gene expression (Fig. 5.3.8.). When compared to NAS2, PD05 astrocytes was observed to secrete significantly lower levels of IL-6 when stimulated with the Liddelow factors ($p<0.001$; Fig. 5.3.8. A). Interestingly, the gene expression levels in PD05 astrocytes were significantly higher when it came to inflammatory related genes, *C3* ($p<0.001$; Fig. 5.3.8. B), *CXCL10* ($p<0.001$; Fig. 5.3.8. C), and *SERPINA3* ($p<0.001$; Fig. 5.3.8. D). Levels of *PTX3*, which is commonly associated with the BBB, were significantly decreased in PD astrocytes when compared to the NAS2 control astrocytes ($p<0.001$; Fig. 5.3.8. E). While no significant difference was observed between PD05 and NAS2 astrocytes in terms of *GFAP* expression when stimulated, PD05 astrocytes expressed significantly more *GFAP* at resting state compared to the NAS2 controls (p0.006; Fig. 5.3.8. F).

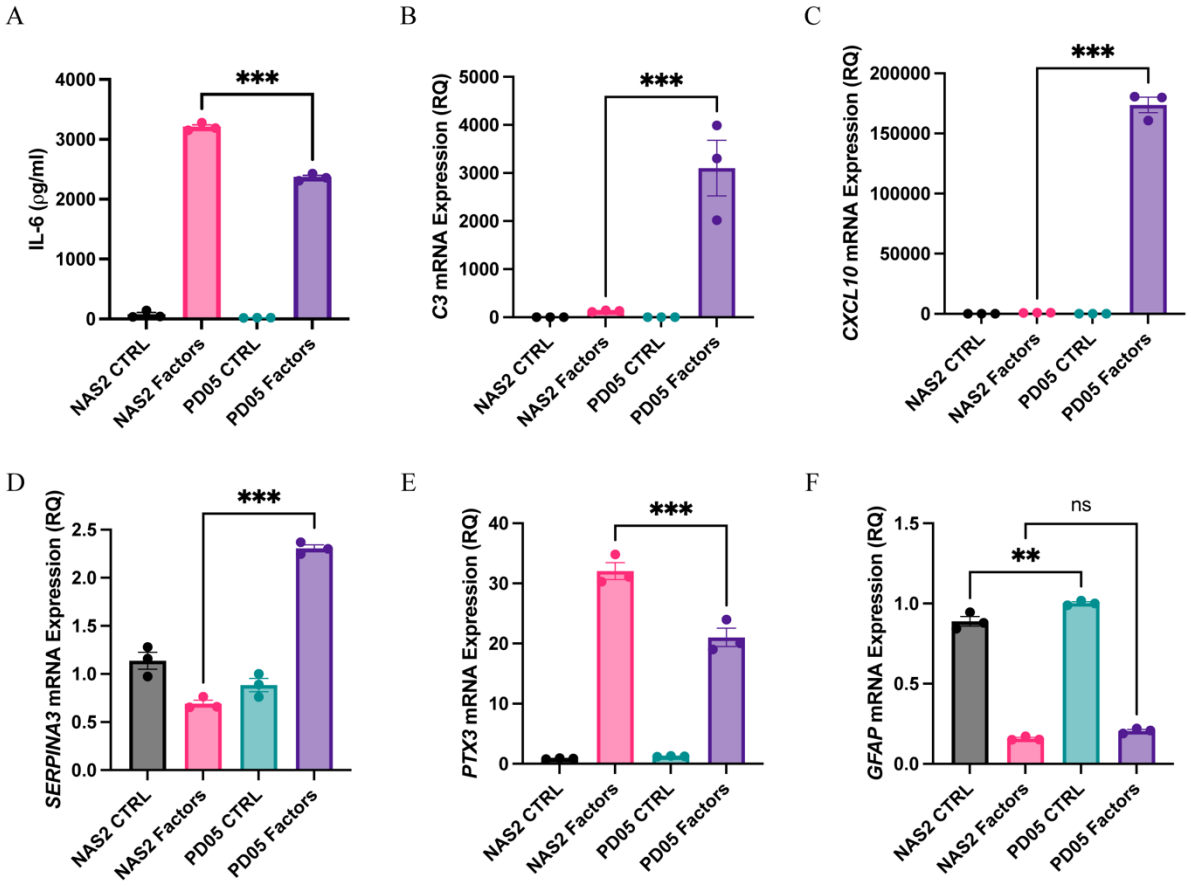

Figure 5.3.9. PD05 vmAstros demonstrate an altered protein and gene expression phenotype compared with control NAS2 vmAstros.

*A) IL-6 protein secretion. Gene expression of B) C3, C) CXCL10, D) SERPINA3, E) PTX3 and F) GFAP. Data expressed as ± SEM (N=3). **p<0.01, ***p<0.001. One-way ANOVA w/ Tukey's post-hoc.*

5.4. Discussion

PD is clinically characterised by the degeneration of neurons in the SNpc of the midbrain. These neurons arise in development through the precise expression of a variety of factors including SHH, FGF8, and activation of the WNT pathway which act to form the ventral floorplate of the midbrain. It is these A9 dopaminergic neurons of the ventral floorplate that are selectively sensitive in PD and the loss of these cells and their projections contribute to the presenting symptoms (Poewe et al., 2017). In order to unmask the mechanisms contributing to this degeneration, we need to study these cells and those in the surrounding environment. There are understandably limitations to the study of these cells and iPSC technology presents a way for us to overcome these limitations (McComish et al., 2022). Through the precisely timed addition of factors known to guide development *in vivo*, we can differentiate these neurons and astrocytes of the ventral midbrain.

5.4.1. Generation of iPSC-derived vmNPC

The first step in this process is to take our generated PD iPSC line, PD05 (see Chapter 4) and a well-characterised control iPSC line, NAS2 and direct them towards the neuroectoderm while simultaneously specifying the cells for the ventral floorplate. After a period of about 20 d we were able to assess the success of this neuralisation by assessing expression of markers; TUJ1, LMX1A, FOXA2 and SOX6 in the cells. Both the PD05 and NAS2 cell lines expressed theses markers, confirming their ventral midbrain neuronal fate. TUJ1, also known as beta III tubulin, is a cytoskeletal protein present in all neuronal cells (Katsetos et al., 2003). It is therefore commonly used to confirm neuronal differentiation of many regions, it is not specific to the midbrain. LMX1A and FOXA2 are well-established markers for the midbrain, they are expressed in development and help drive differentiation of midbrain cells, through regulation

of neurogenin 2, and MSX-1 (Andersson et al., 2006; Cai et al., 2009). These markers have therefore been used for numerous years as confirmation of a successful midbrain differentiation. SOX6 has more recently been highlighted as a potentially useful marker in identifying cells specific to the SNpc (Oosterveen et al., 2021; Pereira Luppi et al., 2021). High levels of SOX6 expression and indeed co-expression of TH is observed in the ventral SN in mouse models, and not in the surrounding VTA (Pereira Luppi et al., 2021). These SOX6/TH+ cells also express aldehyde dehydrogenase 1 A 1 (ALDH1A1). ALDH1A1 is another marker that is well-established as being expressed by these cells in the midbrain. While surrounding areas such as the SN *pars lateralis* and VTA express low levels of SOX6, and high levels of calbindin which should help delineate between areas (Pereira Luppi et al., 2021). Luppi and colleagues also observed that these SOX6 positive neurons increased calcium transients in response to movement (acceleration) but not to reward, while SOX6 negative cells responded with increased calcium transients following reward, and not movement. They therefore, concluded that these SOX6 positive cells from the SNpc are in fact A9 dopaminergic neurons, involved in motor functions, therefore representing the population of interest in PD (Pereira Luppi et al., 2021). Oosterveen and colleagues highlight the importance of SOX6 as a marker of midbrain dopamine neurons. They demonstrate that SOX6 positive neurons are sensitive to PD associated toxin, rotenone, whilst neighbouring orthodenticle homeobox 2 (OTX2) positive cells were not (Oosterveen et al., 2021). SOX6 positivity correlates to a more medial floor plate dopaminergic neuronal population, which is associated with motor tasks and is selectively sensitive (Oosterveen et al., 2021; Pereira Luppi et al., 2021). These data together suggest that these SOX6 positive cells from the SNpc are in fact A9 dopaminergic neurons, involved in motor functions, and represent the population of interest in PD. Researchers are continuously working to improve and adapt protocols for the differentiation of these midbrain dopaminergic neurons to aid the study of PD. The identification of novel markers and gaining a better

understanding of the development of this brain region, and indeed the surrounding areas is benefitting this area of research continuously. It was recently established the markers of FOXA2 and LMX1A do not solely identify the midbrain dopaminergic neuronal progenitors, but also give rise to subthalamic nuclei glutamatergic neurons (Kee et al., 2017). Nolbrant and colleagues describe a protocol that utilises carefully timed addition of FGF8b to steer these developing neurons towards the ventral midbrain dopaminergic fate rather than that of the subthalamic nucleus (Nolbrant et al., 2017). This is the protocol that we utilised in this study. The makers of engrailed 1 (EN1) and canopy FGF signalling regulator 1 (CNPY1) are suggested to confirm midbrain dopaminergic neurons, whilst barH like homeobox 1 (BARHL1) and paired-like homeodomain transcription factor 2 (PITX2) are suggested for the subthalamic nucleus (Nolbrant et al., 2017). The protein calbindin has also been associated with the VTA area and has been used to distinguish neurons from this area from those of the SN (Pereira Luppi et al., 2021). While this area of research is ever growing it is promising that these protocols are demonstrating cellular phenotypes which respond similarly to the selectively vulnerable populations in PD.

While we aimed to use these vmNPC to generate vmAstros, they could also be taken forward and further cultured into mature vmNeurons. The protocols summarised in Table 5.1.1. outline a variety of methods to do this. For prolonged culture of midbrain neural cells, including those vmNPC generated here, neurotrophic factors such as BDNF, GDNF (Binder & Scharfman, 2004; Rakowicz et al., 2002) are utilised. Furthermore, ascorbic acid is commonly implemented due to its ability to improve dopaminergic neuronal yields (Bagga et al., 2008; Yan et al., 2001). Most protocols for generating mature vmNeurons utilise that addition of factors such as TGFβ, dibutyryl cyclic-AMP (dbcAMP), and DAPT to further mature their cells (Table 5.1.1.). It has been demonstrated that dbcAMP specifically aids in specification of

dopaminergic neurons, with its contribution to increased TH expression in cultures. While the factors DAPT and TGFβ are described to improve differentiation and survival, respectively (Sibuea et al., 2023). Sibuea and colleagues recently demonstrated that removal of these factors also increased glial markers such as S100β, highlighting their importance in maintaining a pure neuronal culture (Sibuea et al., 2023). This same study demonstrated that the marker of FOXA2 was down-regulated with removal of TGFβ, while EN1 was dependant on dbcAMP and DAPT, with its expression down-regulated upon their removal. This study concluded that together this cocktail of factors benefits the culture of midbrain A9 dopaminergic neurons and removal of any one of these negatively impacts the culture (Sibuea et al., 2023). Generation of mature vmNeurons enables the investigation of the selectively vulnerable population of cells in PD and thus provides the potential for identification of novel mechanisms which may be targeted therapeutically.

5.4.2. Differentiation of vmAstros

Given the important role of astrocytes in CNS homeostasis, and inflammation, it is no surprise that these cells have been highlighted as being important in the pathogenesis of PD. Understanding how these cells are functioning at a cellular level should aid us in identifying therapeutic avenues for PD. Studying these cells presents a similar issue as with neurons, in that it is near impossible to obtain primary tissue and even then that has its limitations. In order to generate a monolayer culture of ventral midbrain astrocytes to study their responses we utilised iPSC technology. iPSC were first differentiated into vmNPC, from this point vmAPC were generated and finally matured into vmAstros. In order to confirm the generation of mature astrocytes and that a ventral midbrain regionality was maintained astrocytes were assessed for expression of S100β, GFAP, EAAT1, CX43 and LMX1A. S100β and GFAP are well-characterised markers of astrocytes. S100β is a calcium binding protein, expressed mainly by

astrocytes in the CNS (Brozzi et al., 2009). S100β has a plethora of functions intracellularly as well as extracellularly and has been linked to a variety of neurological diseases, including PD (Brozzi et al., 2009; Michetti et al., 2019). GFAP is a key astrocytic intermediate filament protein, which was first described by Eng in 1969 (Eng et al., 2000). Despite its regular use as an astrocyte marker, it has been shown to have variable expression levels within astrocytes and thus is not very reliable (Jurga et al., 2021; Zhang et al., 2019). EAAT1 is located primarily on astrocytes in the CNS and is important for glutamate homeostasis (Parkin et al., 2018). CX43 is an astrocyte gap junction protein that allows exchange of molecules between astrocytes (Dong et al., 2022). The presence of these markers indicate functional capabilities and therefore maturity of the astrocytes. While due to the novelty of the area, the regionality of astrocytes is not often considered when differentiating from iPSC. However, it has been shown repeatedly that astrocyte responses to inflammation will differ depending on the brain region (Crompton et al., 2023; Zhang et al., 2019). Therefore, we aimed to differentiate midbrain specific astrocytes so that our results would be most representative of the PD brain. Hence, the confirmation of the expression of the midbrain marker, LMX1A.

5.4.3. Astrocytes demonstrate differences in their reactive phenotype

In order to assess their ability to behave functionally like astrocytes, and since inflammation is of particular interest to this cell type, their ability to respond to inflammatory stimulus was assessed. Liddelow and colleagues reported in 2017 that the combination of three activated microglial secreted cytokines induced a robust reactive astrocytic phenotype (Liddelow et al., 2017). Of particular interest was the fact that the more pro-inflammatory astrocytes expressed high levels of C3. The group then demonstrated the presence of these C3 positive astrocytes in the post-mortem brain tissue of PD patients (Liddelow et al., 2017). Highlighting this as a plausible stimulus to produce reactive astrocytes similar to those present in PD. In this study

to determine the ability of the astrocytes to adopt a reactive astrocyte phenotype, the iPSC-derived vmAstros were exposed to the Liddelow cocktail of factors; TNFα, IL-1α and C1q. After 24 h the conditioned media and cells were taken for analysis.

Both PD05 and NAS2 vmAstros demonstrated a significant increase in the secretion of IL-6 following stimulation with the Liddelow factors. This increase in IL-6 secretion is consistent with what is observed from pro-inflammatory astrocytes phenotypes. Furthermore, the differentiated astrocytes also followed expected patterns in relation to inflammatory gene expression. Both astrocyte lines demonstrated significantly increased expression of *C3*, *CXCL10*, and *PTX3*. As mentioned, C3 is a pro-inflammatory associated cytokine that has been observed to increase in PD (Liddelow et al., 2017). It is a member of the complement cascade and triggers increased pro-inflammatory pathway activation (Ricklin et al., 2016). CXCL10 is an important immune chemokine, involved in propagating the immune response (Vazirinejad et al., 2014). Elevated plasma CXCL10 levels were associated with poor prognosis on the Hoehn and Yahr scale and poor cognition in PD patients (Rocha et al., 2014). While PTX3 is usually stimulated by pro-inflammatory cytokines, it is known to have neuroprotective roles, including in the BBB (Bonsack et al., 2019). Therefore, it is likely that the increased expression is common following inflammatory insult and represents an attempt of the astrocytes to protect the brain. The reduced expression observed here in the PD astrocytes may have connotations for BBB dysfunction, a phenomenon often described in PD. Expression levels of *IL-6* were also significantly increased compared to controls in NAS2 astrocytes. While *IL-6* expression was increased follow stimulation in the PD05 astrocytes also, the significance could not be assessed due to the control being undetermined. Similarly, levels of *LCN2* expression were increased in both PD05 and NAS2 astrocytes following stimulation, however statistics could not be run due to the control once again remaining undetermined. LCN2 is a common pro-

inflammatory associated protein, that has neurotoxic effects (Kim et al., 2016). Kim and colleagues demonstrated that LCN2 is increase in PD post-mortem brain tissue and confirmed these findings in a MPTP mouse model (Kim et al., 2016). They further associated this increased LCN2 with astrocytes and found LCN2 deficiency is protective in this mouse model (Kim et al., 2016). The expression levels of *GFAP* were observed to significantly decrease following exposure to the Liddelow factors in both PD05 and NAS2 cell lines. This is consistent with literature that describes GFAP levels to decline (Hyvarinen et al., 2019; Soubannier et al., 2020). Interestingly the expression levels of *ITGA6* were observed to decrease in both cell lines following exposure to the Liddelow factors. This gene encodes for the protein CD49f and was recently proposed as a useful marker for astrocytes due to the fact that it remains unaltered despite reactivity profile in the astrocytes (Barbar et al., 2020). As our study directly contradicts these findings it presents an argument for further research into this protein as a consistent marker in astrocytes.

An interesting finding, was that the expression of *SERPINA3* was observed to significantly decrease in NAS2 vmAstros, whilst expression in PD05 vmAstros was significantly increased. This lead to the direct comparison of reactivity phenotypes between the two cell lines in order to asses any other differences. SERPINA3 is indicated by Liddelow and colleagues as a pan-reactive astrocyte marker, in that it is neither wholly pro- nor anti-inflammatory in nature (Liddelow et al., 2017). SERPINA3 has been associated with anti-inflammatory processes and neuroprotection, however, studies have also demonstrated its contribution to inflammation and neuronal damage (Liu et al., 2023). It is therefore, unclear what these differing responses could mean in terms of disease pathogenesis. When compared directly, IL-6 production was significantly reduced in the PD05 astrocytes compared to the NAS2 astrocytes. While, *IL-6* mRNA expression levels also appear reduced in PD05 astrocytes comparatively to NAS2

astrocytes, these were not be directly compared due to no control data being present. Furthermore, PD05 vmAstros expressed significantly higher levels of genes for *C3, CXCL10* and *SERPINA3* compared to the NAS2 control vmAstros. Interestingly, the levels of *PTX3* were significantly lower when compared to those of the NAS2 vmAstros. Finally, while there was no significant difference between PD05 and NAS2 vmAstros in terms of *GFAP* expression following stimulation, there was a significant difference in *GFAP* expression between the control group. While this suggests an overall increased inflammatory phenotype in the PD astrocytes, there is much more work that would need to be down to investigate this potential effect completely. There is a lack of literature investigating iPSC-derived astrocyte reactivity in the context of PD, and any evidence that does exist focuses on genetic forms of PD. One such study utilised iPSC-derived from an individual with the LRRK2 mutation, associated with increased PD risk. The differentiated astrocytes in this study demonstrated an increased pro-inflammatory phenotype compared to health controls, however it is difficult to compare to our sporadic PD data presented here (Sonninen et al., 2020). This study also presented potential differences in inflammatory responses generated upon stimulation between PD astrocytes and controls. Overall these data demonstrates that following developmental cues you can direct the differentiation of pluripotent stem cells towards a specific cell fate, which can then act as a functional model of disease.

Chapter 6 : Investigating the peripheral immune system in Parkinson's disease

6.1. Introduction

6.1.1. The peripheral immune system in Parkinson's disease

While the immune-related processes of astrogliosis and microgliosis have long been established in PD pathogenesis, it is only in recent years that the involvement of the peripheral immune system has really come to the fore. The peripheral immune system and its involvement in PD has been outlined in detail in Chapter 1 of this thesis (see section 1.7.3).

In short, the presence of peripheral $CD4^+$ and $CD8^+$ T cells were observed in the post-mortem brain tissue of PD patients by Brochard and colleagues, which was consistent with findings in animal models of the disease (Brochard et al., 2009; Liu et al., 2017; Liu et al., 2019). While it was $CD4^+$ T cells in particular that have been highlighted as the main contributors to the pathogenesis observed in these models (Brochard et al., 2009). The contributions of T lymphocytes to PD has been summarised in Table 6.1.1. Frequencies of Th1 cells have been demonstrated to increase and also not change at all (Alvarez-Luquin et al., 2019; Baba et al., 2005; Kustrimovic et al., 2018). While it remains unclear whether levels of these cells in PD is altered, a study demonstrated that naïve $CD4^+$ T cells exposed to α-syn differentiated into Th1 or Th17 cells and induced death of TH^+ neurons and exacerbated MPTP associated cell death (Reynolds et al., 2010). Similarly, to the Th1 cells, Th2 cell population levels in PD remain unclear, with studies demonstrating no changes (Alvarez-Luquin et al., 2019), or reductions (Baba et al., 2005; Kustrimovic et al., 2018). However increased IL-13 (Alvarez-Luquin et al., 2019), the Th2 associated cytokine and GATA3, the Th2 associated transcription factor (Kustrimovic et al., 2018) were observed. Sulzer and colleagues were also able to demonstrate that α-syn induced IL-5 secreting Th2 cells (Sulzer et al., 2017). Infiltration of Th17 cells has been demonstrated in the SN of MPTP mouse models (Liu et al., 2017). Furthermore, α-syn stimulated Th17 cells induced neuronal death in the SN also in an MPTP mouse model (Reynolds et al., 2010). Sommer and colleagues in 2017 also demonstrated that

Th17 cells induced neuronal cell death in autologous iPSC-dopamine neuron cultures, which was attenuated with IL-17 inhibition (Sommer et al., 2018). Despite the indication of their contribution to neurodegeneration, the levels of Th17 cells in PD remain inconclusive, with studies observing increased frequencies, lower absolute counts (Kustrimovic et al., 2018), as well as no differences (Alvarez-Luquin et al., 2019). Reduced numbers of Tregs have been observed in PD (Alvarez-Luquin et al., 2019; Baba et al., 2005; Kustrimovic et al., 2018), whilst increase FOXP3 levels have also been observed (Kustrimovic et al., 2018). Studies have demonstrated a neuroprotective role for Tregs in PD models, such as Reynolds an colleagues who observed a beneficial effect of adoptive transfer of Tregs into a MPTP mouse model of PD (Reynolds et al., 2007). Interestingly, studies have observed that cytotoxic T-lymphocyte-associated protein 4 (CTLA-4) expression is reduced in PD, suggesting that immune regulatory mechanisms may be dysfunctional in and perhaps represents a therapeutic approach to PD (Cook et al., 2017). However, we need to fully understand the role of T cells in the disease before any therapeutic approaches can be considered.

Table 6.1.1. Evidence for T cell involvement in Parkinson's disease

PD = Parkinson's disease, HC = Healthy control

Specimens	***Study Groups***	***Main Findings***	***References***
Human whole blood	PD and HC	Decreased absolute lymphocyte numbers, both B and T cells were reduced	(Bas et al., 2001)
Rodent in vivo	$MPTP^+$, $MPTP^-$ 6-$OHDA^+$, 6-OHDA-	Human $CD4^+$ T cells decreased, $CD8^+$ T cells were consistent Significant increase in activated $CD4^+$ T cells and reduction in naïve and memory $CD4^+$ T cells in human samples MPTP, but not 6-OHDA treatment induced activation of $CD4^+$ T cells	
Human whole blood	PD and HC	Absolute lymphocyte numbers were reduced Frequencies of $CD4^+$ T cell were reduced, $CD8^+$ T cells increased Treg cells were significantly reduced IL-4 producing cells were significantly reduced, IFN-γ /IL-4 ratio was significantly increased	(Baba et al., 2005)
Rodent, in vivo, in vitro Treg, Teff and microglia	$MPTP^+$ and $MPTP^-$	Adoptive transfer of Treg attenuates MPTP-induced microglial activation and neuronal cell loss Adoptive transfer of Treg increase neurotrophic factors, BDNF and GDNF.	(Reynolds et al., 2007)

Rodent, in vivo	AAV2-Syn or AAV2-GFP	α-syn overexpression caused increased expression of CD68, IgG deposition and increased ICAM-1, IL-6, IL-1α and TNFα levels COX-2 remained unchanged and iNOS expression decreased at a later time point Increased levels of $CD3^+$ and CD45 $receptor^+$ cells following α-syn overexpression	(Theodore et al., 2008)
Human post-mortem tissue *Rodent in vivo*	PD and HC $MPTP^+$, $MPTP^-$ $Tcrb^{-/-}$, $Rag1^{-/-}$, $CD4^{-/-}$, $CD8^{-/-}$	Post-mortem tissue of PD patients and MPTP-mouse model demonstrates infiltration of $CD8^+$ and $CD4^+$ T cells in PD patients MHCI expression was observed on dopamine neurons of the substantia nigra in PD post-mortem samples MPTP-induced neurodegeneration decreased in the absence of T cells and cell death was attenuated by a lack of $CD4^+$ T cells not $CD8^+$ T cell	(Brochard et al., 2009)
Rodent, in vivo, in vitro $CD4^+$ T cells	$MPTP^+$ and $MPTP^-$	α-syn induced Th1/Th17 cell phenotypes from naïve T cells Adoptive transfer of α-syn stimulated Th1 and Th17 cells caused neuronal death in	(Reynolds et al., 2010)

		the SN, and increases cell death observed in MPTP model	
Human whole blood	PD and HC	Reduced absolute numbers of B and $CD4^+$ T lymphocytes in PD patients	(Stevens et al., 2012)
Rodent in vivo, in vitro primary microglia and $CD4^+$ T cells	AAV2-Syn or AAV2-GFP and WT or $MHCII^-$	Overexpression of α-syn causes increased expression of MHCII on microglia Knockout of MHCII attenuates α-syn induced microglial activation in the SNpc and dopaminergic cell loss	(Harms et al., 2013)
Human post-mortem tissue and hESC	PD and HC	Microglia conditioned media from α-syn and neuromelanin activated microglia cause expression of MHCI in vm-neurons vm-neurons are capable of inducing proliferation of cytotoxic T lymphocytes which in turn cause neuronal cell death	(Cebrian et al., 2014)
Rodent, in vivo	WTS^+ /$Rag2^+$, WTS^+ /$Rag2^-$, WTS^-/Rag^- and WTS^- /$Rag2^+$	Increased levels of insoluble α-syn in Rag^+ mice compared to Rag^- mice $CD4^+$ and $CD8^+$ T cells observed in the brain of WTS^+ /Rag^+ mice but not in WTS^+ /Rag^- or WTS^- M1 phenotype prominent in WTS^+ /Rag^+ mice compared with an M2 phenotype in WTS^+ /Rag^- mice which demonstrate increased phagocytosis of α-syn	(Sommer et al., 2016)

Rodent, in vivo, in vitro neurons and T cells	$MPTP^+$ and $MPTP^-$	$MPTP^+$ mice demonstrate BBB disruption and infiltration of Th17 cells in SN IL-17, IL-1β, TNFα, iNOS, IL-22 and IFN-γ increase in the SN of $MPTP^+$ mice, BDNF and GDNF decrease Co-culture of Th17 cells with vm-neurons causes increased TNFα and IL-1β, and induces neuronal cell death via LFA-1/ICAM-1	(Liu et al., 2017)
Human isolated PBMC's	PD and HC	α-syn peptides presented by both MHCI and MHCII induce T cell proliferation in PD patients T cells mainly either IFN-γ or IL-5 producing	(Sulzer et al., 2017)
Human whole blood and Isolated PBMC's	PD and HC	PD patients demonstrate lower absolute counts but not frequency of Th17 cells and Tregs PHA stimulation caused greater increase in IFN-γ and TNFα in PD patients than HS, however no difference in IL-17A was observed and IL-10 was increased in HS but not in PD patients relative to non-stimulated cells	(Kustrimovic et al., 2018)

		Co-culture of Teff and Treg cells caused ~80% reduction of IFN-γ and TNFα in HS but only ~20% in PD patients	
Human whole blood and CSF	PD and HC	Increased frequencies of $CD4^+$ and $CD8^+$ T cells in CSF and blood of PD patients compared to controls Increased concentrations of IL-2, IL-6, TNFα and MCP-1 in PD CSF Reduced IL-9 in PD CSF compared to controls	(Schroder et al., 2018)
Human iPSC and T cells	PD and HC	Increased frequencies of IL-17 producing $CD4^+$ T cells in PD patients, no significant difference in IFN-γ or IL-4 producing cells Co-culture of iPSC-mid brain neurons with T cells/IL-17 increased neuronal cell death and levels of IL-17, IL-1β, TNFα and IL-6 in PD cells Neuronal cell death in PD co-cultures occurred via IL-17/IL-17 receptor signalling, and potential activation of the NF-κB signalling pathway and preventing IL-17/IL-17 receptor interaction attenuated this	(Sommer et al., 2018)

Human PBMC's and plasma	PD and HC	Decreased Tregs observed in PD patients compared to controls No significant difference in Th1, Th2 and Th17 between patients and control, however the serum concentration of IL-17A were decreased in PD patients Serum concentrations of pro-inflammatory cytokines TNFα, IL-1β, IL-6 and GM-CSF not significantly different between groups	(Alvarez-Luquin et al., 2019)
Rodent, in vivo, in vitro microglia, neurons and Th17 cells	$MPTP^+$ and $MPTP^-$	MPTP caused BBB disfunction and increased IL-17A in SN only Teff cells increase the frequency of $CD4^+$ T cells, reduce TH^+ cell numbers in the SN, decrease dopamine levels in the striatum and increase IL-1β and TNFα levels in MPTP mice. Knockout of IL-17A alleviates these effects IL-17A induced neuronal cell death does not occur in the absence of microglia Silencing IL-17A receptor on microglia prevents IL-17-induced cell death	(Liu et al., 2019)

Human PBMC's	PD, AD and HC	Increased α-syn specific T-cell reactivity prior to PD diagnosis declining post-diagnosis Increased T cell reactivity in response to α-syn in PD patients compared to AD patients and HS	(Lindestam Arlehamn et al., 2020)
Human whole blood and PBMC's	PD and HC	Decreased number of $CD3^+$ T cells in PD patients which is associated with increased disease severity	(Bhatia et al., 2021)
Human whole blood *Isolated lymphocytes, monocytes, Treg, Tresp*	PD and HC	Reduced frequency of Tregs and their functionality in PD No change in absolute numbers of CD3, CD4 or CD8 populations	(Thome et al., 2021)
Human isolated PBMC's	PD and HC	Frequencies of naïve $CD4^+$ and $CD8^+$ T cells decreased in PD Central memory $CD4^+$ T cells increased in PD Increased Th17, Th2, and IFNy-$CD8^+$ T cells	(Yan et al., 2021)
Human whole blood	PD and HC	Increased frequency of late differentiated $CD4^+$ T cells in PD Decreased naïve $CD8^+$ T cells in PD	(He et al., 2022)

		Correlations between immune cell changed and disease associated parameters	
Human isolated CD4$^+$ T cells	PD and HC	PD CD4$^+$ T cells demonstrate reduced migration ability PD CD4$^+$ T cells demonstrated altered mitochondrial function	(Mamula et al., 2022)

6.2. Aims

The contribution of the peripheral immune system to PD pathogenesis is apparent, however we need to gain a better understanding of the role of the immune cell populations before therapeutic strategies can be devised. Therefore, the aim of this study is to:

1. Investigate plasma concentrations of PD associated proteins and cytokines.
2. Investigate cytokine, and chemokine release from PD peripheral immune cells.
3. Investigate lymphocyte populations in PD patients versus aged-matched HC.
    3.1. Investigate levels of associated cytokines.

The hypothesis for this study is that plasma concentrations of inflammatory cytokines such as IL-6, TNFα and IL-17A, as well as α-syn should be elevated in PD individuals compared to HC. Additionally, differences between PD individuals and HC are expected following analysis of cytokines, such as, IL-6, TNFα, IL-17A, CXCL10, CCL5, GM-CSF, IL-10 and IL-1β secreted from PBMC when stimulated with anti-CD3 and anti-CD28. Furthermore, altered levels of immune cell populations such as CD3$^+$ T cells, CD4$^+$ T cells, CD8$^+$ T cells between PD individuals and HC is expected. Finally, differential levels of IL-17A, IFN-γ, IL-2, IL-4,

GM-CSF and TNFα positive $CD4^+$ and $CD8^+$ T cells between PD individuals and HC is also expected. These differences in cytokine secretion may contribute to an altered immune phenotype in PD.

6.2. Materials and methods

6.2.1. Processing of blood samples

Blood samples were collected in collaboration with Professor Tim Lynch's group at the Neurology Clinic in the Mater Hospital. Ethical approval was obtained from the Mater Hospital Research Ethics Committee. HC and PD patients were recruited to provide blood samples after providing informed consent. Blood samples were collected in heparinised tubes and maintained at RT. For all analysis performed in this chapter, each individual was taken as a separate biological N.

6.2.1.1. Isolation of plasma

A small sample of whole blood was centrifuged at 500 x g for 10 min to separate a sample of plasma. Plasma was collected and stored at -20°C.

6.2.1.2. Isolation of peripheral blood mononuclear cells

Whole blood was diluted 1:1 with PBS before being layered over Lymphoprep (VWR International). Layered blood was then centrifuged at 800 x g for 20 min with brake at 0 and acceleration at 1 to separate the blood into layers. Once centrifuged the diluted plasma layer was discarded and PBMC layer was collected into fresh falcon tubes. The PBMC layer was diluted to 50 ml with PBS and centrifuged at 600 x g for 10 min (brake = 9, acceleration = 9). The supernatant was discarded and cell pellet resuspended in a further 50 ml PBS to wash cells. Cells were then centrifuged at 400 x g for 10 min (brake = 9, acceleration = 9). Cell pellet was resuspended in completed RPMI (Appendix 1 Table 6), before being counted. Cells were cryopreserved at concentrations of either $5x10^6$ or $10x10^6$ in 10% DMSO in FBS.

6.2.2. Generation of conditioned media

PBMC conditioned media was generated by stimulating PBMC with plate bound anti-CD3 (1 μg/mL; BD Biosciences, California, US) and soluble anti-CD28 (1 μg/mL; eBioscience, California, US) for 4 d. Conditioned media was then collected and stored at -80°C until use.

6.2.3. Flow Cytometry

PBMCs were thawed and counted. $1x10^6$ cells were seeded per flow cytometry tube. The same batch of internal control PBMCs were used for every run of Flow Cytometry as positive control. The flow cytometry panel was designed to ensure no fluorochrome overlap (Table 6.2.1.). Cells were stimulated with PMA (50 ng/ml), Ionomycin (500 ng/ml) and Brefeldin A (5 μg/ml) for 4 h at 37°C, 5% CO2, the unstimulated group of cells were incubated with Brefeldin A (5 μg/ml) for 4 h at 37°C, 5% CO2. Following stimulation cells were diluted 2:1 with FACS buffer (4% FBS in PBS) before being centrifuged 500 x g for 4 min. The supernatant was discarded and the cells resuspended in extracellular antibody (viability, anti-CD3 and anti-CD8 in BD Horizon™ Brilliant Stain Buffer; Table 6.2.1.). This mix was incubated in the dark for 15 min. The cells were then diluted in FACS buffer, centrifuged at 500 x g for 4 min. The supernatant was discarded and the cells were fixed (Fix and Perm Buffer A) for 10 min at RT in the dark. The cells were diluted in FACS buffer again and centrifuged at 500 x g for 4 min. The supernatant was discarded and the cells resuspended in the intracellular antibody/perm buffer mix (IL-4, IFN-γ, IL-17A, TNFα, GM-CSF and IL-2 in Fix and Perm Buffer B; Table 1). The cells were incubated in the intracellular antibody solution in the dark at RT for 20 min. Following this, the cells were diluted in FACS buffer and centrifuged at 500 x g for 4 min. The supernatant was removed and tubes vortexed to resuspend pellet. The cells stored at 4°C until used. The samples were taken for acquisition using the Aurora, voltage set as FSC 15, SSC 180 and SSCB 50. Data was analysed using FlowJo software.

Table 6.2.1. Flow cytometry antibody panel.

Ch. = Channel, Fluor. = Fluorophore, Man. = Manufacturer. V/R = Volume per reaction

Emission peak (approx.)	***Ch.***	***Target***	***Fluor.***	***Species***	***Man.***	***V/R***
428	V1	IL-4	BV421	Rat	BioLegend®	1.5 µl
542	V7	Viability	FVeF566	Mouse	Novus Bio	0.1µl
615	V10	IFN-γ	BV605	Mouse	BD Horizon™	0.7 µl
720	V13	CD3	BV711	Mouse	BD Horizon™	1.5 µl
525	B2	IL-17A	AF488	Mouse	BioLegend®	1.25 µl
697	B9	TNFα	PerCP-Cy5.5	Mouse	Invitrogen	1.5 µl
581	YG1	GM-CSF	PE	Rat	BioLegend®	1.5 µl
615	YG3	IL-2	PE-CF594	Mouse	BD Horizon™	1.5 µl
780	R7	CD8	APC-eF780	Mouse	Invitrogen	1.5 µl

6.3. Results

6.3.1. Analysis of plasma from individuals with PD and age-matched HC.

We aimed to gain a better understanding of the peripheral immune landscape in people with PD. Current literature is very divided and so it is apparent that further studies are required to gain understanding of the immune status within PD (MacMahon Copas et al., 2021). To begin, we collected plasma from the whole blood samples of people with PD and a collection of age-matched HC participants (Table 6.3.1.). We first analysed the levels of α-syn in these samples and found no apparent differences between the two cohorts (Fig. 6.3.1. A). Following this, we assessed the levels of a variety of cytokines, IL-6 (Fig. 6.3.1. B), TNFα (Fig. 6.3.1. C), and IL-17A (Fig. 6.3.1. D), however, no significant differences were observed here either.

Table 6.3.1. Overview of participants involved in this study.

Data expressed as mean years ± standard deviation

Plasma	***HC n=6***	***PD n=6***
Age (Mean)	63.5 ± 8	71.3 ± 7.5
Sex (Female:Male)	3:3	4:2
Age of onset (Mean)	N/A	64 ± 6.4
Disease duration (Mean)	N/A	7.4 ± 7.7
Conditioned media	***HC n=3***	***PD n=4***
Age (Mean)	57.7 ± 7.5	60.5 ± 11.9
Sex (Female:Male)	1:2	1:3
Age of onset (Mean)	N/A	45.5 ± 9.7
Disease duration (Mean)	N/A	15 ± 5.4
PBMC	***HC n=4***	***PD n=4***
Age (Mean)	63 ± 12.3	60.5 ± 11.9
Sex (Female:Male)	1:3	1:3
Age of onset (Mean)	N/A	45.5 ± 9.7
Disease duration (Mean)	N/A	15 ± 5.4

6.3.2. Investigating differences in stimulated PBMCs protein release.

In order to further investigate potential differences in immune function, we decided to next investigate the peripheral immune cells at the PBMC level. PBMC's were isolated out of whole blood of participants and in this instance, stimulated with anti-CD3 and anti-CD28 for a period of 4 d. After which the conditioned media from the stimulated PBMCs was collected and taken for analysis by ELISA. A variety of proteins associated with immune function were assessed.

Interestingly, the PD samples appeared to have consistently lower secretion levels of proteins assessed than their age-matched HC counterparts. while not all of these reached significance. Levels of granulocyte macrophage colony stimulating factor (GM-CSF; p0.003; Fig. 6.3.2. A) and chemokine ligand 5 (CCL5; p0.04; Fig. 6.3.2. B) were significantly decreased in the PD population compared with controls. While the levels of TNFα (p0.06; Fig. 6.3.2. C), IL-10 (p0.05; Fig. 6.3.2. D) and CXCL10 (p0.06; Fig. 6.3.2. E) appeared down-regulated, this failed to reach significance. Levels of IL-6 (Fig. 6.3.2. F), IL-1β (Fig. 6.3.2. G) and IL-17A (Fig. 6.3.2. H) remain unchanged between the control group and PD samples.

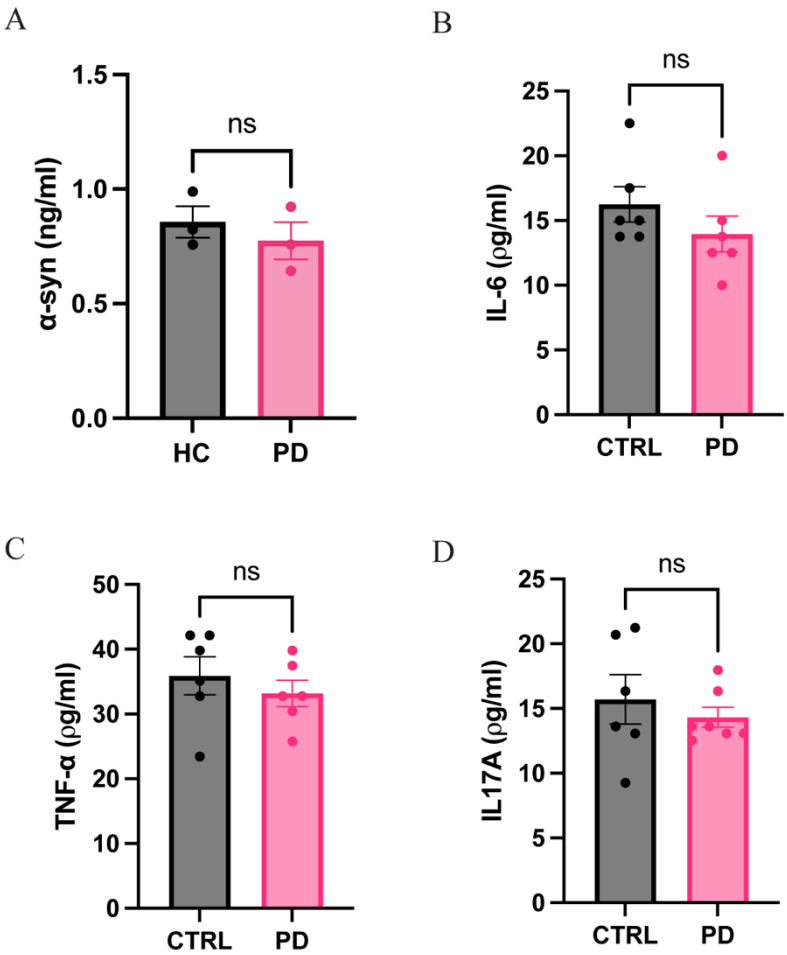

Figure 6.3.1. Analysis of plasma from individuals with PD and aged-matched HC.

Protein concentrations of α-synuclein (A), IL-6 (B), TNF-α (C), IL-17A (D). Data expressed as ± SEM (N=3-6). Unpaired T-test. Significance, $p<0.05$.

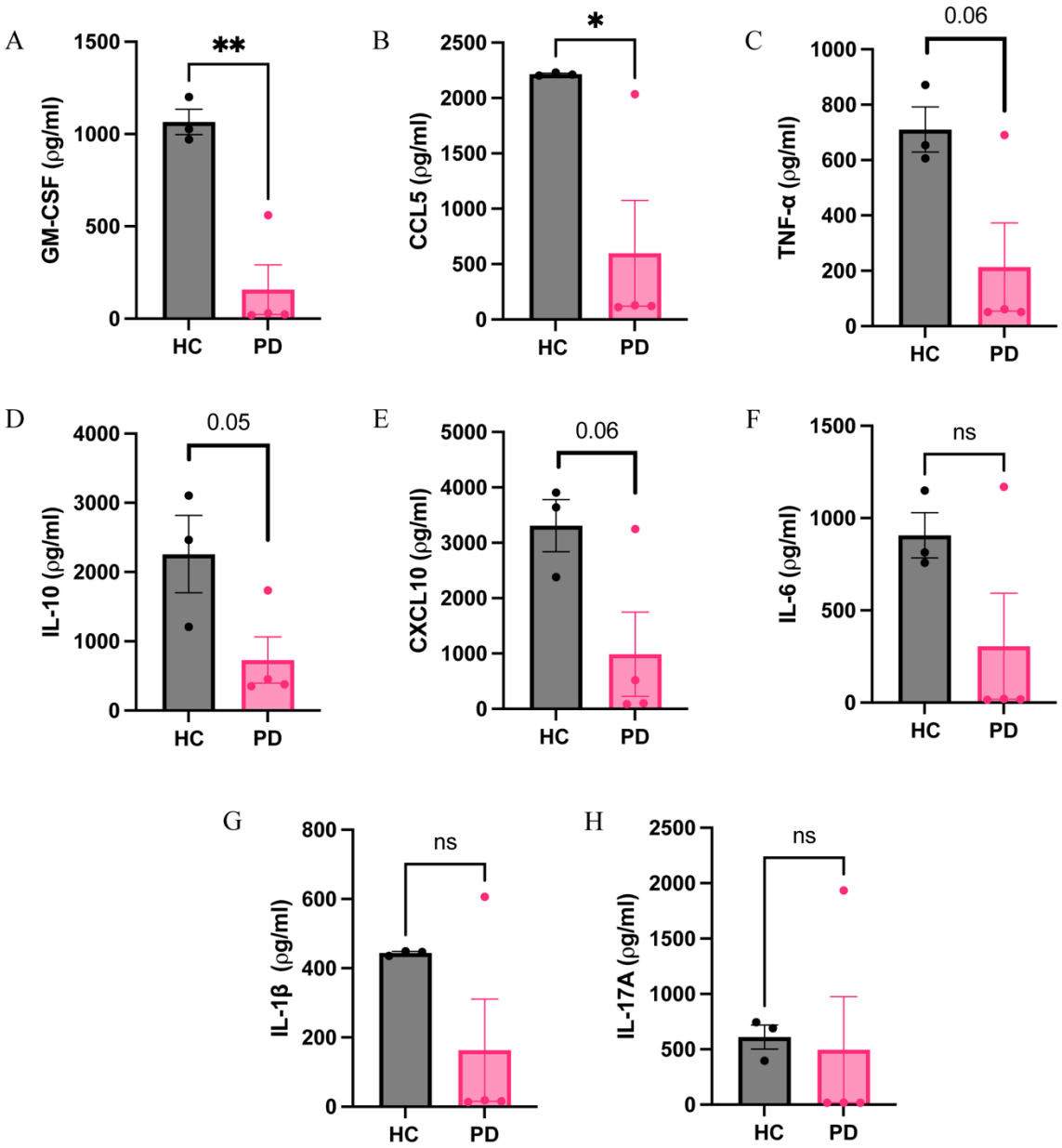

Figure 6.3.2. Analysis of the cytokines released by stimulated PBMC.

*Protein secretion of (A) IL-6, (B) IL-1β, (C) IL-17A, (D) TNF-α (E) GM-CSF, (F) CCL5, (G) CXCL10 and (H) IL-10 from control and PD anti-CD3/anti-CD28 stimulated control and PD PBMC. Data expressed as ± SEM (N=3-4). Unpaired T-test. *p<0.05, **p<0.01, ***p<0.001.*

6.3.3. Investigation of T cell populations using flow cytometry.

To continue our analysis of peripheral immune populations in PD, we took isolated PBMCs and analysed the populations of T cells using flow cytometry. We focused on T cells, due to their apparent contribution to PD pathogenesis (Brochard et al., 2009). The single cells were gated to focus on lymphocytes specifically, then the cells were further divided into $CD3^+$ and $CD3^-$ (Fig. 6.3.3. A-D). From here we focused on the $CD3^+$ T cells and further divided these into $CD8^+$ and $CD8^-$ negative to identify CD8 and CD4 population of T cells (Fig. 6.3.3. E). This approach was adopted due to the down-regulation of CD4 observed following stimulation, a well-established phenomenon (Baran et al., 2001). From here on the $CD8^-$ population will be referred to as CD4. In order to assess the subpopulations of T cells, the cells were stimulated with PMA and ionomycin, brefeldin A was used to prevent release of the cytokines from the cells. We then assessed the production of the following cytokines from both of these subpopulations; IL-17A, IFN-γ, TNFα, GM-CSF, IL-2 and IL-4 (Fig. 6.3.3. F-H). Upon analysis of total $CD3^+$ T cells, there appeared to be a trend towards an increase in frequency for PD samples compared to HC, however this did not reach significance (Fig. 6.3.4. A). A similar trend was observed for CD4 T cells, and a trend towards a decrease observed for $CD8^+$ T cells (Fig. 6.3.4. B and C). The ratio of CD4 to CD8 T cells trended towards an increase but similarly, none of this reached significance (Fig. 6.3.4. D).

Upon assessing the production of cytokines from the CD4 T cell population. We observed a trending decrease in IFNγ (Fig. 6.3.5. A) and cells co-expressing IFNγ and IL-17A (Fig. 6.3.5. C), while IL-17A (Fig. 6.3.5. B) appeared to increase in PD samples compared to aged matched HC. However, none of these reached statistical significance. When observing TNFα (Fig. 6.3.5. D), GM-CSF (Fig. 6.3.5. E) and cells co-expressing TNFα and GM-CSF (Fig. 6.3.5. F), no real differences between the HC cohort and PD cohort were apparent. Interestingly, IL-4 expressing

cells were significantly decreased in PD patients, compared to HC (Fig. 6.3.5. G; p0.05). IL-2 expressing cells trended towards an increase in PD patients, however this failed to reach significance (Fig. 6.3.5. H; p0.08). Finally, IL-4 and IL-2 co-expressing cell frequencies did not differ between the HC and PD samples (Fig. 6.3.5. I).

Interestingly, the frequency of IFNγ, IL-17A and IFNγ, IL-17A co-expressing cells in $CD8^+$ T cell population demonstrated the opposite trends to those seen in the CD4 T cell population. IFNγ (Fig. 6.3.6. A) trended towards an increase, while IL-17A decreased slightly (Fig. 6.3.6. B). The cells expressing both IFNγ and IL-17A appeared to also decrease (Fig. 6.3.6. C). Although, again none of these reached statistical significance. While no significant difference was observed in TNFα expression (Fig. 6.3.6. D), GM-CSF appeared to be increased in the PD samples compared to HC, although it failed to reach significance (Fig. 6.3.6. E; p0.07). Cells co-expressing TNFα and GM-CSF did not significantly increase or decrease between cohorts (Fig. 6.3.6. F). While IL-4 expressing CD4 T cells were significantly decreased in PD patients, $CD8^+$ T cells expressing IL-4 were not significantly altered between groups, although the PD samples trended towards an increase (Fig. 6.3.6. G). Interestingly, while IL-2 expressing cells in the CD4 T cell population trended towards an increase but failed to reach significance, the $CD8^+$ IL-2 expressing T cells were significantly increased in the PD cohort compared to the HC (Fig. 6.3.6. H; p0.02). Lastly, while IL-4 and IL-2 co-expressing cells appeared to be trending towards increase in the PD cohort, this also failed to reach significance (Fig. 6.3.6. I). Overall, these data provides evidence of potential altered peripheral immune status in PD patients.

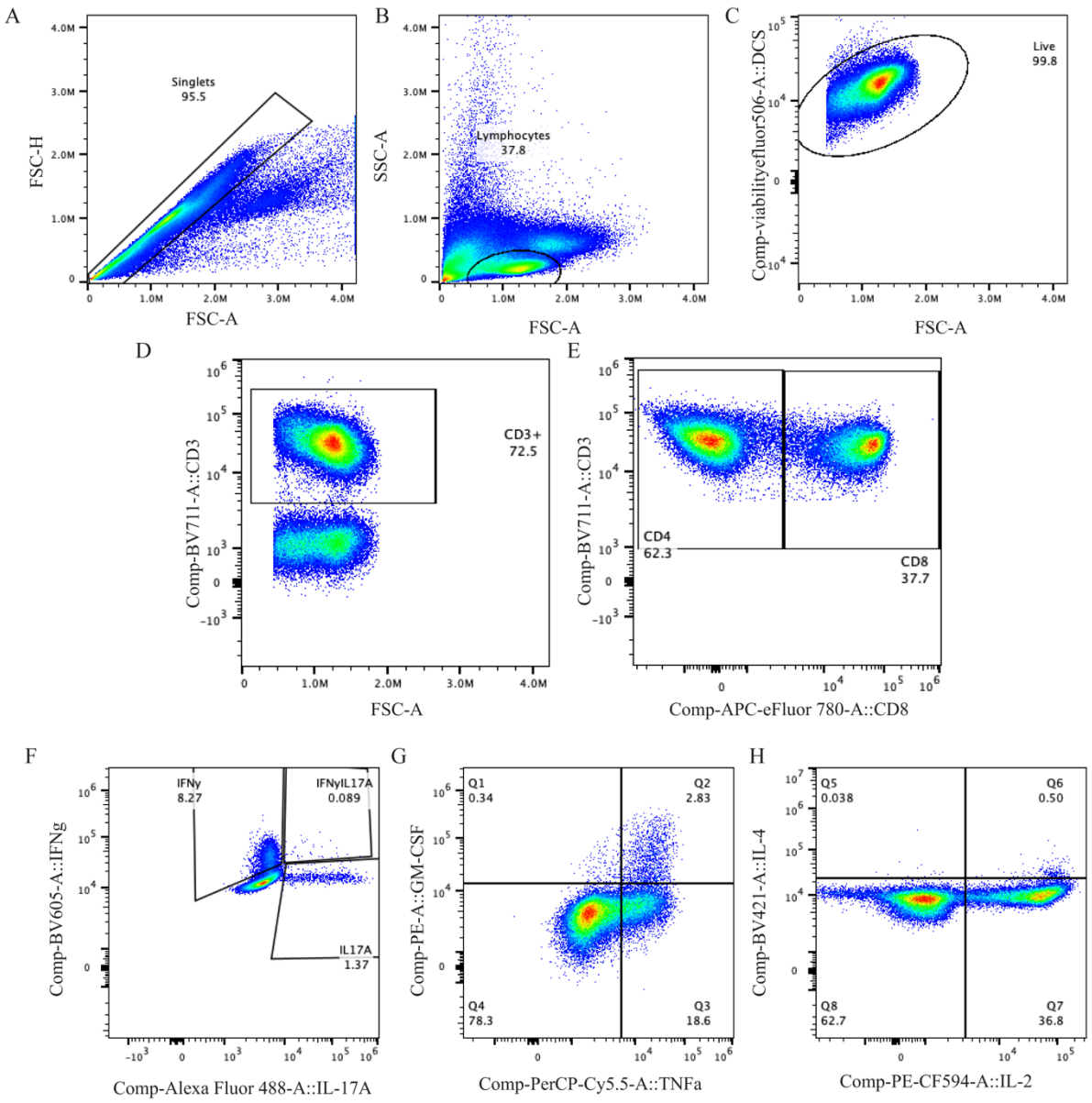

Figure 6.3.3. Outline of the flow cytometry gating strategy.

Cells were gated as follows; (A) single cells, (B) Lymphocytes, (C) Live cells, (D) CD3^{+} cells, (E) CD8 positive and CD8 negative, (F) IFNγ and IL-17A, (G) GM-CSF and TNFα, (H) IL-4 and IL-2.

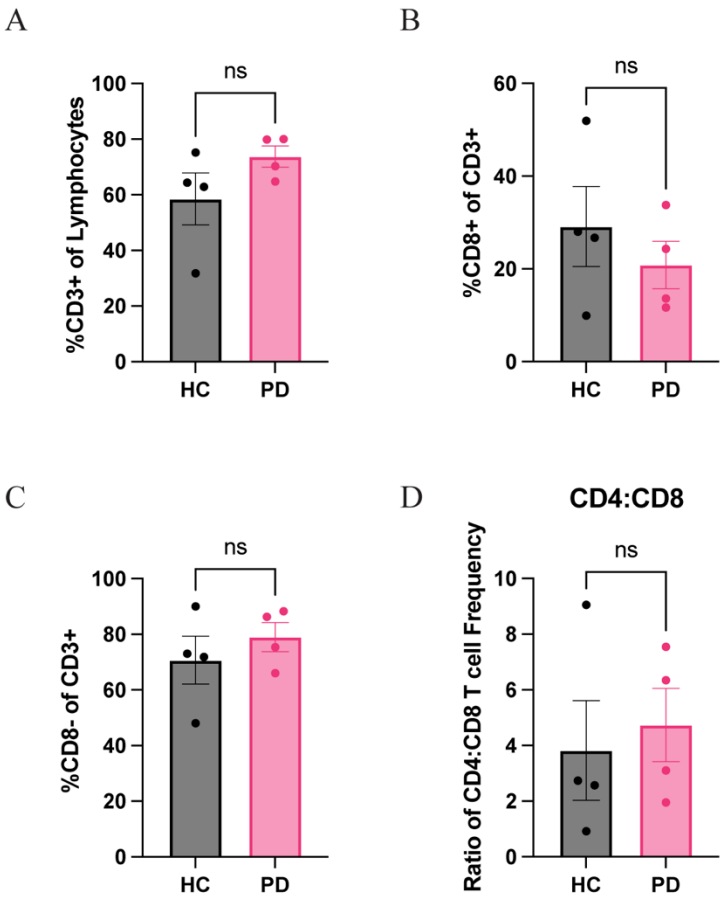

Figure 6.3.4. Analysis of T cell populations

Flow Cytometry analysis of (A) CD3, (B) CD8, (C) CD4 and (D) CD4:CD8 T cell populations in PBMC samples. HC = Healthy Controls, PD = Parkinson's disease. Data expressed as ± SEM (N=4). Unpaired T-test. Significance, $p<0.05$.

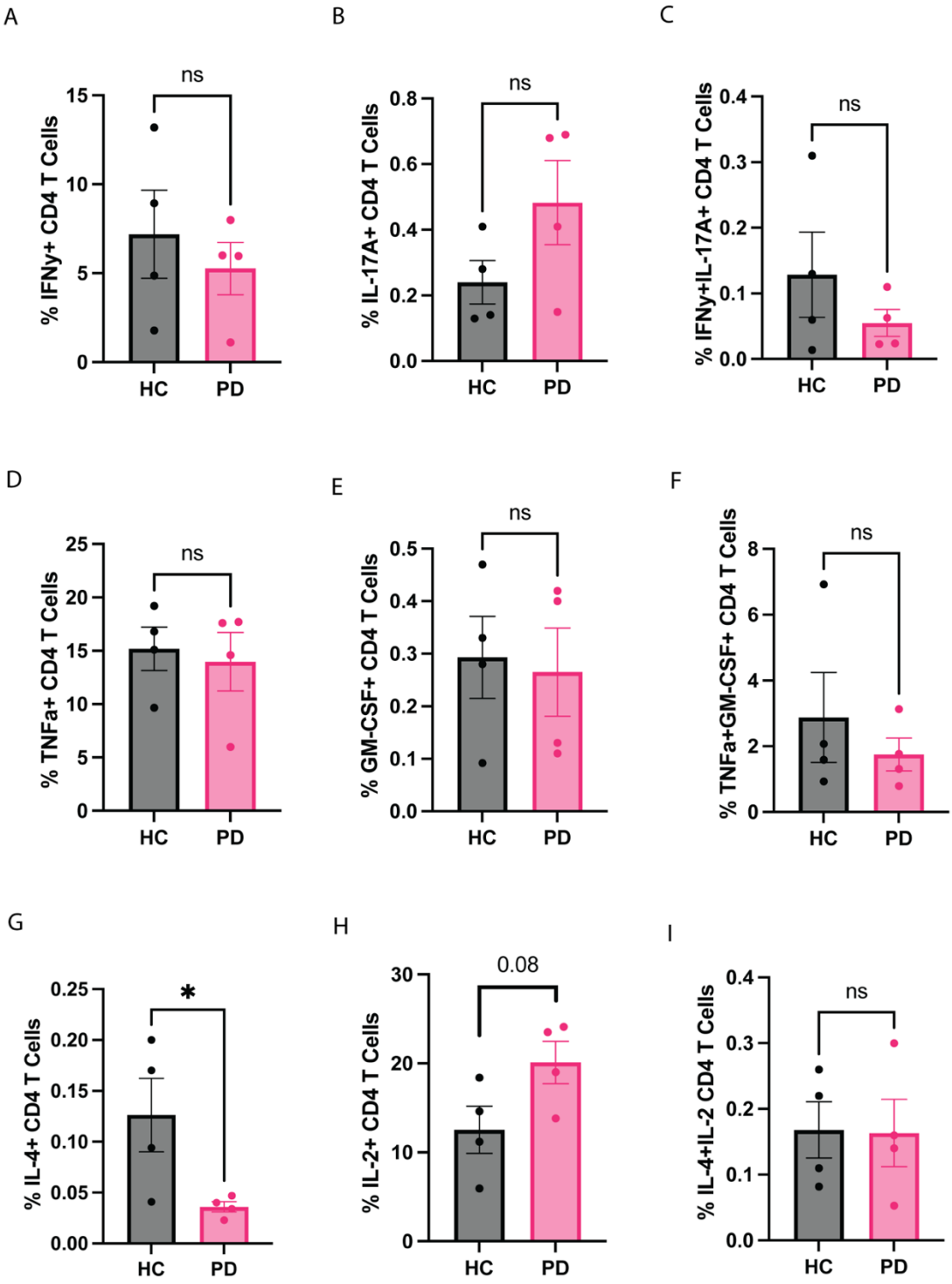

Figure 6.3.5. Analysis of CD4 T cell cytokines.

*Flow Cytometry was used to assess stimulated CD4 T cell intracellular cytokine expression. Expression of (A) IFNγ, (B) IL-17A, (C) IFNγIL-17A, (D) TNFα, (E) GM-CSF, (F) TNFαGM-CSF, (G) IL-4, (H) IL-2 and (I) IL-4IL-2. HC = Healthy Controls, PD = Parkinson's disease. Data expressed as ± SEM (N=4). Unpaired T-test. *p<0.05.*

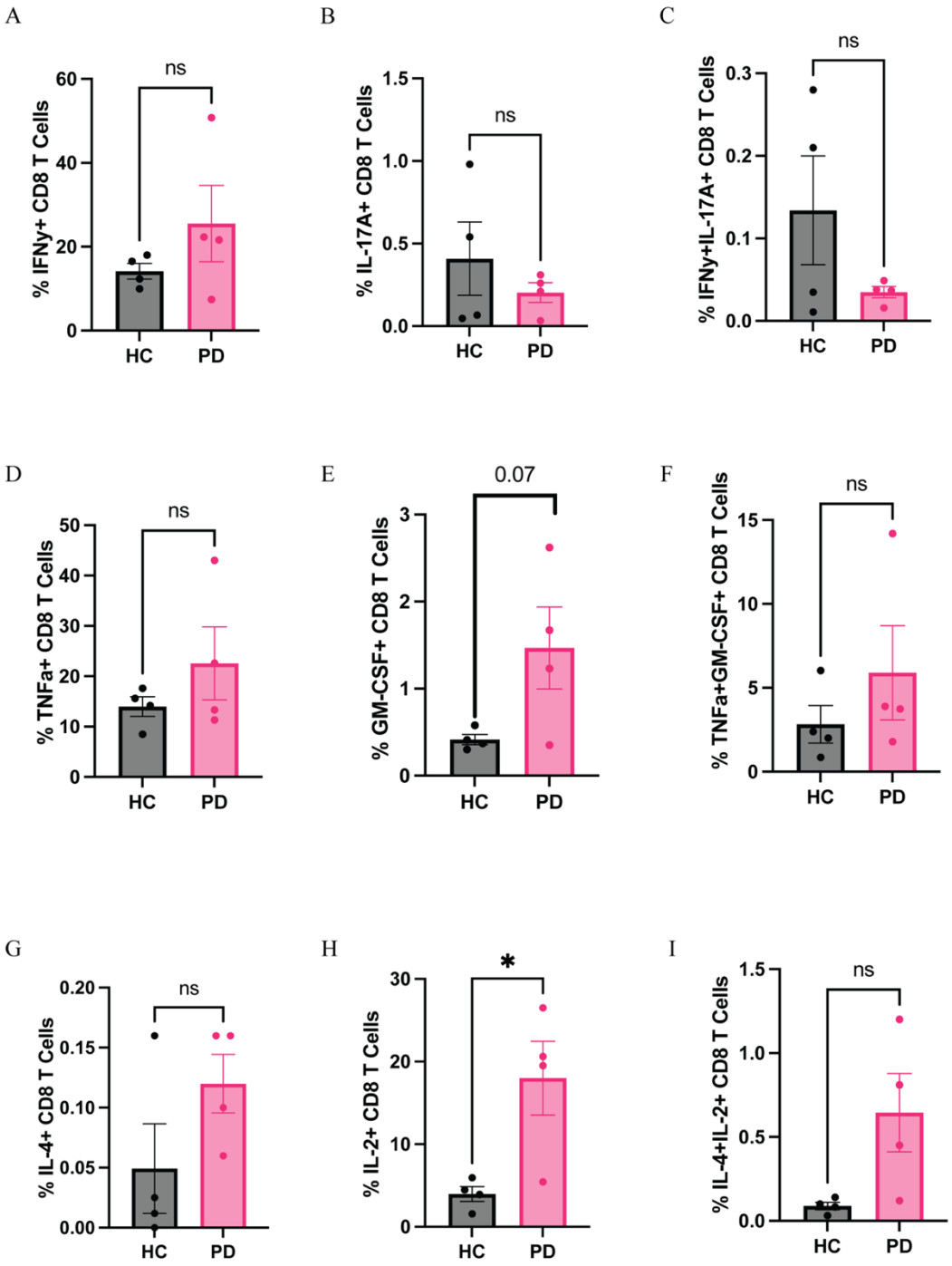

Figure 6.3.6. Analysis of CD8 T cell cytokines.

*Flow Cytometry was used to assess stimulated CD8 T cell intracellular cytokine expression. Expression of (A) IFNγ, (B) IL-17A, (C) IFNγIL-17A, (D) TNFα, (E) GM-CSF, (F) TNFαGM-CSF, (G) IL-4, (H) IL-2 and (I) IL-4IL-2. HC = Healthy Controls, PD = Parkinson's disease. Data expressed as ± SEM (N=4). Unpaired T-test. *p<0.05.*

6.4. Discussion

As mentioned previously, the peripheral immune system has in recent years been flagged as a potential contributing mechanism to PD. There are two main issues currently impeding the understanding of its contribution to this disease and the ability to target this therapeutically. These are both the lack of studies investigating this area and the inconsistencies between studies that make it difficult to arrive at a concrete conclusion. In an attempt to address these issues, this study aimed to both add to the current literature on the distribution of immune cells in PD and also compare these findings with those currently published. To gain a full picture of the immune landscape in PD this study took multiple approaches, in hopes that this would give us an unbiased and overarching analysis of the immune status of PD patients.

In order to achieve the aims, set forth in this study, blood samples were gathered from patients with PD and age-matched HC. From these blood samples plasma and PBMC's were isolated for further analysis. The PBMC's were further divided for *ex vivo* stimulation with anti-CD3 and anti-CD28 to generate conditioned media which could be analysed for proteins secreted, or for stimulation with phorbol myristate acetate (PMA), ionomycin and brefeldin A for analysis via flow cytometry.

In our initial experiments, the plasma levels of a key PD associated protein, α-syn were assessed. α-syn is an important protein, as it is involved in vesicle transport, in particular it is required for neurotransmitter release. α-syn is known to accumulate and aggregate in PD pathogenesis (Calabresi et al., 2023), furthermore, it has been demonstrated to stimulate T cells from PD patients, highlighting its potential role in triggering peripheral immune responses in PD (Lindestam Arlehamn et al., 2020). The data from this study demonstrated no significant differences, between α-syn levels in the plasma of PD patients relative to HC. While these data

does match some other literature that suggests no significant differences in plasma α-syn (Caranci et al., 2013), there is overwhelming literature which demonstrates peripheral α-syn is increased in PD (Calabresi et al., 2023). Limitations for the data presented here include the low sample numbers as well as sensitivity of the test used. The plasma analysis in this study was carried out on low sample numbers of 3 PD and 3 HC. While the data was quite consistent and demonstrates no apparent trends, this is not nearly enough sample to account for variability among participants that is frequently observed in studies. Therefore, future studies should add to these numbers to garner a better understanding of the true results here. The second potential limiting factor here is the assay used to assess levels of α-syn. Whilst the same assay kit has been used for the same purpose in previous studies, the values achieved were much higher than those observed here (J. Li et al., 2023). The methodology applied was described briefly in the latter study and so it is difficult to make a comparison to that used here. A recent meta-analysis described a large variety of studies which assessed α-syn levels in PD patients' serum or plasma. While the choice initially to assess levels in plasma versus in serum may be a point at which variability is introduced, this meta-analysis did not observe this to be factor which contributed to variability (Zubelzu et al., 2022). The overall consensus was in fact that α-syn was increased in PD plasma samples, however, the actual values between studies varied greatly. In this thesis values of approx. 1 ng/ml of α-syn were observed, whilst other studies have reported levels of α-syn including, 1.9-4 pg/ml (Bougea et al., 2020), approximately 10 ng/ml (Caranci et al., 2013), 7.7-9.84 pg/ml x10^7 (Chahine et al., 2020), 110-115,000 pg/ml (Goldman et al., 2018), and approx. 100 – 600 ng/ml (Fan et al., 2020). In future studies obtaining a consistent method of measuring samples for α-syn would be beneficial for comparison across the field.

Following a similar train of thought as the above, the levels of plasma cytokines were measured. The levels of common immune associated cytokines, IL-6, TNFα and IL-17A were assessed using ELISA. IL-6 at high levels is a cytokine with pro-inflammatory actions, involved in immune cell activation and differentiation (Wang et al., 2017). IL-6 was demonstrated to promote differentiation of Th17 cells over Tregs, it aids in migration of immune cells to sites of inflammation through stimulating chemokine release from monocytes (Biswas et al., 1998; Wang et al., 2017). TNFα, is a crucial immune-related cytokine that acts via TNF receptors 1 and 2 to stimulate NFκB and mitogen activated protein kinase (MAPK) induced pro-inflammatory cytokine upregulation, as well as activation and migration of immune cells (Jang et al., 2021). IL-17A, is associated with repair in acute instances, however, chronically, it is associated with damage and is pathogenic in many autoimmune diseases (McGinley et al., 2020). IL-17A potentiates inflammation and is important for release of chemoattractants (J. Chen et al., 2020), it is also demonstrated to be important in many autoimmune diseases (McGinley et al., 2020). While the results shown here also observed no significant differences between HC and PD samples in relation to plasma levels of IL-6, TNFα and IL-17A, the actual concentrations observed do appear consistent with those of other studies (Alvarez-Luquin et al., 2019; Diaz et al., 2022; Wang et al., 2017). Interestingly, Alvarez-Luquin and colleagues observed a reduction in IL-17A in plasma of PD patients, but no difference in IL-6 or TNFα levels in the plasma (Alvarez-Luquin et al., 2019). While Diaz and colleagues observed an increased IL-6 level in serum from PD patients compared with controls, but no difference in other cytokines (Diaz et al., 2022). There is very little literature outlining peripheral circulating levels of cytokines in PD, and this study adds to the current body of literature. However, as the area is in its infancy it will require much more analysis before these data can be translated to the disease therapeutically.

We next aimed to assess the secretion levels of cytokines from stimulated immune cells in order to gauge an idea of the immune phenotype present in PD patients versus HC. The isolated PBMC were stimulated for 4 d with anti-CD3 and anti-CD28. The conditioned media was collected and analysed for the concentrations of various cytokines and chemokines. There are no studies that this author can find which uses PBMC stimulation as a method of assessing cytokine levels in PD. Our study demonstrates an overall significant reduction in levels of IL-6, IL-1β, IL-17A, TNFα, GM-CSF, and CCL5 in PD stimulated PBMC conditioned media compared with age-matched HC, while levels of CXCL10 and IL-10 were unchanged between groups. What these data would suggest is that overall, in PD patients there is a lower number of cells readily producing these proteins. Substantially lower levels of these cytokines might indicate a dysfunctional immune system in PD; however, more work would need to be carried out to tease out these differences.

The final method of analysis utilised in this study to investigate peripheral immune cells and their secretions was flow cytometry. To begin, we assessed levels of T cell populations, $CD3^+$, $CD4^+$, $CD8^+$ T cells and the ratio of CD4:CD8 T cells. As mentioned previously, CD4 was not used as a marker due to its down regulation following stimulation (Baran et al., 2001). Therefore, the $CD3^+$ $CD8^-$ population was used instead. While we observed no significant differences in this analysis, this is not uncommon among studies in the field (Thome et al., 2021). However, it should be noted that this study used very small sample sizes and before a conclusion can be drawn, the N number should be added to. Certain studies observed an overall decrease in $CD4^+$ T cells, while $CD8^+$ T cells are more variable (Baba et al., 2005; Bas et al., 2001; Schroder et al., 2018; Stevens et al., 2012; Yan et al., 2021), whilst again, differences in markers used for flow cytometry and analysis of subpopulations of cells, either naïve or memory cells may be the reason for differing results across studies (see Table 6.1.1.).

Our analysis of $CD4^+$ T cell cytokines yielded a significant change in IL-4, the Th2 cell associated cytokine. IL-4 levels were significantly reduced in PD samples compared with controls. IL-4 is largely recognized for its beneficial effects. It is often regarded as an anti-inflammatory cytokine and can reduce inflammatory effects of other cytokines, such as TNFα. However, it is also beneficial in the brain directly, it has a positive effect on cognition, and is demonstrated to act via astrocytes to increase secretion levels of neurotrophic factors such as BDNF (Gadani et al., 2012). Therefore, if levels of this cytokine are reduced in PD this is likely having detrimental effects on the cells of the brain. Interestingly, Baba and colleagues (2005) observed a reduction in IL-4 producing cells in PD, which is comparable to what we have observed here. While the levels of IL-2 positive cells, was not significantly increased, levels appeared to be trending towards increase in PD patients in this study. IL-2 is an important immunomodulatory cytokine. It plays a critical role in clonal expansion of T cells, but more crucially in this instance, differentiation of Tregs (Ross & Cantrell, 2018). It is possible, that in PD, the body is attempting to induce Treg differentiation in order to combat the chronic inflammatory environment present. However, we do know from studies, that Tregs in PD are observed to not be as suppressive as their control counterparts (Kustrimovic et al., 2018; Thome et al., 2021). Therefore, it is likely, that this just contributes to a vicious cycle of inflammation.

While IL-2 failed to reach significance in our $CD4^+$ T cell population, it was significantly increased in the $CD8^+$ T cell population. In addition to the functions of IL-2 mentioned above, high IL-2 expression has been observed to induce T cells to terminally differentiate rapidly, into short-term effector cells, rather than memory cells, which is induced by lower levels of IL-2 (Ross & Cantrell, 2018). Furthermore, IL-2 has also been demonstrated to induce $CD8^+$ T cell exhaustion (Liu et al., 2021), presenting interesting connotations for the immune landscape in PD. Interestingly, while in this study GM-CSF did not appear to be altered at all

in $CD4^+$ T cells, it was trending towards significance in $CD8^+$ T cells. GM-CSF is named due to its ability to stimulate proliferation of granulocytes and macrophages. However, it is also a potent immune adjuvant and is associated with numerous immune-related, and indeed autoimmune diseases (Bhattacharya et al., 2015). GM-CSF acts to stimulate the immune system overall, therefore, it's increase in PD is likely to contribute to immune cell proliferation.

Another factor to be considered here is the different methods of stimulation used throughout the literature when assessing peripheral immune cells via flow cytometry. While the stimulation techniques used are widely accepted, they have been described to induce differing responses, and this may then induce variability across the field. Here we utilised PMA and ionomycin to stimulate the cells, and brefeldin A to prevent cytokine release. PMA is an activator of protein kinase C, while ionomycin is a calcium ionophore (Ai et al., 2013). Together these compounds are capable of bypassing traditional T cell co-stimulatory molecules to directly induce proliferation. Other methods of stimulation include the use of anti-CD3 and anti-CD28, which provides a more physiological approach to T cell stimulation (Trickett & Kwan, 2003). The study by Alvarez-Luquin and colleagues discussed throughout this thesis, assessed T cell populations in unstimulated lymphocytes, merely exposing the cells to brefeldin A to inhibit cytokine release (Alvarez-Luquin et al., 2019). Their reasoning for doing this was in hopes of bypassing the variable responses achieved with different stimulation methods. However, the vast majority of studies discussed throughout this thesis utilise PMA and ionomycin stimulation. A recent study compared different stimulation methods commonly used prior to flow cytometry staining. This study determined that the combination of PMA and ionomycin produced the best response for T lymphocytes specifically when compared to the combination of anti-CD28 and *Staphylococcal* enterotoxin B or LPS. This study also determined that brefeldin A was the best Golgi stop when comparing with Monensin (Mandala

et al., 2021). A study by Olsen and Sollid in 2013 utilised PMA and ionomycin co-stimulation and compared this to anti-CD3, anti-CD28 beads in assessment of cytokine responses in PBMC's. Both methods yielded robust cytokine responses, however, differences were observed in the production of IL-17 and IL-10. The stimulation of cells with PMA and ionomycin induced greater IL-17 production that the anit-CD3 and anti-CD28 stimulation. Whilst higher levels of IL-10 were observed in the anti-CD3 and anti-CD28 stimulation group (Olsen & Sollid, 2013). Other studies have also observed no increase in IL-10 and even IL-4 when stimulation with PMA and ionomycin was utilised (Ai et al., 2013). These data indicates that stimulation methods is something worth keeping in mind when comparing studies across the field as responses may vary. While our data provides interesting additions to the analysis of peripheral immune cell populations in PD, until the data can be further validated by increasing the sample number, there is little that can be said conclusively. However, the field in general remains in disarray, with no consensus yet emerging on the state of the peripheral immune cell populations in PD.

Overall, the involvement of the peripheral immune system in PD is an exciting area of research in terms of the potential therapeutic avenues it opens. However, the field is in desperate need of further research and a consistent approach to analysis so that we are able to compare studies to one another more seamlessly.

Chapter 7 : Final Discussion

7.1. Summary

PD is particularly interesting, as it is associated primarily with the loss of a small, specific population of cells, the A9 dopaminergic neurons. It would be easy to assume this should make it a straightforward disease to unravel, alas, it has been quite the opposite. Whilst these A9 dopaminergic neurons are selectively vulnerable in PD, and there must be a reason for that, there are numerous other aspects which have come into play that are less easily explained. One such aspect is the misfolding and accumulation of α-syn, while there are genetic reasons for this, why does it occur seemingly unprompted in other instances? The involvement of the immune system is another, why is it that these peripheral cells infiltrate the otherwise content, immune sequestered CNS? Until we can unravel the mysteries of these mechanisms, the loss of dopaminergic neurons will remain an issue, despite our best efforts. Therefore, in order to add to the already impressive body of literature pertaining to this disease, this thesis set out to elucidate some of these mechanisms at play.

To begin, in Chapter 3 we utilised iPSC-derived midbrain astrocytes to investigate the response, if any, of these cells to peripheral immune cell secretions. Increasing literature supports the presence of peripheral immune cells in the PD brain, and their contribution to neurodegeneration (see Chapter 1 and Chapter 6). However, there is little known about their interactions with astrocytes. As previously discussed, astrocytes are critical homeostatic regulators of the CNS and their dysfunction can prove to be detrimental. We observed a robust, pro-inflammatory astrocyte phenotype following exposure to $CD4^+$ T cell conditioned media, at both acute and chronic timepoints. Furthermore, the cytokines TNFα and IL-17A, both of which are secreted by $CD4^+$ T cells, synergistically induced a similar pro-inflammatory phenotype in the vmAstros. Lastly, this chronic reactive phenotype induced damage to cellular membranes, observed through increased LDH release, as well as increased expression of the

DNA damage marker, γH2AX. Together, these data provides evidence that peripheral immune cells, upon entering the brain, contribute to astrocyte-induced inflammation and potential dysfunction of astrocytic processes. Whilst these data was interesting, we wanted to improve the translatability of the research. This leads us on to Chapter 4, in which we aimed to generate patient specific iPSC. We successfully generated iPSC lines from the skin biopsies of different sporadic PD patients. These cells expressed the established markers of pluripotency and demonstrated their pluripotent capabilities by generating cells of the three germ layers; the endoderm, mesoderm and ectoderm. Furthermore, we successfully generated midbrain neural progenitor cells and then astrocytes from these patient iPSC alongside a healthy control iPSC line. The importance of having the healthy control line is that it acts as a baseline and positive control for any experiments carried out with the patient lines. This line originates from the healthy sibling of a PD patient, not included in these studies, and has already been well-characterised as iPSC, neurons and astrocytes. The differentiated cells were exposed to the Liddelow factors to induce a reactive astrocyte phenotype. These factors have been widely established to potently induce a reactive astrocyte phenotype and are regularly implemented for this purpose (Liddelow et al., 2017). In this study we utilised this as a method of functionally characterising the cells as astrocytes, as it is well known that astrocytes will take on a reactive phenotype in responses to stimulus. However, we unexpectedly observed differences in the reactive phenotype of the PD derived astrocytes versus the control astrocytes. There was an increase in many pro-inflammatory related genes including C3, which has been previously linked to neurodegenerative diseases such as PD and AD (Liddelow et al., 2017). Due to the potential contribution of the peripheral immune system to the inflammatory environment within the brain in PD, in Chapter 6 we aimed to gain a better understanding of the immune landscape in PD. We investigated the profile of peripheral immune cells isolated from PD patients versus controls using different methods of analysis. Whilst there was a great

degree of variability in this study, we did observe some differences in the immune cell populations between PD individuals and their age-matched healthy control counterparts that are observed elsewhere in the literature.

Overall this thesis provides novel evidence that peripheral immune cell secreted cytokines contribute to astrogliosis and potential astrocyte dysfunction. Furthermore, we demonstrate that PD astrocytes may produce a more pro-inflammatory phenotype than healthy control astrocytes. Finally, peripheral immune cells in PD patients have an altered phenotype compared to those of healthy control individuals which may indicate a dysregulated immune landscape.

7.2. Peripheral immune cells contribute to chronic astrogliosis

As we have discussed previously in this thesis, astrocytes are crucial mediators of homeostasis in the CNS. There is little evidence of the interactions between peripheral immune cells and astrocytes in PD, however the data generated in this thesis adds support to the previously published data and furthermore identified a previously unreported dynamic. The fact that this study was able to demonstrate that peripheral immune cell have the capability to induce astrogliosis has large implications for PD pathogenesis. These data outlines a chronic pro-inflammatory environment of not only microglia and astrocytes but also now peripheral immune cells. These cells all appear to activate one another, therefore contributing to a vicious cycle of inflammation. A recent study by Rostami and colleagues demonstrated that astrocytes have antigen presenting capabilities in response to pre-formed α-syn fibrils. These astrocytes expressed the co-stimulatory molecules of MHCII, CD80, CD86 and CD40 which are necessary to activate $CD4^+$ T cells (Rostami et al., 2020). Furthermore, it has been observed that T cell activation of astrocytes promotes Th17 cell infiltration, microglial migration, and phagocytosis (Prajeeth et al., 2017). Additionally, Miklossy and colleagues observed ICAM-1

positive astrocytes in close proximity to LFA-1 positive microglia and leukocytes in the SN of PD patients (Miklossy et al., 2006). Overall these studies suggest a key role of T cell and astrocyte interactions in contributing to PD, whilst this requires further investigation it has exciting implications for PD therapeutics.

Future studies that wish to advance on this research should investigate pathways other than NFκB activation as was explored in this study, which could be behind the synergistic effects of TNFα and IL-17A. While TNFα is commonly associated with NFκB activation, it can trigger activity of AKT, MAPK and caspase 8 also (Jang et al., 2021). Similarly, IL-17A can act to increase activator protein 1 (AP-1)/MAPK pathways and of course NFκB (J. Chen et al., 2020). TNFα and IL-17A have been demonstrated to produce synergistic effects in other cell types, however, this is cell type dependent and the combined cytokines are just as likely to produce an additive response as a synergistic one (Beringer et al., 2018; Chiricozzi et al., 2011; Claire Q.F. Wang, 2013,; Elain et al., 2014; Noack et al., 2019; Zrioual et al., 2008). Inhibition of the NFκB pathway components would aid in fully ruling out this pathway. Similarly, using other techniques such as western immunoblotting to assess whether there is an increase in components of the pathways would be beneficial. Furthermore, to assess whether it is in fact the TNFα and IL-17A responsible for the reactive astrocyte phenotype induced by the conditioned media, inhibitors of these cytokines or their receptors could be used to demonstrate attenuation of the response. Seckunimab, the anti-IL-17 antibody was utilised by Sommer and colleagues in 2018 to confirm that IL-17 was responsible for the neuronal cell death observed in their study (Sommer et al., 2018). Due to studies demonstrating variability in the expression of various genes, it would be interesting to also include timepoints earlier than 24 h in future studies. Trindade and colleagues have observed significant upregulation of gene expression as early as 1.5 h post-stimulation (Trindade et al., 2020). Therefore, inclusion of earlier timepoints

would potentially identify gene expression alterations that may have been missed in this study and would provide a more robust illustration of the reactive astrocyte phenotype produced. Similarly, a timepoint between 3 and 7 d, such as a 5 d timepoint, would be beneficial. The γH2AX increase observed here occurred at 3 d but returned to baseline at 7 d, whilst LDH was increased at 7 d but not at 3 d. There is more information to be teased out here between these two timepoints to establish what pathological mechanisms are at play in the astrocytes. Furthermore, due to these being unexpected findings, this chapter only dealt with initial investigation of potential detrimental damage to the astrocytes. However, these results present interesting and important connotations for astrocyte health in disease. Therefore, a future study should focus on how chronic cytokine exposure and the reactive state of the astrocytes has negative effects on the cell itself. It would be interesting to look for further signs of cell damage and potential death, such as caspase activity. Furthermore, assessing astrocyte homeostatic functioning, such as glutamate uptake, calcium signalling, or glycolytic metabolism following chronic reactivity would be interesting, and thus determining if these astrocytes are capable of carrying out their necessary functions. It would be interesting to see if cytokine exposure was ceased after 7 d, would the astrocytes recover, would they be able to restore homeostasis. The new evidence supporting astrocytes as immune cells with memory capabilities identifies endless interesting questions for future research, especially in an area such as this where there is already the peripheral-central immune cross-over (Lee et al., 2024). Trialling a similar approach here could also provide interesting results, exposure of the cells to the initial stimulus for 24 h, then allowing time to recover before reintroducing the stimulus. It would be interesting to see if we achieve a similar result as continuous exposure or if it induced an even further increase in response, or perhaps it would be identical to the initial stimulus.

7.4. Cell replacement therapy

This study generated multiple iPSC lines from sporadic PD patients. While the aim of this study was to utilise these cells to generate an *in vitro* disease model, iPSC are following their ESC counterparts and becoming more frequently utilised for PD cell replacement therapies. While few exist, there are trials utilising iPSC for the treatment of PD. The Kyoto trial utilised human iPSC-derived dopaminergic neural progenitor cells from a healthy individual (UMIN000033564, JMA-IIA00384; Yamanaka, 2020). They generated these cells from an individual with the most common HLA phenotype in Japan. The hope in utilising HLA-matching is that there should be a reduced risk of graft rejection (Morizane et al., 2017). However, this study still utilised immunosuppressants. Schweitzer and colleagues utilised an autologous cell transplant approach in a single case study in 2020. They transplanted the patient's own iPSC-derived dopamine neural progenitor cells and demonstrated successful transplantation without the need for immunosuppressant therapy (Schweitzer et al., 2020). The cells used in these studies differ from those produced here in that they would undergo much more extensive characterisation and phenotyping to ensuring their safety for use in the clinic. However, the results generated thus far from these trials and the continuously growing body of research pertaining to iPSC and their midbrain derivatives represents promising avenues for disease modifying therapies for PD.

7.3. Reactive phenotype differences in PD vmAstros

In order to increase the translatability of this research this thesis also aimed to generate patient derived iPSC and thus midbrain astrocytes, relevant for studying PD. This was achieved successfully. While differences were observed between the PD astrocytes and the healthy controls in terms of reactivity profile, there still needs to be further investigation of this

response before any conclusion can be drawn. Future researchers should differentiate the other PD iPSC lines into midbrain astrocytes and perform the same set of experiments to either confirm our findings are consistent across sporadic PD lines or help in identifying the difference that resulted in our findings. Due to the well-established response of astrocytes to the Liddelow factors, their use allows for variability within cell lines to be identified. It would be important to carry out multiple neuralisations from the same cell lines to confirm consistency in their response, before repeating the experiments described in this thesis with these new PD lines. Whilst iPSC derived cells from PD patients have been demonstrated to be more pro-inflammatory than their control counterparts, these have usually been genetic PD cases. The sporadic nature of these cells means that if an inflammatory phenotype is observed, the origin of this will require more investigation to be understood. Although, due to the selective vulnerability of A9 dopamine neurons, it would not be surprising if a similar individualistic phenotype existed for astrocytes of this area. Interestingly, studies have observed differences in the response of astrocytes from different brain regions (Crompton et al., 2023). It might be tempting to attach these phenotypic differing responses to the recent revelation that astrocytes have immunological memory, and therefore if the cells are derived from PD patients, may well be responding due to previous inflammatory exposure. However, due to the epigenetic reset associated with the generation of iPSC, this should not be the case. In order to study that phenomenon, the use of direct reprogramming would be more appropriate as this would prevent the loss of these epigenetic signals.

7.4. Alterations in peripheral immune cell populations

The final aspect of this thesis was the investigation of peripheral immune cell populations. While this preliminary data demonstrates some interesting differences in PD immune cell populations compared to healthy controls, there still remains a lot to be done before this can be

applied to the disease overall. This study had very low sample numbers which limits the accuracy of the data due to variability among individuals. Variability is quite common in the analysis of peripheral immune cells, and while studies of as few as ten participants exist (Sommer et al., 2018), it is more common to have at least an N of 30 (Alvarez-Luquin et al., 2019; Baba et al., 2005; Bas et al., 2001). As was mentioned, the current state of peripheral immune cell analysis in PD is up in the air. There are no concrete trends emerging as of yet, however, this is largely due to the novelty of the area. At the present moment, any contribution to the field is going to be beneficial, we need to continue to add data to the equation in order to get a concrete grasp on the state of the immune system in PD. The importance of studying the peripheral immune population is the connotations these cells have on pathogenesis in the brain, and directly on the research we do at a cellular level. There is little value in investigating the response of peripheral immune cells on brain cells if we don't know how they are responding in the disease. Similarly, there is little benefit in knowing a certain population of cells is increased or decreased if we don't know how this might impact the brain. Therefore, future studies should investigate in more detail these immune cell populations, as well as further analyse the presence or absence of peripheral immune populations in post-mortem brain tissue. Determining the effects of these immune cells in the brain is also crucial. As Sommer and colleagues demonstrated Th17 cells are capable of inducing neurodegeneration (Sommer et al., 2018). The interesting addition to this research is that this effect only occurred if it was the patient's own immune cells on their iPSC-derived dopamine neurons. This suggests it is an allogenic response, i.e. the patient's own immune cells are responding to a self-antigen. This study, is primely situated to continue on from this research. Here we have generated iPSC derived astrocytes from PD patient's and could collect further peripheral immune cells from those same individuals. This would enable future studies the ability to investigate any allogenic or autologous responses between the peripheral immune cells and the iPSC-derived astrocytes

we have generated. Furthermore, iPSC-derived microglia could also be differentiated to further explore the immune cell interactions. The generation of midbrain organoids also represents an important step towards more translatable research of cellular interactions in terms of PD. The iPSC generated in this study could be utilised to form midbrain organoids to investigate the responses of multiple cell types to peripheral immune cells.

Another aspect that should be considered in future studies of the peripheral immune system in PD is the importance of comparing early-onset PD (EOPD) and late-onset PD (LOPD). While the range of ages observed in this thesis are not dissimilar to those in other studies, there are a number of participants who would fall under the category of EOPD. EOPD is PD that presents before the age of 50 years, with any presenting cases above the age of 50 being considered LOPD (Nascimento et al., 2023). It is no surprise that differences in disease progression and presentation have been observed between these two cohorts. Separation of these cohorts is rarely done when comparing peripheral immune populations. However, a recent study by Tian and colleagues observed a significant reduction in $CD57^-$ naïve $CD8^+$ T cells in LOPD patients when compared with EOPD patients (Tian et al., 2022). While other trends were observed none reached statistical significance. Despite this, future studies should consider including this as an extra division of populations in case these individuals display differing peripheral immune landscapes and thus may account for some of the variability observed across studies.

The importance of understanding differences in immune presentation is crucial if we are to identify therapeutic targets to treat PD. The immune system is successfully targeted in numerous diseases, including rheumatoid arthritis where Th17 cells are largely involved. In this sense the repurposing of existing immune targeting therapeutics would be an ideal approach to disease-modification of PD.

7.5. Targeting the immune system therapeutically

The immune system offers an interesting therapeutic target for potential disease-modifying therapies for the treatment of PD. Glucagon like peptide 1 (GLP-1) receptor agonists are currently FDA approved in the treatment of type 2 diabetes mellitus. Exenatide, a GLP-1 receptor agonist, is currently in the midst of phase 3 clinical trials and due to be completed later on this year (NCT04232969, ISRCTN14552789; Vijiaratnam et al., 2021). While the mechanism by which the GLP-1 receptor agonists exert their protective effects in PD remain to be fully elucidated, Yun in colleagues in 2018 demonstrated a link to astrocyte reactivity. Their study demonstrated that the NLY01 GLP-1 receptor agonist was capable of preventing pro-inflammatory astrocyte induction by microglia and also observed that prevention of this inflammatory phenotype resulted in reduced neuronal cell death (Yun et al., 2018). Based on the potential benefits this drug may have in PD pathogenesis, NLY01 is currently also undergoing phase 2 clinical trials for use as a PD therapeutic (NCT04154072).

Due to the indication that α-syn may act as the immune stimulating antigen in PD (Sulzer et al., 2017), targeting this protein may aid in interrupting the detrimental inflammatory cascades associated with this disease. Monoclonal antibodies have been generated against α-syn and there are currently numerous active clinical trials utilising this approach. Prasinezumab, is a monoclonal IgG 1 antibody targeting the C-terminal region of aggregated α-syn. Despite uncertainty of its effectiveness at Phase 2 clinical trials, there is some evidence of its ability to slow progression on the MDS-UPDRS scale. Phase 2 b clinical trials of this compound are currently ongoing (NCT04777331). BIIB054, Cinpanemab, is another example of α-syn targeting antibody therapies trialled for PD. This antibody made it to phase 2 clinical trials, where it failed to meet its primary endpoint targets and thus was not moved forward (NCT03318523; Lang et al., 2022). Other α-syn targeting antibodies including MEDI1341 are

being tested for use in PD (NCT04449484, NCT03272165; Schofield et al., 2019). The anti-α-syn vaccine, PD01A which has previously successfully gone through phase 1 clinical trials for use in PD, has since been renamed ACI-7104.056 (Volc et al., 2020). However, despite the rename, this vaccine against α-syn is currently undergoing phase 2 clinical trials (NCT06015841). Azathioprine, which targets immune cell proliferation including both B and T lymphocytes and is currently used as a therapeutic for numerous diseases, including multiple sclerosis (ISRCTN14616801; Greenland et al., 2020), has completed its phase 2 clinical trial as a PD therapeutic this year, with results pending. Sargramostim, a GM-CSF, promotes proliferation of T reg cells over T effector cells. It has been shown to be effective in numerous diseases and is currently FDA approved. A number of clinical trials have been carried out on the potential use of this drug for PD therapy, however it has yet to reach FDA approval (NCT03790670, NCT01882010; Gendelman et al., 2017; Olson et al., 2023; Olson et al., 2021).

As was mentioned above, groups have demonstrated the potential benefits of targeting specific immune cells, such as Th17 cells, in terms of PD pathogenesis (Sommer et al., 2018). Therapeutics targeting IL-17 and even TNFα, the two cytokines most implicated throughout this study, are utilised for treatment of inflammatory related diseases, such as Psoriasis or rheumatoid arthritis (Buckland, 2014; Jiraskova Zakostelska et al., 2023). The fact that these drugs are currently approved for therapeutic use indicates their tolerance in the body and therefore provides the potential for their repurposing for disease modifying therapy of PD.

Another interesting avenue for PD therapy would be to utilise the newly emerging technology of nanoparticles. Numerous groups are optimising nanoparticle technology to target immune-related disease such as cancer and HIV (Cevaal et al., 2021). Nanoparticles can be altered to

target specific cells such as $CD3^+$, $CD4^+$ or $CD8^+$ T cells (Ramishetti et al., 2015; Smith et al., 2017; Yang et al., 2018). They can then deliver intracellular cargo that can alter the activation state of these T cells. If this technology could be utilised to modulate activation of specific T cells subsets, this could be used to manipulate the peripheral immune cell landscape in PD.

7.6. Conclusions

To summarise, this thesis provided novel insights into the reactive state of midbrain astrocytes, both in relation to their stimulation by peripheral immune-associated cytokines, as well as the differing responses between PD and controls. The data presented here provides an interesting foundation on which future studies could build to truly identify novel therapeutic targets for disease modifying therapies to treat PD.

Appendix 1

Table 1. Human fibroblast medium

Component	***Concentration***
DMEM	80.9%
Fetal Bovine Serum	16%
Non-Essential Amino Acids	1%
GlutaMAX	1%
Penicillin-Streptomycin	1%
2-mercaptoethanol	0.1%

Table 2. Mouse embryonic fibroblast medium

Component	***Concentration***
DMEM	88%
Fetal Bovine Serum	10%
GlutaMAX	1%
Penicillin-Streptomycin	1%

Table 3. Human embryonic stem cell medium

Component	***Concentration***
DMEM F-12	77.8%
Knock-out serum replacement	20%

GlutaMAX	1%
Non-Essential Amino Acids	1%
2-mercaptoethanol	0.2%

Table 4. Reprogramming medium

Component	***Concentration***
DMEM F-12	77.8%
Knock-out serum replacement	20%
GlutaMAX	1%
Non-Essential Amino Acids	1%
2-mercaptoethanol	0.2%
Fibroblast Growth Factor 2	100 ng/ml
PD0325901	0.5 μM
Chir99021	3 μM
Sodium Butyrate	0.5 mM
A-83-01	0.5 μM

Table 5. Embryoid body medium

Component	***Concentration***
DMEM F-12	80%
Fetal Bovine Serum	20%

Table 6. Completed RPMI

Component	***Concentration***
RPMI	88%
FBS	10%
Penicillin-Streptomycin	1%
GlutaMAX	1%

Table 7. Neural differentiation medium

Component	***Concentration***
Neurobasal Medium	24%
DMEM F-12 + GlutaMAX	24%
Non-Essential Amino Acids	1%
GlutaMAX	0.5%
Penicillin-Streptomycin	1%
N2	0.5%
B27	1%
Insulin	0.1%
SB431542	10 μM
LDN193189	100 ng/ml
Sonic Hedgehog	300 ng/ml
CHIR99021	0.6 – 1.0 μM

Table 8. Neural maintenance medium

Component	***Concentration***
Neurobasal Medium	24%
DMEM F-12 + GlutaMAX	24%
Non-Essential Amino Acids	1%
GlutaMAX	0.5%
Penicillin-Streptomycin	1%
N2	0.5%
B27	1%
Insulin	0.1%
BDNF	20 ng/ml
GDNF	20 ng/ml
Ascorbic Acid	0.2 mM

Table 9. Astrocyte medium

Component	***Concentration***
Advanced DMEM	98%
Non-Essential Amino Acids	1%
GlutaMAX	1%
Penicillin-Streptomycin	1%
N2	1%
B27	0.2%
EGF	20 ng/ml
hLIF	20 ng/ml

Table 10. Astrocyte maturation medium

Component	***Concentration***
Advanced DMEM	98%
Non-Essential Amino Acids	1%
GlutaMAX	1%
Penicillin-Streptomycin	1%
N2	1%
B27	0.2%
BMP4	20 ng/ml
hLIF	20 ng/ml

Appendix 2

Publications

MacMahon Copas AN, McComish SF, Fletcher JM and Caldwell MA (2021) The Pathogenesis of Parkinson's Disease: A Complex Interplay Between Astrocytes, Microglia, and T Lymphocytes? *Front. Neurol.* 12:666737. doi: 10.3389/fneur.2021.666737

McComish SF, **MacMahon Copas AN** and Caldwell MA (2022) Human Brain Based Models Provide a Powerful Tool for the Advancement of Parkinson's Disease Research and Therapeutic Development. *Front. Neurosci.* 16:851058. doi: 10.3389/fnins.2022.851058

MacMahon Copas AN, McComish SF, Petrasca A, McCormack R, Ivers D, Stricker A, Fletcher JM and Caldwell MA (In Submission) $CD4^+$ T cell-associated cytokines induce a chronic pro-inflammatory phenotype in induced pluripotent stem cell-derived midbrain astrocytes.

McComish SF, O'Sullivan J, **MacMahon Copas AN,** Imiolek M, Boyle NT, Crompton LA, Lane JD, Caldwell MA (In preparation) Reactive astrocytes generated from human iPSC are pro-inflammatory and display altered metabolism.

Oral Presentations

2022, NECTAR, Virtual "Peripheral Immune Cells Induce Reactive Phenotype in Human iPSC-derived Midbrain Astrocytes"

2021, NSI, Virtual “Peripheral immune cells induce a reactive phenotype in human iPSC-derived astrocytes”

2021, NECTAR-INTR, Virtual “Peripheral immune cells induce reactive astrocyte phenotype in human iPSC-derived astrocytes”

Poster Presentations

2023, **XVI European Meeting on Glial Cells in Health and Disease, Berlin, Germany** “*Investigating the effect of peripheral immune cytokines on astrocyte reactivity in Parkinson’s disease”*

2023, ADPD, Gothenburg, Sweden “Peripheral immune cells induce a reactive phenotype in human iPSC-derived midbrain astrocytes“

2022, NSI-ECRN, Dublin, Ireland “Peripheral immune cells induce a reactive phenotype in human iPSC-derived astrocytes”

2021, NSI, Virtual “Peripheral immune cells induce a reactive phenotype in human iPSC-derived astrocytes”

Bibliography

Abeliovich, A., Schmitz, Y., Farinas, I., Choi-Lundberg, D., Ho, W. H., Castillo, P. E., Shinsky, N., Verdugo, J. M., Armanini, M., Ryan, A., Hynes, M., Phillips, H., Sulzer, D., & Rosenthal, A. (2000). Mice lacking alpha-synuclein display functional deficits in the nigrostriatal dopamine system. *Neuron*, *25*(1), 239-252. https://doi.org/10.1016/s0896-6273(00)80886-7

Ai, W., Li, H., Song, N., Li, L., & Chen, H. (2013). Optimal method to stimulate cytokine production and its use in immunotoxicity assessment. *Int J Environ Res Public Health*, *10*(9), 3834-3842. https://doi.org/10.3390/ijerph10093834

Alekseenko, Z., Dias, J. M., Adler, A. F., Kozhevnikova, M., van Lunteren, J. A., Nolbrant, S., Jeggari, A., Vasylovska, S., Yoshitake, T., Kehr, J., Carlen, M., Alexeyenko, A., Parmar, M., & Ericson, J. (2022). Robust derivation of transplantable dopamine neurons from human pluripotent stem cells by timed retinoic acid delivery. *Nat Commun*, *13*(1), 3046. https://doi.org/10.1038/s41467-022-30777-8

Alvarez, J. I., Katayama, T., & Prat, A. (2013). Glial influence on the blood brain barrier. *Glia*, *61*(12), 1939-1958. https://doi.org/10.1002/glia.22575

Alvarez-Luquin, D. D., Arce-Sillas, A., Leyva-Hernandez, J., Sevilla-Reyes, E., Boll, M. C., Montes-Moratilla, E., Vivas-Almazan, V., Perez-Correa, C., Rodriguez-Ortiz, U., Espinoza-Cardenas, R., Fragoso, G., Sciutto, E., & Adalid-Peralta, L. (2019). Regulatory impairment in untreated Parkinson's disease is not restricted to Tregs: other regulatory populations are also involved. *J Neuroinflammation*, *16*(1), 212. https://doi.org/10.1186/s12974-019-1606-1

Andersson, E., Tryggvason, U., Deng, Q., Friling, S., Alekseenko, Z., Robert, B., Perlmann, T., & Ericson, J. (2006). Identification of intrinsic determinants of midbrain dopamine neurons. *Cell*, *124*(2), 393-405. https://doi.org/10.1016/j.cell.2005.10.037

Andrews, P. W., Banting, G., Damjanov, I., Arnaud, D., & Avner, P. (1984). Three monoclonal antibodies defining distinct differentiation antigens associated with different high molecular weight polypeptides on the surface of human embryonal carcinoma cells. *Hybridoma*, *3*(4), 347-361. https://doi.org/10.1089/hyb.1984.3.347

Arenas, E., Denham, M., & Villaescusa, J. C. (2015). How to make a midbrain dopaminergic neuron. *Development*, *142*(11), 1918-1936. https://doi.org/10.1242/dev.097394

Avilion, A. A., Nicolis, S. K., Pevny, L. H., Perez, L., Vivian, N., & Lovell-Badge, R. (2003). Multipotent cell lineages in early mouse development depend on SOX2 function. *Genes Dev*, *17*(1), 126-140. https://doi.org/10.1101/gad.224503

Azevedo, F. A., Carvalho, L. R., Grinberg, L. T., Farfel, J. M., Ferretti, R. E., Leite, R. E., Jacob Filho, W., Lent, R., & Herculano-Houzel, S. (2009). Equal numbers of neuronal and nonneuronal cells make the human brain an isometrically scaled-up primate brain. *J Comp Neurol*, *513*(5), 532-541. https://doi.org/10.1002/cne.21974

Baba, Y., Kuroiwa, A., Uitti, R. J., Wszolek, Z. K., & Yamada, T. (2005). Alterations of T-lymphocyte populations in Parkinson disease. *Parkinsonism Relat Disord*, *11*(8), 493-498. https://doi.org/10.1016/j.parkreldis.2005.07.005

Bagga, V., Dunnett, S. B., & Fricker-Gates, R. A. (2008). Ascorbic acid increases the number of dopamine neurons in vitro and in transplants to the 6-OHDA-lesioned rat brain. *Cell Transplant*, *17*(7), 763-773. https://doi.org/10.3727/096368908786516774

Baldwin, K. T., Murai, K. K., & Khakh, B. S. (2023). Astrocyte morphology. *Trends Cell Biol*. https://doi.org/10.1016/j.tcb.2023.09.006

Bandres-Ciga, S., Diez-Fairen, M., Kim, J. J., & Singleton, A. B. (2020). Genetics of Parkinson's disease: An introspection of its journey towards precision medicine. *Neurobiol Dis*, *137*, 104782. https://doi.org/10.1016/j.nbd.2020.104782

Baran, J., Kowalczyk, D., Ozog, M., & Zembala, M. (2001). Three-color flow cytometry detection of intracellular cytokines in peripheral blood mononuclear cells: comparative analysis of phorbol myristate acetate-ionomycin and phytohemagglutinin stimulation. *Clin Diagn Lab Immunol*, *8*(2), 303-313. https://doi.org/10.1128/CDLI.8.2.303-313.2001

Barbar, L., Jain, T., Zimmer, M., Kruglikov, I., Sadick, J. S., Wang, M., Kalpana, K., Rose, I. V. L., Burstein, S. R., Rusielewicz, T., Nijsure, M., Guttenplan, K. A., di Domenico, A., Croft, G., Zhang, B., Nobuta, H., Hebert, J. M., Liddelow, S. A., & Fossati, V. (2020). CD49f Is a Novel Marker of Functional and Reactive Human iPSC-Derived Astrocytes. *Neuron*, *107*(3), 436-453 e412. https://doi.org/10.1016/j.neuron.2020.05.014

Barros, L. F., & Weber, B. (2018). CrossTalk proposal: an important astrocyte-to-neuron lactate shuttle couples neuronal activity to glucose utilisation in the brain. *J Physiol*, *596*(3), 347-350. https://doi.org/10.1113/JP274944

Bas, J., Calopa, M., Mestre, M., Mollevi, D. G., Cutillas, B., Ambrosio, S., & Buendia, E. (2001). Lymphocyte populations in Parkinson's disease and in rat models of parkinsonism. *J Neuroimmunol*, *113*(1), 146-152. https://doi.org/10.1016/s0165-5728(00)00422-7

Ben-Shlomo, Y., Darweesh, S., Llibre-Guerra, J., Marras, C., San Luciano, M., & Tanner, C. (2024). The epidemiology of Parkinson's disease. *Lancet*, *403*(10423), 283-292. https://doi.org/10.1016/S0140-6736(23)01419-8

Bentivoglio, M., & Morelli, M. (2005). The organization and circuits of mesencephalic dopaminergic neurons and the distribution of dopamine receptors in the brain. Dopamine. In: Elsevier BV.

Beringer, A., Thiam, N., Molle, J., Bartosch, B., & Miossec, P. (2018). Synergistic effect of interleukin-17 and tumour necrosis factor-alpha on inflammatory response in hepatocytes through interleukin-6-dependent and independent pathways. *Clin Exp Immunol*, *193*(2), 221-233. https://doi.org/10.1111/cei.13140

Bernheimer, H., Birkmayer, W., Hornykiewicz, O., Jellinger, K., & Seitelberger, F. (1973). Brain dopamine and the syndromes of Parkinson and Huntington. Clinical, morphological and neurochemical correlations. *J Neurol Sci*, *20*(4), 415-455. https://doi.org/10.1016/0022-510x(73)90175-5

Betarbet, R., Sherer, T. B., MacKenzie, G., Garcia-Osuna, M., Panov, A. V., & Greenamyre, J. T. (2000). Chronic systemic pesticide exposure reproduces features of Parkinson's disease. *Nat Neurosci*, *3*(12), 1301-1306. https://doi.org/10.1038/81834

Bhargava, N., Jaitly, S., Goswami, S. G., Jain, S., Chakraborty, D., & Ramalingam, S. (2019). Generation and characterization of induced pluripotent stem cell line (IGIBi001-A) from a sickle cell anemia patient with homozygous beta-globin mutation. *Stem Cell Res*, *39*, 101484. https://doi.org/10.1016/j.scr.2019.101484

Bhatia, D., Grozdanov, V., Ruf, W. P., Kassubek, J., Ludolph, A. C., Weishaupt, J. H., & Danzer, K. M. (2021). T-cell dysregulation is associated with disease severity in Parkinson's Disease. *J Neuroinflammation*, *18*(1), 250. https://doi.org/10.1186/s12974-021-02296-8

Bhattacharya, P., Budnick, I., Singh, M., Thiruppathi, M., Alharshawi, K., Elshabrawy, H., Holterman, M. J., & Prabhakar, B. S. (2015). Dual Role of GM-CSF as a Pro-

Inflammatory and a Regulatory Cytokine: Implications for Immune Therapy. *J Interferon Cytokine Res*, *35*(8), 585-599. https://doi.org/10.1089/jir.2014.0149

Bhatti, M. S., & Frostig, R. D. (2023). Astrocyte-neuron lactate shuttle plays a pivotal role in sensory-based neuroprotection in a rat model of permanent middle cerebral artery occlusion. *Sci Rep*, *13*(1), 12799. https://doi.org/10.1038/s41598-023-39574-9

Binder, D. K., & Scharfman, H. E. (2004). Brain-derived neurotrophic factor. *Growth Factors*, *22*(3), 123-131. https://doi.org/10.1080/08977190410001723308

Biswas, P., Delfanti, F., Bernasconi, S., Mengozzi, M., Cota, M., Polentarutti, N., Mantovani, A., Lazzarin, A., Sozzani, S., & Poli, G. (1998). Interleukin-6 induces monocyte chemotactic protein-1 in peripheral blood mononuclear cells and in the U937 cell line. *Blood*, *91*(1), 258-265. https://www.ncbi.nlm.nih.gov/pubmed/9414293

Bjorklund, A., & Dunnett, S. B. (2007). Dopamine neuron systems in the brain: an update. *Trends Neurosci*, *30*(5), 194-202. https://doi.org/10.1016/j.tins.2007.03.006

Blauwendraat, C., Nalls, M. A., & Singleton, A. B. (2020). The genetic architecture of Parkinson's disease. *Lancet Neurol*, *19*(2), 170-178. https://doi.org/10.1016/S1474-4422(19)30287-X

Blocq, P., & Marinescu, G. (1892). *Sur les lésions et la pathogénie de l'épilepsie dite essentielle*.

Bonifati, V., Rizzu, P., van Baren, M. J., Schaap, O., Breedveld, G. J., Krieger, E., Dekker, M. C., Squitieri, F., Ibanez, P., Joosse, M., van Dongen, J. W., Vanacore, N., van Swieten, J. C., Brice, A., Meco, G., van Duijn, C. M., Oostra, B. A., & Heutink, P. (2003). Mutations in the DJ-1 gene associated with autosomal recessive early-onset parkinsonism. *Science*, *299*(5604), 256-259. https://doi.org/10.1126/science.1077209

Bonsack, B., Borlongan, M. C., Lo, E. H., & Arai, K. (2019). Brief overview: Protective roles of astrocyte-derived pentraxin-3 in blood-brain barrier integrity. *Brain Circ*, *5*(3), 145-149. https://doi.org/10.4103/bc.bc_37_19

Borghammer, P. (2021). The alpha-Synuclein Origin and Connectome Model (SOC Model) of Parkinson's Disease: Explaining Motor Asymmetry, Non-Motor Phenotypes, and Cognitive Decline. *J Parkinsons Dis*, *11*(2), 455-474. https://doi.org/10.3233/JPD-202481

Borghammer, P., Just, M. K., Horsager, J., Skjaerbaek, C., Raunio, A., Kok, E. H., Savola, S., Murayama, S., Saito, Y., Myllykangas, L., & Van Den Berge, N. (2022). A postmortem study suggests a revision of the dual-hit hypothesis of Parkinson's disease. *NPJ Parkinsons Dis*, *8*(1), 166. https://doi.org/10.1038/s41531-022-00436-2

Bougea, A., Stefanis, L., Emmanouilidou, E., Vekrelis, K., & Kapaki, E. (2020). High discriminatory ability of peripheral and CFSF biomarkers in Lewy body diseases. *J Neural Transm (Vienna)*, *127*(3), 311-322. https://doi.org/10.1007/s00702-019-02137-2

Braak, H., Del Tredici, K., Rub, U., de Vos, R. A., Jansen Steur, E. N., & Braak, E. (2003). Staging of brain pathology related to sporadic Parkinson's disease. *Neurobiol Aging*, *24*(2), 197-211. https://doi.org/10.1016/s0197-4580(02)00065-9

Braak, H., Rub, U., Gai, W. P., & Del Tredici, K. (2003). Idiopathic Parkinson's disease: possible routes by which vulnerable neuronal types may be subject to neuroinvasion by an unknown pathogen. *J Neural Transm (Vienna)*, *110*(5), 517-536. https://doi.org/10.1007/s00702-002-0808-2

Bravery, C. A. (2015). Do human leukocyte antigen-typed cellular therapeutics based on induced pluripotent stem cells make commercial sense? *Stem Cells Dev*, *24*(1), 1-10. https://doi.org/10.1089/scd.2014.0136

Brissaud, E. (1899). *Leçons sur les maladies nerveuses* (Vol. 2). Masson.

Brochard, V., Combadiere, B., Prigent, A., Laouar, Y., Perrin, A., Beray-Berthat, V., Bonduelle, O., Alvarez-Fischer, D., Callebert, J., Launay, J. M., Duyckaerts, C., Flavell, R. A., Hirsch, E. C., & Hunot, S. (2009). Infiltration of CD4+ lymphocytes into the brain contributes to neurodegeneration in a mouse model of Parkinson disease. *J Clin Invest*, *119*(1), 182-192. https://doi.org/10.1172/JCI36470

Brozzi, F., Arcuri, C., Giambanco, I., & Donato, R. (2009). S100B Protein Regulates Astrocyte Shape and Migration via Interaction with Src Kinase: IMPLICATIONS FOR ASTROCYTE DEVELOPMENT, ACTIVATION, AND TUMOR GROWTH. *J Biol Chem*, *284*(13), 8797-8811. https://doi.org/10.1074/jbc.M805897200

Buckland, J. (2014). Rheumatoid arthritis: Anti-TNF and anti-IL-17 antibodies--better together! *Nat Rev Rheumatol*, *10*(12), 699. https://doi.org/10.1038/nrrheum.2014.183

Cabezas, R., Avila, M., Gonzalez, J., El-Bacha, R. S., Baez, E., Garcia-Segura, L. M., Jurado Coronel, J. C., Capani, F., Cardona-Gomez, G. P., & Barreto, G. E. (2014). Astrocytic modulation of blood brain barrier: perspectives on Parkinson's disease. *Front Cell Neurosci*, *8*, 211. https://doi.org/10.3389/fncel.2014.00211

Cai, J., Donaldson, A., Yang, M., German, M. S., Enikolopov, G., & Iacovitti, L. (2009). The role of Lmx1a in the differentiation of human embryonic stem cells into midbrain dopamine neurons in culture and after transplantation into a Parkinson's disease model. *Stem Cells*, *27*(1), 220-229. https://doi.org/10.1634/stemcells.2008-0734

Caiazzo, M., Giannelli, S., Valente, P., Lignani, G., Carissimo, A., Sessa, A., Colasante, G., Bartolomeo, R., Massimino, L., Ferroni, S., Settembre, C., Benfenati, F., & Broccoli, V. (2015). Direct conversion of fibroblasts into functional astrocytes by defined transcription factors. *Stem Cell Reports*, *4*(1), 25-36. https://doi.org/10.1016/j.stemcr.2014.12.002

Calabresi, P., Mechelli, A., Natale, G., Volpicelli-Daley, L., Di Lazzaro, G., & Ghiglieri, V. (2023). Alpha-synuclein in Parkinson's disease and other synucleinopathies: from overt neurodegeneration back to early synaptic dysfunction. *Cell Death Dis*, *14*(3), 176. https://doi.org/10.1038/s41419-023-05672-9

Cao, F., Lin, S., Xie, X., Ray, P., Patel, M., Zhang, X., Drukker, M., Dylla, S. J., Connolly, A. J., Chen, X., Weissman, I. L., Gambhir, S. S., & Wu, J. C. (2006). In vivo visualization of embryonic stem cell survival, proliferation, and migration after cardiac delivery. *Circulation*, *113*(7), 1005-1014. https://doi.org/10.1161/CIRCULATIONAHA.105.588954

Cappella, M., Elouej, S., & Biferi, M. G. (2021). The Potential of Induced Pluripotent Stem Cells to Test Gene Therapy Approaches for Neuromuscular and Motor Neuron Disorders. *Front Cell Dev Biol*, *9*, 662837. https://doi.org/10.3389/fcell.2021.662837

Caranci, G., Piscopo, P., Rivabene, R., Traficante, A., Riozzi, B., Castellano, A. E., Ruggieri, S., Vanacore, N., & Confaloni, A. (2013). Gender differences in Parkinson's disease: focus on plasma alpha-synuclein. *J Neural Transm (Vienna)*, *120*(8), 1209-1215. https://doi.org/10.1007/s00702-013-0972-6

Carlsson, A. (1959). The occurrence, distribution and physiological role of catecholamines in the nervous system. *Pharmacol Rev*, *11*(2, Part 2), 490-493. https://www.ncbi.nlm.nih.gov/pubmed/13667431

Castro-Vinuelas, R., Sanjurjo-Rodriguez, C., Pineiro-Ramil, M., Hermida-Gomez, T., Rodriguez-Fernandez, S., Oreiro, N., de Toro, J., Fuentes, I., Blanco, F. J., & Diaz-Prado, S. (2020). Generation and characterization of human induced pluripotent stem cells (iPSCs) from hand osteoarthritis patient-derived fibroblasts. *Sci Rep*, *10*(1), 4272. https://doi.org/10.1038/s41598-020-61071-6

Cebrian, C., Zucca, F. A., Mauri, P., Steinbeck, J. A., Studer, L., Scherzer, C. R., Kanter, E., Budhu, S., Mandelbaum, J., Vonsattel, J. P., Zecca, L., Loike, J. D., & Sulzer, D. (2014). MHC-I expression renders catecholaminergic neurons susceptible to T-cell-mediated degeneration. *Nat Commun*, *5*, 3633. https://doi.org/10.1038/ncomms4633

Cerri, S., Mus, L., & Blandini, F. (2019). Parkinson's Disease in Women and Men: What's the Difference? *J Parkinsons Dis*, *9*(3), 501-515. https://doi.org/10.3233/JPD-191683

Cevaal, P. M., Ali, A., Czuba-Wojnilowicz, E., Symons, J., Lewin, S. R., Cortez-Jugo, C., & Caruso, F. (2021). In Vivo T Cell-Targeting Nanoparticle Drug Delivery Systems: Considerations for Rational Design. *ACS Nano*, *15*(3), 3736-3753. https://doi.org/10.1021/acsnano.0c09514

Chahine, L. M., Beach, T. G., Brumm, M. C., Adler, C. H., Coffey, C. S., Mosovsky, S., Caspell-Garcia, C., Serrano, G. E., Munoz, D. G., White, C. L., 3rd, Crary, J. F., Jennings, D., Taylor, P., Foroud, T., Arnedo, V., Kopil, C. M., Riley, L., Dave, K. D., Mollenhauer, B., & Systemic Synuclein Sampling, S. (2020). In vivo distribution of alpha-synuclein in multiple tissues and biofluids in Parkinson disease. *Neurology*, *95*(9), e1267-e1284. https://doi.org/10.1212/WNL.0000000000010404

Chambers, I., Colby, D., Robertson, M., Nichols, J., Lee, S., Tweedie, S., & Smith, A. (2003). Functional expression cloning of Nanog, a pluripotency sustaining factor in embryonic stem cells. *Cell*, *113*(5), 643-655. https://doi.org/10.1016/s0092-8674(03)00392-1

Chambers, S. M., Fasano, C. A., Papapetrou, E. P., Tomishima, M., Sadelain, M., & Studer, L. (2009). Highly efficient neural conversion of human ES and iPS cells by dual inhibition of SMAD signaling. *Nat Biotechnol*, *27*(3), 275-280. https://doi.org/10.1038/nbt.1529

Chan, F. K., Moriwaki, K., & De Rosa, M. J. (2013). Detection of necrosis by release of lactate dehydrogenase activity. *Methods Mol Biol*, *979*, 65-70. https://doi.org/10.1007/978-1-62703-290-2_7

Charcot, J. M. (1892). *Leçons sur les maladies du système nerveux* (Vol. 1). Bureau du Progrès médical.

Chaudhry, G. R., Fecek, C., Lai, M. M., Wu, W. C., Chang, M., Vasquez, A., Pasierb, M., & Trese, M. T. (2009). Fate of embryonic stem cell derivatives implanted into the vitreous of a slow retinal degenerative mouse model. *Stem Cells Dev*, *18*(2), 247-258. https://doi.org/10.1089/scd.2008.0057

Chehelgerdi, M., Behdarvand Dehkordi, F., Chehelgerdi, M., Kabiri, H., Salehian-Dehkordi, H., Abdolvand, M., Salmanizadeh, S., Rashidi, M., Niazmand, A., Ahmadi, S., Feizbakhshan, S., Kabiri, S., Vatandoost, N., & Ranjbarnejad, T. (2023). Exploring the promising potential of induced pluripotent stem cells in cancer research and therapy. *Mol Cancer*, *22*(1), 189. https://doi.org/10.1186/s12943-023-01873-0

Chen, J., Liu, X., & Zhong, Y. (2020). Interleukin-17A: The Key Cytokine in Neurodegenerative Diseases. *Front Aging Neurosci*, *12*, 566922. https://doi.org/10.3389/fnagi.2020.566922

Chen, W., Yan, X., Lv, H., Liu, Y., He, Z., & Luo, X. (2020). Gender differences in prevalence of LRRK2-associated Parkinson disease: A meta-analysis of observational studies. *Neurosci Lett*, *715*, 134609. https://doi.org/10.1016/j.neulet.2019.134609

Chiricozzi, A., Guttman-Yassky, E., Suarez-Farinas, M., Nograles, K. E., Tian, S., Cardinale, I., Chimenti, S., & Krueger, J. G. (2011). Integrative responses to IL-17 and TNF-alpha in human keratinocytes account for key inflammatory pathogenic circuits in psoriasis. *J Invest Dermatol*, *131*(3), 677-687. https://doi.org/10.1038/jid.2010.340

Chocarro, J., Rico, A. J., Ariznabarreta, G., Roda, E., Honrubia, A., Collantes, M., Penuelas, I., Vazquez, A., Rodriguez-Perez, A. I., Labandeira-Garcia, J. L., Vila, M., & Lanciego, J. L. (2023). Neuromelanin accumulation drives endogenous synucleinopathy in non-human primates. *Brain*, *146*(12), 5000-5014. https://doi.org/10.1093/brain/awad331

Claire Q.F. Wang, Y. T. A., Mayte Suarez-Farinas, Juana Gonzalez, Hiroshi Mitsui, Michelle A. Lowes, Seth J. Orlow, Prashiela Manga, James G. Krueger,. (2013,). IL-17 and TNF Synergistically Modulate Cytokine Expression while Suppressing Melanogenesis: Potential Relevance to Psoriasis, . *Journal of Investigative Dermatology,*, *Volume 133, Issue 12,*(ISSN 0022-202X,), Pages 2741-2752,.

Claire, Q. F. W., Yemsratch, T. A., Mayte, S.-F., Juana, G., Hiroshi, M., Michelle, A. L., Seth, J. O., Prashiela, M., & James, G. K. (2013). IL-17 and TNF Synergistically Modulate Cytokine Expression while Suppressing Melanogenesis: Potential Relevance to Psoriasis, . *Journal of Investigative Dermatology,*, *Volume 133, Issue 12,*(ISSN 0022-202X,), Pages 2741-2752,.

Clementi, M. E., Sampaolese, B., Di Sante, G., Ria, F., Di Liddo, R., Romano Spica, V., & Michetti, F. (2023). S100B Expression Plays a Crucial Role in Cytotoxicity, Reactive Oxygen Species Generation and Nitric Oxide Synthase Activation Induced by Amyloid beta-Protein in an Astrocytoma Cell Line. *Int J Mol Sci*, *24*(6). https://doi.org/10.3390/ijms24065213

Collaborators, G. B. D. P. s. D. (2018). Global, regional, and national burden of Parkinson's disease, 1990-2016: a systematic analysis for the Global Burden of Disease Study 2016. *Lancet Neurol*, *17*(11), 939-953. https://doi.org/10.1016/S1474-4422(18)30295-3

Cook, D. A., Kannarkat, G. T., Cintron, A. F., Butkovich, L. M., Fraser, K. B., Chang, J., Grigoryan, N., Factor, S. A., West, A. B., Boss, J. M., & Tansey, M. G. (2017). LRRK2 levels in immune cells are increased in Parkinson's disease. *NPJ Parkinsons Dis*, *3*, 11. https://doi.org/10.1038/s41531-017-0010-8

Cowan, C. A., Atienza, J., Melton, D. A., & Eggan, K. (2005). Nuclear reprogramming of somatic cells after fusion with human embryonic stem cells. *Science*, *309*(5739), 1369-1373. https://doi.org/10.1126/science.1116447

Crompton, L. A., McComish, S. F., Stathakos, P., Cordero-Llana, O., Lane, J. D., & Caldwell, M. A. (2021). Efficient and Scalable Generation of Human Ventral Midbrain Astrocytes from Human-Induced Pluripotent Stem Cells. *J Vis Exp*(176). https://doi.org/10.3791/62095

Crompton, L. A., McComish, S. F., Steward, T. G. J., Whitcomb, D. J., Lane, J. D., & Caldwell, M. A. (2023). Human stem cell-derived ventral midbrain astrocytes exhibit a region-specific secretory profile. *Brain Commun*, *5*(2), fcad114. https://doi.org/10.1093/braincomms/fcad114

D'Amato, R. J., Alexander, G. M., Schwartzman, R. J., Kitt, C. A., Price, D. L., & Snyder, S. H. (1987). Evidence for neuromelanin involvement in MPTP-induced neurotoxicity. *Nature*, *327*(6120), 324-326. https://doi.org/10.1038/327324a0

d'Azyr, F. V. (1786). *Traite d'anatomie et de physiologie* (Vol. 1). Didot.

Damier, P., Hirsch, E. C., Agid, Y., & Graybiel, A. M. (1999). The substantia nigra of the human brain. I. Nigrosomes and the nigral matrix, a compartmental organization based on calbindin D(28K) immunohistochemistry. *Brain*, *122 (Pt 8)*, 1421-1436. https://doi.org/10.1093/brain/122.8.1421

De Bock, M., Decrock, E., Wang, N., Bol, M., Vinken, M., Bultynck, G., & Leybaert, L. (2014). The dual face of connexin-based astroglial Ca(2+) communication: a key player in brain physiology and a prime target in pathology. *Biochim Biophys Acta*, *1843*(10), 2211-2232. https://doi.org/10.1016/j.bbamcr.2014.04.016

de Rus Jacquet, A., Alpaugh, M., Denis, H. L., Tancredi, J. L., Boutin, M., Decaestecker, J., Beauparlant, C., Herrmann, L., Saint-Pierre, M., Parent, M., Droit, A., Breton, S., & Cicchetti, F. (2023). The contribution of inflammatory astrocytes to BBB impairments in a brain-chip model of Parkinson's disease. *Nat Commun*, *14*(1), 3651. https://doi.org/10.1038/s41467-023-39038-8

Devine, M. J., Ryten, M., Vodicka, P., Thomson, A. J., Burdon, T., Houlden, H., Cavaleri, F., Nagano, M., Drummond, N. J., Taanman, J. W., Schapira, A. H., Gwinn, K., Hardy, J., Lewis, P. A., & Kunath, T. (2011). Parkinson's disease induced pluripotent stem cells with triplication of the alpha-synuclein locus. *Nat Commun*, *2*, 440. https://doi.org/10.1038/ncomms1453

Diaz, K., Kohut, M. L., Russell, D. W., & Stegemoller, E. L. (2022). Peripheral inflammatory cytokines and motor symptoms in persons with Parkinson's disease. *Brain Behav Immun Health*, *21*, 100442. https://doi.org/10.1016/j.bbih.2022.100442

Dolgacheva, L. P., Berezhnov, A. V., Fedotova, E. I., Zinchenko, V. P., & Abramov, A. Y. (2019). Role of DJ-1 in the mechanism of pathogenesis of Parkinson's disease. *J Bioenerg Biomembr*, *51*(3), 175-188. https://doi.org/10.1007/s10863-019-09798-4

Donato, R., Sorci, G., Riuzzi, F., Arcuri, C., Bianchi, R., Brozzi, F., Tubaro, C., & Giambanco, I. (2009). S100B's double life: intracellular regulator and extracellular signal. *Biochim Biophys Acta*, *1793*(6), 1008-1022. https://doi.org/10.1016/j.bbamcr.2008.11.009

Dong, R., Han, Y., Jiang, L., Liu, S., Zhang, F., Peng, L., Wang, Z., Ma, Z., Xia, T., & Gu, X. (2022). Connexin 43 gap junction-mediated astrocytic network reconstruction attenuates isoflurane-induced cognitive dysfunction in mice. *J Neuroinflammation*, *19*(1), 64. https://doi.org/10.1186/s12974-022-02424-y

Dorsey, E. R., Sherer, T., Okun, M. S., & Bloem, B. R. (2018). The Emerging Evidence of the Parkinson Pandemic. *J Parkinsons Dis*, *8*(s1), S3-S8. https://doi.org/10.3233/JPD-181474

Dovonou, A., Bolduc, C., Soto Linan, V., Gora, C., Peralta Iii, M. R., & Levesque, M. (2023). Animal models of Parkinson's disease: bridging the gap between disease hallmarks and research questions. *Transl Neurodegener*, *12*(1), 36. https://doi.org/10.1186/s40035-023-00368-8

Du, Y., Ma, Z., Lin, S., Dodel, R. C., Gao, F., Bales, K. R., Triarhou, L. C., Chernet, E., Perry, K. W., Nelson, D. L., Luecke, S., Phebus, L. A., Bymaster, F. P., & Paul, S. M. (2001). Minocycline prevents nigrostriatal dopaminergic neurodegeneration in the MPTP model of Parkinson's disease. *Proc Natl Acad Sci U S A*, *98*(25), 14669-14674. https://doi.org/10.1073/pnas.251341998

Dulski, J., Uitti, R. J., Ross, O. A., & Wszolek, Z. K. (2022). Genetic architecture of Parkinson's disease subtypes - Review of the literature. *Front Aging Neurosci*, *14*, 1023574. https://doi.org/10.3389/fnagi.2022.1023574

Ehringer, H., & Hornykiewicz, O. (1960). [Distribution of noradrenaline and dopamine (3-hydroxytyramine) in the human brain and their behavior in diseases of the extrapyramidal system]. *Klin Wochenschr*, *38*, 1236-1239. https://doi.org/10.1007/BF01485901

Eichmuller, O. L., & Knoblich, J. A. (2022). Human cerebral organoids - a new tool for clinical neurology research. *Nat Rev Neurol*, *18*(11), 661-680. https://doi.org/10.1038/s41582-022-00723-9

Elain, G., Jeanneau, K., Rutkowska, A., Mir, A. K., & Dev, K. K. (2014). The selective anti-IL17A monoclonal antibody secukinumab (AIN457) attenuates IL17A-induced levels of IL6 in human astrocytes. *Glia*, *62*(5), 725-735. https://doi.org/10.1002/glia.22637

Elsworth, J. D., & Roth, R. H. (1997). Dopamine synthesis, uptake, metabolism, and receptors: relevance to gene therapy of Parkinson's disease. *Exp Neurol*, *144*(1), 4-9. https://doi.org/10.1006/exnr.1996.6379

Emamzadeh, F. N. (2016). Alpha-synuclein structure, functions, and interactions. *J Res Med Sci*, *21*, 29. https://doi.org/10.4103/1735-1995.181989

Eng, L. F., Ghirnikar, R. S., & Lee, Y. L. (2000). Glial fibrillary acidic protein: GFAP-thirty-one years (1969-2000). *Neurochem Res*, *25*(9-10), 1439-1451. https://doi.org/10.1023/a:1007677003387

Escartin, C., Galea, E., Lakatos, A., O'Callaghan, J. P., Petzold, G. C., Serrano-Pozo, A., Steinhauser, C., Volterra, A., Carmignoto, G., Agarwal, A., Allen, N. J., Araque, A., Barbeito, L., Barzilai, A., Bergles, D. E., Bonvento, G., Butt, A. M., Chen, W. T., Cohen-Salmon, M., . . . Verkhratsky, A. (2021). Reactive astrocyte nomenclature, definitions, and future directions. *Nat Neurosci*, *24*(3), 312-325. https://doi.org/10.1038/s41593-020-00783-4

Evans, M. J., & Kaufman, M. H. (1981). Establishment in culture of pluripotential cells from mouse embryos. *Nature*, *292*(5819), 154-156. https://doi.org/10.1038/292154a0

Fan, Z., Pan, Y. T., Zhang, Z. Y., Yang, H., Yu, S. Y., Zheng, Y., Ma, J. H., & Wang, X. M. (2020). Systemic activation of NLRP3 inflammasome and plasma alpha-synuclein levels are correlated with motor severity and progression in Parkinson's disease. *J Neuroinflammation*, *17*(1), 11. https://doi.org/10.1186/s12974-019-1670-6

Farrer, M., Kachergus, J., Forno, L., Lincoln, S., Wang, D. S., Hulihan, M., Maraganore, D., Gwinn-Hardy, K., Wszolek, Z., Dickson, D., & Langston, J. W. (2004). Comparison of kindreds with parkinsonism and alpha-synuclein genomic multiplications. *Ann Neurol*, *55*(2), 174-179. https://doi.org/10.1002/ana.10846

Funayama, M., Nishioka, K., Li, Y., & Hattori, N. (2023). Molecular genetics of Parkinson's disease: Contributions and global trends. *J Hum Genet*, *68*(3), 125-130. https://doi.org/10.1038/s10038-022-01058-5

Fuxe, K., Manger, P., Genedani, S., & Agnati, L. (2006). The nigrostriatal DA pathway and Parkinson's disease. *J Neural Transm Suppl*(70), 71-83. https://doi.org/10.1007/978-3-211-45295-0_13

Gadani, S. P., Cronk, J. C., Norris, G. T., & Kipnis, J. (2012). IL-4 in the brain: a cytokine to remember. *J Immunol*, *189*(9), 4213-4219. https://doi.org/10.4049/jimmunol.1202246

Garcia, L., Gonzalez, C. D., Gagne, A., McGuire, J. A., French, D., Takanohashi, A., Almad, A., Vanderver, A., & Sase, S. (2024). Generation of three induced pluripotent stem cell lines from individuals with Aicardi-Goutieres syndrome caused by a c.3019G>A (p.G1007R) autosomal dominant pathogenic variant in ADAR1. *Stem Cell Res*, *74*, 103299. https://doi.org/10.1016/j.scr.2023.103299

Ge, P., Dawson, V. L., & Dawson, T. M. (2020). PINK1 and Parkin mitochondrial quality control: a source of regional vulnerability in Parkinson's disease. *Mol Neurodegener*, *15*(1), 20. https://doi.org/10.1186/s13024-020-00367-7

Gendelman, H. E., Zhang, Y., Santamaria, P., Olson, K. E., Schutt, C. R., Bhatti, D., Shetty, B. L. D., Lu, Y., Estes, K. A., Standaert, D. G., Heinrichs-Graham, E., Larson, L., Meza, J. L., Follett, M., Forsberg, E., Siuzdak, G., Wilson, T. W., Peterson, C., & Mosley, R. L. (2017). Evaluation of the safety and immunomodulatory effects of sargramostim in a randomized, double-blind phase 1 clinical Parkinson's disease trial. *NPJ Parkinsons Dis*, *3*, 10. https://doi.org/10.1038/s41531-017-0013-5

German, D. C., Manaye, K., Smith, W. K., Woodward, D. J., & Saper, C. B. (1989). Midbrain dopaminergic cell loss in Parkinson's disease: computer visualization. *Ann Neurol*, *26*(4), 507-514. https://doi.org/10.1002/ana.410260403

German, D. C., & Manaye, K. F. (1993). Midbrain dopaminergic neurons (nuclei A8, A9, and A10): three-dimensional reconstruction in the rat. *J Comp Neurol*, *331*(3), 297-309. https://doi.org/10.1002/cne.903310302

Giasson, B. I., Duda, J. E., Quinn, S. M., Zhang, B., Trojanowski, J. Q., & Lee, V. M. (2002). Neuronal alpha-synucleinopathy with severe movement disorder in mice expressing

A53T human alpha-synuclein. *Neuron*, *34*(4), 521-533. https://doi.org/10.1016/s0896-6273(02)00682-7

Goetz, C. G., Fahn, S., Martinez-Martin, P., Poewe, W., Sampaio, C., Stebbins, G. T., Stern, M. B., Tilley, B. C., Dodel, R., Dubois, B., Holloway, R., Jankovic, J., Kulisevsky, J., Lang, A. E., Lees, A., Leurgans, S., LeWitt, P. A., Nyenhuis, D., Olanow, C. W., . . . LaPelle, N. (2007). Movement Disorder Society-sponsored revision of the Unified Parkinson's Disease Rating Scale (MDS-UPDRS): Process, format, and clinimetric testing plan. *Mov Disord*, *22*(1), 41-47. https://doi.org/10.1002/mds.21198

Gok-Yurtseven, D., Kafa, I. M., Minbay, Z., & Eyigor, O. (2019). Glutamatergic activation of A1 and A2 noradrenergic neurons in the rat brain stem. *Croat Med J*, *60*(4), 352-360. https://doi.org/10.3325/cmj.2019.60.352

Goldman, J. G., Andrews, H., Amara, A., Naito, A., Alcalay, R. N., Shaw, L. M., Taylor, P., Xie, T., Tuite, P., Henchcliffe, C., Hogarth, P., Frank, S., Saint-Hilaire, M. H., Frasier, M., Arnedo, V., Reimer, A. N., Sutherland, M., Swanson-Fischer, C., Gwinn, K., . . . Kang, U. J. (2018). Cerebrospinal fluid, plasma, and saliva in the BioFIND study: Relationships among biomarkers and Parkinson's disease Features. *Mov Disord*, *33*(2), 282-288. https://doi.org/10.1002/mds.27232

Gray, M. T., & Woulfe, J. M. (2015). Striatal blood-brain barrier permeability in Parkinson's disease. *J Cereb Blood Flow Metab*, *35*(5), 747-750. https://doi.org/10.1038/jcbfm.2015.32

Greenland, J. C., Cutting, E., Kadyan, S., Bond, S., Chhabra, A., & Williams-Gray, C. H. (2020). Azathioprine immunosuppression and disease modification in Parkinson's disease (AZA-PD): a randomised double-blind placebo-controlled phase II trial protocol. *BMJ Open*, *10*(11), e040527. https://doi.org/10.1136/bmjopen-2020-040527

Grigor'eva, E. V., Kopytova, A. E., Yarkova, E. S., Pavlova, S. V., Sorogina, D. A., Malakhova, A. A., Malankhanova, T. B., Baydakova, G. V., Zakharova, E. Y., Medvedev, S. P., Pchelina, S. N., & Zakian, S. M. (2023). Biochemical Characteristics of iPSC-Derived Dopaminergic Neurons from N370S GBA Variant Carriers with and without Parkinson's Disease. *Int J Mol Sci*, *24*(5). https://doi.org/10.3390/ijms24054437

Gurdon, J. B., Lane, C. D., Woodland, H. R., & Marbaix, G. (1971). Use of frog eggs and oocytes for the study of messenger RNA and its translation in living cells. *Nature*, *233*(5316), 177-182. https://doi.org/10.1038/233177a0

Gwag, B. J., Lobner, D., Koh, J. Y., Wie, M. B., & Choi, D. W. (1995). Blockade of glutamate receptors unmasks neuronal apoptosis after oxygen-glucose deprivation in vitro. *Neuroscience*, *68*(3), 615-619. https://doi.org/10.1016/0306-4522(95)00232-8

Harms, A. S., Cao, S., Rowse, A. L., Thome, A. D., Li, X., Mangieri, L. R., Cron, R. Q., Shacka, J. J., Raman, C., & Standaert, D. G. (2013). MHCII is required for alpha-synuclein-induced activation of microglia, CD4 T cell proliferation, and dopaminergic neurodegeneration. *J Neurosci*, *33*(23), 9592-9600. https://doi.org/10.1523/JNEUROSCI.5610-12.2013

Hawkes, C. H., Del Tredici, K., & Braak, H. (2007). Parkinson's disease: a dual-hit hypothesis. *Neuropathol Appl Neurobiol*, *33*(6), 599-614. https://doi.org/10.1111/j.1365-2990.2007.00874.x

He, Y., Peng, K., Li, R., Zhang, Z., Pan, L., Zhang, T., Lin, A., Hong, R., Nie, Z., Guan, Q., & Jin, L. (2022). Changes of T lymphocyte subpopulations and their roles in predicting the risk of Parkinson's disease. *J Neurol*, *269*(10), 5368-5381. https://doi.org/10.1007/s00415-022-11190-z

Hegarty, S. V., Sullivan, A. M., & O'Keeffe, G. W. (2013). Midbrain dopaminergic neurons: a review of the molecular circuitry that regulates their development. *Dev Biol*, *379*(2), 123-138. https://doi.org/10.1016/j.ydbio.2013.04.014

Hinz, M., Stilmann, M., Arslan, S. C., Khanna, K. K., Dittmar, G., & Scheidereit, C. (2010). A cytoplasmic ATM-TRAF6-cIAP1 module links nuclear DNA damage signaling to ubiquitin-mediated NF-kappaB activation. *Mol Cell*, *40*(1), 63-74. https://doi.org/10.1016/j.molcel.2010.09.008

Hirsch, E. C. (1994). Biochemistry of Parkinson's disease with special reference to the dopaminergic systems. *Mol Neurobiol*, *9*(1-3), 135-142. https://doi.org/10.1007/BF02816113

Hochedlinger, K., & Jaenisch, R. (2015). Induced Pluripotency and Epigenetic Reprogramming. *Cold Spring Harb Perspect Biol*, *7*(12). https://doi.org/10.1101/cshperspect.a019448

Hoehn, M. M., & Yahr, M. D. (1967). Parkinsonism: onset, progression and mortality. *Neurology*, *17*(5), 427-442. https://doi.org/10.1212/wnl.17.5.427

Horvath, S. (2013). DNA methylation age of human tissues and cell types. *Genome Biol*, *14*(10), R115. https://doi.org/10.1186/gb-2013-14-10-r115

Hughes, S. M., Lillien, L. E., Raff, M. C., Rohrer, H., & Sendtner, M. (1988). Ciliary neurotrophic factor induces type-2 astrocyte differentiation in culture. *Nature*, *335*(6185), 70-73. https://doi.org/10.1038/335070a0

Huh, Y. E., Usnich, T., Scherzer, C. R., Klein, C., & Chung, S. J. (2023). GBA1 Variants and Parkinson's Disease: Paving the Way for Targeted Therapy. *J Mov Disord*, *16*(3), 261-278. https://doi.org/10.14802/jmd.23023

Hyvarinen, T., Hagman, S., Ristola, M., Sukki, L., Veijula, K., Kreutzer, J., Kallio, P., & Narkilahti, S. (2019). Co-stimulation with IL-1beta and TNF-alpha induces an

inflammatory reactive astrocyte phenotype with neurosupportive characteristics in a human pluripotent stem cell model system. *Sci Rep*, *9*(1), 16944. https://doi.org/10.1038/s41598-019-53414-9

Isaacson, S. H., Hauser, R. A., Pahwa, R., Gray, D., & Duvvuri, S. (2023). Dopamine agonists in Parkinson's disease: Impact of D1-like or D2-like dopamine receptor subtype selectivity and avenues for future treatment. *Clin Park Relat Disord*, *9*, 100212. https://doi.org/10.1016/j.prdoa.2023.100212

Jang, D. I., Lee, A. H., Shin, H. Y., Song, H. R., Park, J. H., Kang, T. B., Lee, S. R., & Yang, S. H. (2021). The Role of Tumor Necrosis Factor Alpha (TNF-alpha) in Autoimmune Disease and Current TNF-alpha Inhibitors in Therapeutics. *Int J Mol Sci*, *22*(5). https://doi.org/10.3390/ijms22052719

Jiang, Y., Jahagirdar, B. N., Reinhardt, R. L., Schwartz, R. E., Keene, C. D., Ortiz-Gonzalez, X. R., Reyes, M., Lenvik, T., Lund, T., Blackstad, M., Du, J., Aldrich, S., Lisberg, A., Low, W. C., Largaespada, D. A., & Verfaillie, C. M. (2002). Pluripotency of mesenchymal stem cells derived from adult marrow. *Nature*, *418*(6893), 41-49. https://doi.org/10.1038/nature00870

Jiao, J., Dang, Y., Yang, Y., Gao, R., Zhang, Y., Kou, Z., Sun, X. F., & Gao, S. (2013). Promoting reprogramming by FGF2 reveals that the extracellular matrix is a barrier for reprogramming fibroblasts to pluripotency. *Stem Cells*, *31*(4), 729-740. https://doi.org/10.1002/stem.1318

Jiraskova Zakostelska, Z., Reiss, Z., Tlaskalova-Hogenova, H., & Rob, F. (2023). Paradoxical Reactions to Anti-TNFalpha and Anti-IL-17 Treatment in Psoriasis Patients: Are Skin and/or Gut Microbiota Involved? *Dermatol Ther (Heidelb)*, *13*(4), 911-933. https://doi.org/10.1007/s13555-023-00904-4

Joksimovic, M., Yun, B. A., Kittappa, R., Anderegg, A. M., Chang, W. W., Taketo, M. M., McKay, R. D., & Awatramani, R. B. (2009). Wnt antagonism of Shh facilitates midbrain floor plate neurogenesis. *Nat Neurosci*, *12*(2), 125-131. https://doi.org/10.1038/nn.2243

Juarez Olguin, H., Calderon Guzman, D., Hernandez Garcia, E., & Barragan Mejia, G. (2016). The Role of Dopamine and Its Dysfunction as a Consequence of Oxidative Stress. *Oxid Med Cell Longev*, *2016*, 9730467. https://doi.org/10.1155/2016/9730467

Jurga, A. M., Paleczna, M., Kadluczka, J., & Kuter, K. Z. (2021). Beyond the GFAP-Astrocyte Protein Markers in the Brain. *Biomolecules*, *11*(9). https://doi.org/10.3390/biom11091361

Kam, T. I., Hinkle, J. T., Dawson, T. M., & Dawson, V. L. (2020). Microglia and astrocyte dysfunction in parkinson's disease. *Neurobiol Dis*, *144*, 105028. https://doi.org/10.1016/j.nbd.2020.105028

Kamath, T., Abdulraouf, A., Burris, S. J., Langlieb, J., Gazestani, V., Nadaf, N. M., Balderrama, K., Vanderburg, C., & Macosko, E. Z. (2022). Single-cell genomic profiling of human dopamine neurons identifies a population that selectively degenerates in Parkinson's disease. *Nat Neurosci*, *25*(5), 588-595. https://doi.org/10.1038/s41593-022-01061-1

Kamishibahara, Y., Okamoto, S., Ohkuma, T., & Taniguchi, H. (2023). Stabilized generation of human iPSC-derived liver organoids using a modified coating approach. *Biol Methods Protoc*, *8*(1), bpac034. https://doi.org/10.1093/biomethods/bpac034

Kang, C., Xu, Q., Martin, T. D., Li, M. Z., Demaria, M., Aron, L., Lu, T., Yankner, B. A., Campisi, J., & Elledge, S. J. (2015). The DNA damage response induces inflammation and senescence by inhibiting autophagy of GATA4. *Science*, *349*(6255), aaa5612. https://doi.org/10.1126/science.aaa5612

Karami, Z., Moradi, S., Eidi, A., Soleimani, M., & Jafarian, A. (2022). Induced pluripotent stem cells: Generation methods and a new perspective in COVID-19 research. *Front Cell Dev Biol*, *10*, 1050856. https://doi.org/10.3389/fcell.2022.1050856

Katsetos, C. D., Herman, M. M., & Mork, S. J. (2003). Class III beta-tubulin in human development and cancer. *Cell Motil Cytoskeleton*, *55*(2), 77-96. https://doi.org/10.1002/cm.10116

Kawatani, K., Nambara, T., Nawa, N., Yoshimatsu, H., Kusakabe, H., Hirata, K., Tanave, A., Sumiyama, K., Banno, K., Taniguchi, H., Arahori, H., Ozono, K., & Kitabatake, Y. (2021). A human isogenic iPSC-derived cell line panel identifies major regulators of aberrant astrocyte proliferation in Down syndrome. *Commun Biol*, *4*(1), 730. https://doi.org/10.1038/s42003-021-02242-7

Kee, N., Volakakis, N., Kirkeby, A., Dahl, L., Storvall, H., Nolbrant, S., Lahti, L., Bjorklund, A. K., Gillberg, L., Joodmardi, E., Sandberg, R., Parmar, M., & Perlmann, T. (2017). Single-Cell Analysis Reveals a Close Relationship between Differentiating Dopamine and Subthalamic Nucleus Neuronal Lineages. *Cell Stem Cell*, *20*(1), 29-40. https://doi.org/10.1016/j.stem.2016.10.003

Kerepesi, C., Zhang, B., Lee, S. G., Trapp, A., & Gladyshev, V. N. (2021). Epigenetic clocks reveal a rejuvenation event during embryogenesis followed by aging. *Sci Adv*, *7*(26). https://doi.org/10.1126/sciadv.abg6082

Kettenmann, H., Hanisch, U. K., Noda, M., & Verkhratsky, A. (2011). Physiology of microglia. *Physiol Rev*, *91*(2), 461-553. https://doi.org/10.1152/physrev.00011.2010

Kim, B. W., Jeong, K. H., Kim, J. H., Jin, M., Kim, J. H., Lee, M. G., Choi, D. K., Won, S. Y., McLean, C., Jeon, M. T., Lee, H. W., Kim, S. R., & Suk, K. (2016). Pathogenic Upregulation of Glial Lipocalin-2 in the Parkinsonian Dopaminergic System. *J Neurosci*, *36*(20), 5608-5622. https://doi.org/10.1523/JNEUROSCI.4261-15.2016

Kirkeby, A., Grealish, S., Wolf, D. A., Nelander, J., Wood, J., Lundblad, M., Lindvall, O., & Parmar, M. (2012). Generation of regionally specified neural progenitors and functional neurons from human embryonic stem cells under defined conditions. *Cell Rep*, *1*(6), 703-714. https://doi.org/10.1016/j.celrep.2012.04.009

Klein, C., & Westenberger, A. (2012). Genetics of Parkinson's disease. *Cold Spring Harb Perspect Med*, *2*(1), a008888. https://doi.org/10.1101/cshperspect.a008888

Ko, H. C., & Gelb, B. D. (2014). Concise review: drug discovery in the age of the induced pluripotent stem cell. *Stem Cells Transl Med*, *3*(4), 500-509. https://doi.org/10.5966/sctm.2013-0162

Kostic, M., Zivkovic, N., Cvetanovic, A., Stojanovic, I., & Colic, M. (2017). IL-17 signalling in astrocytes promotes glutamate excitotoxicity: Indications for the link between inflammatory and neurodegenerative events in multiple sclerosis. *Mult Scler Relat Disord*, *11*, 12-17. https://doi.org/10.1016/j.msard.2016.11.006

Kouroupi, G., Antoniou, N., Prodromidou, K., Taoufik, E., & Matsas, R. (2020). Patient-Derived Induced Pluripotent Stem Cell-Based Models in Parkinson's Disease for Drug Identification. *Int J Mol Sci*, *21*(19). https://doi.org/10.3390/ijms21197113

Krencik, R., & Zhang, S. C. (2011). Directed differentiation of functional astroglial subtypes from human pluripotent stem cells. *Nat Protoc*, *6*(11), 1710-1717. https://doi.org/10.1038/nprot.2011.405

Kriks, S., Shim, J. W., Piao, J., Ganat, Y. M., Wakeman, D. R., Xie, Z., Carrillo-Reid, L., Auyeung, G., Antonacci, C., Buch, A., Yang, L., Beal, M. F., Surmeier, D. J., Kordower, J. H., Tabar, V., & Studer, L. (2011). Dopamine neurons derived from human ES cells efficiently engraft in animal models of Parkinson's disease. *Nature*, *480*(7378), 547-551. https://doi.org/10.1038/nature10648

Kuang, Y. L., Munoz, A., Nalula, G., Santostefano, K. E., Sanghez, V., Sanchez, G., Terada, N., Mattis, A. N., Iacovino, M., Iribarren, C., Krauss, R. M., & Medina, M. W. (2019). Evaluation of commonly used ectoderm markers in iPSC trilineage differentiation. *Stem Cell Res*, *37*, 101434. https://doi.org/10.1016/j.scr.2019.101434

Kumar, D., Hussain, A., Srivastava, A. K., Mukerji, M., Mukherjee, O., & Faruq, M. (2018). Generation of three spinocerebellar ataxia type-12 patients derived induced pluripotent stem cell lines (IGIBi002-A, IGIBi003-A and IGIBi004-A). *Stem Cell Res*, *31*, 216-221. https://doi.org/10.1016/j.scr.2018.08.008

Kustrimovic, N., Comi, C., Magistrelli, L., Rasini, E., Legnaro, M., Bombelli, R., Aleksic, I., Blandini, F., Minafra, B., Riboldazzi, G., Sturchio, A., Mauri, M., Bono, G., Marino, F., & Cosentino, M. (2018). Parkinson's disease patients have a complex phenotypic and functional Th1 bias: cross-sectional studies of CD4+ Th1/Th2/T17 and Treg in drug-naive and drug-treated patients. *J Neuroinflammation*, *15*(1), 205. https://doi.org/10.1186/s12974-018-1248-8

Ladewig, J., Mertens, J., Kesavan, J., Doerr, J., Poppe, D., Glaue, F., Herms, S., Wernet, P., Kogler, G., Muller, F. J., Koch, P., & Brustle, O. (2012). Small molecules enable highly efficient neuronal conversion of human fibroblasts. *Nat Methods*, *9*(6), 575-578. https://doi.org/10.1038/nmeth.1972

Lane, E., & Dunnett, S. (2008). Animal models of Parkinson's disease and L-dopa induced dyskinesia: how close are we to the clinic? *Psychopharmacology (Berl)*, *199*(3), 303-312. https://doi.org/10.1007/s00213-007-0931-8

Lang, A. E., Siderowf, A. D., Macklin, E. A., Poewe, W., Brooks, D. J., Fernandez, H. H., Rascol, O., Giladi, N., Stocchi, F., Tanner, C. M., Postuma, R. B., Simon, D. K., Tolosa, E., Mollenhauer, B., Cedarbaum, J. M., Fraser, K., Xiao, J., Evans, K. C., Graham, D.

L., . . . Investigators, S. (2022). Trial of Cinpanemab in Early Parkinson's Disease. *N Engl J Med*, *387*(5), 408-420. https://doi.org/10.1056/NEJMoa2203395

Langeh, U., & Singh, S. (2021). Targeting S100B Protein as a Surrogate Biomarker and its Role in Various Neurological Disorders. *Curr Neuropharmacol*, *19*(2), 265-277. https://doi.org/10.2174/1570159X18666200729100427

Lee, H. G., Rone, J. M., Li, Z., Akl, C. F., Shin, S. W., Lee, J. H., Flausino, L. E., Pernin, F., Chao, C. C., Kleemann, K. L., Srun, L., Illouz, T., Giovannoni, F., Charabati, M., Sanmarco, L. M., Kenison, J. E., Piester, G., Zandee, S. E. J., Antel, J. P., . . . Quintana, F. J. (2024). Disease-associated astrocyte epigenetic memory promotes CNS pathology. *Nature*. https://doi.org/10.1038/s41586-024-07187-5

Lewy, F. H. (1912). Paralysis agitans. I. Pathologische anatomie. *Handbuch der neurologie*, *3*, 920-958.

Li, C., Li, Y., Zhang, W., Ma, Z., Xiao, S., Xie, W., Miao, S., Li, B., Lu, G., Liu, Y., Bai, W., & Yu, S. (2023). Dopaminergic Projections from the Hypothalamic A11 Nucleus to the Spinal Trigeminal Nucleus Are Involved in Bidirectional Migraine Modulation. *Int J Mol Sci*, *24*(23). https://doi.org/10.3390/ijms242316876

Li, D., Wang, L., Hou, J., Shen, Q., Chen, Q., Wang, X., Du, J., Cai, X., Shan, Y., Zhang, T., Zhou, T., Shi, X., Li, Y., Zhang, H., & Pan, G. (2016). Optimized Approaches for Generation of Integration-free iPSCs from Human Urine-Derived Cells with Small Molecules and Autologous Feeder. *Stem Cell Reports*, *6*(5), 717-728. https://doi.org/10.1016/j.stemcr.2016.04.001

Li, J., Zhao, J., Chen, L., Gao, H., Zhang, J., Wang, D., Zou, Y., Qin, Q., Qu, Y., Li, J., Xiong, Y., Min, Z., Yan, M., Mao, Z., & Xue, Z. (2023). alpha-Synuclein induces Th17 differentiation and impairs the function and stability of Tregs by promoting RORC

transcription in Parkinson's disease. *Brain Behav Immun*, *108*, 32-44. https://doi.org/10.1016/j.bbi.2022.10.023

Lian, H., Yang, L., Cole, A., Sun, L., Chiang, A. C., Fowler, S. W., Shim, D. J., Rodriguez-Rivera, J., Taglialatela, G., Jankowsky, J. L., Lu, H. C., & Zheng, H. (2015). NFkappaB-activated astroglial release of complement C3 compromises neuronal morphology and function associated with Alzheimer's disease. *Neuron*, *85*(1), 101-115. https://doi.org/10.1016/j.neuron.2014.11.018

Liddelow, S. A., & Barres, B. A. (2017). Reactive Astrocytes: Production, Function, and Therapeutic Potential. *Immunity*, *46*(6), 957-967. https://doi.org/10.1016/j.immuni.2017.06.006

Liddelow, S. A., Guttenplan, K. A., Clarke, L. E., Bennett, F. C., Bohlen, C. J., Schirmer, L., Bennett, M. L., Munch, A. E., Chung, W. S., Peterson, T. C., Wilton, D. K., Frouin, A., Napier, B. A., Panicker, N., Kumar, M., Buckwalter, M. S., Rowitch, D. H., Dawson, V. L., Dawson, T. M., . . . Barres, B. A. (2017). Neurotoxic reactive astrocytes are induced by activated microglia. *Nature*, *541*(7638), 481-487. https://doi.org/10.1038/nature21029

Lin, H., Li, Q., Du, Q., Wang, O., Wang, Z., Akert, L., Carlson, M. A., Zhang, C., Subramanian, A., Zhang, C., Lunning, M., Li, M., & Lei, Y. (2019). Integrated generation of induced pluripotent stem cells in a low-cost device. *Biomaterials*, *189*, 23-36. https://doi.org/10.1016/j.biomaterials.2018.10.027

Lindestam Arlehamn, C. S., Dhanwani, R., Pham, J., Kuan, R., Frazier, A., Rezende Dutra, J., Phillips, E., Mallal, S., Roederer, M., Marder, K. S., Amara, A. W., Standaert, D. G., Goldman, J. G., Litvan, I., Peters, B., Sulzer, D., & Sette, A. (2020). alpha-Synuclein-specific T cell reactivity is associated with preclinical and early Parkinson's disease. *Nat Commun*, *11*(1), 1875. https://doi.org/10.1038/s41467-020-15626-w

Liu, C., Zhao, X. M., Wang, Q., Du, T. T., Zhang, M. X., Wang, H. Z., Li, R. P., Liang, K., Gao, Y., Zhou, S. Y., Xue, T., Zhang, J. G., Han, C. L., Shi, L., Zhang, L. W., & Meng, F. G. (2023). Astrocyte-derived SerpinA3N promotes neuroinflammation and epileptic seizures by activating the NF-kappaB signaling pathway in mice with temporal lobe epilepsy. *J Neuroinflammation*, *20*(1), 161. https://doi.org/10.1186/s12974-023-02840-8

Liu, G., David, B. T., Trawczynski, M., & Fessler, R. G. (2020). Advances in Pluripotent Stem Cells: History, Mechanisms, Technologies, and Applications. *Stem Cell Rev Rep*, *16*(1), 3-32. https://doi.org/10.1007/s12015-019-09935-x

Liu, M. L., Zang, T., Zou, Y., Chang, J. C., Gibson, J. R., Huber, K. M., & Zhang, C. L. (2013). Small molecules enable neurogenin 2 to efficiently convert human fibroblasts into cholinergic neurons. *Nat Commun*, *4*, 2183. https://doi.org/10.1038/ncomms3183

Liu, Y., Zhou, N., Zhou, L., Wang, J., Zhou, Y., Zhang, T., Fang, Y., Deng, J., Gao, Y., Liang, X., Lv, J., Wang, Z., Xie, J., Xue, Y., Zhang, H., Ma, J., Tang, K., Fang, Y., Cheng, F., . . . Huang, B. (2021). IL-2 regulates tumor-reactive CD8(+) T cell exhaustion by activating the aryl hydrocarbon receptor. *Nat Immunol*, *22*(3), 358-369. https://doi.org/10.1038/s41590-020-00850-9

Liu, Z., Huang, Y., Cao, B. B., Qiu, Y. H., & Peng, Y. P. (2017). Th17 Cells Induce Dopaminergic Neuronal Death via LFA-1/ICAM-1 Interaction in a Mouse Model of Parkinson's Disease. *Mol Neurobiol*, *54*(10), 7762-7776. https://doi.org/10.1007/s12035-016-0249-9

Liu, Z., Qiu, A. W., Huang, Y., Yang, Y., Chen, J. N., Gu, T. T., Cao, B. B., Qiu, Y. H., & Peng, Y. P. (2019). IL-17A exacerbates neuroinflammation and neurodegeneration by activating microglia in rodent models of Parkinson's disease. *Brain Behav Immun*, *81*, 630-645. https://doi.org/10.1016/j.bbi.2019.07.026

Long, H., Zhang, S., Zeng, S., Tong, Y., Liu, J., Liu, C., & Li, D. (2022). Interaction of RAGE with alpha-synuclein fibrils mediates inflammatory response of microglia. *Cell Rep*, *40*(12), 111401. https://doi.org/10.1016/j.celrep.2022.111401

Loria, F., Vargas, J. Y., Bousset, L., Syan, S., Salles, A., Melki, R., & Zurzolo, C. (2017). alpha-Synuclein transfer between neurons and astrocytes indicates that astrocytes play a role in degradation rather than in spreading. *Acta Neuropathol*, *134*(5), 789-808. https://doi.org/10.1007/s00401-017-1746-2

Lotz, S., Goderie, S., Tokas, N., Hirsch, S. E., Ahmad, F., Corneo, B., Le, S., Banerjee, A., Kane, R. S., Stern, J. H., Temple, S., & Fasano, C. A. (2013). Sustained levels of FGF2 maintain undifferentiated stem cell cultures with biweekly feeding. *PLoS One*, *8*(2), e56289. https://doi.org/10.1371/journal.pone.0056289

Luo, S. X., & Huang, E. J. (2016). Dopaminergic Neurons and Brain Reward Pathways: From Neurogenesis to Circuit Assembly. *Am J Pathol*, *186*(3), 478-488. https://doi.org/10.1016/j.ajpath.2015.09.023

MacMahon Copas, A. N., McComish, S. F., Fletcher, J. M., & Caldwell, M. A. (2021). The Pathogenesis of Parkinson's Disease: A Complex Interplay Between Astrocytes, Microglia, and T Lymphocytes? *Front Neurol*, *12*, 666737. https://doi.org/10.3389/fneur.2021.666737

MacVicar, B. A., & Newman, E. A. (2015). Astrocyte regulation of blood flow in the brain. *Cold Spring Harb Perspect Biol*, *7*(5). https://doi.org/10.1101/cshperspect.a020388

Maherali, N., Sridharan, R., Xie, W., Utikal, J., Eminli, S., Arnold, K., Stadtfeld, M., Yachechko, R., Tchieu, J., Jaenisch, R., Plath, K., & Hochedlinger, K. (2007). Directly reprogrammed fibroblasts show global epigenetic remodeling and widespread tissue contribution. *Cell Stem Cell*, *1*(1), 55-70. https://doi.org/10.1016/j.stem.2007.05.014

Mamula, D., Khosousi, S., He, Y., Lazarevic, V., & Svenningsson, P. (2022). Impaired migratory phenotype of CD4(+) T cells in Parkinson's disease. *NPJ Parkinsons Dis*, *8*(1), 171. https://doi.org/10.1038/s41531-022-00438-0

Mandala, W., Harawa, V., Munyenyembe, A., Soko, M., & Longwe, H. (2021). Optimization of stimulation and staining conditions for intracellular cytokine staining (ICS) for determination of cytokine-producing T cells and monocytes. *Curr Res Immunol*, *2*, 184-193. https://doi.org/10.1016/j.crimmu.2021.10.002

Markey, K. M., Saunders, J. C., Smuts, J., von Reyn, C. R., & Garcia, A. D. R. (2023). Astrocyte development-More questions than answers. *Front Cell Dev Biol*, *11*, 1063843. https://doi.org/10.3389/fcell.2023.1063843

Marshall, J. S., Warrington, R., Watson, W., & Kim, H. L. (2018). An introduction to immunology and immunopathology. *Allergy Asthma Clin Immunol*, *14*(Suppl 2), 49. https://doi.org/10.1186/s13223-018-0278-1

Martin, L. J., Pan, Y., Price, A. C., Sterling, W., Copeland, N. G., Jenkins, N. A., Price, D. L., & Lee, M. K. (2006). Parkinson's disease alpha-synuclein transgenic mice develop neuronal mitochondrial degeneration and cell death. *J Neurosci*, *26*(1), 41-50. https://doi.org/10.1523/JNEUROSCI.4308-05.2006

Masato, A., Plotegher, N., Boassa, D., & Bubacco, L. (2019). Impaired dopamine metabolism in Parkinson's disease pathogenesis. *Mol Neurodegener*, *14*(1), 35. https://doi.org/10.1186/s13024-019-0332-6

Masui, S., Nakatake, Y., Toyooka, Y., Shimosato, D., Yagi, R., Takahashi, K., Okochi, H., Okuda, A., Matoba, R., Sharov, A. A., Ko, M. S., & Niwa, H. (2007). Pluripotency governed by Sox2 via regulation of Oct3/4 expression in mouse embryonic stem cells. *Nat Cell Biol*, *9*(6), 625-635. https://doi.org/10.1038/ncb1589

McComish, S. F., MacMahon Copas, A. N., & Caldwell, M. A. (2022). Human Brain-Based Models Provide a Powerful Tool for the Advancement of Parkinson's Disease Research and Therapeutic Development. *Front Neurosci*, *16*, 851058. https://doi.org/10.3389/fnins.2022.851058

McFleder, R. L., Makhotkina, A., Groh, J., Keber, U., Imdahl, F., Pena Mosca, J., Peteranderl, A., Wu, J., Tabuchi, S., Hoffmann, J., Karl, A. K., Pagenstecher, A., Vogel, J., Beilhack, A., Koprich, J. B., Brotchie, J. M., Saliba, A. E., Volkmann, J., & Ip, C. W. (2023). Brain-to-gut trafficking of alpha-synuclein by CD11c(+) cells in a mouse model of Parkinson's disease. *Nat Commun*, *14*(1), 7529. https://doi.org/10.1038/s41467-023-43224-z

McGeer, P. L., Itagaki, S., Boyes, B. E., & McGeer, E. G. (1988). Reactive microglia are positive for HLA-DR in the substantia nigra of Parkinson's and Alzheimer's disease brains. *Neurology*, *38*(8), 1285-1291. https://doi.org/10.1212/wnl.38.8.1285

McGinley, A. M., Sutton, C. E., Edwards, S. C., Leane, C. M., DeCourcey, J., Teijeiro, A., Hamilton, J. A., Boon, L., Djouder, N., & Mills, K. H. G. (2020). Interleukin-17A Serves a Priming Role in Autoimmunity by Recruiting IL-1beta-Producing Myeloid Cells that Promote Pathogenic T Cells. *Immunity*, *52*(2), 342-356 e346. https://doi.org/10.1016/j.immuni.2020.01.002

Mertens, J., Paquola, A. C. M., Ku, M., Hatch, E., Bohnke, L., Ladjevardi, S., McGrath, S., Campbell, B., Lee, H., Herdy, J. R., Goncalves, J. T., Toda, T., Kim, Y., Winkler, J., Yao, J., Hetzer, M. W., & Gage, F. H. (2015). Directly Reprogrammed Human Neurons Retain Aging-Associated Transcriptomic Signatures and Reveal Age-Related Nucleocytoplasmic Defects. *Cell Stem Cell*, *17*(6), 705-718. https://doi.org/10.1016/j.stem.2015.09.001

Michetti, F., D'Ambrosi, N., Toesca, A., Puglisi, M. A., Serrano, A., Marchese, E., Corvino, V., & Geloso, M. C. (2019). The S100B story: from biomarker to active factor in neural injury. *J Neurochem*, *148*(2), 168-187. https://doi.org/10.1111/jnc.14574

Miklossy, J., Doudet, D. D., Schwab, C., Yu, S., McGeer, E. G., & McGeer, P. L. (2006). Role of ICAM-1 in persisting inflammation in Parkinson disease and MPTP monkeys. *Exp Neurol*, *197*(2), 275-283. https://doi.org/10.1016/j.expneurol.2005.10.034

Miller, R. A., & Ruddle, F. H. (1976). Pluripotent teratocarcinoma-thymus somatic cell hybrids. *Cell*, *9*(1), 45-55. https://doi.org/10.1016/0092-8674(76)90051-9

Mishra, A., Singh, S., & Shukla, S. (2018). Physiological and Functional Basis of Dopamine Receptors and Their Role in Neurogenesis: Possible Implication for Parkinson's disease. *J Exp Neurosci*, *12*, 1179069518779829. https://doi.org/10.1177/1179069518779829

Mitsui, K., Tokuzawa, Y., Itoh, H., Segawa, K., Murakami, M., Takahashi, K., Maruyama, M., Maeda, M., & Yamanaka, S. (2003). The homeoprotein Nanog is required for maintenance of pluripotency in mouse epiblast and ES cells. *Cell*, *113*(5), 631-642. https://doi.org/10.1016/s0092-8674(03)00393-3

Mohamed, M. A., Zeng, Z., Gennaro, M., Lao-Kaim, N. P., Myers, J. F. M., Calsolaro, V., Femminella, G. D., Tyacke, R. J., Martin-Bastida, A., Gunn, R. N., Nutt, D. J., Edison, P., Piccini, P., & Roussakis, A. A. (2022). Astrogliosis in aging and Parkinson's disease dementia: a new clinical study with (11)C-BU99008 PET. *Brain Commun*, *4*(5), fcac199. https://doi.org/10.1093/braincomms/fcac199

Morizane, A., Kikuchi, T., Hayashi, T., Mizuma, H., Takara, S., Doi, H., Mawatari, A., Glasser, M. F., Shiina, T., Ishigaki, H., Itoh, Y., Okita, K., Yamasaki, E., Doi, D., Onoe, H., Ogasawara, K., Yamanaka, S., & Takahashi, J. (2017). MHC matching improves

engraftment of iPSC-derived neurons in non-human primates. *Nat Commun*, *8*(1), 385. https://doi.org/10.1038/s41467-017-00926-5

Mulia, G. E., Picanco-Castro, V., Stavrou, E. F., Athanassiadou, A., & Figueiredo, M. L. (2021). Advances in the Development and the Applications of Nonviral, Episomal Vectors for Gene Therapy. *Hum Gene Ther*, *32*(19-20), 1076-1095. https://doi.org/10.1089/hum.2020.310

Murillo, M. D. P., Aronsson, P., Winder, M., & Carlsson, T. (2020). Desipramine, commonly used as a noradrenergic neuroprotectant in 6-OHDA-lesions, leads to local functional changes in the urinary bladder and gastrointestinal tract in healthy rats. *Heliyon*, *6*(11), e05472. https://doi.org/10.1016/j.heliyon.2020.e05472

Mv, L. (1895). Der feinere Bau des Nervensystems im Lichte neuester Forschung. *Fischer's Medicinische Buchhandlung H, Kornfield, Berlin*.

Nascimento, I., Nobrega, K. C. C., Souza, B. R. A., Barone, I. C., Checchio, G., Ponciano, V. P., de Paula, C. G. C., Possani, A. N., Penha, N. C., Helene, A. F., Roque, A. C., Savica, R., & Piemonte, M. E. P. (2023). Comparison of disability level between Early and Late Onset Parkinson's Disease using WHODAS 2. *Front Neurol*, *14*, 1281537. https://doi.org/10.3389/fneur.2023.1281537

Natunen, S., Satomaa, T., Pitkanen, V., Salo, H., Mikkola, M., Natunen, J., Otonkoski, T., & Valmu, L. (2011). The binding specificity of the marker antibodies Tra-1-60 and Tra-1-81 reveals a novel pluripotency-associated type 1 lactosamine epitope. *Glycobiology*, *21*(9), 1125-1130. https://doi.org/10.1093/glycob/cwq209

Ng, Y. H., Chanda, S., Janas, J. A., Yang, N., Kokubu, Y., Sudhof, T. C., & Wernig, M. (2021). Efficient generation of dopaminergic induced neuronal cells with midbrain characteristics. *Stem Cell Reports*, *16*(7), 1763-1776. https://doi.org/10.1016/j.stemcr.2021.05.017

Nichols, J., Zevnik, B., Anastassiadis, K., Niwa, H., Klewe-Nebenius, D., Chambers, I., Scholer, H., & Smith, A. (1998). Formation of pluripotent stem cells in the mammalian embryo depends on the POU transcription factor Oct4. *Cell*, *95*(3), 379-391. https://doi.org/10.1016/s0092-8674(00)81769-9

Nicklas, W. J., Youngster, S. K., Kindt, M. V., & Heikkila, R. E. (1987). MPTP, MPP+ and mitochondrial function. *Life Sci*, *40*(8), 721-729. https://doi.org/10.1016/0024-3205(87)90299-2

Noack, M., Beringer, A., & Miossec, P. (2019). Additive or Synergistic Interactions Between IL-17A or IL-17F and TNF or IL-1beta Depend on the Cell Type. *Front Immunol*, *10*, 1726. https://doi.org/10.3389/fimmu.2019.01726

Nolbrant, S., Heuer, A., Parmar, M., & Kirkeby, A. (2017). Generation of high-purity human ventral midbrain dopaminergic progenitors for in vitro maturation and intracerebral transplantation. *Nat Protoc*, *12*(9), 1962-1979. https://doi.org/10.1038/nprot.2017.078

Okita, K., Ichisaka, T., & Yamanaka, S. (2007). Generation of germline-competent induced pluripotent stem cells. *Nature*, *448*(7151), 313-317. https://doi.org/10.1038/nature05934

Okita, K., Matsumura, Y., Sato, Y., Okada, A., Morizane, A., Okamoto, S., Hong, H., Nakagawa, M., Tanabe, K., Tezuka, K., Shibata, T., Kunisada, T., Takahashi, M., Takahashi, J., Saji, H., & Yamanaka, S. (2011). A more efficient method to generate integration-free human iPS cells. *Nat Methods*, *8*(5), 409-412. https://doi.org/10.1038/nmeth.1591

Olsen, I., & Sollid, L. M. (2013). Pitfalls in determining the cytokine profile of human T cells. *J Immunol Methods*, *390*(1-2), 106-112. https://doi.org/10.1016/j.jim.2013.01.015

Olson, K. E., Abdelmoaty, M. M., Namminga, K. L., Lu, Y., Obaro, H., Santamaria, P., Mosley, R. L., & Gendelman, H. E. (2023). An open-label multiyear study of

sargramostim-treated Parkinson's disease patients examining drug safety, tolerability, and immune biomarkers from limited case numbers. *Transl Neurodegener*, *12*(1), 26. https://doi.org/10.1186/s40035-023-00361-1

Olson, K. E., Namminga, K. L., Lu, Y., Schwab, A. D., Thurston, M. J., Abdelmoaty, M. M., Kumar, V., Wojtkiewicz, M., Obaro, H., Santamaria, P., Mosley, R. L., & Gendelman, H. E. (2021). Safety, tolerability, and immune-biomarker profiling for year-long sargramostim treatment of Parkinson's disease. *EBioMedicine*, *67*, 103380. https://doi.org/10.1016/j.ebiom.2021.103380

Olszewska, D. A., McCarthy, A., Soto-Beasley, A. I., Walton, R. L., Magennis, B., McLaughlin, R. L., Hardiman, O., Ross, O. A., & Lynch, T. (2020). Association Between Glucocerebrosidase Mutations and Parkinson's Disease in Ireland. *Front Neurol*, *11*, 527. https://doi.org/10.3389/fneur.2020.00527

Omole, A. E., & Fakoya, A. O. J. (2018). Ten years of progress and promise of induced pluripotent stem cells: historical origins, characteristics, mechanisms, limitations, and potential applications. *PeerJ*, *6*, e4370. https://doi.org/10.7717/peerj.4370

Oosterveen, T., Garcao, P., Moles-Garcia, E., Soleilhavoup, C., Travaglio, M., Sheraz, S., Peltrini, R., Patrick, K., Labas, V., Combes-Soia, L., Marklund, U., Hohenstein, P., & Panman, L. (2021). Pluripotent stem cell derived dopaminergic subpopulations model the selective neuron degeneration in Parkinson's disease. *Stem Cell Reports*, *16*(11), 2718-2735. https://doi.org/10.1016/j.stemcr.2021.09.014

Paisan-Ruiz, C., Jain, S., Evans, E. W., Gilks, W. P., Simon, J., van der Brug, M., Lopez de Munain, A., Aparicio, S., Gil, A. M., Khan, N., Johnson, J., Martinez, J. R., Nicholl, D., Marti Carrera, I., Pena, A. S., de Silva, R., Lees, A., Marti-Masso, J. F., Perez-Tur, J., . . . Singleton, A. B. (2004). Cloning of the gene containing mutations that cause

PARK8-linked Parkinson's disease. *Neuron*, *44*(4), 595-600. https://doi.org/10.1016/j.neuron.2004.10.023

Pan, G. J., Chang, Z. Y., Scholer, H. R., & Pei, D. (2002). Stem cell pluripotency and transcription factor Oct4. *Cell Res*, *12*(5-6), 321-329. https://doi.org/10.1038/sj.cr.7290134

Park, I. H., Arora, N., Huo, H., Maherali, N., Ahfeldt, T., Shimamura, A., Lensch, M. W., Cowan, C., Hochedlinger, K., & Daley, G. Q. (2008). Disease-specific induced pluripotent stem cells. *Cell*, *134*(5), 877-886. https://doi.org/10.1016/j.cell.2008.07.041

Parkin, G. M., Udawela, M., Gibbons, A., & Dean, B. (2018). Glutamate transporters, EAAT1 and EAAT2, are potentially important in the pathophysiology and treatment of schizophrenia and affective disorders. *World J Psychiatry*, *8*(2), 51-63. https://doi.org/10.5498/wjp.v8.i2.51

Parkinson, J. (2002). An essay on the shaking palsy. 1817. *J Neuropsychiatry Clin Neurosci*, *14*(2), 223-236; discussion 222. https://doi.org/10.1176/jnp.14.2.223

Parra-Rivas, L. A., Madhivanan, K., Aulston, B. D., Wang, L., Prakashchand, D. D., Boyer, N. P., Saia-Cereda, V. M., Branes-Guerrero, K., Pizzo, D. P., Bagchi, P., Sundar, V. S., Tang, Y., Das, U., Scott, D. A., Rangamani, P., Ogawa, Y., & Subhojit, R. (2023). Serine-129 phosphorylation of alpha-synuclein is an activity-dependent trigger for physiologic protein-protein interactions and synaptic function. *Neuron*, *111*(24), 4006-4023 e4010. https://doi.org/10.1016/j.neuron.2023.11.020

Pennock, N. D., White, J. T., Cross, E. W., Cheney, E. E., Tamburini, B. A., & Kedl, R. M. (2013). T cell responses: naive to memory and everything in between. *Adv Physiol Educ*, *37*(4), 273-283. https://doi.org/10.1152/advan.00066.2013

Pereira Luppi, M., Azcorra, M., Caronia-Brown, G., Poulin, J. F., Gaertner, Z., Gatica, S., Moreno-Ramos, O. A., Nouri, N., Dubois, M., Ma, Y. C., Ramakrishnan, C., Fenno,

L., Kim, Y. S., Deisseroth, K., Cicchetti, F., Dombeck, D. A., & Awatramani, R. (2021). Sox6 expression distinguishes dorsally and ventrally biased dopamine neurons in the substantia nigra with distinctive properties and embryonic origins. *Cell Rep*, *37*(6), 109975. https://doi.org/10.1016/j.celrep.2021.109975

Perrier, A. L., Tabar, V., Barberi, T., Rubio, M. E., Bruses, J., Topf, N., Harrison, N. L., & Studer, L. (2004). Derivation of midbrain dopamine neurons from human embryonic stem cells. *Proc Natl Acad Sci U S A*, *101*(34), 12543-12548. https://doi.org/10.1073/pnas.0404700101

Petrasca, A., Phelan, J. J., Ansboro, S., Veale, D. J., Fearon, U., & Fletcher, J. M. (2020). Targeting bioenergetics prevents CD4 T cell-mediated activation of synovial fibroblasts in rheumatoid arthritis. *Rheumatology (Oxford)*, *59*(10), 2816-2828. https://doi.org/10.1093/rheumatology/kez682

Pfisterer, U., Kirkeby, A., Torper, O., Wood, J., Nelander, J., Dufour, A., Bjorklund, A., Lindvall, O., Jakobsson, J., & Parmar, M. (2011). Direct conversion of human fibroblasts to dopaminergic neurons. *Proc Natl Acad Sci U S A*, *108*(25), 10343-10348. https://doi.org/10.1073/pnas.1105135108

Poewe, W., Seppi, K., Tanner, C. M., Halliday, G. M., Brundin, P., Volkmann, J., Schrag, A. E., & Lang, A. E. (2017). Parkinson disease. *Nat Rev Dis Primers*, *3*, 17013. https://doi.org/10.1038/nrdp.2017.13

Polymeropoulos, M. H., Lavedan, C., Leroy, E., Ide, S. E., Dehejia, A., Dutra, A., Pike, B., Root, H., Rubenstein, J., Boyer, R., Stenroos, E. S., Chandrasekharappa, S., Athanassiadou, A., Papapetropoulos, T., Johnson, W. G., Lazzarini, A. M., Duvoisin, R. C., Di Iorio, G., Golbe, L. I., & Nussbaum, R. L. (1997). Mutation in the alpha-synuclein gene identified in families with Parkinson's disease. *Science*, *276*(5321), 2045-2047. https://doi.org/10.1126/science.276.5321.2045

Pons-Espinal, M., Blasco-Agell, L., Fernandez-Carasa, I., Andres-Benito, P., di Domenico, A., Richaud-Patin, Y., Baruffi, V., Marruecos, L., Espinosa, L., Garrido, A., Tolosa, E., Edel, M. J., Otero, M. J., Mosquera, J. L., Ferrer, I., Raya, A., & Consiglio, A. (2024). Blocking IL-6 signaling prevents astrocyte-induced neurodegeneration in an iPSC-based model of Parkinson's disease. *JCI Insight*, *9*(3). https://doi.org/10.1172/jci.insight.163359

Prajeeth, C. K., Kronisch, J., Khorooshi, R., Knier, B., Toft-Hansen, H., Gudi, V., Floess, S., Huehn, J., Owens, T., Korn, T., & Stangel, M. (2017). Effectors of Th1 and Th17 cells act on astrocytes and augment their neuroinflammatory properties. *J Neuroinflammation*, *14*(1), 204. https://doi.org/10.1186/s12974-017-0978-3

Qin, J., Ma, Z., Chen, X., & Shu, S. (2023). Microglia activation in central nervous system disorders: A review of recent mechanistic investigations and development efforts. *Front Neurol*, *14*, 1103416. https://doi.org/10.3389/fneur.2023.1103416

Rakowicz, W. P., Staples, C. S., Milbrandt, J., Brunstrom, J. E., & Johnson, E. M., Jr. (2002). Glial cell line-derived neurotrophic factor promotes the survival of early postnatal spinal motor neurons in the lateral and medial motor columns in slice culture. *J Neurosci*, *22*(10), 3953-3962. https://doi.org/10.1523/JNEUROSCI.22-10-03953.2002

Ramishetti, S., Kedmi, R., Goldsmith, M., Leonard, F., Sprague, A. G., Godin, B., Gozin, M., Cullis, P. R., Dykxhoorn, D. M., & Peer, D. (2015). Systemic Gene Silencing in Primary T Lymphocytes Using Targeted Lipid Nanoparticles. *ACS Nano*, *9*(7), 6706-6716. https://doi.org/10.1021/acsnano.5b02796

Ransom, B. R., Kunis, D. M., Irwin, I., & Langston, J. W. (1987). Astrocytes convert the parkinsonism inducing neurotoxin, MPTP, to its active metabolite, MPP+. *Neurosci Lett*, *75*(3), 323-328. https://doi.org/10.1016/0304-3940(87)90543-x

Rappold, P. M., Cui, M., Chesser, A. S., Tibbett, J., Grima, J. C., Duan, L., Sen, N., Javitch, J. A., & Tieu, K. (2011). Paraquat neurotoxicity is mediated by the dopamine transporter and organic cation transporter-3. *Proc Natl Acad Sci U S A*, *108*(51), 20766-20771. https://doi.org/10.1073/pnas.1115141108

Reynolds, A. D., Banerjee, R., Liu, J., Gendelman, H. E., & Mosley, R. L. (2007). Neuroprotective activities of CD4+CD25+ regulatory T cells in an animal model of Parkinson's disease. *J Leukoc Biol*, *82*(5), 1083-1094. https://doi.org/10.1189/jlb.0507296

Reynolds, A. D., Stone, D. K., Hutter, J. A., Benner, E. J., Mosley, R. L., & Gendelman, H. E. (2010). Regulatory T cells attenuate Th17 cell-mediated nigrostriatal dopaminergic neurodegeneration in a model of Parkinson's disease. *J Immunol*, *184*(5), 2261-2271. https://doi.org/10.4049/jimmunol.0901852

Ribes, V., Balaskas, N., Sasai, N., Cruz, C., Dessaud, E., Cayuso, J., Tozer, S., Yang, L. L., Novitch, B., Marti, E., & Briscoe, J. (2010). Distinct Sonic Hedgehog signaling dynamics specify floor plate and ventral neuronal progenitors in the vertebrate neural tube. *Genes Dev*, *24*(11), 1186-1200. https://doi.org/10.1101/gad.559910

Ricklin, D., Reis, E. S., Mastellos, D. C., Gros, P., & Lambris, J. D. (2016). Complement component C3 - The "Swiss Army Knife" of innate immunity and host defense. *Immunol Rev*, *274*(1), 33-58. https://doi.org/10.1111/imr.12500

Rocha, N. P., Scalzo, P. L., Barbosa, I. G., Souza, M. S., Morato, I. B., Vieira, E. L., Christo, P. P., Teixeira, A. L., & Reis, H. J. (2014). Cognitive Status Correlates with CXCL10/IP-10 Levels in Parkinson's Disease. *Parkinsons Dis*, *2014*, 903796. https://doi.org/10.1155/2014/903796

Ross, S. B., Fraser, S. T., Bagnall, R. D., & Semsarian, C. (2017). Peripheral blood derived induced pluripotent stem cells (iPSCs) from a female with familial hypertrophic cardiomyopathy. *Stem Cell Res*, *20*, 76-79. https://doi.org/10.1016/j.scr.2017.02.016

Ross, S. H., & Cantrell, D. A. (2018). Signaling and Function of Interleukin-2 in T Lymphocytes. *Annu Rev Immunol*, *36*, 411-433. https://doi.org/10.1146/annurev-immunol-042617-053352

Rostami, J., Fotaki, G., Sirois, J., Mzezewa, R., Bergstrom, J., Essand, M., Healy, L., & Erlandsson, A. (2020). Astrocytes have the capacity to act as antigen-presenting cells in the Parkinson's disease brain. *J Neuroinflammation*, *17*(1), 119. https://doi.org/10.1186/s12974-020-01776-7

Roybon, L., Lamas, N. J., Garcia, A. D., Yang, E. J., Sattler, R., Lewis, V. J., Kim, Y. A., Kachel, C. A., Rothstein, J. D., Przedborski, S., Wichterle, H., & Henderson, C. E. (2013). Human stem cell-derived spinal cord astrocytes with defined mature or reactive phenotypes. *Cell Rep*, *4*(5), 1035-1048. https://doi.org/10.1016/j.celrep.2013.06.021

Schmid, B., Holst, B., Clausen, C., Bahnassawy, L., Reinhardt, P., Bakker, M. H. M., Diaz-Guerra, E., Vicario, C., Martino-Adami, P. V., Thoenes, M., Ramirez, A., Fliessbach, K., Grezella, C., Brustle, O., Peitz, M., Ebneth, A., & Cabrera-Socorro, A. (2021). Generation of a set of isogenic iPSC lines carrying all APOE genetic variants (E2/E3/E4) and knock-out for the study of APOE biology in health and disease. *Stem Cell Res*, *52*, 102180. https://doi.org/10.1016/j.scr.2021.102180

Schofield, D. J., Irving, L., Calo, L., Bogstedt, A., Rees, G., Nuccitelli, A., Narwal, R., Petrone, M., Roberts, J., Brown, L., Cusdin, F., Dosanjh, B., Lloyd, C., Dobson, C., Gurrell, I., Fraser, G., McFarlane, M., Rockenstein, E., Spencer, B., . . . Perkinton, M. S. (2019). Preclinical development of a high affinity α-synuclein antibody, MEDI1341, that can

enter the brain, sequester extracellular α-synuclein and attenuate α-synuclein spreading in vivo. *Neurobiol Dis*, *132*, 104582. https://doi.org/10.1016/j.nbd.2019.104582

Scholze, A. R., Foo, L. C., Mulinyawe, S., & Barres, B. A. (2014). BMP signaling in astrocytes downregulates EGFR to modulate survival and maturation. *PLoS One*, *9*(10), e110668. https://doi.org/10.1371/journal.pone.0110668

Schondorf, D. C., Aureli, M., McAllister, F. E., Hindley, C. J., Mayer, F., Schmid, B., Sardi, S. P., Valsecchi, M., Hoffmann, S., Schwarz, L. K., Hedrich, U., Berg, D., Shihabuddin, L. S., Hu, J., Pruszak, J., Gygi, S. P., Sonnino, S., Gasser, T., & Deleidi, M. (2014). iPSC-derived neurons from GBA1-associated Parkinson's disease patients show autophagic defects and impaired calcium homeostasis. *Nat Commun*, *5*, 4028. https://doi.org/10.1038/ncomms5028

Schroder, J. B., Pawlowski, M., Meyer Zu Horste, G., Gross, C. C., Wiendl, H., Meuth, S. G., Ruck, T., & Warnecke, T. (2018). Immune Cell Activation in the Cerebrospinal Fluid of Patients With Parkinson's Disease. *Front Neurol*, *9*, 1081. https://doi.org/10.3389/fneur.2018.01081

Schwarz, J., Schwarz, S. C., & Storch, A. (2006). Developmental perspectives on human midbrain-derived neural stem cells. *Neurodegener Dis*, *3*(1-2), 45-49. https://doi.org/10.1159/000092092

Schweitzer, J. S., Song, B., Herrington, T. M., Park, T. Y., Lee, N., Ko, S., Jeon, J., Cha, Y., Kim, K., Li, Q., Henchcliffe, C., Kaplitt, M., Neff, C., Rapalino, O., Seo, H., Lee, I. H., Kim, J., Kim, T., Petsko, G. A., . . . Kim, K. S. (2020). Personalized iPSC-Derived Dopamine Progenitor Cells for Parkinson's Disease. *N Engl J Med*, *382*(20), 1926-1932. https://doi.org/10.1056/NEJMoa1915872

Serio, A., Bilican, B., Barmada, S. J., Ando, D. M., Zhao, C., Siller, R., Burr, K., Haghi, G., Story, D., Nishimura, A. L., Carrasco, M. A., Phatnani, H. P., Shum, C., Wilmut, I.,

Maniatis, T., Shaw, C. E., Finkbeiner, S., & Chandran, S. (2013). Astrocyte pathology and the absence of non-cell autonomy in an induced pluripotent stem cell model of TDP-43 proteinopathy. *Proc Natl Acad Sci U S A*, *110*(12), 4697-4702. https://doi.org/10.1073/pnas.1300398110

Shaltouki, A., Peng, J., Liu, Q., Rao, M. S., & Zeng, X. (2013). Efficient generation of astrocytes from human pluripotent stem cells in defined conditions. *Stem Cells*, *31*(5), 941-952. https://doi.org/10.1002/stem.1334

Sherer, T. B., Kim, J. H., Betarbet, R., & Greenamyre, J. T. (2003). Subcutaneous rotenone exposure causes highly selective dopaminergic degeneration and alpha-synuclein aggregation. *Exp Neurol*, *179*(1), 9-16. https://doi.org/10.1006/exnr.2002.8072

Shuvalova, L. D., Eremeev, A. V., Bogomazova, A. N., Novosadova, E. V., Zerkalenkova, E. A., Olshanskaya, Y. V., Fedotova, E. Y., Glagoleva, E. S., Illarioshkin, S. N., Lebedeva, O. S., & Lagarkova, M. A. (2020). Generation of induced pluripotent stem cell line RCPCMi004-A derived from patient with Parkinson's disease with deletion of the exon 2 in PARK2 gene. *Stem Cell Res*, *44*, 101733. https://doi.org/10.1016/j.scr.2020.101733

Sibuea, S., Ho, J. K., Pouton, C. W., & Haynes, J. M. (2023). TGFbeta3, dibutyryl cAMP and a notch inhibitor modulate phenotype late in stem cell-derived dopaminergic neuron maturation. *Front Cell Dev Biol*, *11*, 1111705. https://doi.org/10.3389/fcell.2023.1111705

Simola, N., Morelli, M., & Carta, A. R. (2007). The 6-hydroxydopamine model of Parkinson's disease. *Neurotox Res*, *11*(3-4), 151-167. https://doi.org/10.1007/BF03033565

Singleton, A. B., Farrer, M., Johnson, J., Singleton, A., Hague, S., Kachergus, J., Hulihan, M., Peuralinna, T., Dutra, A., Nussbaum, R., Lincoln, S., Crawley, A., Hanson, M., Maraganore, D., Adler, C., Cookson, M. R., Muenter, M., Baptista, M., Miller, D., . . .

Gwinn-Hardy, K. (2003). alpha-Synuclein locus triplication causes Parkinson's disease. *Science*, *302*(5646), 841. https://doi.org/10.1126/science.1090278

Skorvanek, M., Martinez-Martin, P., Kovacs, N., Rodriguez-Violante, M., Corvol, J. C., Taba, P., Seppi, K., Levin, O., Schrag, A., Foltynie, T., Alvarez-Sanchez, M., Arakaki, T., Aschermann, Z., Aviles-Olmos, I., Benchetrit, E., Benoit, C., Bergareche-Yarza, A., Cervantes-Arriaga, A., Chade, A., . . . Stebbins, G. T. (2017). Differences in MDS-UPDRS Scores Based on Hoehn and Yahr Stage and Disease Duration. *Mov Disord Clin Pract*, *4*(4), 536-544. https://doi.org/10.1002/mdc3.12476

Smith, T. T., Stephan, S. B., Moffett, H. F., McKnight, L. E., Ji, W., Reiman, D., Bonagofski, E., Wohlfahrt, M. E., Pillai, S. P. S., & Stephan, M. T. (2017). In situ programming of leukaemia-specific T cells using synthetic DNA nanocarriers. *Nat Nanotechnol*, *12*(8), 813-820. https://doi.org/10.1038/nnano.2017.57

Soldner, F., Hockemeyer, D., Beard, C., Gao, Q., Bell, G. W., Cook, E. G., Hargus, G., Blak, A., Cooper, O., Mitalipova, M., Isacson, O., & Jaenisch, R. (2009). Parkinson's disease patient-derived induced pluripotent stem cells free of viral reprogramming factors. *Cell*, *136*(5), 964-977. https://doi.org/10.1016/j.cell.2009.02.013

Sommer, A., Fadler, T., Dorfmeister, E., Hoffmann, A. C., Xiang, W., Winner, B., & Prots, I. (2016). Infiltrating T lymphocytes reduce myeloid phagocytosis activity in synucleinopathy model. *J Neuroinflammation*, *13*(1), 174. https://doi.org/10.1186/s12974-016-0632-5

Sommer, A., Marxreiter, F., Krach, F., Fadler, T., Grosch, J., Maroni, M., Graef, D., Eberhardt, E., Riemenschneider, M. J., Yeo, G. W., Kohl, Z., Xiang, W., Gage, F. H., Winkler, J., Prots, I., & Winner, B. (2018). Th17 Lymphocytes Induce Neuronal Cell Death in a Human iPSC-Based Model of Parkinson's Disease. *Cell Stem Cell*, *23*(1), 123-131 e126. https://doi.org/10.1016/j.stem.2018.06.015

Sonninen, T. M., Hamalainen, R. H., Koskuvi, M., Oksanen, M., Shakirzyanova, A., Wojciechowski, S., Puttonen, K., Naumenko, N., Goldsteins, G., Laham-Karam, N., Lehtonen, M., Tavi, P., Koistinaho, J., & Lehtonen, S. (2020). Metabolic alterations in Parkinson's disease astrocytes. *Sci Rep*, *10*(1), 14474. https://doi.org/10.1038/s41598-020-71329-8

Sorrentino, Z. A., Xia, Y., Funk, C., Riffe, C. J., Rutherford, N. J., Ceballos Diaz, C., Sacino, A. N., Price, N. D., Golde, T. E., Giasson, B. I., & Chakrabarty, P. (2018). Motor neuron loss and neuroinflammation in a model of alpha-synuclein-induced neurodegeneration. *Neurobiol Dis*, *120*, 98-106. https://doi.org/10.1016/j.nbd.2018.09.005

Soubannier, V., Maussion, G., Chaineau, M., Sigutova, V., Rouleau, G., Durcan, T. M., & Stifani, S. (2020). Characterization of human iPSC-derived astrocytes with potential for disease modeling and drug discovery. *Neurosci Lett*, *731*, 135028. https://doi.org/10.1016/j.neulet.2020.135028

Spillantini, M. G., Schmidt, M. L., Lee, V. M., Trojanowski, J. Q., Jakes, R., & Goedert, M. (1997). Alpha-synuclein in Lewy bodies. *Nature*, *388*(6645), 839-840. https://doi.org/10.1038/42166

Stanberry, I., Cunningham, D., Ye, S., Alonzo, M., Zhao, M. T., Garg, V., & Lilly, B. (2023). Characterization of an induced pluripotent stem cell line NCHi011-A from a 23-year-old female with Alagille Syndrome harboring a heterozygous JAG1 pathogenic variant. *Stem Cell Res*, *72*, 103213. https://doi.org/10.1016/j.scr.2023.103213

Stevens, C. H., Rowe, D., Morel-Kopp, M.-C., Orr, C., Russell, T., Ranola, M., Ward, C., & Halliday, G. M. (2012). Reduced T helper and B lymphocytes in Parkinson's disease. *Journal of Neuroimmunology*, *252*(1-2), 95-99. https://doi.org/10.1016/j.jneuroim.2012.07.015

Stoker, T. B., Torsney, K. M., & Barker, R. A. (2018). Emerging Treatment Approaches for Parkinson's Disease. *Front Neurosci*, *12*, 693. https://doi.org/10.3389/fnins.2018.00693

Sulzer, D., Alcalay, R. N., Garretti, F., Cote, L., Kanter, E., Agin-Liebes, J., Liong, C., McMurtrey, C., Hildebrand, W. H., Mao, X., Dawson, V. L., Dawson, T. M., Oseroff, C., Pham, J., Sidney, J., Dillon, M. B., Carpenter, C., Weiskopf, D., Phillips, E., . . . Sette, A. (2017). T cells from patients with Parkinson's disease recognize alpha-synuclein peptides. *Nature*, *546*(7660), 656-661. https://doi.org/10.1038/nature22815

Tada, M., Takahama, Y., Abe, K., Nakatsuji, N., & Tada, T. (2001). Nuclear reprogramming of somatic cells by in vitro hybridization with ES cells. *Curr Biol*, *11*(19), 1553-1558. https://doi.org/10.1016/s0960-9822(01)00459-6

Takahashi, K., Tanabe, K., Ohnuki, M., Narita, M., Ichisaka, T., Tomoda, K., & Yamanaka, S. (2007). Induction of pluripotent stem cells from adult human fibroblasts by defined factors. *Cell*, *131*(5), 861-872. https://doi.org/10.1016/j.cell.2007.11.019

Takahashi, K., & Yamanaka, S. (2006). Induction of pluripotent stem cells from mouse embryonic and adult fibroblast cultures by defined factors. *Cell*, *126*(4), 663-676. https://doi.org/10.1016/j.cell.2006.07.024

Tanner, C. M., Kamel, F., Ross, G. W., Hoppin, J. A., Goldman, S. M., Korell, M., Marras, C., Bhudhikanok, G. S., Kasten, M., Chade, A. R., Comyns, K., Richards, M. B., Meng, C., Priestley, B., Fernandez, H. H., Cambi, F., Umbach, D. M., Blair, A., Sandler, D. P., & Langston, J. W. (2011). Rotenone, paraquat, and Parkinson's disease. *Environ Health Perspect*, *119*(6), 866-872. https://doi.org/10.1289/ehp.1002839

Theodore, S., Cao, S., McLean, P. J., & Standaert, D. G. (2008). Targeted overexpression of human alpha-synuclein triggers microglial activation and an adaptive immune response

in a mouse model of Parkinson disease. *J Neuropathol Exp Neurol*, *67*(12), 1149-1158. https://doi.org/10.1097/NEN.0b013e31818e5e99

Thiruchelvam, M., Brockel, B. J., Richfield, E. K., Baggs, R. B., & Cory-Slechta, D. A. (2000). Potentiated and preferential effects of combined paraquat and maneb on nigrostriatal dopamine systems: environmental risk factors for Parkinson's disease? *Brain Res*, *873*(2), 225-234. https://doi.org/10.1016/s0006-8993(00)02496-3

Thome, A. D., Atassi, F., Wang, J., Faridar, A., Zhao, W., Thonhoff, J. R., Beers, D. R., Lai, E. C., & Appel, S. H. (2021). Ex vivo expansion of dysfunctional regulatory T lymphocytes restores suppressive function in Parkinson's disease. *NPJ Parkinsons Dis*, *7*(1), 41. https://doi.org/10.1038/s41531-021-00188-5

Thomson, J. A., Itskovitz-Eldor, J., Shapiro, S. S., Waknitz, M. A., Swiergiel, J. J., Marshall, V. S., & Jones, J. M. (1998). Embryonic stem cell lines derived from human blastocysts. *Science*, *282*(5391), 1145-1147. https://doi.org/10.1126/science.282.5391.1145

Tian, J., Dai, S. B., Jiang, S. S., Yang, W. Y., Yan, Y. Q., Lin, Z. H., Dong, J. X., Liu, Y., Zheng, R., Chen, Y., Zhang, B. R., & Pu, J. L. (2022). Specific immune status in Parkinson's disease at different ages of onset. *NPJ Parkinsons Dis*, *8*(1), 5. https://doi.org/10.1038/s41531-021-00271-x

Trétiakoff, C. (1919). Contribution a l'etude de l'Anatomie pathologique du Locus Niger de Soemmering avec quelques deduction relatives a la pathogenie des troubles du tonus musculaire et de la maladie de Parkinson. *Theses de Paris*.

Trickett, A., & Kwan, Y. L. (2003). T cell stimulation and expansion using anti-CD3/CD28 beads. *J Immunol Methods*, *275*(1-2), 251-255. https://doi.org/10.1016/s0022-1759(03)00010-3

Trindade, P., Loiola, E. C., Gasparotto, J., Ribeiro, C. T., Cardozo, P. L., Devalle, S., Salerno, J. A., Ornelas, I. M., Ledur, P. F., Ribeiro, F. M., Ventura, A. L. M., Moreira, J. C. F.,

Gelain, D. P., Porciuncula, L. O., & Rehen, S. K. (2020). Short and long TNF-alpha exposure recapitulates canonical astrogliosis events in human-induced pluripotent stem cells-derived astrocytes. *Glia*, *68*(7), 1396-1409. https://doi.org/10.1002/glia.23786

Van Craenenbroeck, K., Vanhoenacker, P., & Haegeman, G. (2000). Episomal vectors for gene expression in mammalian cells. *Eur J Biochem*, *267*(18), 5665-5678. https://doi.org/10.1046/j.1432-1327.2000.01645.x

Vaz, I. M., Borgonovo, T., Kasai-Brunswick, T. H., Santos, D. S. D., Mesquita, F. C. P., Vasques, J. F., Gubert, F., Rebelatto, C. L. K., Senegaglia, A. C., & Brofman, P. R. S. (2021). Chromosomal aberrations after induced pluripotent stem cells reprogramming. *Genet Mol Biol*, *44*(3), e20200147. https://doi.org/10.1590/1678-4685-GMB-2020-0147

Vazirinejad, R., Ahmadi, Z., Kazemi Arababadi, M., Hassanshahi, G., & Kennedy, D. (2014). The biological functions, structure and sources of CXCL10 and its outstanding part in the pathophysiology of multiple sclerosis. *Neuroimmunomodulation*, *21*(6), 322-330. https://doi.org/10.1159/000357780

Vierbuchen, T., Ostermeier, A., Pang, Z. P., Kokubu, Y., Sudhof, T. C., & Wernig, M. (2010). Direct conversion of fibroblasts to functional neurons by defined factors. *Nature*, *463*(7284), 1035-1041. https://doi.org/10.1038/nature08797

Vijiaratnam, N., Girges, C., Auld, G., Chau, M., Maclagan, K., King, A., Skene, S., Chowdhury, K., Hibbert, S., Morris, H., Limousin, P., Athauda, D., Carroll, C. B., Hu, M. T., Silverdale, M., Duncan, G. W., Chaudhuri, R., Lo, C., Del Din, S., . . . Foltynie, T. (2021). Exenatide once weekly over 2 years as a potential disease-modifying treatment for Parkinson's disease: protocol for a multicentre, randomised, double blind, parallel group, placebo controlled, phase 3 trial: The 'Exenatide-PD3' study. *BMJ Open*, *11*(5), e047993. https://doi.org/10.1136/bmjopen-2020-047993

Vilarino-Guell, C., Wider, C., Ross, O. A., Dachsel, J. C., Kachergus, J. M., Lincoln, S. J., Soto-Ortolaza, A. I., Cobb, S. A., Wilhoite, G. J., Bacon, J. A., Behrouz, B., Melrose, H. L., Hentati, E., Puschmann, A., Evans, D. M., Conibear, E., Wasserman, W. W., Aasly, J. O., Burkhard, P. R., . . . Farrer, M. J. (2011). VPS35 mutations in Parkinson disease. *Am J Hum Genet*, *89*(1), 162-167. https://doi.org/10.1016/j.ajhg.2011.06.001

Viti, J., Feathers, A., Phillips, J., & Lillien, L. (2003). Epidermal growth factor receptors control competence to interpret leukemia inhibitory factor as an astrocyte inducer in developing cortex. *J Neurosci*, *23*(8), 3385-3393. https://doi.org/10.1523/JNEUROSCI.23-08-03385.2003

Vlahos, K., Sourris, K., Mayberry, R., McDonald, P., Bruveris, F. F., Schiesser, J. V., Bozaoglu, K., Lockhart, P. J., Stanley, E. G., & Elefanty, A. G. (2019). Generation of iPSC lines from peripheral blood mononuclear cells from 5 healthy adults. *Stem Cell Res*, *34*, 101380. https://doi.org/10.1016/j.scr.2018.101380

Volc, D., Poewe, W., Kutzelnigg, A., Luhrs, P., Thun-Hohenstein, C., Schneeberger, A., Galabova, G., Majbour, N., Vaikath, N., El-Agnaf, O., Winter, D., Mihailovska, E., Mairhofer, A., Schwenke, C., Staffler, G., & Medori, R. (2020). Safety and immunogenicity of the alpha-synuclein active immunotherapeutic PD01A in patients with Parkinson's disease: a randomised, single-blinded, phase 1 trial. *Lancet Neurol*, *19*(7), 591-600. https://doi.org/10.1016/S1474-4422(20)30136-8

Wang, C., Yang, T., Liang, M., Xie, J., & Song, N. (2021). Astrocyte dysfunction in Parkinson's disease: from the perspectives of transmitted alpha-synuclein and genetic modulation. *Transl Neurodegener*, *10*(1), 39. https://doi.org/10.1186/s40035-021-00265-y

Wang, L., Miyahira, A. K., Simons, D. L., Lu, X., Chang, A. Y., Wang, C., Suni, M. A., Maino, V. C., Dirbas, F. M., Yim, J., Waisman, J., & Lee, P. P. (2017). IL6 Signaling in

Peripheral Blood T Cells Predicts Clinical Outcome in Breast Cancer. *Cancer Res*, *77*(5), 1119-1126. https://doi.org/10.1158/0008-5472.CAN-16-1373

Wang, L. M., Wu, Q., Kirk, R. A., Horn, K. P., Ebada Salem, A. H., Hoffman, J. M., Yap, J. T., Sonnen, J. A., Towner, R. A., Bozza, F. A., Rodrigues, R. S., & Morton, K. A. (2018). Lipopolysaccharide endotoxemia induces amyloid-beta and p-tau formation in the rat brain. *Am J Nucl Med Mol Imaging*, *8*(2), 86-99. https://www.ncbi.nlm.nih.gov/pubmed/29755842

Wang, Y., Chou, B. K., Dowey, S., He, C., Gerecht, S., & Cheng, L. (2013). Scalable expansion of human induced pluripotent stem cells in the defined xeno-free E8 medium under adherent and suspension culture conditions. *Stem Cell Res*, *11*(3), 1103-1116. https://doi.org/10.1016/j.scr.2013.07.011

Wilmut, I., Schnieke, A. E., McWhir, J., Kind, A. J., & Campbell, K. H. (1997). Viable offspring derived from fetal and adult mammalian cells. *Nature*, *385*(6619), 810-813. https://doi.org/10.1038/385810a0

Wooten, G. F., Currie, L. J., Bovbjerg, V. E., Lee, J. K., & Patrie, J. (2004). Are men at greater risk for Parkinson's disease than women? *J Neurol Neurosurg Psychiatry*, *75*(4), 637-639. https://doi.org/10.1136/jnnp.2003.020982

Yamanaka, S. (2007). Strategies and new developments in the generation of patient-specific pluripotent stem cells. *Cell Stem Cell*, *1*(1), 39-49. https://doi.org/10.1016/j.stem.2007.05.012

Yamanaka, S. (2020). Pluripotent Stem Cell-Based Cell Therapy-Promise and Challenges. *Cell Stem Cell*, *27*(4), 523-531. https://doi.org/10.1016/j.stem.2020.09.014

Yan, J., Studer, L., & McKay, R. D. (2001). Ascorbic acid increases the yield of dopaminergic neurons derived from basic fibroblast growth factor expanded mesencephalic

precursors. *J Neurochem*, *76*(1), 307-311. https://doi.org/10.1046/j.1471-4159.2001.00073.x

Yan, Y., Ding, X., Li, K., Ciric, B., Wu, S., Xu, H., Gran, B., Rostami, A., & Zhang, G. X. (2012). CNS-specific therapy for ongoing EAE by silencing IL-17 pathway in astrocytes. *Mol Ther*, *20*(7), 1338-1348. https://doi.org/10.1038/mt.2012.12

Yan, Z., Yang, W., Wei, H., Dean, M. N., Standaert, D. G., Cutter, G. R., Benveniste, E. N., & Qin, H. (2021). Dysregulation of the Adaptive Immune System in Patients With Early-Stage Parkinson Disease. *Neurol Neuroimmunol Neuroinflamm*, *8*(5). https://doi.org/10.1212/NXI.0000000000001036

Yang, K., Liu, Y., & Zhang, M. (2024). The Diverse Roles of Reactive Astrocytes in the Pathogenesis of Amyotrophic Lateral Sclerosis. *Brain Sci*, *14*(2). https://doi.org/10.3390/brainsci14020158

Yang, N., Zhao, Y., Liu, Z., Zhang, R., He, Y., Zhou, Y., Xu, Q., Sun, Q., Yan, X., Guo, J., & Tang, B. (2019). Systematically analyzing rare variants of autosomal-dominant genes for sporadic Parkinson's disease in a Chinese cohort. *Neurobiol Aging*, *76*, 215 e211-215 e217. https://doi.org/10.1016/j.neurobiolaging.2018.11.012

Yang, Y. S., Moynihan, K. D., Bekdemir, A., Dichwalkar, T. M., Noh, M. M., Watson, N., Melo, M., Ingram, J., Suh, H., Ploegh, H., Stellacci, F. R., & Irvine, D. J. (2018). Targeting small molecule drugs to T cells with antibody-directed cell-penetrating gold nanoparticles. *Biomater Sci*, *7*(1), 113-124. https://doi.org/10.1039/c8bm01208c

You, T., Bi, Y., Li, J., Zhang, M., Chen, X., Zhang, K., & Li, J. (2017). IL-17 induces reactive astrocytes and up-regulation of vascular endothelial growth factor (VEGF) through JAK/STAT signaling. *Sci Rep*, *7*, 41779. https://doi.org/10.1038/srep41779

Yu, J., Chau, K. F., Vodyanik, M. A., Jiang, J., & Jiang, Y. (2011). Efficient feeder-free episomal reprogramming with small molecules. *PLoS One*, *6*(3), e17557. https://doi.org/10.1371/journal.pone.0017557

Yu, J., Hu, K., Smuga-Otto, K., Tian, S., Stewart, R., Slukvin, II, & Thomson, J. A. (2009). Human induced pluripotent stem cells free of vector and transgene sequences. *Science*, *324*(5928), 797-801. https://doi.org/10.1126/science.1172482

Yu, J., Vodyanik, M. A., He, P., Slukvin, II, & Thomson, J. A. (2006). Human embryonic stem cells reprogram myeloid precursors following cell-cell fusion. *Stem Cells*, *24*(1), 168-176. https://doi.org/10.1634/stemcells.2005-0292

Yu, J., Vodyanik, M. A., Smuga-Otto, K., Antosiewicz-Bourget, J., Frane, J. L., Tian, S., Nie, J., Jonsdottir, G. A., Ruotti, V., Stewart, R., Slukvin, II, & Thomson, J. A. (2007). Induced pluripotent stem cell lines derived from human somatic cells. *Science*, *318*(5858), 1917-1920. https://doi.org/10.1126/science.1151526

Yun, S. P., Kam, T. I., Panicker, N., Kim, S., Oh, Y., Park, J. S., Kwon, S. H., Park, Y. J., Karuppagounder, S. S., Park, H., Kim, S., Oh, N., Kim, N. A., Lee, S., Brahmachari, S., Mao, X., Lee, J. H., Kumar, M., An, D., . . . Ko, H. S. (2018). Block of A1 astrocyte conversion by microglia is neuroprotective in models of Parkinson's disease. *Nat Med*, *24*(7), 931-938. https://doi.org/10.1038/s41591-018-0051-5

Zhang, Z., Ma, Z., Zou, W., Guo, H., Liu, M., Ma, Y., & Zhang, L. (2019). The Appropriate Marker for Astrocytes: Comparing the Distribution and Expression of Three Astrocytic Markers in Different Mouse Cerebral Regions. *Biomed Res Int*, *2019*, 9605265. https://doi.org/10.1155/2019/9605265

Zhang, Z., Xiang, D., & Wu, W. S. (2014). Sodium butyrate facilitates reprogramming by derepressing OCT4 transactivity at the promoter of embryonic stem cell-specific miR-

302/367 cluster. *Cell Reprogram*, *16*(2), 130-139. https://doi.org/10.1089/cell.2013.0070

Zhou, Q., Viollet, C., Efthymiou, A., Khayrullina, G., Moritz, K. E., Wilkerson, M. D., Sukumar, G., Dalgard, C. L., & Doughty, M. L. (2019). Neuroinflammatory astrocytes generated from cord blood-derived human induced pluripotent stem cells. *J Neuroinflammation*, *16*(1), 164. https://doi.org/10.1186/s12974-019-1553-x

Zimprich, A., Biskup, S., Leitner, P., Lichtner, P., Farrer, M., Lincoln, S., Kachergus, J., Hulihan, M., Uitti, R. J., Calne, D. B., Stoessl, A. J., Pfeiffer, R. F., Patenge, N., Carbajal, I. C., Vieregge, P., Asmus, F., Muller-Myhsok, B., Dickson, D. W., Meitinger, T., . . . Gasser, T. (2004). Mutations in LRRK2 cause autosomal-dominant parkinsonism with pleomorphic pathology. *Neuron*, *44*(4), 601-607. https://doi.org/10.1016/j.neuron.2004.11.005

Ziolkowska, B. (2021). The Role of Mesostriatal Dopamine System and Corticostriatal Glutamatergic Transmission in Chronic Pain. *Brain Sci*, *11*(10). https://doi.org/10.3390/brainsci11101311

Zrioual, S., Toh, M. L., Tournadre, A., Zhou, Y., Cazalis, M. A., Pachot, A., Miossec, V., & Miossec, P. (2008). IL-17RA and IL-17RC receptors are essential for IL-17A-induced ELR+ CXC chemokine expression in synoviocytes and are overexpressed in rheumatoid blood. *J Immunol*, *180*(1), 655-663. https://doi.org/10.4049/jimmunol.180.1.655

Zubelzu, M., Morera-Herreras, T., Irastorza, G., Gomez-Esteban, J. C., & Murueta-Goyena, A. (2022). Plasma and serum alpha-synuclein as a biomarker in Parkinson's disease: A meta-analysis. *Parkinsonism Relat Disord*, *99*, 107-115. https://doi.org/10.1016/j.parkreldis.2022.06.001